

# **Neural extracellular matrix remodelling as a potential target for cognitive enhancement in the aging brain**

Thesis

for the degree of  
doctor rerum naturalium (Dr. rer. nat.)

approved by the Faculty of Natural Sciences of Otto von Guericke University Magdeburg

by M.Sc. David Baidoe-Ansah  
born on April 24, 1987 in Kumasi (Ghana)

Examiner: Prof. Dr. Alexander Dityatev  
Prof. Dr. Juan Nacher

submitted on: March 31, 2022

defended on: December 07, 2022

**SUMMARY**

Age-dependent accumulation of extracellular matrix (ECM) molecules is implicated in the age-associated decline in synaptic and cognitive functions, which is the common phenotype of both normal and pathological aging. Therefore, understanding age-associated changes in the expression of genes involved in regulating various ECM components can provide an insight into the role of ECM in aging and identify targets to potentially rejuvenate the aging brain and rescue synaptic plasticity and cognition. Hence, in this study, we investigated the cell-type-specific expression of major ECM-degrading and modifying enzymes in the hippocampus of three groups of C57BL/6/J male mice: 2- to 3-month-old (2-3M), 22- to 24-month-old (22-24M), and more than 30-month-old (>30M). Using qPCR, we discovered a downregulation of the majority of ECM-related genes in the hippocampus of >30M mice, which was not the case in 22-24M mice, although genes related to neuroinflammation were highly upregulated in both aged groups. Interestingly, we found a consistent for both 22-24M and >30M old mice downregulation of two genes known to regulate proteolysis of ECM proteoglycans, the carbohydrate sulfotransferase 3 (CHST3) responsible for 6-sulfation of chondroitin sulfates and a disintegrin and metalloproteinase with thrombospondin motifs 5 (ADAMTS-5). Therefore, I tried to rejuvenate the aged hippocampus of 22-24M mice by overexpressing ADAMTS-5 using an adeno-associated virus (AAV) delivery, which indeed improved the hippocampus-dependent synaptic and cognitive functions. Immunohistochemical studies of ADAMTS-5 overexpressing 22-24M mice revealed a loss of ECM chondroitin sulfate proteoglycans, in particular of aggrecan as the major component of perineuronal nets around parvalbumin-expressing (PV+) interneurons and readjustment of both excitatory and inhibitory synaptic inputs to PV+ cells to the levels matching those in 2-3M mice. Degradation of ECM was accompanied by changes in astroglia, microglia, and oligodendrocytes, which may improve clearance and long-range interactions in the aged brains. I also found enhanced long-term potentiation (LTP) and CREB signaling in the CA1 region, presumably due to inhibition of signaling through the extrasynaptic GluN2B-NMDA receptors, which activation has been previously shown to impair synaptic plasticity in aged brains. Moreover, overexpression of ADAMTS-5 rescued behavioral performance of 22-24M mice in the novel object location test and finding a reward in a dry maze test. Altogether, I demonstrated that age-dependent dysregulation of the ECM proteolytic remodeling culminates in the accumulation of neural ECM, while its partial degradation by overexpression of ADAMTS-5 abrogates multiple aging-associated cellular alterations and restores cognitive functions.

## ZUSAMMENFASSUNG

Altersabhängige Ansammlungen von extrazelluläre Matrix (EZM)-Molekülen werden mit der altersbedingten Abnahme der synaptischen und kognitiven Funktionen in Verbindung gebracht, die ein gemeinsamer Phänotyp sowohl des normalen als auch des pathologischen Alterns sind. Daher kann das Verständnis altersbedingter Veränderungen in der Expression von Genen, die an der Regulierung verschiedener EZM-Komponenten beteiligt sind, einen Einblick in die Rolle der EZM beim Altern geben und Ziele identifizieren, die das alternde Gehirn verjüngen und die synaptische Plastizität und Kognition retten könnten. In dieser Studie untersuchten wir daher die zelltypspezifische Expression der wichtigsten EZM-abbauenden und -modifizierenden Enzyme im Hippocampus von drei Gruppen männlicher C57BL6/J-Mäuse: 2- bis 3 Monate alt (2-3M), 22- bis 24 Monate alt (22-24M) und älter als 30 Monate (>30M). Mithilfe von qPCR entdeckten wir eine Herunterregulierung der meisten EZM-bezogenen Gene im Hippocampus der >30M-Mäuse, was bei 22-24M-Mäusen nicht der Fall war, obwohl Gene, die mit der Neuroinflammation zusammenhängen, in beiden Altersgruppen stark hochreguliert waren. Interessanterweise fanden wir sowohl bei 22-24M-Mäusen als auch bei >30M-Mäusen eine konsistente Herunterregulierung von zwei Genen, die bekanntermaßen die Proteolyse von EZM-Proteoglykanen regulieren: die Kohlenhydrat-Sulfotransferase 3 (CHST3), die für die 6-Sulfatierung von Chondroitinsulfaten verantwortlich ist, und eine Desintegrin- und Metalloproteinase mit Thrombospondin-Motif-5 (ADAMTS-5). Deshalb habe ich versucht, den gealterten Hippocampus von 22-24M-Mäusen zu verjüngen, indem ich ADAMTS-5 mit Hilfe eines adeno-assoziierten (AAV)-Virus überexprimiert habe, was tatsächlich die vom Hippocampus abhängigen synaptischen und kognitiven Funktionen verbesserte. Immunhistochemische Untersuchungen an ADAMTS-5-überexprimierenden 22-24M-Mäusen ergaben einen Verlust von EZM-Chondroitinsulfat-Proteoglykanen, insbesondere von Aggrecan, dem Hauptbestandteil perineuronaler Netze um Parvalbumin-exprimierende (PV+)-Interneurone, und eine Anpassung sowohl der exzitatorischen als auch der inhibitorischen synaptischen Eingänge zu PV+-Zellen auf ein Niveau, das dem von 2-3M-Mäusen entspricht. Der Abbau der EZM ging mit Veränderungen der Astroglia, Mikroglia und Oligodendrozyten einher, was die Clearance und die weitreichenden Wechselwirkungen im gealterten Gehirn verbessern könnte. Ich fand auch eine verstärkte Langzeitpotenzierung (LTP) und CREB- Signalübertragung in der CA1-Region, vermutlich aufgrund der Hemmung der Signalübertragung durch die extrasynaptischen GluN2B-NMDA-Rezeptoren, deren Aktivierung nachweislich die synaptische Plastizität in gealterten Gehirnen beeinträchtigt. Darüber hinaus rettete die Überexpression von ADAMTS-5 die Verhaltensleistung von 22-24M-Mäusen im Novel-Object-Location-Test (Test zur Lokalisierung neuartiger Objekte) und bei der Suche nach einer Belohnung im

Trockenlabyrinthtest. Insgesamt konnte ich zeigen, dass eine altersabhängige Regulationsstörung des proteolytischen Umbaus der EZM zu einer Anhäufung neuronaler EZM führt, während ihr teilweiser Abbau durch Überexpression von ADAMTS-5 mehrere altersbedingte zelluläre Veränderungen aufhebt und die kognitiven Funktionen wiederherstellt.

**TABLE OF CONTENTS**

1	INTRODUCTION .....	12
1.1	ECM.....	12
1.1.1	Molecular composition of brain ECM .....	13
1.1.2	Functions of ECM in the developing brain: cell differentiation, cell migration, axon guidance, myelination, synaptogenesis .....	18
1.1.3	Functions of ECM in the adult brain: synaptic transmission and plasticity, learning and memory, regulation of immune functions .....	23
1.1.4	CSPG biosynthesis and glycosylation.....	27
1.1.5	Sulfation of chondroitin sulfates in developing and adult brain .....	30
1.2	Proteolytic remodeling of ECM in the brain.....	32
1.2.1	Matrix metalloproteinase (MMPs).....	33
1.2.2	Matrix metalloproteinase-9 (MMP-9).....	35
1.2.3	Cathepsins .....	39
1.2.4	Cathepsins and CNS.....	40
1.2.5	ADAMTS family .....	42
1.2.6	ADAMTS-4 .....	45
1.2.7	ADAMTS-4 and CNS.....	46
1.2.8	ADAMTS-5 .....	47
1.2.9	ADAMTS-5 and CNS.....	49
1.3	Aging.....	51
1.3.1	Pathological and normal aging.....	52
1.3.2	Learning and memory in normal aging.....	55
1.3.3	Aging and impaired synaptic plasticity.....	56
1.3.4	Aging and ECM .....	58
2	AIMS AND OBJECTIVES .....	61
3	MATERIALS AND METHODS.....	62
3.1	Animals.....	62
	Tissue isolation, RNA extraction and RT-qPCR .....	62
3.1.1	Tissue isolation .....	64
3.1.2	RNA extraction, cDNA conversion, and qPCR .....	64
3.2	3.2.3 FACS technology .....	65
3.2.1	FACS sorting for neuronal and glial nuclei extraction .....	66

3.3	Immunohistochemistry (IHC) and Immunocytochemistry (ICC).....	67
3.3.1	Immunohistochemistry.....	68
3.3.2	Immunocytochemistry .....	69
3.4	Generation, characterization and stereotaxic injection of hADAMTS-5 AAVs.....	69
3.4.1	Generation of pAAV_hPGK_hADAMTS5_T2A_eGFP and pAAV_hPGK_eGFP .....	69
3.4.2	Cell culture and characterization of pAAV_hPGK_hADAMTS5_T2A_EGFP and pAAV_hPGK_EGFP .....	70
3.4.3	Stereotaxic injection of pAAV_hPGK_hADAMTS5_T2A_EGFP and pAAV_hPGK_EGFP into the hippocampal CA1 .....	72
3.5	Behavioral experiments.....	72
3.5.1	Open field.....	73
3.5.2	Novel object location and recognition tests .....	73
3.5.3	Labyrinth (dry maze) .....	74
3.5.4	Optimization of the quadrant-based labyrinth task (dry maze).....	74
3.5.5	Asymmetrical-quadrant-based labyrinth task .....	76
3.6	Microscopy and image analysis .....	78
3.6.1	Confocal microscopy, High-resolution imaging, image acquisition, processing, and analysis	78
3.6.2	Cell-type specific analysis .....	79
3.6.3	Perineuronal and synaptic puncta analysis.....	80
3.6.4	Analysis of PV-network configuration .....	80
3.6.5	GluN2B staining and image analysis .....	80
3.7	Electrophysiological experiments .....	81
3.8	Statistical analysis.....	82
4	RESULTS .....	84
4.1	Increased ECM protein levels in the aged brains do not correlate with mRNA levels of CSPG core-proteins .....	84
4.1.1	Expression of CSPG core-proteins and enzymes regulating synthesis and sulfation of GAG chains in the hippocampus of 22-24 and >30M old mice .....	84
4.1.2	Reduced Adamts-5 expression in the hippocampus of 22-24 and >30M old mice.....	86
4.1.3	Cell-specific reduction of Adamts-5 and Chst3 in the hippocampus of 22-24M old mice.	88
4.1.4	Cell-specific increase in ADAMTS-5 and CHST3 expression in the hippocampus of 22-24M mice .....	89
4.1.5	Reduced activity of CHST3 and ADAMTS-5 in the hippocampus of 22-24M old mice ...	92

4.2	ECM remodelling by overexpressing hADAMTS-5 in the hippocampus of 22-24M old mice .	94
4.2.1	Increased ECM cleavage by hADAMTS-5 in the hippocampus of 22-24M old mice and in hippocampal cultures .....	94
4.2.2	Removal of Aggrecan and Brevican in CA1, CA2, and CA3 of 22-24M old mice injected with pAAV_hPGK_hADAMTS5_EGFP .....	96
4.2.3	pAAV_hPGK_hADAMTS-5_EGFP cleaved other CSPGs in the hippocampus of 22-24M old mice .....	100
4.2.4	Effect of overexpressing hADAMTS-5 on neuroinflammation in hippocampal CA1 of 22-24-month-old mice .....	102
4.2.5	Effect of overexpressing hADAMTS-5 on myelination in the hippocampus of 22-24M mice	107
4.2.6	Overexpression of ADAMTS5 improved long-term memory of NOLT in 22-24M mice	108
4.2.7	Overexpression of ADAMTS-5 improved spatial learning and memory in 22-24M mice	111
4.2.8	Overexpression of ADAMTS5 improved synaptic plasticity in 22-24M mice.....	113
4.2.9	CSPG remodelling does not change expression of synaptic GluN2B expression in 22-24M mice	117
4.2.10	CSPG remodelling enhanced pCREB signaling in aged ADAMATS-5 mice.....	117
4.2.11	CSPG remodelling partially restored both excitatory and inhibitory synaptic inputs in aged ADAMATS-5 mice to young controls.....	119
5	DISCUSSION .....	125
5.1	mRNA levels of CSPGs core-proteins and glycosylation enzymes do not correlate with PNN protein levels in aged mice .....	126
5.2	mRNA levels of CSPGs proteases did not change in aged mice compared to young controls except for <i>Adamts-5</i> and <i>MMP-12</i> .....	127
5.3	CHST-3 and ADAMTS-5 are upregulated in 22-24M old mice.....	128
5.4	Effects of overexpressing hADAMTS-5 on CSPGs cleavage, neuroinflammation and distribution of oligodendrocytes .....	129
5.5	CSPG remodeling improved long-term NOLT memory and spatial learning and memory in 22-24-month-old mice.....	131
5.6	Molecular and cellular mechanisms behind cognitive enhancement in hADAMTS-5 injected mice	132
6	CONCLUSIONS.....	136
7	REFERENCES .....	137

**LIST OF ABBREVIATIONS**

AAV	Adeno-associated virus
ACAN	Aggrecan
ACSF	Artificial cerebrospinal fluid
AD	Alzheimer's disease
ADAMTS	A disintegrin and metalloproteinase with thrombospondin motifs
AIS	Axon initial segment
AMPAR	$\alpha$ -amino-3-hydroxy-5-methyl-4-isoxazolepropionic acid receptor
APP	Amyloid precursor protein
BCAN	Brevican
BSA	Bovine serum albumin
C4ST1	Chondroitin 4-O-sulfotransferase 1
C4ST3	Chondroitin 4-O-sulfotransferase 3
C6ST1	Chondroitin 6-O-sulfotransferase 1
CA1	Cornus ammonis 1
CA2	Cornus ammonis 2
CA3	Cornus ammonis 3
CaMKII	Ca <sup>2+</sup> /Calmodulin-dependent protein kinase
c-FOS	Fos proto-oncogene
chABC	Chondroitinase ABC
ChPf2	Chondroitin polymerizing factor 2
Chst11	Carbohydrate sulfotransferase 11
Chst13	Carbohydrate sulfotransferase 13
Chst3	Carbohydrate sulfotransferase 3
Chst7	Carbohydrate sulfotransferase 7

ChSy1	Chondroitin sulfate synthases 1
ChSy3	Chondroitin sulfate synthase 3
CNS	Central nervous system
CREB	cAMP response element-binding protein
CS-GAGs	Glycosaminoglycan
CSPGs	Chondroitin sulfate proteoglycans
DIV	Days <i>in vitro</i>
DMEM	Dulbecco's Modified Eagle's Medium
DZNE	Deutsches Zentrum für Neurodegenerative Erkrankungen e.V.
ECM	Extracellular matrix
EGFP	Enhanced green fluorescent protein
EPSPs	Excitatory postsynaptic potentials
ER	Endoplasmic reticulum
FACS	Fluorescence-activated cell sorting
fEPSPs	Field excitatory postsynaptic potentials
GABA	Gamma-aminobutyric acid
Gal	Galactose
GalNAc	N-acetylgalactosamine
GFAP	Glial fibrillary acidic protein
GlcA	Glucuronic acid
HA	Hyaluronan acid
HAPLN	Hyaluronan and proteoglycan link proteins
hPGK	Human phosphoglycerate kinase
IBA1	Allograft inflammatory factor 1
IHC	Immunohistochemistry
IL	Interleukin

IL1beta	Interleukin 1 beta
L-LTP	Late-phase of LTP
LTD	Long-term depression
LTP	Long-term potentiation
MAP	Mitogen-activated protein
ML	Medio-lateral
MMP	Matrix metalloproteinase
MT-MMPs	Membrane-bound MMPs
MWM	Morris water maze
NARP	Neuronal activity-regulated pentraxin
NB	Neurobasal medium
NCAM	Neuronal cell adhesion molecule
NCAN	Neurocan
NMDAR	N-methyl-D-aspartate receptor
NMDAR-LTD	NMDAR-dependent LTD
NOLT	Novel object location test
NORT	Novel object recognition test
NrCAM	Neuron glia-related CAM
OA	Osteoarthritis
OLIG2	Oligodendrocyte transcription factor
OPCs	Oligodendrocyte precursor cells
OTX2	Orthodenticle homeobox 2
PAPS	3'-phosphoadenosine 5'-phosphosulfate
PB	Phosphate-buffered
PBS	Phosphate-buffered saline
PCAN	Phosphacan

pCREB	Phosphorylated CREB
PFA	Paraformaldehyde
PFC	Prefrontal cortex
PGs	Proteoglycans
PNN	Perineuronal nets
PSD	Post-synaptic density protein
PV	Parvalbumin
ROS	Reactive oxygen species
RT-PCR	Reverse transcription-polymerase chain reaction
Sema3A	Semaphorin 3A
STP	Short-term potentiation
TIMP	Tissue inhibitor of metalloproteinases
TNF- $\alpha$	Tumor necrosis factor- $\alpha$
TNR	Tenascin-R
TOP1	Topoisomerase I
TSR	Thrombospondin 1-like repeats
UST	Uranyl 2-O-sulfotransferase
VCAN	Versican
vGAT	Vesicular GABA transporter
vGLUT	Vesicular glutamate transporter
WFA	<i>Wisteria floribunda</i> agglutinin

## 1 INTRODUCTION

### 1.1 ECM

The extracellular matrix (ECM) is a complex network of macromolecules present within tissues and organs, including collagens, fibronectin, laminins, fibrillins, proteoglycans, and several other glycoproteins (Lockhart et al., 2011; Ulbrich et al., 2021). In the past, ECM was viewed to solely confer structural support such as strength and elasticity, to cells and tissues within their microenvironment. Recent findings have unraveled more complex biomechanical, biochemical and physiological functions (Frantz et al., 2010). These include cell to cell signaling, volume transmission, regulation of cell proliferation and differentiation (Lockhart et al., 2011; Syková and Nicholson, 2008).

In the mammalian brain, ECM occupies a volume fraction of 10%-20% of the total volume of the normal adult brain, and is interspersed between neurons and glia cells (Bonneh-Barkay and Wiley, 2009; Ulbrich et al., 2021). Neurons and glial cells synthesize and secrete various ECM molecules into extracellular space (ECS) where they **aggregate** around cell soma, dendrites, the axon initial segment, the nodes of Ranvier and synapses (Rasband and Peles, 2021). The composition and density of ECM molecules within the brain are region-specific and depend on neural activity (Carulli et al., 2010; Dityatev et al., 2007; Syková and Nicholson, 2008). During brain development, ECM molecules are mostly diffuse and influence cell proliferation, migration and differentiation because of their ability to adhere to cell surface receptors such as integrins and syndecans (Itoh, 2021; Kleiser and Nyström, 2020). The switch from juvenile to the more heterogeneous and compact adult ECM (El-Tabbal et al., 2021) strongly correlates with the development of essential brain functions including the closure of the critical period, synaptic plasticity, synaptogenesis, learning and memory, synaptic stabilization and neural regeneration (Frischknecht et al., 2014). Additionally, the ECM protects the integrity of the brain microenvironment by using its buffering properties to maintain physiological ion and water concentration (Bonnans et al., 2014; Frantz et al., 2010) (**Figure 1.1**).

Overall, ECM molecules are highly dynamic and several studies have unraveled the varying organization of brain ECM and the diverse alterations during brain development. These studies have shown a strong correlation between certain brain functions and specific components of ECM which will be elaborated on in the next sections.

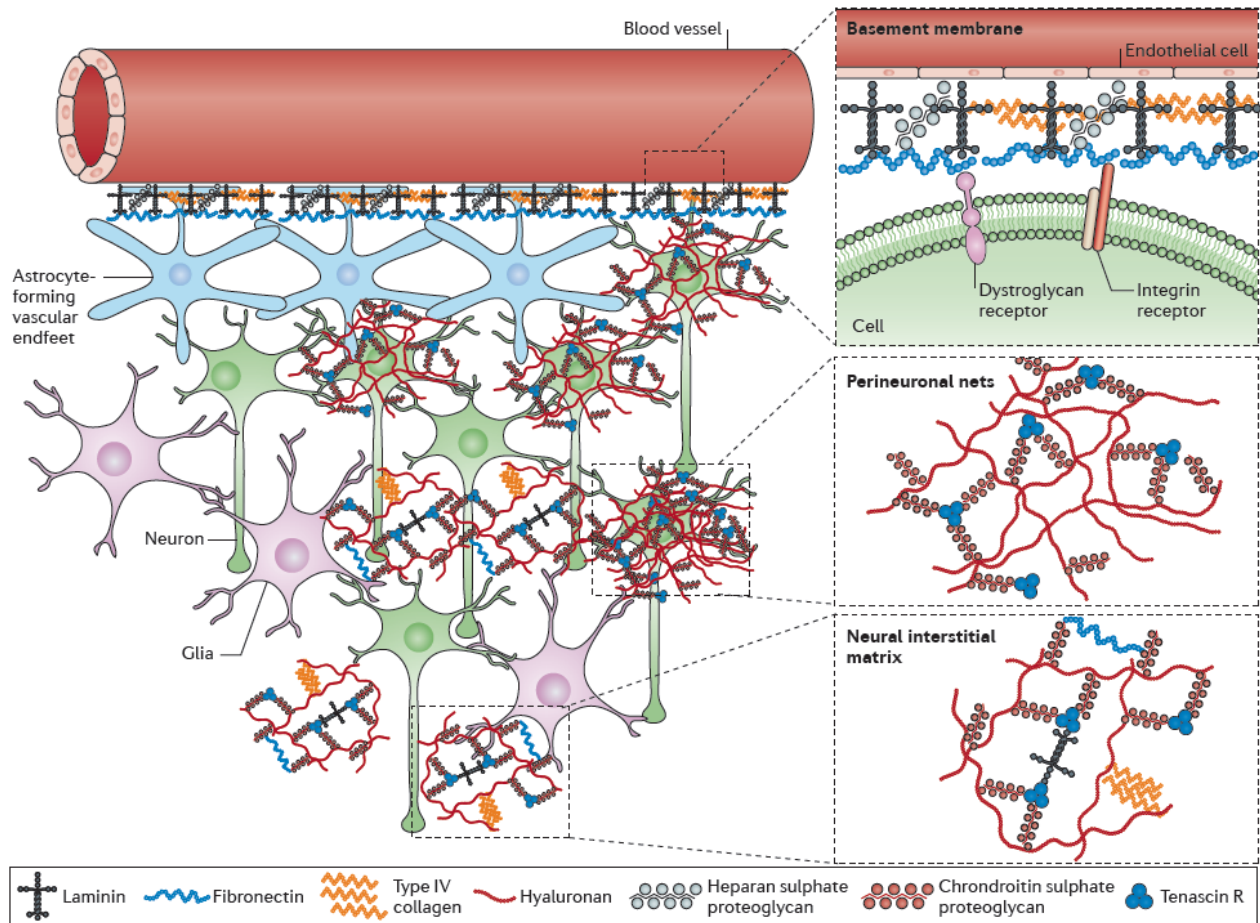


**Figure 1.1: Localization of ECM in the CNS**

In the brain, ECM molecules are localized at the basement membranes, around soma and proximal dendrites in a condensed lattice-like form called perineuronal nets (PNNs). In addition, ECM can be found in the interstitial space, where it is called the neural interstitial matrix. This form can be found around neuronal synapses (Lau et al., 2013).

### 1.1.1 Molecular composition of brain ECM

Here I will differentiate between the two forms of neural ECM: a more diffuse form within the extracellular space and a condensed form that is tethered to the surfaces of cells, known as perineuronal nets (PNNs) (Dityatev and Schachner, 2003; Bruckner et al., 2006; Fawcett et al., 2019). In the brain, ECM consists of proteoglycans and glycoproteins, such as chondroitin sulfate proteoglycans (CSPGs), heparin sulfate

proteoglycan (HSPGs), tenascins and link proteins (Harlow and Macklin, 2014; Lundell et al., 2004). PNNs are predominantly enriched around the soma, proximal dendrites, and axon initial segments of parvalbumin-expressing (PV+), gamma-aminobutyric acid (GABA)ergic interneurons and a subtype of excitatory neurons (Ulbrich et al., 2021) in the hippocampus, cerebral cortex and cerebellum as well as other brain regions (Song & Dityatev, 2018; Ulbrich et al., 2021). The formation and maturation of PNNs are essential for the onset and closure of the critical period during brain development. This process can be reopened by digesting the chondroitin sulfate glycosaminoglycans (CS-GAGs) of PNNs with the bacterial enzyme, chondroitinase ABC (chABC) (Hou et al., 2003; Pizzorusso et al., 2002).

A typical PNN contains CSPGs bound to HA through the N-terminal hyaluronan binding domain, with the CSPG - HA complex stabilized by the hyaluronan and proteoglycan link proteins (HAPLN1-4), and the carboxylic ends cross-linked to the ECM glycoprotein, Tenascin-R (TNR) (Dityatev & Schachner, 2003, Morawski et al., 2014). HA is a non-sulfated linear polysaccharide made up of D-glucuronic acid and N-acetyl-D-glucosamine units, and it is synthesized by a family of transmembrane hyaluronan synthases (HASs) that includes HAS1, HAS2, HAS3 and HAS4 (Bikbaev et al., 2015; Weigel et al., 2015). CSPGs are sulfated proteoglycans with two major families, the lecticans and non-lecticans. Each CSPG lectican consists of a core protein attached covalently to CS-GAGs side chains and they include; aggrecan (ACAN), brevican (BCAN), neurocan (NCAN), and versican (VCAN). The core protein of lecticans is, thus, divided into 3 major domains namely the G1, G2 and G3 (Gottschall and Howell, 2015). The G2 domain is bound to the CS-GAGs which are long, unbranched, varying-length chains of polysaccharides with repeating disaccharide units of amino sugar, either N-acetylglucosamine (GlcNAc) or N-acetylgalactosamine (GalNAc), and glucuronic acid (GlcA) (Sethi and Zaia, 2017). The differences in core protein, the number of GAG chains and sulfation patterns influence the varying functions in CSPGs (Pendleton et al., 2013a; Properzi et al., 2003). The second family of CSPGs, the non-lecticans, include phosphacan (PCAN), the cell-surface glycoprotein, CD44 antigen (CD44), the transmembrane proteoglycan, neural/glia antigen 2 (NG2), and others (Long & Huttner, 2019). Currently, PNNs are visualized using the plant lectin molecule, *Wisteria floribunda* agglutinin (WFA) that specifically labels the highly abundant N-acetylglucosamine of CSPGs (Djrbal et al., 2017). Recent findings have identified both orthodenticle homeobox 2 (OTX2) and semaphorin 3A (Sema3A) to bind to the GAGs of CSPGs (Carulli and Verhaagen, 2021). Interestingly, OTX2 has been shown to influence maturation of PV interneurons through internalization and this is essential for the critical period (Sugiyama et al., 2008), whereas the accumulation of sema3A in an activity-

dependent manner coincides with the closure of the critical period (Boggio et al., 2019) (**Figure 1.2 & 1.3**).

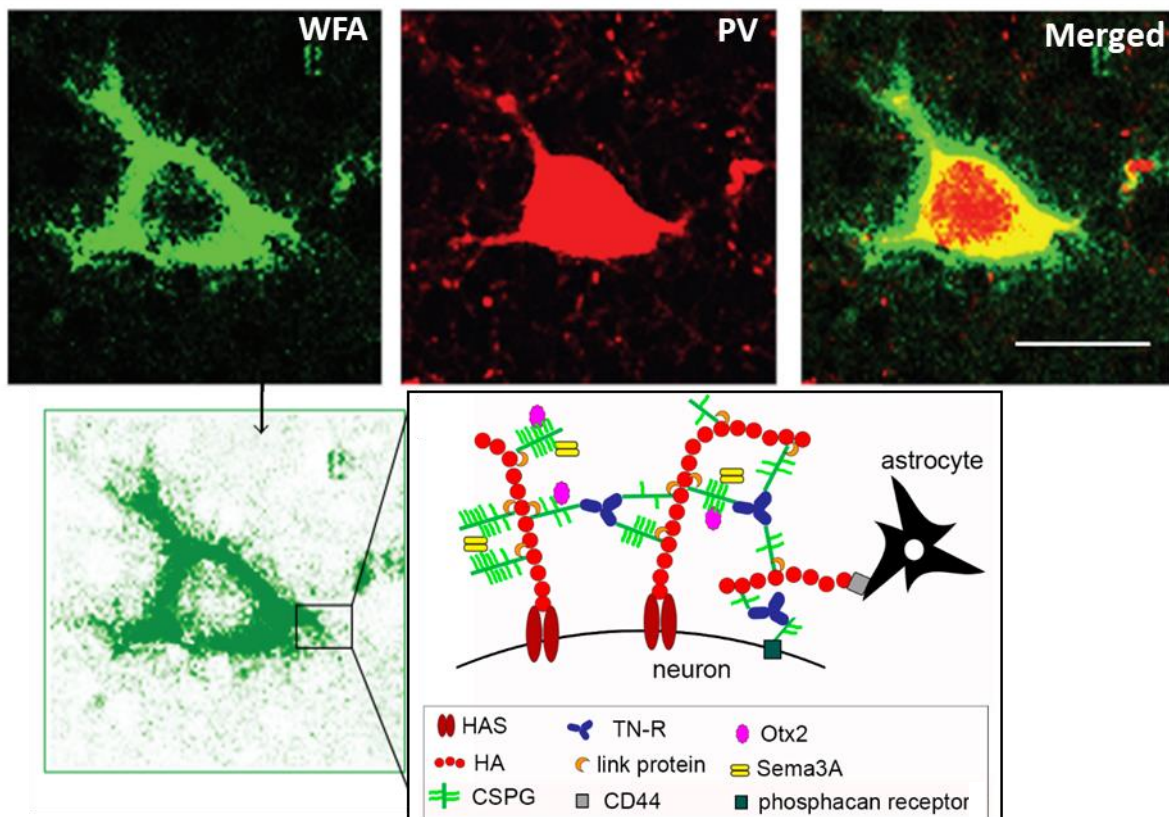


**Figure 1.2: Molecular composition of PNN around PV+-interneurons**

Immunostaining to visualize PNN around PV+ interneurons with WFA (green) and PV(red) antibodies. The individual composition of PNNs including CSPGs, ACAN, VCAN, NCAN and BCAN bound to the (HA) backbone, stabilized by link proteins and the lecticans are cross-linked by the glycoprotein, TNR. Both OTX2 and Sema3A bind to CSPG via the GAGs. This scheme is modified from both Lorenzo and Carulli (Carulli and Verhaagen, 2021; Lorenzo Bozzelli et al., 2018).

Along axons, ECM is prominent at the axon initial segment (AIS), the nodes of Ranvier of myelinated axons and at the axonal terminals (perisynaptic ECM) (Krishnaswamy et al., 2019). The AIS and nodes of Ranvier are composed of clusters of voltage-gated  $\text{Na}^+$  channels [Nav], which are required for the generation and propagation of action potentials (Hedstrom et al., 2007). Furthermore, at the AIS, the clustering of these ion channels in addition to cell adhesion molecules CAMs; neurofascin-186 [NF-186] and neuron glia-related CAM [NrCAM] depend on the cytoskeletal proteins, ankyrin G and  $\beta 4$  spectrin (Hedstrom et al., 2007; Rasband and Peles, 2021). Surprisingly, these regions are highly enriched by ECM,

whereby BCAN, whose localization at the AIS depends on NF-186 and NrCAMs expression, is the major ECM molecule enriched at the AIS (Hedstrom et al., 2007; Zonta et al., 2011). Meanwhile, at the nodes of Ranvier, VCAN, PCAN and TNR are enriched in addition to BCAN, with VCAN functioning as the major organizer of ECM at this region (Bekku et al., 2009; Dours-Zimmermann et al., 2009). At synapses, ECM has been identified as a major component (Yuzaki, 2018), giving rise to the tetrapartite synapse model which includes presynapse (axon terminal), the postsynapse, the astrocytic endfoot and, the synaptic cleft with perisynaptic ECM around (Dityatev and Rusakov, 2011; Ferrer-Ferrer and Dityatev, 2018; Korotchenko et al., 2014). Several ECM molecules secreted by neurons and glia function by facilitating the interaction between dendrites and axons of neurons. These molecules are also known as the extracellular scaffolding proteins (ESPs) and they include Cerebellin 1 (Cbln1), neuronal pentraxins, Hevin, thrombospondins, and glypicans (Yuzaki, 2018). (**Figure 1.4**).

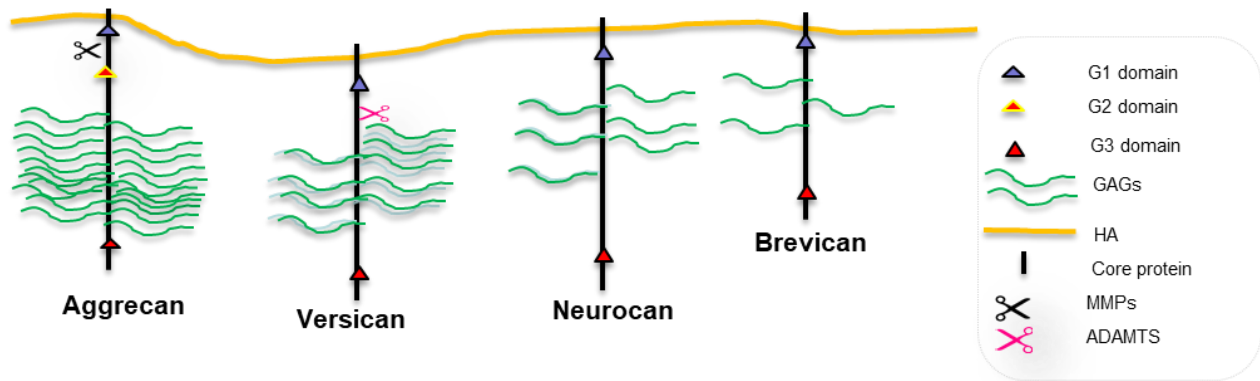


**Figure 1.3: Structure of CSPGs of the lectican family**

Each CSPG includes a core protein with varying number of sugar chains, the GAGs, of which ACAN has the highest number of GAGs followed by VCAN. BCAN, on the other hand, has the least number of GAGs and the shortest length of core proteins.

The interactions of ECM molecules with their respective receptors at the pre- and postsynapse are essential for their organization, function and modification (Korotchenko et al., 2014). A review by Korotchenko shows that the secreted protein leucine-rich glioma-inactivated 1 (LGI1), neuronal activity-regulated pentraxin (NARP) and neuronal pentraxin 1 (NP1) are localized in the synaptic cleft (Xu et al., 2003) and they interact with their receptors to organize synapses. Furthermore, the perisynaptic extracellular space of glutamatergic synapses contains BCAN and NCAN associated with HA and they are interconnected via TNR and TNC, that function in the organization and modification of synapses (Korotchenko et al., 2014) (Figure 1.4 and 1.5).

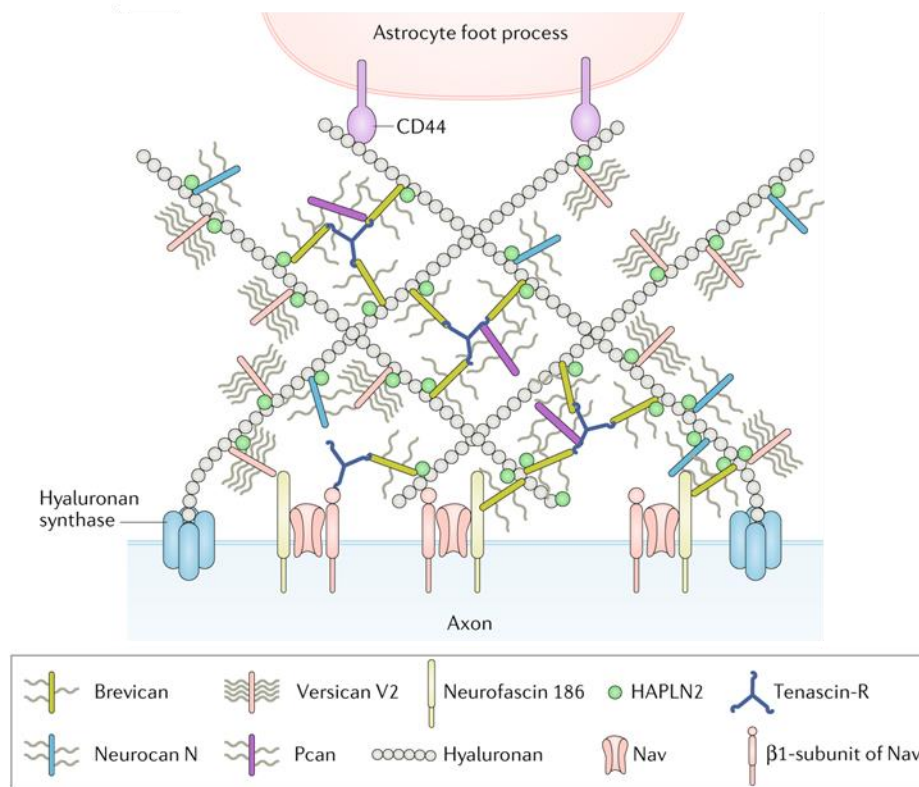


**Figure 1.4 ECM organization around various compartments of neurons**

PNN around soma and dendrites of PV+ interneurons consist of the CSPGs, versican, neurocan and brevicane, bound to the backbone hyaluronan and stabilized by link proteins, HAPLN2. At the nodes of Ranvier, ECM molecules are found to stabilize and regulate interactions between glia and neurons through association with cell adhesion molecules such as Neurofascin 186 and NrCAM. Sodium channels (Nav) at axonal membrane are stabilized by Neurofascin 186 and B1-subunits. From (Fawcett et al., 2019).

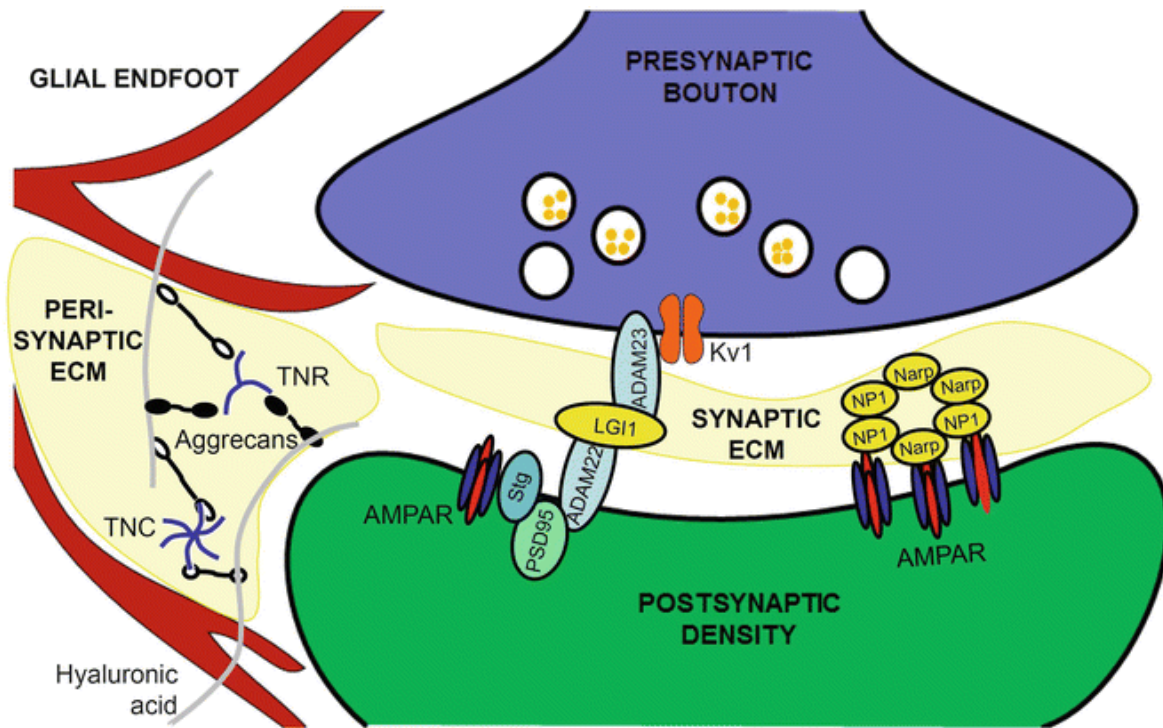


**Figure 1.5 Zooming in at the tetrapartite synapse**

The composition of the tetrapartite synapse includes pre- and postsynaptic terminals coupled with synaptic and perisynaptic ECM such as ACAN, TNR and TNC along with the astrocytic end feet. AMPA receptors colocalize with neuronal pentraxins NP1 and NARP in synaptic domains (Korotchenko et al., 2014).

### *1.1.2 Functions of ECM in the developing brain: cell differentiation, cell migration, axon guidance, myelination, synaptogenesis*

The mammalian brain development can be divided into two distinct stages. Firstly, the developing brain which includes the embryonic brain in utero together with the postnatal brain, and secondly the adult brain. CNS development in both rodents and humans starts with the formation of the neural tube which gives rise to the spinal cord and brain (Semple et al., 2013). This process (called neurulation) finishes on gestational days eight to eleven days in rodents and after three to four weeks in humans (Kolb and Gibb, 2011; Semple et al., 2013; Urbán and Guillemot, 2014). The brain development is influenced by unique cues produced in the maternal environment in the embryonic stage, the environment together with experience-dependent

brain activity in the postnatal stage, and a more complex and matured extracellular space in the adult brain (Chini and Hanganu-Opatz, 2021; Kolb and Gibb, 2011). Recent findings also point to the epigenetic modifications as another cue, that can regulate brain development via alteration to the normal gene expression that can occur at any stage of brain development (Blumberg et al., 2009). One common factor that is found to influence brain development at any stage is the ECM.

The brain development in rodents and humans follows a similar sequence. First of all, the cell type, either neurons (neurogenesis) or glia cells (gliogenesis) is determined by the proliferation and differentiation of neural progenitor cells (Urbán and Guillemot, 2014). The newly formed cells then migrate to their destinations such as the hippocampus and cortical locations. This is followed by cell maturation, synapse formation and pruning, and finally myelination (Kolb and Gibb, 2011; Williams et al., 2010). Studies have demonstrated that ECM facilitates intracellular signaling that regulates these embryonic processes (Dityatev and Schachner, 2003). For instance, HA in the developing brain maintains neural progenitor cells proliferation but not their differentiation (Wang et al., 2012). Other examples are NCAN, exclusively produced by neurons in the CNS, and PCAN derived from astrocytes (Grumet et al., 1994), which are all abundantly expressed in the developing brain as they regulate neurite outgrowth and cell adhesion. NCAN is a known CSPG with a high affinity for the neural adhesion molecules namely NCAM and Ng-CAM but has little or no affinity for laminin (Friedlander et al., 1994). The association of NCAN to NCAM and Ng-CAM inhibits neurite growth and cell adhesion in neurons cultured on surfaces coated with the said molecules. On the other hand, PCAN, a secreted form of receptor-type protein-tyrosine phosphatase  $\zeta$  (RPTP $\zeta$ ), enhances neurite outgrowth in hippocampal and cortical neurons (Maeda & Noda, 1996). Other lecticans also inhibit neurite outgrowth such as BCAN in rat cerebellum along with ACAN in dorsal root ganglion neurons (Chan et al., 2008). The distribution of CSPGs as well as sulfation of GAGs side chains are altered during brain development (Mencio et al., 2021), indicating a potential developmental function for sulfated sugar chains in the brain. Case in point, a study shows that the digestion of CSPGs GAGs with chABC in the developing neocortex of mice reduced neural progenitor proliferation to neurons whereas the density of glia, specifically astrocytes, increased, indicating a switch in the fate of progenitor cells (Sirko et al., 2007). Moreover, ECM proteoglycans, like CSPG content in the embryonic brain is constant but starts to increase at birth until it reaches adult levels post-birth (Margolis and Margolis, 1993; Oohira et al., 1986), suggesting they are vital for brain development. This implies that CSPGs GAGs play vital role in proliferation and differentiation during brain development (**Figure 1.6**).

Once neurons migrate to their respective functional sites and differentiate, they begin to form connections that requires both axonal growth and dendritic formation. Axonal pathfinding also called axonal guidance, is an aspect of neural development whereby neurons send axons to their targets, and this process is critical for the wiring or neuronal network of the developing brain. ECM proteoglycans and glycoproteins function as adhesive cues during axonal guidance by facilitating neurite elongation or outgrowth (Kappler et al., 1997). In addition, cell adhesion proteins fibronectin and laminin interact with lecticans in controlling axonal growth by repelling the inhibiting effects of CSPGs towards axonal pathfinding (Katoh-Semba et al., 1995). In rodents and humans, the neural network relies on dendritic development and synaptogenesis which begins at the mid embryonic stage and continues after birth. The overall function of the brain arises from the appropriate connections between neuronal populations, and these connections rely on the efficient axonal guidance to the exact target zones, recognition of receptive target cells and formation of synapses on the postsynaptic neuron. CSPGs interact with NCAM to facilitate synaptogenesis and synapse stabilization (Mencio et al., 2021), like BCAN influencing synaptogenesis in the postnatal brain (Shabani et al., 2021). Another essential process in the developing brain is synaptic pruning, which occurs postnatally in rodents and humans. It is influenced by NCAN through inhibiting synaptic pruning via control of SEMA 3F signaling (**Figure 1.6**).

Finally, in the brain, myelination of neurons by oligodendrocytes is pivotal and this process is highly intense, especially during brain development, and therefore requires high expression of myelin proteins and lipids. Myelination begins before birth in humans compared to after birth in rodents, and originates in the caudal brain and progresses towards the forebrain with fibers of cerebral cortex being the last site to be myelinated (Santos et al., 2020). During myelination, the glia oligodendrocyte precursor cells (OPCs) rapidly proliferate, mature into oligodendrocytes, align their long and elaborated membrane along neuronal axons (Keough et al., 2016; Webb, 2017). Brain ECM has been found to both positively and negatively influence myelination (Williams et al., 2007). For instance, on the bright side, laminins are strongly detected in the white matter tracts, which surprisingly, are completely lost in fully-myelinated axons (Colognato et al., 2005). Strikingly, laminin expression reappears in demyelinated fiber tracts (Zhao et al., 2009), indicating laminin as one of the major ECM molecules necessary for myelination. Besides being essential for the proliferation, migration, and differentiation of progenitor cells during brain development, CSPGs also function in neuronal myelination. In the developing brain, VCAN, BCAN and TNR are synthesized by oligodendrocytes (Harlow and Macklin, 2014) with BCAN observed at membrane extension around axon fibers (Ogawa et al., 2001). Also, in the context of CNS injury and diseases, new oligodendrocytes

and astrocytes are recruited at and around the injury site, yet they are less effective in remyelinating demyelinated axons (Harlow and Macklin, 2014). At the injury site, the inhibitory glial scar, which is made up of excess expression of CSPGs from astrocytes and oligodendrocytes like BCAN, NCAN, VCAN as well as PCAN with decreased ACAN (Andrews et al., 2012; Jones et al., 2003; Lemons et al., 2001), is known to inhibit functions of oligodendrocytes. This suppression has been known to depend on the interaction between CSPGs and the protein tyrosine phosphatase sigma (PTP $\sigma$ ) receptor (Coles et al., 2011; Harlow and Macklin, 2014), as well as the leukocyte common antigen-related phosphatase (LAR) (Fisher et al., 2011). The interaction between the said molecules inhibits the outgrowth of oligodendrocytes and myelination, and this effect is reversed or rescued in experiments using chABC to degrade CSPGs as well as RNA interference-mediated down regulation of THE protein tyrosine phosphatase sigma (PTP $\sigma$ ) receptor (Harlow and Macklin, 2014; Pendleton et al., 2013a), and in LAR knockout animal models (Fisher et al., 2011) (**Figure 1.6 and Table 1.1**).

**Table 1.1: Stages cell development**

Developmental stage	Neuronal function	Glial function	ECM
Cell birth	Neurogenesis	Gliogenesis	HA, NCAN
Cell migration			NCAN, PCAN
Cell differentiation	Formation of dendrites and axon		NCAN, PCAN, BCAN
Cell maturation	Dendrite and axon growth	Glia processes	NCAN, PCAN, Laminin, Fibronectin
Contact formation	Synaptogenesis	Myelogenesis (Myelination), astroglial contacts, e.g. around vessels and synapses	BCAN, NCAN, VCAN, TNF, Laminin
Cell death	Neuronal death and synaptic pruning	Glial death	NCAN, PCAN

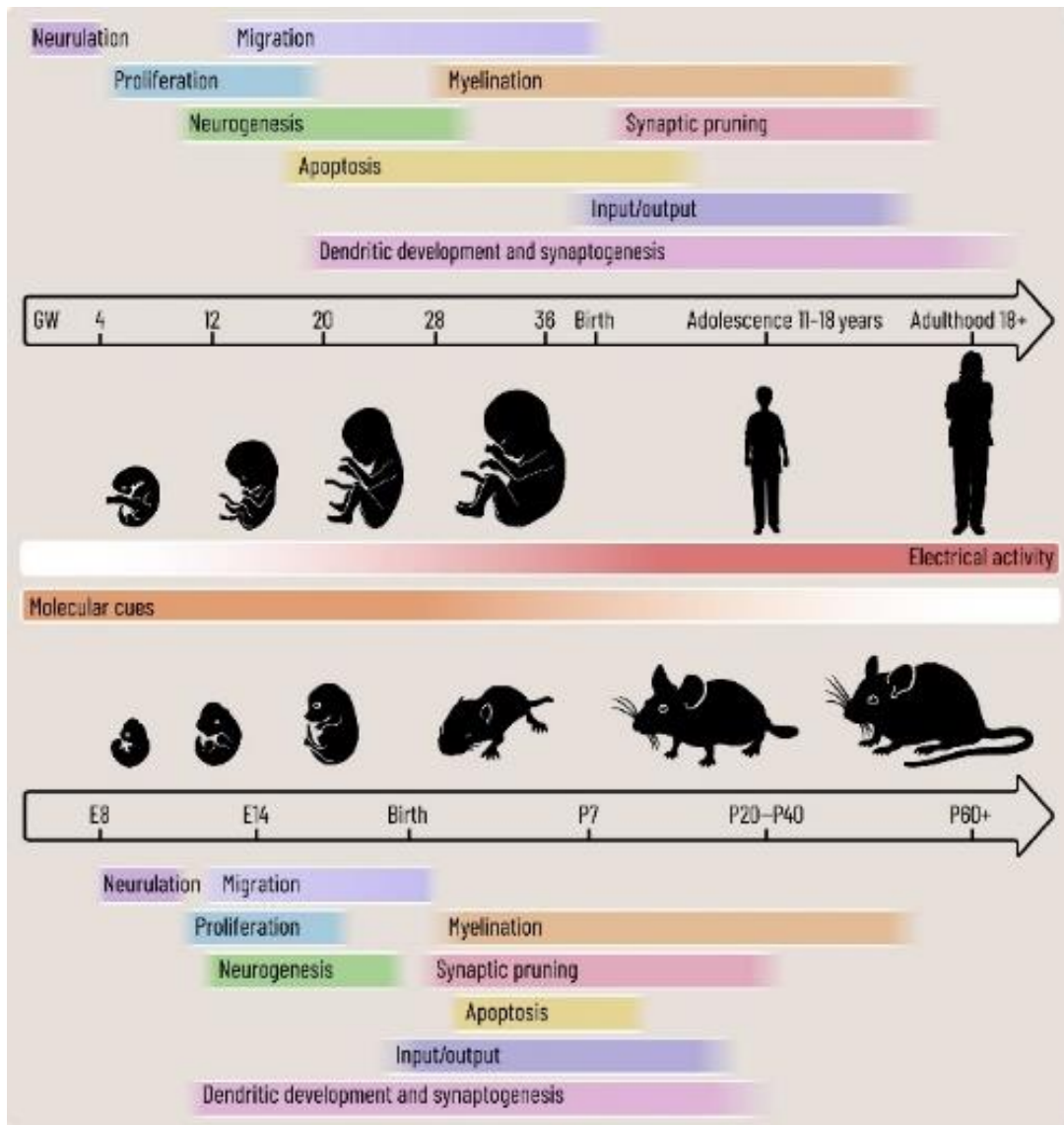


**Figure 1.6 Brain development in rodent and human**

Rodents and humans have similar embryonic and post-natal brain developmental processes. This includes neurulation, proliferation, migration and neurogenesis representing the embryonic phase of brain development followed by postnatal processes like myelination and synaptic pruning. However, dendritic development and synaptogenesis begin before birth in both animals but terminate by P40 in rodents whereas in humans it continues even into adulthood (Chini and Hanganu-Opatz, 2021).

### *1.1.3 Functions of ECM in the adult brain: synaptic transmission and plasticity, learning and memory, regulation of immune functions*

The transition from postnatal to adulthood brain is accompanied by extensive maturation of neuronal networks (Pujol et al., 2021) through the formation, elimination and reorganization of synapses (synaptogenesis and synaptic pruning) (Mencio et al., 2021; Pires-Neto et al., 1999), and elimination of cells (apoptosis) (Chan et al., 2002; Khundrakpam et al., 2016; Orlando et al., 2012). This transition also significantly influences functional and behavioral properties such as synaptic transmission and plasticity, and learning and memory. During this period, CSPGs such as NCAN and VCAN are upregulated for the first couple of weeks after birth in mice but downregulated in adulthood, with ACAN and BCAN increasing especially during the critical period (Zimmermann and Dours-Zimmermann, 2008). The critical period coincides with extreme synaptogenesis, and in humans, this period starts from infancy to early childhood which corresponds to P1-P20 in mice. The plastic nature of this period shapes the cognitive and behavioral developments serving as a platform for the acquisition of future skills (Cao et al., 2017). The closure of this period coincides with the maturation of PNNs along with an increase in the number of PV+ interneurons and less dynamic dendritic spines, which is an important aspect of structural plasticity (Orlando et al., 2012).

Studies have demonstrated that PNNs are essential for controlling critical period via maturation of PV cells and this phenomenon is known to depend on OTX2, which once trapped in PNNs enhances PV maturation and eventually closes the critical period (Bernard and Prochiantz, 2016). The transition from the critical period to the adult brain involves synaptic refinement through synaptic pruning, that is the elimination of excess synapses. A typical synapse includes axonal terminal(s) and a dendritic spine(s), and these spines are extensions from dendritic shafts. Dendritic spines are very dynamic in structure and function during brain development, but stable synaptic connections in the adult brain are stabilized by PNNs (Hering and Sheng, 2001). The stabilization of synapses requires appropriate adjustment of spines as well as regular remodeling, and impairment of these processes results in brain diseases like Alzheimer's disease (Levy et al., 2014). Although PNNs regulate spine and synapse stabilization, they also influence synaptic pruning. The removal of PNN in the hippocampus, for example, impairs synaptic pruning (Orlando et al., 2012), and this is observed in diseases like autism and schizophrenia (Bitanhirwe and Woo, 2014). Additionally, neuronal cell death is another process essential for the maturation of adult brain as about half of neurons do not reach adulthood (Vanderhaeghen and Cheng, 2010; Yuan et al., 2003).

Under the scope of synaptic transmission, plasticity, learning and memory, recent evidence show these processes share common structural and physiological features. They involve the long-term potentiation (LTP) and long-term depression (LTD) of dendritic spines to strengthen or weaken synaptic connections respectively (Ashby et al., 2021; Bliss and Collingridge, 1993), and they can be induced in rodents and humans (Cooke and Bliss, 2006). Both LTP and LTD are activity-dependent modulation of synaptic transmission between the pre and post-synapses (Abraham et al., 2019), and they are characterized by several factors such as changes in neurotransmitter release probability and alterations in postsynaptic receptors (Collingridge et al., 2010). In the mammalian brain, three glutamate-gated ion channels localized at the post-synapse are the  $\alpha$ -amino-3-hydroxy-5-methyl-4-isoxazolepropionic acid receptor (AMPA), the N-methyl-D-aspartate receptor (NMDAR) and kainate receptors (Blanke and VanDongen, 2009). These receptors are anchored in the post-synaptic membrane by the scaffold post-synaptic density protein with a molecular weight of 95 kDa, hence the name PSD-95 (Blanke and VanDongen, 2009; Sheng, 2001). NMDAR and AMPAR are known to induce the formation, maintenance, and maturation of dendritic spines, especially of excitatory synapses, and also influence synaptic remodeling via calcium-dependent modifications of filamentous actin (F-actin) (Malenka and Bear, 2004; Tian et al., 2007).

AMPA is a tetrameric ion channel formed in the ER with four subunits, namely GluA1-4, which regulate the conductance and gating properties of the channel (Greger et al., 2007). Functionally, AMPARs facilitate the fast excitatory transmission and depolarization of the post-synapse during synaptic transmission (Greger et al., 2007). Comparatively, NMDARs are also heterotetrameric as AMPARs, but they can bind to glutamate and glycine/D-serine. NMDAR subunits include one GluN1, four GluN2 (GluN2A, GluN2B, GluN2C, GluN2D) and two GluN3 (GluN3A and GluN3B) subunit genes (Paoletti et al., 2013a). All NMDARs are composed of 2 GluN1 in combination with either GluN2 and GluN3 (Traynelis et al., 2010). Interestingly, NMDARs conduction of cations is voltage-dependent even after binding to glutamate, the reason being, specific sites on the receptor are usually bound to extracellular magnesium ( $Mg^{2+}$ ) and zinc ( $Zn^{2+}$ ) at resting membrane potential, blocking the ion pore (Hatton and Paoletti, 2005; Mayer, 2005) **(Figure 1.7)**.

However, following the depolarization of post-synapse by AMPAR conductance,  $Mg^{2+}$  and  $Zn^{2+}$  are removed and repelled from the pore, therefore, allowing the influx of both  $Na^{+}$  and  $Ca^{2+}$  ions into dendritic spines whereas potassium goes the opposite direction (Malenka and Bear, 2004). The sharp rise in intracellular  $Ca^{2+}$  activates  $Ca^{2+}$ /Calmodulin-dependent protein kinase (CaMKII), which represents the

important step in the induction of LTP. Progression of LTP involves stabilization of changes at dendritic spines as a result of LTP expression, which includes the enlargement of dendritic spines and recruitment of extra AMPAR. The trafficking of AMPAR at synapses relies on phosphorylation of the GluR1 subunit which is catalyzed by activated CaMKII (Malenka and Bear, 2004). This stage of LTP, termed the LTP maintenance, involves protein synthesis and gene transcription, and eventually the polymerization of F-actin to stabilize the new spine shape and anchoring of trafficked AMPAR via PSD-95 (Tian et al., 2007). This is one of the major molecular signatures for memory formation as well as memory consolidation. With LTD, the gradual and prolonged increase in the intracellular  $\text{Ca}^{2+}$  via NMDAR induces LTD also known as the NMDAR-dependent LTD (NMDAR-LTD) (Mango et al., 2019; Neveu and Zucker, 1996). It is essential for some learning properties, especially with the novelty exploration in hippocampal CA1 of mice (Dong et al., 2012; Manahan-Vaughan and Braunewell, 1999). Additionally,  $\text{Ca}^{2+}$ -permeable AMPAR can induce LTD as observed in some hippocampal CA3 interneurons (Laezza et al., 1999). Generally, LTD occurs when the slow rise in  $\text{Ca}^{2+}$  sensed by Calmodulin (CaM) activates protein phosphatase 1 (PP1) which dephosphorylates GluR1 of AMPAR and PSD-95 (Collingridge et al., 2010). This results in the lateral diffusion of AMPAR from the synaptic cleft to the extra-synaptic zone for endocytosis (**Figure 1.7**).

The removal of CSPGs by chABC and knockout of TNR reduced LTP in CA1 of hippocampal slices (Saghatelian et al., 2000; Bukalo et al., 2001; Senkov et al., 2014) whilst the degradation of HA with hyaluronidase impaired LTP and affected the retention of contextual fear memory in the hippocampus (Kochlamazashvili et al., 2010a). Furthermore, the removal of PNN with chABC impairs memory consolidation and reconsolidation whereas upregulation of the PNN component, HAPLN1, maintains or enhances both recent and remote memory stabilization (Shi et al., 2019). An interesting study demonstrated an improvement in the long-term recognition memory coupled with the altered synaptic transmission in the perirhinal cortex of HAPLN1 KO mice. From this study, they also show that recognition memory is dependent on LTD which was enhanced in HAPLN1 KO mice, and similar memory results were produced using chABC, although, the effect diminished over time due to PNN recovery (Romberg et al., 2013). Interestingly, deletion of the CSPG lectican, BCAN, in the hippocampus influenced the expression of other CSPGs, e.g. reduced NCAN expression along with impaired LTP, however, no overall defects in learning and memory were reported (Ogawa et al., 2001). These data suggest the varying effect of CSPG core proteins and the GAG chains on synaptic plasticity and learning and memory.

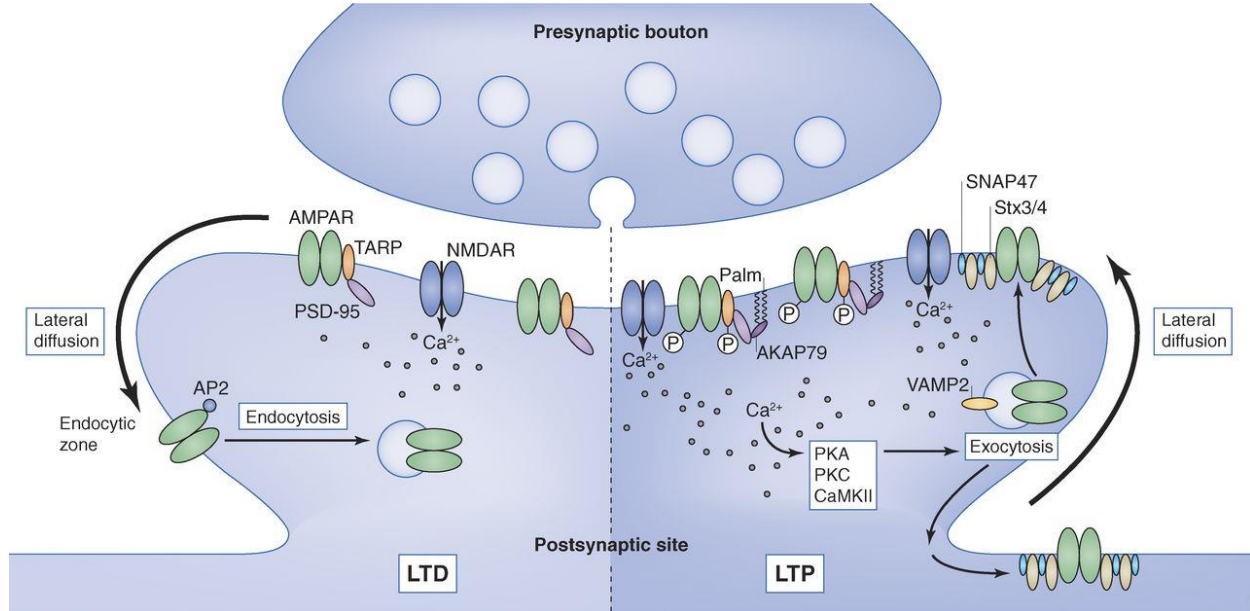


**Figure 1.7 Synaptic changes during LTD and LTP**

Molecular organization of synapses during synaptic plasticity, i.e. LTD and LTP. With LTP, activation of NMDAR results in a rapid influx of  $\text{Ca}^{2+}$  activating several kinases such as PKA, PKC and CaMKII. These kinases phosphorylate GluA1 subunits of AMPAR facilitating lateral diffusion of AMPAR from extrasynaptic sites to synaptic domains. Contrarily, during LTD  $\text{Ca}^{2+}$  increase is gradual and this activates phosphatases that dephosphorylate GluA1 subunits causing endocytosis of AMPAR at synapses (Vitureira and Goda, 2013).

In the adult brain, there is increased inflammation and tissue damage which CSPGs are known to be vital to these processes. Following an injury, activation of astrocytes by factors like interleukin-6 (IL-6) and transforming growth factor (TGF) released from microglia is the first event to occur (Jang et al., 2020), and upon arrival to injury sites they secrete more inflammatory cytokines like tumor necrosis factor- $\alpha$  (TNF- $\alpha$ ) and IL1beta (Pekny et al., 2014; Santos-Galindo et al., 2011), and CSPGs around the injury site (Pendleton et al., 2013a). CSPGs at this region form a barrier termed glia scar, that prevents axonal growth or regeneration, impairs the repair of demyelinated fibers, and results in the death and dysfunction of oligodendrocytes (Pendleton et al., 2013a; Silver and Miller, 2004). In multiple sclerosis (MS), for example, remyelination of injured neurons is impaired due to the suppression of OPCs migration (Keough et al., 2016) along with reduced maturation (Back et al., 2005). Studies have related OPC's suppression with the

myelin-associated inhibitors and ECM (Keough et al., 2016). Removal of CSPGs with chABC or inhibition of CSPGs synthesis restores myelination, indicating an inhibitory role played by glycan chains as well as their sulfation (Keough et al., 2016; Zhai et al., 2021). Furthermore, the relationship between neural ECM and inflammation is extensively studied at the moment.

#### 1.1.4 CSPG biosynthesis and glycosylation

The amount of ECM at any time point during the development of the mammalian brain depends on the balance between synthesis and degradation. Almost 90% of brain ECM proteins are glycosylated, which is necessary for their molecular recognition functions in cell adhesion and differentiation (Li and Wang, 2016). The formation of ECM CSPGs follows the sequence of: **1.** the initial synthesis of the core proteins **2.** translocation to the endoplasmic reticulum (ER) and Golgi apparatus for glycosylation, which includes GAG initiation, elongation and sulfation, and **3.** CSPG secretion. Glycosylation, an enzyme-catalyzed post-translational modification, involves the covalent attachment of a carbohydrate donor to the functional group of CSPG core protein to give rise to a glycoconjugate (Dalziel et al., 2014). Here, the enzyme xylosyltransferase that initiates glycosylation is encoded by the xylosyltransferase 1 & 2 (XYLT1 and 2) genes. These genes are differentially expressed in tissues with XYLT1 mostly expressed and localized in the ER of neuronal and glial cells (Luderman et al., 2017). At the ER, XylT1 transfers the monosaccharide, xylose, from UDP-xylose to the serine residue of CSPG core protein through the following recognition sites (G-S-G or G-S-X-G) (Kimata et al., 2007; Luderman et al., 2017; Olson and Esko, 2004). After this step, the developing CSPG molecule is transferred to the Golgi apparatus for further GAG synthesis (Dalziel et al., 2014) (**Figure 1.8**).

At the Golgi apparatus, two galactose (Gal) residues and one glucuronic acid (GlcA) residue are sequentially added to the CSPG core protein and xylose-complex to give rise to the tetrasaccharide linkage region, GlcA- $\beta$ -1,3--Gal- $\beta$ -1,3--Gal- $\beta$ -1,4--Xyl- $\beta$ -O-Ser, also called the GAG-protein linkage region (Li and Wang, 2016; Mikami and Kitagawa, 2013a; Noti and Seeberger, 2005). These reactions are catalyzed by their appropriate glycosyltransferases including XylT1, GalT-1( $\beta$ 1,4-galactosyltransferase 1), GalT-2( $\beta$ 1,3-galactosyltransferase 2, and dGlcAT-1 ( $\beta$ 1,3-glucuronyltransferase 1)(Bai et al., 2001, 1999; Kitagawa et al., 1998; Wei et al., 1999). Then, the GAG-protein linkage region is further modified through sulfation of the Gal residues together with the phosphorylation of the xylose (Olson and Esko, 2013, 2004), after which the GAG chains are synthesized.

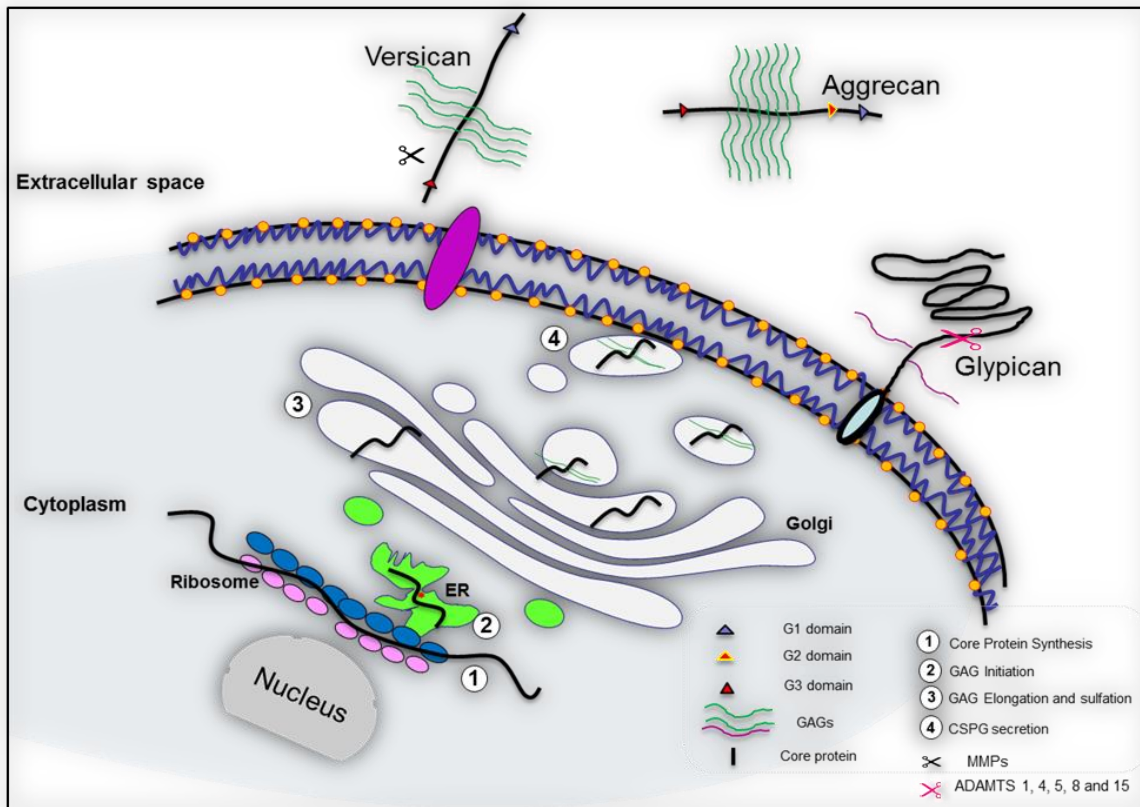


**Figure 1.8 Biosynthesis and function of chondroitin sulfate**

CSPGs synthesis follows a sequence of four events including the core protein synthesis, GAG initiation in the ER, and then the GAG elongation and sulfation, which take place in the Golgi apparatus and, finally, secretion. Once secreted, CSPGs can either diffuse or be membrane-bound.

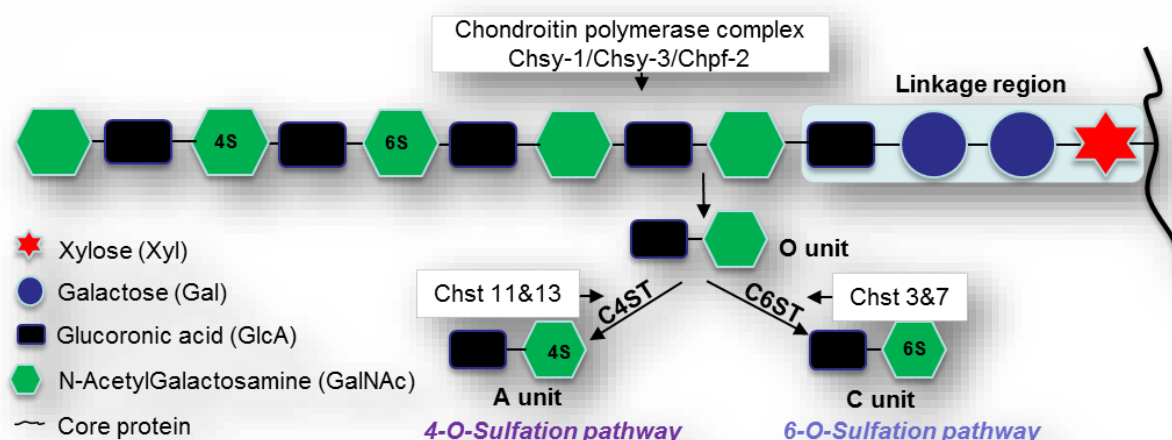


**Figure 1.9 Glycosylation and sulfation of CSPGs**

The CSPG-GAGs are catalyzed by the chondroitin polymerase complex that includes Chsy-1, Chsy-3 and Chpf-2. This complex can only synthesize the GAGs once the linkage region is formed, which depends on the initial association of xylose to the core protein. The GAGs of CSPGs are modified via sulfation of the 4<sup>th</sup> and 6<sup>th</sup> carbon of disaccharide units catalyzed by the C4ST and C6ST enzymes respectively.

Surprisingly, recent findings suggest that the said modification of the GAG-protein linkage region, especially the phosphorylation of xylose, regulates the synthesis and turnover of CSPGs and HSPGs (Wen et al., 2014). One study demonstrated that overexpressing the Golgi secretory kinase, FAM20B, which phosphorylates xylose, increased the expression of CSPGs and HSPGs but this effect was lost when FAM20B was downregulated (Koike et al., 2009). A truncated GAG-protein linkage region that could not initiate as well as elongate GAG chains was also observed in FAM20 knockout cells (Wen et al., 2014). This, therefore, indicates that the phosphorylation of xylose is essential for the maturation of the linkage region, which eventually, makes it a good acceptor and stimulator of the initiation stage of GAG chain synthesis (Koike et al., 2014; Mikami and Kitagawa, 2013a; Wen et al., 2014). Although, GAG biosynthesis depends on the formation and modification of the GAG-protein linkage region which serves as the primer for either CSPGs or HSPGs synthesis, however, this process also relies on the exact type of the initial sugar residue covalently added to this region (Wei et al., 1999). For CSPGs, the addition of the amino sugar unit, N-Acetyl-D-galactosamine (GalNAc $\beta$ 1-4), to the linkage region (Gotoh et al., 2002; Li and Wang, 2016) by the GalNAc transferase family (GalNAcT) also known as the chondroitin GalNAc transferase (ChGn) (Uyama et al., 2003), initiates GAG synthesis. The ChGn-1 (GalNAcT-I) and the ChGn-2 (GalNAcT-II)

make up the GalNAc transferase family and both catalyze the initiation of CSPG GAG chains, and recent studies show that they can also regulate chain length and number (Uyama et al., 2003) (**Figure 1.9**).

After GAG chain initiation, the assembly of the GAG-protein linkage region and GalNAc $\beta$ 1-4 is elongated through the sequential and alternate addition of the uronic acid, D-Glucuronic acid (GlcA $\beta$ 1-3) and GalNAc $\beta$ 1-4 units to form the repeating disaccharide units. This reaction is catalyzed by the GalNAc transferase family together with the chondroitin synthase family also known as the chondroitin polymerase complex (Olson & Esko, 2004), and all these enzymes are localized in the Golgi apparatus. The chondroitin polymerase complex comprises the chondroitin polymerizing factor 2 (ChPf2), chondroitin sulfate synthases 1 (ChSy 1) and chondroitin sulfate synthase 3 (ChSy3), as all possess dual glycosyltransferase activities, and that is both GalNAcT-II and GlcAT-II activities (Izumikawa et al., 2008; Sato et al., 2003). However, the individual components of the chondroitin polymerase complex cannot polymerize GAG chains on their own except in combinations, and this eventually contributes to the variable chain length observed in the various CSPGs (Izumikawa et al., 2008; Kitagawa et al., 2003). Together, they elongate GAG chains that are subsequently modified through sulfation to give rise to a matured CSPG (Mikami and Kitagawa, 2013a). In the end, matured CSPGs are either secreted into the extracellular space or membrane-bound (**Figure 1.8 and 1.9**).

#### *1.1.5 Sulfation of chondroitin sulfates in developing and adult brain*

The sulfation of CSPG GAGs is necessary for their maturation and function. This is tightly controlled by various carbohydrate sulfotransferases such as the carbohydrate sulfotransferase 3 (Chst3), carbohydrate sulfotransferase 7 (Chst7), carbohydrate sulfotransferase 11 (Chst11), and carbohydrate sulfotransferase 13 (Chst13). These sulfotransferases are also known as chondroitin 6-O-sulfotransferase 1 (C6ST1), chondroitin 6-O-sulfotransferase 2 (C6ST2), chondroitin 4-O-sulfotransferase 1 (C4ST1) and chondroitin 4-O-sulfotransferase 3 (C4ST3), respectively. The sulfation reaction involves the addition of a sulfate group from the universal sulfate donor, 3'-phosphoadenosine 5'-phosphosulfate (PAPS), to various positions on the universal disaccharide acceptor, the O unit (GlcA $\beta$ 1-3 and GalNAc $\beta$ 1-4) (Mikami and Kitagawa, 2013a). Additionally, the reaction varies in several pathways including the 2-O-sulfation, 4-O-sulfation and the 6-O-Sulfation pathways. With the 6-O-sulfation pathway, both Chst3 (C6ST1) and Chst7 (C6ST2) catalyze the addition of a sulfate group at the C-6 position (C6S) of GalNAc residues. On the other hand, the addition of the sulfate group at the C-4 position (C4S) of GalNAc, catalyzed by Chst11 (C4ST1) and Chst13 (C4ST3), comprises the 4-O-sulfation pathway. The enzyme uranyl 2-O-sulfotransferase (UST)

catalyzes the 2-O-sulfation of the GluA residues (Mikami and Kitagawa, 2013a; Miyata and Kitagawa, 2017). Overall, diverse disaccharide units of CSPGs namely; O, A, C, D and E are formed due to variation in sulfation patterns. The O unit (GlcA and GalNAc) is the non-sulfated disaccharide whereas the monosulfated are A (GlcA and GalNAc [C4S]) and C units (GlcA and GalNAc [C6S]), and the disulfated are D (GlcA [C2S] and GalNAc [C6S]) and E units (GlcA and GalNAc [C4S & C6S])(Mikami and Kitagawa, 2013a) (**Figure 1.10**).

Different sulfation patterns influence brain development and have distinct functions. For instance, in the developing brain, most CSPGs are 6-O-sulfated and they enhance migration, differentiation and myelination of neurons. CSPGs quantification studies over the years have observed upregulation of the 6-sulfating catalases compared to 4-O-sulfation (Mikami and Kitagawa, 2013a; Sugahara et al., 2003) during early brain development. On the flip side, in the adult brain the ratio of 6 to 4-O-sulfated CSPGs shift to 4-O-sulfation, which influences the length of GAG chains, as shown in a loss of function study that C4ST1 (Chst11) elongates GAG chains (Uyama et al., 2006). Furthermore, sulfated CSPGs have been associated with the inhibition or enhancement of neural regeneration after injury, suggesting a potential role for CSPGs-GAGs in proliferation, migration and differentiation (Lin et al., 2011; H. Wang et al., 2008). Additionally, overexpressing C6ST-1 delays the termination of the critical period possible due to reduced ACAN expression which is a major component for PNN formation (Shinji Miyata and Kitagawa, 2016). Although CSPGs are inhibitory to axonal regeneration during injury, upregulation of 6-O-sulfation positively influences axonal regeneration, as glia scar predominantly 4-O-sulfated (Miyata and Kitagawa, 2017). This means 4-O-sulfation inhibits whereas 6-O-sulfation enhances axonal growth (Lin et al., 2011; H. Wang et al., 2008). This explains why 6-sulfated, and both 6- and 4- sulfated CSPGs GAGs are predominant in the embryonic brain (Carulli et al., 2010; Lin et al., 2011). Furthermore, sulfation patterns of CSPGs are pivotal for synaptic plasticity and memory retention (Yang et al., 2021). In this study, the authors showed that lack of chondroitin 6-sulfotransferase (Chst3) resulted in a loss of memory in 11-18 month-old mice. They also showed that overexpressing Chst3 rescued the cognitive and LTP impairments observed in aged mice (Yang et al., 2021).

In humans, mutations as well as post-transcriptional regulation of the *Chst3* gene have been implicated in defects like the spondyloepiphyseal dysplasia (Srivastava et al., 2017) and the lumbar disc degeneration (LDD) (Song et al., 2013), respectively. Interestingly, mutation of arginine to glutamine (R304Q) at the PAPs binding site of a recombinant CHST3 completely impairs sulfation activity, which correlates with

reduced sulfated CSPG in urine of patients with spondyloepiphyseal dysplasia (Thiele et al., 2004). This indicates that 6-O-sulfation is also essential for CNS development in humans.

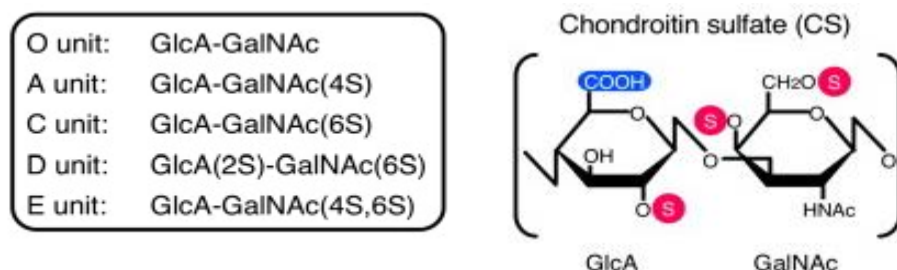


**Figure 1.10 Disaccharide units found in Chondroitin sulfates proteoglycans (CSPGs)**

CSPGs consist of GlcA and GalNAc residues that are sulfated at the 4<sup>th</sup> or 6<sup>th</sup> carbon on GalNAc residues to give rise to the A and C units respectively. In addition, sulfation of the 2<sup>nd</sup> carbon of GlcA and 6<sup>th</sup> carbon of GalNAc residues give rise to the D-unit and the E-unit when both the 4<sup>th</sup> and 6<sup>th</sup> carbon of GalNAc residues are sulfated (modified from (Mikami and Kitagawa, 2013a)).

## 1.2 Proteolytic remodeling of ECM in the brain

Within the microenvironment of cells during development, the synthesis, modification, secretion and degradation or remodeling of ECM requires an intricate balance between ECM production and remodeling, which is termed as ECM homeostasis (turnover) (Cox and Erler, 2011). Dysregulation of this balance at any point in time can result in structural (developmental) or physiological abnormalities that constitute pathological conditions. For instance, the physiological cleavage of ECM facilitates cell migration that is prevented under insufficient degradation conditions whereas uncontrolled cleavage inhibits cell-matrix interactions, and this is a major cause of some connective tissue pathologies (Chakraborti et al., 2003). In addition, accumulation of ECM due to impaired remodeling or degradation can result in fibrotic tissues or organs like seen in lungs during multiple sclerosis (Gagliano, 2019). Other conditions like cancer and cardiovascular disorders have been associated with altered ECM remodeling (Brinckerhoff and Matrisian, 2002). Studies show that remodeling enzymes are expressed throughout development and maturation of tissues and organs at varying degrees, to regulate CSPGs turnover at any level of organization. As during tissue and organ formation in vertebrates it is imperative to have a well-controlled dynamism of CSPGs,

this is, therefore, orchestrated by matrix-degrading enzymes such as the matrix metalloproteinase (MMPs), cathepsins and a disintegrin and metalloproteinase with thrombospondin motifs (ADAMTS).

### 1.2.1 *Matrix metalloproteinase (MMPs)*

Matrix metalloproteinases (MMPs), also known as matrixins are calcium-dependent, zinc-containing endopeptidases that belong to the metzincin superfamily. MMPs are one class of the major matrix-degrading enzymes expressed in several organs and tissues in vertebrates and thus essential for ECM remodeling during development. MMPs cleave various ECM such as collagens, elastin, gelatins, glycoprotein and proteoglycans (Verma and Hansch, 2007). The physiological expression of MMPs has been associated with several processes like angiogenesis, inflammation, neurogenesis and wound healing (Verma and Hansch, 2007), as its expression is regulated by the endogenous inhibitors, the tissue inhibitors of metalloproteinases (TIMPs) and  $\alpha$ 2-macroglobulins (Aranapakam et al., 2003). Therefore, activation of MMP proenzymes (zymogens) by other MMPs or enzymes (Nagase et al., 2006), along with posttranslational modifications (Chakraborti et al., 2003) also regulates their activities. The regulation of MMPs is critical to maintaining a balance in ECM turnover throughout the life of an organism as altered expression of MMPs and TIMPs have been associated with several development aberrations as well as pathological processes (Chakraborti et al., 2003; Verslegers et al., 2013). For example, the overexpression of MMPs coupled to downregulation of TIMPs is implicated in pathologies such as arthritis, multiple sclerosis as well as tumor formation and progression (Grobewska et al., 2012; Herszényi et al., 2012). On the other hand, reduced MMP expression results in excess accumulation of ECM as seen in the formation of cleft palate in organisms lacking specific collagen cleaving MMPs resulting in limited collagenolytic activity (Shi et al., 2008). In addition, MMP inhibition or loss of function studies show that impaired embryogenesis is a result of disrupted cell proliferation and migration due to reduced ECM remodeling (Brauer, 2006; Ries et al., 2007; Vu & Werb, 2000).

In vertebrates, various MMPs of varying substrates preference and composition are produced by several structural cell types including endothelial and epithelial cells, and by inflammatory cells like macrophages and neutrophils (Shin et al., 2007). Once formed and secreted, MMPs attach to cell membranes and this enhances their interaction to respective substrates (Chakraborti et al., 2003). The general composition of MMPs consists of 4 domains namely the N-terminal pro-domain which includes the signal and pro-peptides, followed by the catalytic (CAT) region, the hinge region (linker 1) and four hemopexin-like (HPX) domains (carboxylic-terminal domain) (Brauer et al., 2011), whereas membrane-bound MMPs (MT-MMPs) have

an additional transmembrane and cytoplasmic domains after another linker region (linker 2)(Cerofolini et al., 2016). Some domains offer unique functions like observed in the hemopexin-like domain of MMP-2 where it facilitates cell surface activation of pro-MMP-2 by the MT1-MMP (Strongin et al., 1995). About 13 MMPs upon secretion are processed with the help of the signal peptide serving as bait due to its susceptibility to proteolysis releasing the pro-MMPs for further processing (Nagase et al., 2006). The pro-MMPs are subsequently cleaved by other active MMPs. Interestingly, about 10 MMPs have a furin-like pro-peptide region that is cleaved intracellularly before being secreted as inactive pro-MMPs (Nagase et al., 2006). Overall, thus far, in vertebrates more than 25 MMPs with different substrate specificities have been described (Löffek et al., 2011) including 24 found in humans. MMPs are further categorized into 6 classes based on composition and function (as well as substrate specificities), and these classes are 4 collagenases, 2 gelatinases, 4 stromelysins, 2 matrilysins, 6 MT-MMPs and 8 other enzymes (Sternlicht and Werb, 2001) (**Figure 1.11 and Table 1.2**).

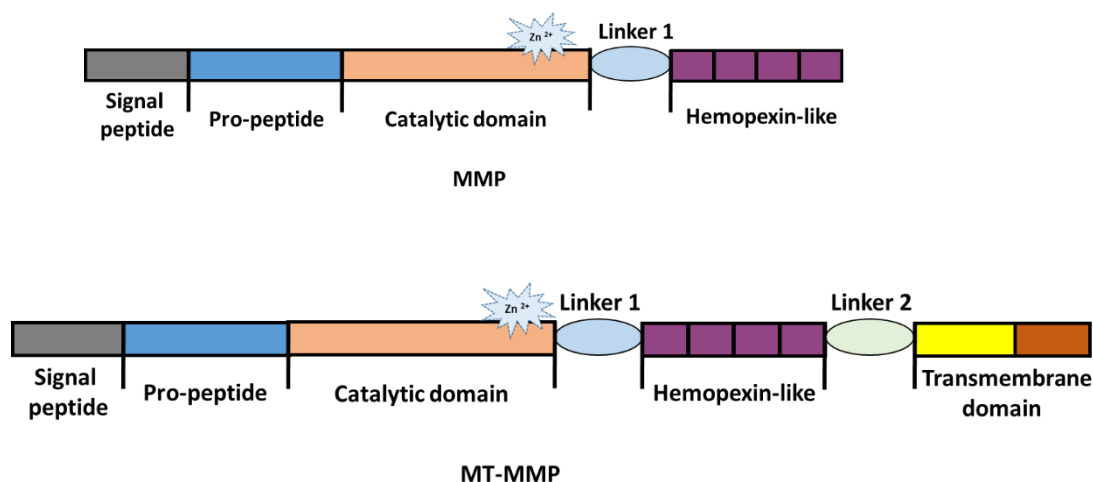


**Figure 1.11 Domain organization of secreted and membrane-bound MMPs**

MMPs have domain organization similar to ADAMTS which includes signal peptide, pro-peptide, a catalytic domain and the hemopexin-like domain. However, the membrane-bound MMPs have an additional transmembrane domain.

### 1.2.2 Matrix metalloproteinase-9 (MMP-9)

MMP-9 belongs to the gelatinase family of MMPs and it is also known as the gelatinase B that cleaves gelatin, collagens and elastin (Sindhu et al., 2016). Uniquely, MMP-9 contains 3 fibronectins type II repeats at the catalytic domain which defines its specificity to the said substrates (Steffensen et al., 1995; Verslegers et al., 2013), especially for gelatin/collagen. MMP-9 is initially synthesized as a pre-proenzyme of 707 amino acid sequence which is then processed and secreted as a stable 92kDa inactive pro-MMP-9. The secreted inactive pro-MMP-9 attaches to the cell surface by binding to CD44 (Yu and Stamenkovic, 2000), and it is then activated by a protease cascade that includes plasmin and inactive MMP-3 (Stromelysin-1). Activation of MMP-9 involves the initial activation of pro-MMP-3 by plasmin, making active MMP-3 a potent activator of MMP-9. The activated MMP-3 then functions by removing the pro-peptide off pro-MMP-9 to produce 82-kDa active MMP-9 that contains two  $Zn^{2+}$  and three  $Ca^{2+}$  at the catalytic domain (Ramos-DeSimone et al., 1999). The presence of these ions at the catalytic domain confers stability and is necessary for MMP-9 activity (Nagase and Woessner, 1999). Studies indicate that the expression of MMP-9 and other MMPs are inducible and are produced from several cell types or tissues in both developmental or adult stages. MMP-9 expression is induced by certain growth factors, like epidermal growth factor as seen in human breast cancer cells (Kondapaka et al., 1997) facilitating tumor progression (invasion and metastasis) (Himmelstein et al., 1994; Itoh et al., 1999). Additionally, cytokines such as TNF- $\alpha$  and IL1beta from cancer cells (Unemori et al., 1991), and from cultured rat astrocytes (Gottschall and Yu, 1995; Spiegel et al., 1996), together with hormones and cell-matrix interactions induce MMP-9 expression. Also, other chemical agents such as lipopolysaccharides (LPS) or tumor progressing agents like phorbol esters influence MMP-9 expression (Lee et al., 2003).

In the developing brain of mice, several MMPs are expressed such as MMP-2 but MMP-9 is highly upregulated at early postnatal stages which later decreases (Verslegers et al., 2013). In the CNS, astrocytes synthesize MMP-2 whereas MMP-9 is expressed in neuronal dendrites (Tian et al., 2007). Interestingly, MMP-9 expression is highly increased parallel to cellular proliferation (neurogenesis) and migration during brain development. This is observed in rat cortical neural stem cells (NSCs) (Beurden and Hoff, 2018; Ingraham et al., 2011), and in neuronal differentiation (Higgins et al., 2009). Furthermore, a study by Vaillant and colleagues, demonstrated by *in vitro* experiments that MMP-9 is critical for postnatal brain development specifically with migration and axonal outgrowth of cerebellar granule explant cells. From their study, MMP-9 deficiency in mice delayed migration of granular precursors cells and apoptosis (Vaillant et al., 2003), which indicates that MMP-9 plays a role in cerebellar morphogenesis (Ayoub et al.,

2005). The interactions between CAMs and ECM molecules are involved in forming and modifying synapses like observed for NCAMs (Dityatev et al., 2004) during early synaptogenesis, as well as for reelin and laminins (Tian et al., 2007). Another CAM, the intercellular adhesion molecule-5 (ICAM-5), which is expressed in dendritic spines of excitatory neurons during postnatal development (Mitsui et al., 2005; Yoshihara et al., 1994), has been found to function in the formation and stabilization of dendrites, however, this is dependent on MMP-9 activity (Tian et al., 2007). Here, the association of intercellular adhesion molecule-5 with actin filaments favors dendrite formation and synaptogenesis by inhibiting its cleavage by MMP-9. Neuronal apoptosis is also known to be one of the essential processes for brain development as well as maturation. Hence, a study by Murase and McKay in 2012 advocated the involvement of MMP-9 in neuronal death. They show that deficiency or inhibition of MMP-9 enhances neuronal survival via laminin-integrin interaction (Murase and McKay, 2012), conferring neuroprotection (**Figure 12**).

Regarding the effect of MMP-9 on synaptic plasticity, several studies highlight the contribution of MMP-9 to synaptic ECM proteolysis along with trafficking and activation of glutamate receptors during synaptic transmission (Bozdagi et al., 2007; Verslegers et al., 2013). One study shows that the increase in MMP-9 proteolytic activity depends on the activation of NMDAR, and this is a physiological regulatory role of MMP-9 (Bozdagi et al., 2007). Another study shows that the late-phase of LTP (L-LTP) in CA1 along with memory retention depends on MMP-9 expression and activity (Nagy et al., 2006), indicating a function of MMP-9 on LTP maintenance. Other experiments have been carried out on the dentate gyrus and mossy fibers to CA3 projections, and all conclude that MMP-9 regulates LTP (Gawlak et al., 2009; Wang et al., 2008). However, no effect of MMP-9 on the LTP induction as well as LTD has been observed. In MMP-9 deficient mice, Nagy and colleagues demonstrate that MMP-9 function on synaptic physiology is via integrin receptors, and it also offers structural modification of synapses. Additionally, MMP-9 enhances synaptic plasticity through NMDARs surface diffusion which depends on integrin  $\beta 1$  signaling but not on ECM cleavage or AMPAR trafficking (Michaluk et al., 2009).

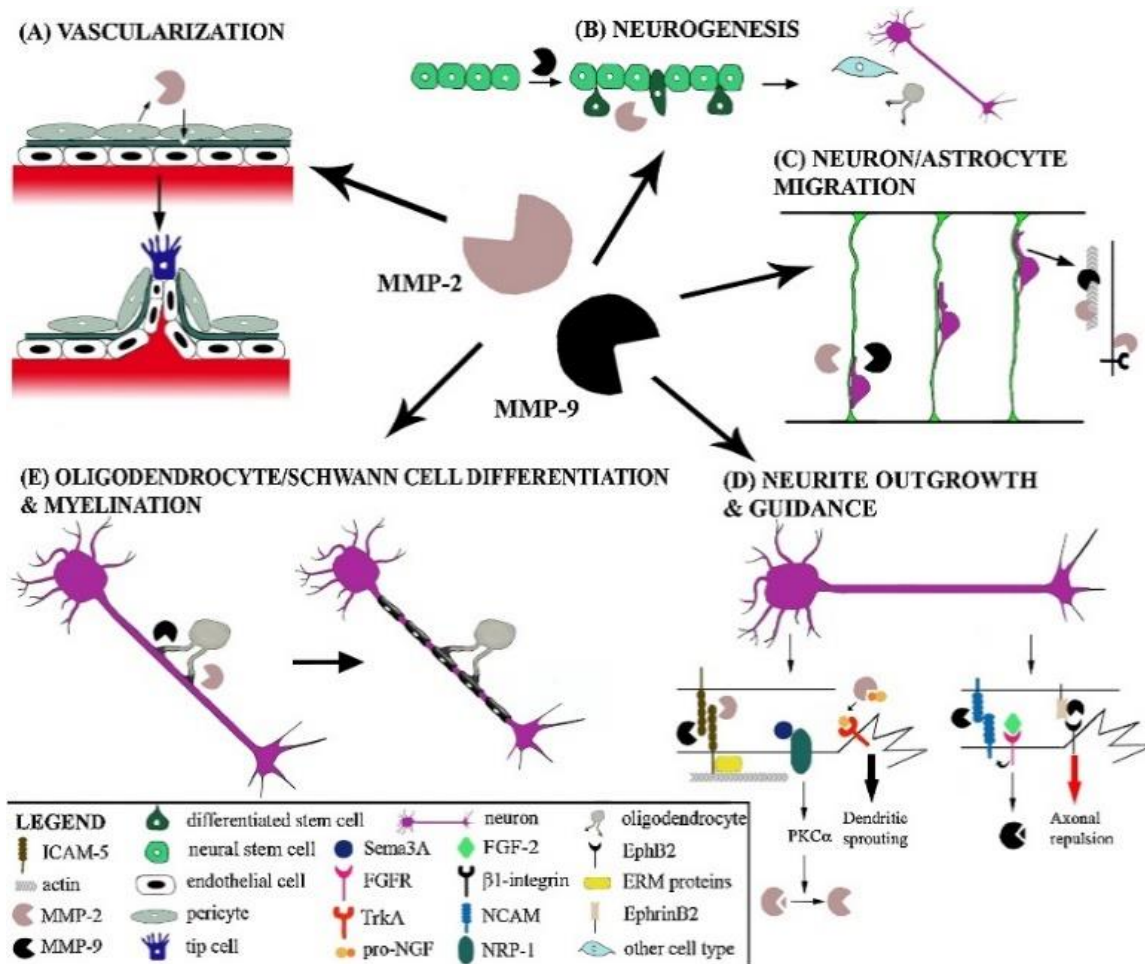


**Figure 1.12 Effect of MMP-2 and -9 in developing brain**

In the developing brain, both MMP-2 and -9 degradation of ECM influence processes such as vascularization, neurogenesis, neuron and astrocyte migration, axonal growth and guidance as well as myelination (Verslegers et al., 2013).

**Table 1.2. Classification of matrix metalloproteinase enzymes (adopted from (Beurden and Hoff, 2018)).**

No.	MMP No.	Class	Enzyme
1	MMP-1	Collagenases	Collagenase-1
2	MMP-8		Neutrophil collagenase
3	MMP-13		Collagenase-3
4	MMP-18		Collagenase-4
5	MMP-2	Gelatinases	Gelatinase-A
6	MMP-9		Gelatinases-B
7	MMP-3	Stromelysins	Stromelysin-1
8	MMP-10		Stromelysin-2
9	MMP-11		Stromelysin-3
10	MMP-27		Homology to stromelysin-2 (51.6%)
11	MMP-7	Matrilysins	Matrilysin
12	MMP-26		Matrilysin-2
13	MMP-14	MT-MMP (membrane type)	MT1-MMP
14	MMP-15		MT2-MMP
15	MMP-16		MT3-MMP
16	MMP-17		MT4-MMP
17	MMP-24		MT5-MMP
18	MMP-25		MT6-MMP
19	MMP-12	Other enzymes	Macrophage metalloelastase
20	MMP-19		RASI 1
21	MMP-20		Enamelysin
22	MMP-21		MMP identified on chromosome 1
23	MMP-22		MMP identified on chromosome 1
24	MMP-23		From human ovary cDNA
25	MMP-28		Epilysin
26	MMP-29		Unnamed

### 1.2.3 Cathepsins

Lysosomes sometimes referred to as “*lord of destruction*” are membrane-bound acidic degrading organelles that recycle proteins or macromolecules by resident hydrolytic enzymes, also known as lysosomal peptidases (Somiya, 2020). About 50 lysosomal peptidases are known thus far, and these peptidases require an acidic environment, usually around a pH of 5, for efficient protein degradation (Jakoš et al., 2019). Cathepsins are the main group of lysosomal peptidases, and they are a large family of enzymes that are ubiquitously expressed in humans and rodents (Wartmann et al., 2010). This includes 3 major classes of peptidases namely the aspartic, serine and cysteine peptidases. The aspartic peptidases are cathepsins D and E, whereas cathepsins A and G are serine peptidases and the papain-like thiol proteases form the cysteine peptidases group. Eleven (11) members of the cysteine peptidases are observed in humans, namely; cathepsins B, C, F, H, K, L, O, S, V, W and X (Turk et al., 2012), meanwhile, mice lack the cathepsins V and have 8 additional cathepsins (Mason, 2008). Interestingly, cysteine cathepsins are highly expressed in endosomes and lysosomes as they have some extra-lysosomal function including cytosol, cell membrane and extracellular space proteolytic activity (Rossi et al., 2004; Turk et al., 2012; Verma et al., 2016). Such proteolytic functions are essential for lysosomal-dependent processes like antigen presentation, cell death and metabolism, and maintaining steady protein turnover (Turk et al., 2012) (**Figure 1.13**).

To prevent unnecessary activity-dependent degradation of proteins as well as developmental aberrations, cathepsins are usually produced in an inactive form, which includes the signal peptide followed by the pro-domain and the heavy and light chain domains (Cheng et al., 2012). Interestingly, differences in the length and sequence composition of the pro-domain constitute the various groups of cysteine peptidases (Brömme and Wilson, 2011), namely the endopeptidases, exopeptidases and the unknown groups *as shown in the figure below*. Proenzyme cathepsins once synthesized are initially localized to the ER with the help of the signal peptide. In the ER, the signal peptide is removed, and the remaining cathepsin residue is glycosylated, followed by phosphorylation in the Golgi apparatus. From the Golgi apparatus, the inactive cathepsins are translocated to early endosomes in an acidic environment where the pro-domain are removed resulting in the active cathepsin (Cheng et al., 2012). Pro-cathepsin activation can be done by other proteases as well as other cathepsins as observed with cathepsin D and papain-like cysteine proteases activating cathepsins-B, S and K (Brömme et al., 2004; Turk et al., 2000). Although, activation of cathepsins through the removal of pro-domain can be done by other cathepsins (Olson & Joyce, 2015), however, this can also occur through auto-activation. For example, auto-activation of the pro-cathepsin-B is seen to be accelerated by ECM,

especially the CSPG GAGs (Caglič et al., 2007). Once activated, cathepsins are either localized in endosomes or lysosomes as well as secreted into the extracellular space.

#### 1.2.4 Cathepsins and CNS

In the CNS, cysteine cathepsins are secreted by microglia (Lively and Schlichter, 2013), astrocyte and neurons, and are known to function in normal and diseased brain. For instance, neurological hallmarks like gliosis (reactive change in glial cells) along with reduced motor functions are observed in cathepsin-F deficient aged mice (Tang et al., 2006). As cysteine cathepsins function both intracellularly and extracellularly, they are, therefore, essential for ECM degradation, which is one of the major relationships between cathepsin activity and cancer invasion (Sevenich and Joyce, 2014). Regarding ECM degradation, cysteine cathepsins are secreted to degrade ECM in the extracellular space whilst endocytosed-ECM are degraded by endosome or lysosome localized-cathepsins (Brömme and Wilson, 2011). Within the extracellular space, the degradation of ECM by secreted cysteine cathepsins is prevented at neutral or higher pH due to their stability once bound to CSPG GAGs (Song et al., 2000). Cathepsin-B and other cysteine cathepsins like cathepsin-L cleave ECM proteins like fibronectin (Buck et al., 1992; Taleb et al., 2006), in addition, cathepsin-S cleaves laminin (Buck et al., 1992; Ishidoh and Kominami, 1995; Lah et al., 1989) and nidogen-1, a component of the basement membrane of tissues in CNS (Sage et al., 2012). Moreover, lecticans like ACAN and human link proteins are cleaved by cathepsins-K, L, S and B (Hou et al., 2003; Nguyen et al., 1990).

Cathepsins' activities towards ECM are mostly during pathological conditions relative to MMPs that function during development. For instance, *in vivo* studies show that cathepsin-B and Tenascin-C are upregulated in gliomas, specifically in astrocytoma and glioblastomas, whereas *in vitro* experiments show that Tenascin-C is cleaved by cathepsin-B (Lu et al., 2011). However, other studies have implicated cysteine cathepsins in brain development and maturation. For instance, the expression and activity of cathepsins, especially cathepsin-B, promotes axonal outgrowth by removing the inhibitory effect of CSPGs (Tran et al., 2018; Tran & Silver, 2021), such as ACAN (Rodríguez-Manzaneque et al., 2015) as well as axonal regeneration (Tran et al., 2018b). Cathepsin expression and activity are strictly regulated, otherwise, may result in CNS pathologies like neuroinflammation and Alzheimer's disease (Butler et al., 2011). In rats, 7 days after spinal cord injury, excessive cathepsin-D and B are secreted by microglia and invading macrophages to the injury site (Moon et al., 2008; Tran and Silver, 2021) which degrades ECM. Cathepsin-S, known to cleave ECM, is also upregulated in activated microglia at injury sites (Tran and Silver, 2021).

Amyloid precursor protein (APP) as well as amyloid- $\beta$  peptides (A $\beta$ ) are cleaved by cathepsins (Cermak et al., 2016), and studies by Embury and Fabrizio show that cathepsin-B activity enhances learning and memory in demented mice (Embury et al., 2017; Farizatto et al., 2017), whereas lack of cathepsin-B increases amyloid- $\beta$  load (Cermak et al., 2016). Surprisingly, inhibition of cathepsin-B and L decreases the formation and accumulation of Amyloid- $\beta$  oligomers (Butler et al., 2011; Zheng et al., 2012). Cathepsins also play role in synaptic plasticity, for example, cathepsin-B is secreted from lysosomes after calcium influx during neuronal transmission, and activates MMP-9 which subsequently digests (remodels) CSPGs (Ibata et al., 2019; Padamsey et al., 2017). Findings from Padamsey and colleagues suggest that inhibition of cathepsin-B secretion modifies structural and functional properties of dendritic spines. Additionally, cathepsin-S and L influence neuronal plasticity by eliminating spine and synapse densities through actin remodeling (Graber et al., 2004; Hayashi et al., 2013).

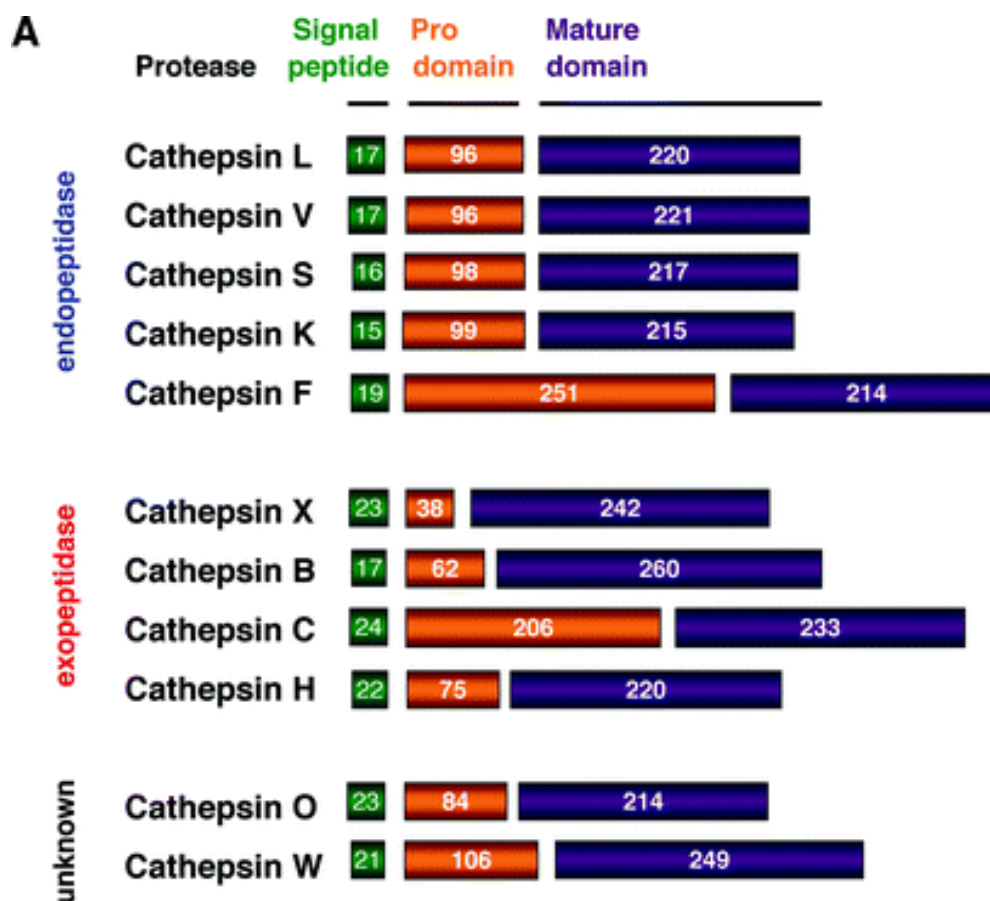


**Figure 1.13 Domain organization of cysteine cathepsins in humans**

The cysteine cathepsins have a similar domain organization as MMPs, which includes the signal peptide, the pro-domain and the mature domain. In humans, the cysteine cathepsins are divided into 3 subclasses

that are the endopeptidases (cathepsins L, V, S, K and F), exopeptidases (cathepsins X, B, C, and H) and unknown class including Cathepsins O and W (Brömme and Wilson, 2011).

### 1.2.5 ADAMTS family

Although ECM is regulated by proteases like MMPs and cathepsins, however, ADAMTS also have a major proteolytic effect on CSPGs, especially during tissue and organ formation. MMPs and ADAMTS belong to the metzincin protease family that has  $Zn^{2+}$  at their active sites (Gomis-Rüth, 2009). Unlike lysosomal cathepsins and MMPs, ADAMTS with their multiple thrombospondin 1-like repeats (TSR) (Nagase and Fushimi, 2008), lack a transmembrane domain (Porter et al., 2005), and therefore, they are generally secreted once synthesized and modified (Kelwick et al., 2015). In humans, about 19 ADAMTS have been studied and these are further classified into subclasses based on their substrate specificities. Seven are aggrecanases including the ADAMTS-1, 4, 5, 8, 9, 15 and 20, with ADAMTS-2, -3 and -14 belonging to the procollagen class, the cartilage degrading ADAMTS are ADAMTS-7 and -12, one von-Willebrand Factor proteinase ADAMTS-13, and, finally, the orphan enzymes which includes ADAMTS-6, 10, 16, 17, 18 and 19 (Kelwick et al., 2015) (**Figure 1.14**).

All ADAMTS have a similar structure which comes in two major domains, the peptidase and the ancillary domains (Lemarchant et al., 2013). The peptidase domain includes the signal peptide followed by the pro-domain, a metalloproteinase and finally the disintegrin-like domain. On the other hand, the ancillary domain that gives variability to ADAMTS includes one or more TSR motifs, a cysteine-rich domain and a spacer region (Kelwick et al., 2015; Nagase and Fushimi, 2008). ADAMTS, like in MMPs, are synthesized in a pre-pro-ADAMTS form and then secreted in a pro-ADAMTS format and then activated by MMPs and cathepsins in the extracellular space (Kelwick et al., 2015). Although the pro-domains of MMPs, cathepsins and ADAMTS function to regulate the folding and latency of these enzymes, however, with ADAMTS, they also have additional functions. The pro-domains of ADAMTS have conserved unique recognition sites localized between the pro-protein and metalloproteinase domains (Hatsuzawa et al., 1992; Molloy et al., 1992), and these sites are cleaved by furin or furin-like protein convertase (PPC) resulting in an intracellular activation of ADAMTS. For example, the activation of ADAMTS-1 by furin and MMPs yield two active forms; namely p87 and p65 (Rodriguez-Manzanique et al., 2000), with the former occurring inside the cell. In addition, pro-ADAMTS-4 with its 3 multiple furin-susceptible sites in its pro-domain is activated at the trans-Golgi (Wang et al., 2004), contrary to the extracellular activation of pro-ADAMTS-5 and the cell surface activation of pro-ADAMTS-9 (Koo et al., 2007, Longpré et al., 2009). The disintegrin-like domain

which is part of the metalloproteinase domain has been shown to function in determining the cleavage specificity of ADAMTS, as shown for ADAMTS-13 (de Groot et al., 2009)(**Figure 1.14**).

The ancillary domain, on the other hand, determines the association with, and specificities of ECM substrates. This is because all ADAMTS have at least one TSR with ADAMTS-9 and -20 having the largest number of TSRs (Kelwick et al., 2015). The TSR domain, especially in the vascular system, has been shown to have an anti-angiogenic function in ADAMTS-1 and -8, as well as non-enzymatic effects in other ADAMTS (Rodríguez-Manzaneque et al., 2015). Proteolytic modification of ancillary domains together with overall glycosylation of ADAMTS regulates the spatial and functional properties of ADAMTS. Like MMPs and cathepsins, ADAMTS expression and activities are regulated or inhibited by four TIMPs, namely TIMP-1, -2, -3 and -4 (Murphy, 2011), with TIMP-3 proving to be the most effective inhibitor of ADAMTS (Rodríguez-Manzaneque et al., 2002). TIMPS-1, -2 and -3 are secreted in their active forms whereas TIMP-3 is also active intracellularly with TIMP-4 less or not expressed in some tissues, especially in fibroblasts (Takizawa et al., 2000). Studies show that ADAMTS regulation relies on the interaction between the ancillary domain and the N-terminal domain of TIMPs as seen in ADAMTS-4 and -5 with TIMP-3 (Kashiwagi et al., 2001; Troeberg et al., 2009). Generally, ADAMTS are known to function in diverse developmental and physiological processes via their proteolytic activity. ADAMTS activity has been found, through analysis of human pathologies and knockout rodent models, to be critical for the development and maintenance of tissues and organs. For instance, the cleavage of essential embryonic CSPGs by aggrecanases (ADAMTS-1, -4, -5, -8, -9, -15 and -20), is critical for development of heart tissues (Sandy et al., 2001), and ovulation (Russell et al., 2003).

In the CNS, several ADAMTS such as ADAMTS-1, -4, -5, -8, and -9, are expressed in several brain regions like DG, cortex and striatum (Lemarchant et al., 2013; Yuan et al., 2002), as well as in developing mice embryo (Jungers et al., 2005). ADAMTS proteolytic properties are essential for both developmental and physiological processes in CNS. For instance, the lack of ADAMTS-1 reduces the expression of some synaptic proteins such as the synaptosomal nerve-associated protein 25 (SNAP-25) and PSD-95, indicating how essential ADAMTS are for synaptic activity (Lemarchant et al., 2013). Furthermore, from *in vitro* experiments, ADAMTS can induce neurite elongation which is a central piece in CNS development (Gottschall and Howell, 2015). ADAMTS family members have also been implicated in several of CNS-related developmental and physiological conditions like ADAMTS-1 associated with Downs syndrome and with demented conditions such as Alzheimer's and Pick's disease (Miguel et al., 2005).

In the next two sections, we will discuss current findings regarding the expression and function of the two major aggrecanases, which are ADAMTS-4 and -5.

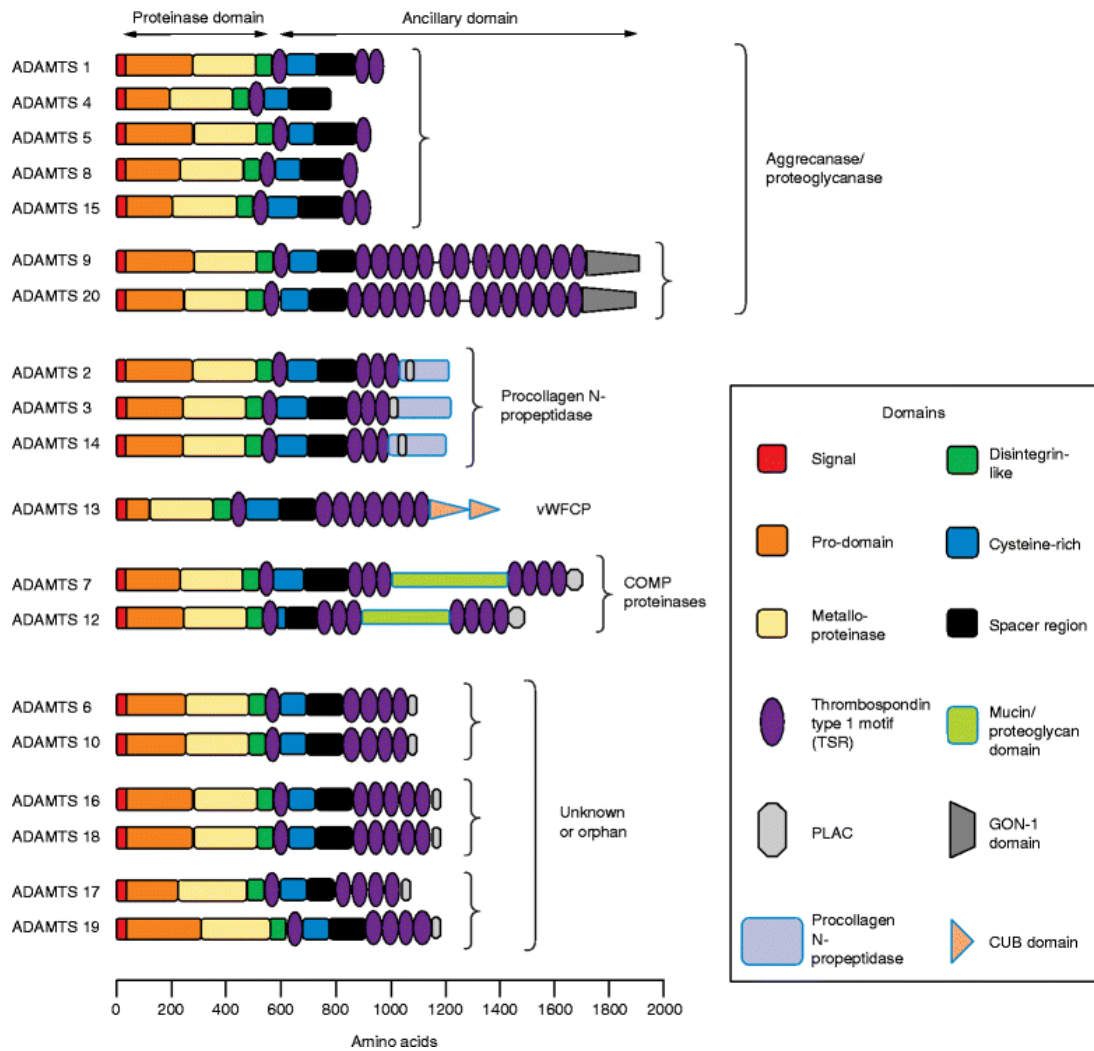


**Figure 1.14 Members of the ADAMTS family and their domain organization**

In the ADAMTS family, about 20 ADAMTS of which 7 members constitute the aggrecanases such as ADAMTS-4 and-5. All ADAMTS are divided into two major domains which are the proteinase domain that comprises the signal peptide, the pro-domain metalloproteinase and the disintegrin-like regions, and the ancillary domain. The ancillary domain includes the thrombospondin type1 motif (TSR), the cysteine-rich and the spacer domains (Kelwick et al., 2015).

### 1.2.6 ADAMTS-4

ADAMTS-4 also known as aggrecanase-1 belongs to the adamalysin family of zinc-binding metalloprotease and is one of the major ECM proteases that cleave CSPGs around tissues and organs (M. D. Tortorella et al., 2000). ADAMTS-4's overall structure consists of 837 amino acid residue protein with a 1-207 prodomain residue, 208-212 furin-sensitive site, a catalytic domain of 213-440 residue, residues from 441 to 547 for a disintegrin-like and TSR, along with residues from 548-694 and 695-837 constituting the cysteine-rich and c-terminal spacer domains respectively (Gao et al., 2002; Mosyak et al., 2008). Comparatively, ADAMTS-4 has a similar zinc-binding motif to MMPs, and has a similar number of domains as ADAMTS-5 but has less TSR (Tortorella et al., 2000; Tortorella et al., 1999). An early study identified that the TSR domain function in the recognition, binding and cleavage activity of ADAMTS-4 to its substrates, as cleavage is dependent on binding efficiency (M. Tortorella et al., 2000).

ADAMTS-4 is known to cleave several aggregating proteoglycans, like ACAN, specifically, the bond at the inter-globular domain (IGD) between glutamic and alanine amino acids, Glu<sup>373</sup>-Ala<sup>374</sup> (Gao et al., 2004; Tortorella et al., 2000). BCAN is also cleaved at the bond between glutamic acid at 395 and serine at 396, Glu<sup>395</sup>-Ser<sup>396</sup> (Matthews et al., 2000), and for VCAN the bond between glutamic and alanine amino acids with Glu<sup>441</sup>-Ala<sup>442</sup> site for V1, Glu<sup>405</sup> for V2 and Glu<sup>405</sup> and 1428 for V0 (Sandy et al., 2001). However, ADAMTS-4 does not cleave other extracellular matrix proteins such as fibronectin, thrombospondin and type I and II collagens (Tortorella et al., 2002). Interestingly, the efficient interaction between the recognition site of ECM and ADAMTS-4 depends on the modification of non-catalytic domains. In 2002, Gao and colleagues demonstrated how ADAMTS-4 is activated *in vitro* using human chondrosarcoma cell lines. Here, they show that the full-length ADAMTS-4 (p100) contains a furin-recognition site that yields a p75 form once cleaved by furin (Gao et al., 2002). Moreover, they also reported that only the p75 form of ADAMTS-4 can be further processed to yield two active forms, that is p60 and p50, via c-terminal spacer domain truncation. Two years later, Gao's group explored further to elucidate the enzyme that performs the c-terminal truncation. They reported that the inactive ADAMTS-4 is catalyzed by the glycosylphosphatidyl inositol-anchored membrane-type 4 matrix metalloproteinase (MT4-MMP) (Gao et al., 2004). Surprisingly, studies by Kashiwagi using several variants of ADAMTS-4 found the full length without the pro-domain as well as without both pro-domain and c-terminal spacer domain to be most effective in cleaving ACAN compared to variants lacking the TSR and cysteine-rich domain (Kashiwagi et al., 2004). Additionally, the binding of ADAMTS-4 to ACAN is found to be GAG chain dependent, and more importantly, this requires the function of the cysteine-rich domain as lack of this domain reduced affinity between ADAMTS-4 and

ACAN (Flannery et al., 2002; Tortorella et al., 2000). This indicates that both TSR and cysteine-rich domains are essential for substrate interaction as well as catalytic functions of ADAMTS-4 (Malfait et al., 2002; Schlatmann and Becker, 1977).

### 1.2.7 ADAMTS-4 and CNS

In the CNS, ADAMTS-4 is expressed in several brain regions including the cortex and hippocampus (Nguyen et al., 2020), and in the spinal cord (Hamel et al., 2005; Lemarchant et al., 2017). ADAMTS-4 mRNA is found in the murine cortex as early as p8 and at maturity, with adult mice showing the most abundant levels of ADAMTS-4 compared to other ADAMTS both in the cortex and the spinal cord (Howell et al., 2012). Meanwhile, a contrasting result was reported by Levy and colleagues when they show that ADAMTS-4 mRNA during hippocampal and cortical development using *in situ* hybridization did not colocalize with neurons, microglia and astrocytes but rather with oligodendrocytes (Levy et al., 2015). This means, ADAMTS-4 is expressed by oligodendrocytes during development and later taken over by neurons, astrocytes and microglia. A study by Haddock and co-workers observed ADAMTS-4 expressed in snap-frozen human white matter tissues from both normal and diseased states like multiple sclerosis (Haddock et al., 2006). This was further corroborated by studies in Alzheimer's patients (Pehlivan et al., 2016). In the brain, ADAMTS-4 cleaves ACAN, BCAN, NCAN and VCAN and other CSPGs like PCAN, and the extracellular signaling molecule, reelin (Lemarchant et al., 2017). ADAMTS-4 activity has been associated with specific physiological and pathological events in the CNS. For instance, like MMP-9, ADAMTS-4 has been found to function on neurite growth of cortical and spinal cord neurons by removing the inhibitory effect of CSPGs (Cua et al., 2013). Reelin is found to be essential in preventing the transition between normal and pathological aging (Doehner and Knuesel, 2010). Furthermore, as ADAMTS-4 cleaves reelin which is known to influence migration and maturation of neurons during development as well as synaptic activity of adult neurons, therefore ADAMTS-4 expression is rigorously regulated (Krstic et al., 2012a).

As spinal cord results in excessive production of CSPGs that inhibits axonal regeneration, it has been shown that the exogenous and *in vivo* proteoglycanase activities of ADAMTS-4 on BCAN, NCAN and PCAN enhance the functional recovery of motor neurons by improving axonal regeneration (Tauchi et al., 2012) and myelination (Pruvost et al., 2017). From Tauchi, the inhibitory effects of CSPGs were reversed in cerebellar granule neurons cultured on surfaces coated with proteoglycan and ADAMTS-4 compared to only proteoglycan, and this effect was comparable to the effect of chABC (Tauchi et al., 2012).

Inflammatory-induced upregulation of ADAMTS-4 by TNF- $\alpha$  was also shown in rats with cerebral artery occlusion (Cross et al., 2006) as well as following induced seizures in rats.

ADAMTS-4 also has an anti-inflammatory effect as demonstrated by Lemarchant and colleagues in mouse models of ischemic stroke. They show that downregulation of ADAMTS-4 to about 50% via siRNA technology prior to exposure to lipopolysaccharides increased the production of pro-inflammatory cytokines like TNF- $\alpha$  and IL1beta. They also show that ADAMTS-4 results in the expression of anti-inflammatory cytokines like IL-10 and IL-6 around the ischemic area (Lemarchant et al., 2016).

### 1.2.8 ADAMTS-5

Just like ADAMTS-4, ADAMTS-5 (aggrecanase-2), also called ADAMTS-11 belongs to the adamalysin family of metalloprotease and these aggrecanases have about 48% sequence similarity beyond the signal peptide and pro-domain (Mosyak et al., 2008). ADAMTS-5 is expressed in several tissues including adipocytes, skeletal tissues, uterus, breasts and in the brain. Moreover, ADAMTS-5 expression is associated with several factors such as the cytokines IL-1 & -6, and TNF- $\alpha$  (Kelwick et al., 2015). Once formed, the full-length pre-pro-ADAMTS-5 has a similar domain organization as ADAMTS-4. In the case of ADAMTS-5, there are 2 TSR domains flanking the cysteine and spacer domains (Gendron et al., 2007). After the signal peptide is removed from the pre-pro-ADAMTS-5, the pro-ADAMTS-5 is processed differently to ADAMTS-4. Both ADAMTS-4 and -5 have furin recognition sites, however, furin processing of ADAMTS-5 takes place extracellularly contrary to intracellular processing of ADAMTS-1 and -4 (Longpré et al., 2009). Three furin recognition sites are located in the pro-domain of mice and human ADAMTS-5 (Fosang et al., 2008). Additionally, the cleaved pro-peptide and the mature ADAMTS-5 localized extracellularly do not bind to the cell surface as seen in the processing of pro-ADAMTS-9, indicating distinct processing of pro-ADAMTS-5 to the other ADAMTS (Fosang et al., 2008).

As previously described, the non-catalytic ancillary domain of ADAMTS-4 and -5 regulates both matrix interaction as well as cleaving properties, but for ADAMTS-5, there are some fundamental differences. The cysteine-rich domain of ADAMTS-5, for instance, regulates its attachment to matrix substrates contrary to the spacer domain for ADAMTS-4 (Gendron et al., 2007). Also, the TSR 1 and 2 of ADAMTS-5 facilitate affinity to sulfated GAGs as well as fibronectin (Vankemmelbeke et al., 2001). The catalytic domain of ADAMTS-5 can only cleave matrix at a very low efficiency whereas further addition of any of the c-

terminal domains enhances activity. ADAMTS-5 is very effective under a wide pH range, that is from 7.0 to 9.5 (Gendron et al., 2007).

Interestingly, the biochemical signature of ADAMTS-5 is not as elaborate as ADAMTS-4. However, both ADAMTS-4 and -5 have similar aggrecanase activity which is higher than for other proteoglycanases like ADAMTS-1, -8 and -9 (Collins-Racie et al., 2004; Kuno et al., 2000; Somerville et al., 2003). Comparatively, ADAMTS-5 aggrecanase activity is more than 1,000 times higher compared to ADAMTS-4 under physiological conditions (Gendron et al., 2007). Meanwhile, both aggrecanases cleave ACAN at similar sites, that is at the Glu<sup>373</sup>-Ala<sup>374</sup> bond (Abbaszade et al., 1999; Tortorella et al., 1999). Furthermore, ADAMTS-4 and -5 also have four additional aggrecanase-sensitive sites localized in the chondroitin sulfate-rich regions of ACAN. These sites are the GELE<sup>1480-1481</sup>GRGD, KEEE<sup>1667-1668</sup>GLGS, TAQE<sup>1771-1772</sup>AGEG, and VSQE<sup>1871-1872</sup>LGQR that exist between the G2 and G3 domains of the core-protein, and they are conserved in various species (Nagase & Kashiwagi, 2003; Tortorella et al., 2000). Just like ADAMTS-4, ADAMTS-5 cleaves other CSPGs like VCAN and BCAN (Demircan et al., 2014), and also HA in cartilage extracts potentially through its disintegrin and spacer domains (Plaas et al., 2007), but it has weak activity on fibronectin (Fosang et al., 2008), and it cleaves CSPG biglycan and link proteins (Didangelos et al., 2012) (**Figure 1.15**).

ADAMTS-5 proteolytic activity has been associated with several developmental and physiological processes in various tissues. In the heart, VCAN is highly expressed in the developing valves especially in endothelial cells but this is reduced in adult valves (Zhou et al., 2015). The lack of ADAMTS-5 in mice enlarges the developing valves and it is associated with adult cardiac valve diseases such as the aortic valve sclerosis (Hinton and Yutzey, 2011). ADAMTS-5 remodeling of adult skin proteoglycan has been studied and ACAN and VCAN accumulates in the dermis of ADAMTS-5 knockout mice affecting wound healing (Velasco et al., 2011). Furthermore, the extensive degradation of ACAN by ADAMTS-5 has been observed in cartilages of mouse models of inflammatory arthritis (Nagase and Kashiwagi, 2003; Stanton et al., 2005). In human, cartilage diseases like OA and rheumatoid arthritis, there is a significant reduction in cartilage matrix content as a result of excessive degradation of ACAN by ADAMTS-5 (Nagase and Kashiwagi, 2003; Stanton et al., 2005), and in mice (Abbaszade et al., 1999; Stanton et al., 2005). Furthermore, studies in ADAMTS-5 knockout female and male mice by Sonya in 2005, demonstrated that ADAMTS-5 has limited developmental functions. Here, ADAMTS-5 knockout mice developed normal organs like heart, lungs, testis, eye and others, in addition to no aberrations in body weight and blood analysis (Glasson et al., 2005). The relationship between inflammation, expression and activity of ADAMTS-5 has also been

demonstrated in cultured articular cartilages with factors like IL-1 and retinoic acid reducing the release of proteoglycans (Glasson et al., 2005).

During normal development, TIMP-3, the most potent inhibitor of ADAMTS-5, is expressed in skeletal tissues (in epithelia, cartilage and muscle) of mice embryos (Apte et al., 1994), as well as in bovine and human chondrocytes (Su et al., 1999). However, under disease conditions, the expression of TIMP-3 is upregulated as seen in the synovium of human OA as well as in cultured medium and lysates of rheumatoid synovial fibroblasts (Takizawa et al., 2000).

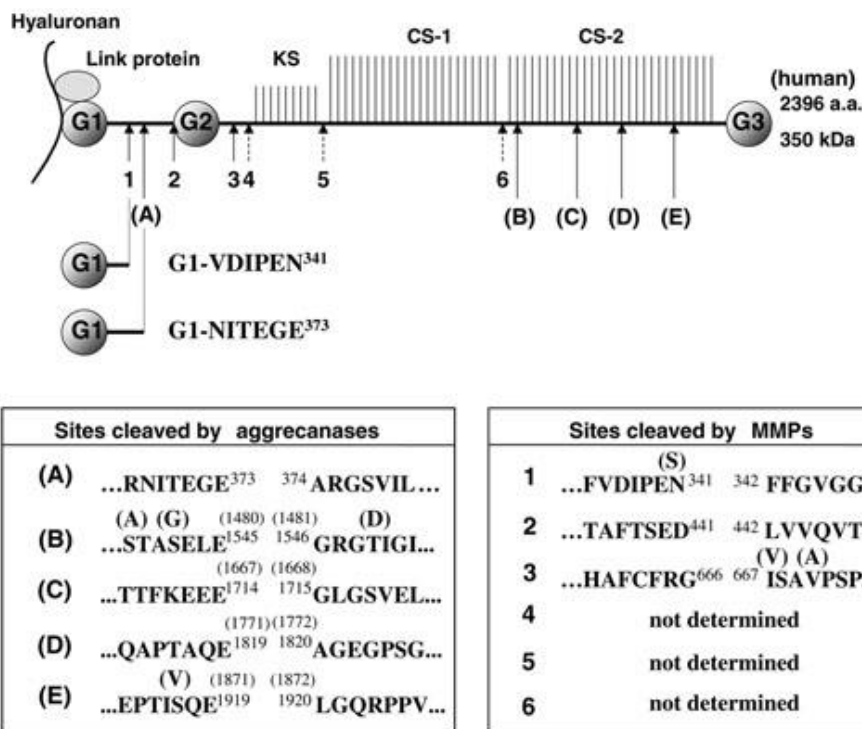
### 1.2.9 ADAMTS-5 and CNS

In the CNS, thus far, little knowledge has been gathered regarding the role of ADAMTS-5 in brain development as well as synaptic functions. At the moment, ADAMTS-5 is known to be expressed in neurons, astrocytes and microglia of several brain regions like *striatum radiatum* of hippocampus of aged mice (Ferrer-Ferrer and Dityatev, 2018; Krstic et al., 2012a), cerebral cortex of rodents (Reid et al., 2009; Zamanian et al., 2012) and humans (Cross et al., 2006), and in the spinal cord (Demircan et al., 2013). Using IHC, ADAMTS-5 is located in the dendrites of rat hippocampus which supports findings by Krstic in 2012 (Dubey et al., 2017). In mice hippocampus, Levy and colleagues demonstrated using *in situ* hybridization and quantitative RT-PCR (*qPCR*) that ADAMTS-5 mRNA peaks at P7 which is about 6-fold abundant to ADAMTS-4 levels, but by P15 ADAMTS-5 mRNA decreases and reaches minimum levels by P56. ADAMTS-4 mRNA, on the other hand, peaks at P15 but also reaches minimum levels by P56 and P60 in hippocampus and cortex respectively. They show that ADAMTS-5, in particular, is essential for hippocampal development (Levy et al., 2015). Complementary findings were also reported by Gottschall and Howell in 2012, where they also confirm peak expression of ADAMTS-5 at P8 which reduces even at P160 in the frontal cortex, and here, the expression pattern is not sex-dependent (Gottschall and Howell, 2015; Howell et al., 2012). ADAMTS-5 protein levels are extensively reduced in AD mice models (Ferrer-Ferrer and Dityatev, 2018) but both mRNA and protein levels remained unchanged in animal model of status epilepticus (Dubey et al., 2017). This might explain why ECM accumulates in AD mice models. In contrast, the nerve fibers of Multiple sclerosis in humans have very low mRNA and protein levels of ADAMTS-5 and this is about 50-fold less expressed relative to ADAMTS-4 (Haddock et al., 2006).

Functionally, ADAMTS-5 cleaves brain lecticans such as BCAN, VCAN and ACAN, as well as PCAN and reelin (Krstic et al., 2012a; Nakada et al., 2005). Although ADAMTS-5 offers a protective effect in the

aorta wall, but in the brain and the spinal cord cleavage of BCAN by ADAMTS-5, which is extensively expressed in human glioblastoma cells, is strongly associated with glioblastoma compared to normal brain (Nakada et al., 2005). Moreover, VCAN cleavage in brain endothelial cells by ADAMTS-5 has been implicated with the cerebral cavernous malformations (Hong et al., 2020) and this is prevented in ADAMTS-5 knockout mice. In the spinal cord, ADAMTS-5 and ADAMTS-4 knockout mice are protected from the degradation of VCAN which is known to be upregulated during injury, however, ACAN and BCAN are cleaved potentially by ADAMTS-1 (Demircan et al., 2014). This indicates that in mice CNS, both ADAMTS-4 and -5 are the most effective proteases of VCAN.

One interesting feature of ECM during spinal cord injury is the upregulation of CSPGs like BCAN and VCAN but not ACAN (Asher et al., 2002; Lemons et al., 2001), however, ADAMTS-5 is also upregulated at those sites. The upregulation of ADAMTS-5 mRNA levels during conditions like the transient middle cerebral artery occlusion (tMCAO) and spinal cord injuries (Cross et al., 2006; Demircan et al., 2013; Zamanian et al., 2012) promotes neurite outgrowth by cleaving BCAN and VCAN. This effect has also been shown to occur without ECM cleavage through the mitogen-activated protein (MAP) kinase and extracellular signal-regulated kinase 1/2 (ERK1/2) pathway. This was demonstrated by Hamel in 2008, whereby adding recombinant ADAMTS-5 to neuronal cultures enhanced neurite growth. Meanwhile, irrespective of ECM cleavage, the addition of selective MAP kinase inhibitors impaired neurite growth indicating that ADAMTS-5 effect on neurite growth can also be through MAP ERK1/2 kinase signaling (Hamel et al., 2008). Furthermore, cleavage of reelin by ADAMTS-5 has been implicated to function in neurodevelopment and synaptic plasticity (Krstic et al., 2012a). Unfortunately, not much information exists regarding the detailed effect of ADAMTS-5 during adult ECM remodeling and learning and memory. The perisynaptic proteolysis of BCAN and ACAN by ADAMT-4 and -5 at excitatory synapses has been demonstrated to be enhanced through dopamine receptor activation, specifically the D1-type DA receptor (Mitlöhner et al., 2020).



Arthritis Research &amp; Therapy

**Figure: 1.15** Cleavage sites of ACAN by ADAMTS and MMPs (Nagase and Kashiwagi, 2003).

### 1.3 Aging

Aging is a dynamic process in the life span of every organism. In humans, the aging population is rapidly growing and it is currently one of the major risk factors associated with some detrimental pathologies. Aging is a fundamental phenomenon for the development and maturation of an organism from juvenile towards adulthood. The rate at which rodents grow is about 150x faster compared to humans after birth which decreases to about 25x after 6-months, and both organisms experience similar burdens of aging (Flurkey et al., 2007) (**Figure 1.16**). Aging is a continuous and dynamic process, mostly occurring after adulthood in every organism's life and it is accompanied by significant changes in essential processes (Flurkey et al., 2007). Such processes include alterations in biological (structural), physiological and behavioral processes that are essential for the survival of organisms in their environment. Studies show that these phenomena culminate from the basic changes in single cells (cellular senescence) due to insults from stimulators like oxidative stress, cytokines, mitochondrial and DNA damage (Papadopoulos et al., 2020). Eventually, they disrupt the homeostasis and health of tissues and organs (Gorgoulis et al., 2019) as well

as the integrity of their microenvironment. In ideal situations, once these detrimental changes or stimulators occur in cells they are either removed or reversed, however, failure of cells in this regard activates death pathways (Gorgoulis et al., 2019). From a broad perspective, aging can be classified into two classes namely pathological and non-pathological also known as normal aging.

### *1.3.1 Pathological and normal aging*

Although aging is essential for development and maturation, however, with pathological aging, tissue and organs are both structurally and functionally altered to the point of dysfunction and degeneration. For instance, aging has been associated with pathological changes in several organs like the heart, lungs, kidneys and the brain. Aging heart comes with a decreased rate of ventricular filling due to fibrosis and stiffening of walls of the left ventricles and these are critical defects observed in patients and animals with atrial fibrillation (Keller and Howlett, 2016). Atrial fibrillation in recent studies is associated with an increased risk of sudden cardiac death (Waldmann et al., 2020) which also occurs in patients with ventricular fibrillation as well as atrial fibrillation (Ritchie et al., 2013). Also, an age-dependent decrease in ventricular myocytes as a result of cell death has been associated with some cardiac diseases in men but not in women (Ritchie et al., 2013). Aging increases adipose tissues (Silaghi et al., 2008), calcification and inflammation of heart tissues (New and Aikawa, 2011), and decreased cardiac conduction due to reduced activity of pacemaker cells (Jones, 2006; Ritchie et al., 2013). Moreover, aging has strongly been associated with a significant decrease in lung function such as reduced physiological expiratory volume and the development of lung diseases like cancer and pulmonary fibrosis (Navarro and Driscoll, 2017).

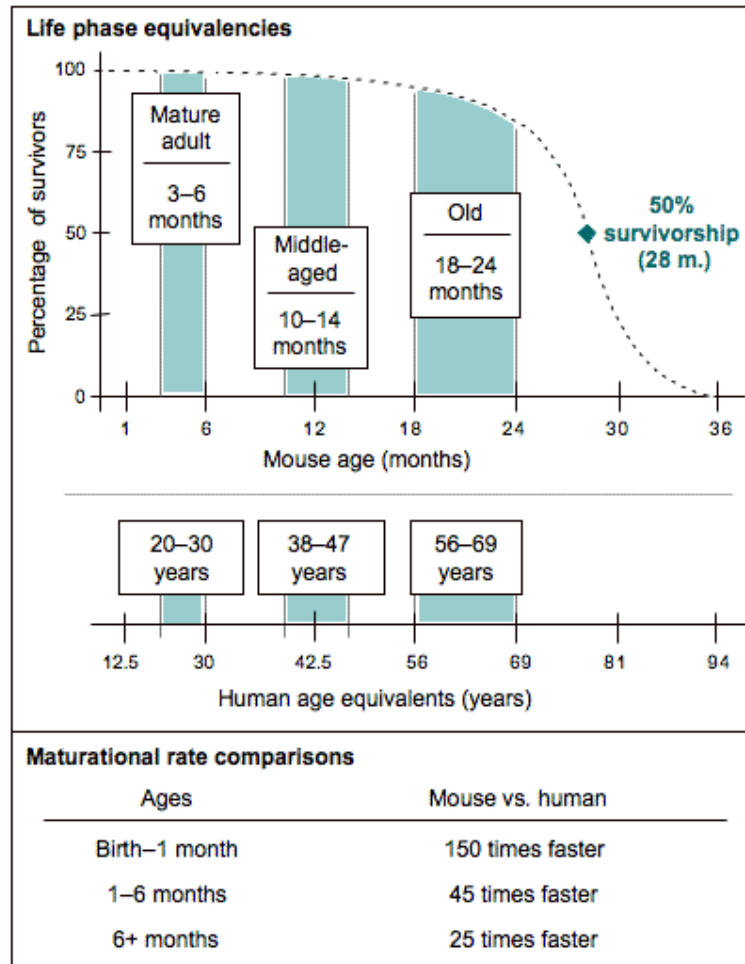


**Figure 1.16 Comparison between the various life stages of C57BL/6J mice to human beings** (Flurkey et al., 2007).

CNS pathologies such as dementia, small vessel disease, stroke, spinal cord injuries and others are highly prevalent in aged human and animal populations (Rosso et al., 2013). In the CNS, aging negatively alters the microenvironment of various cells of several brain regions including the hippocampus, which, eventually, decreases CNS functions. Such alterations include activation of microglia and astrocytes, which results in neuroinflammation (Chee and Solito, 2021), a common event found in several pathophysiological diseases in the CNS like in AD animal models as well as in physiologically aged organisms (Jurga et al.,

2020; Schwab et al., 2010). Microglia, the brain's resident macrophage, in the resting state functions as an immune cell by maintaining the integrity of neurons through its processes, regulating synaptic plasticity and also monitoring the microenvironment (Hornik et al., 2016). However, once activated, a common phenomenon in the aging brain, microglia release a host of molecules including reactive oxygen species (ROS) that eventually damage neurons, and they also secrete pro-inflammatory cytokines like IL-6, TNF- $\alpha$ , IL1beta, and IL-8 (Cleeland et al., 2019; Jurga et al., 2020). These factors together with cytotoxic factors like nitric oxide (NO) function in activating astrocytes, especially the A1 astrocytes, initiate neuronal death through phagocytosis by microglia (Liddel et al., 2017). The A1 astrocytes are unable to perform normal functions of supporting neuronal survival, rather they stimulate the death of neurons and oligodendrocytes as seen in AD animals (Liddel et al., 2017; Peters, 2002; Tuppo and Arias, 2005). Both microglia and astrocytes also function amongst others in the release of ECM molecules as well as proteases and these functions are also altered in most CNS pathologies like dementia and epilepsy (Schwab et al., 2010).

With normal aging, tissues and organs of animals encounter a decrease in their functional efficiencies as a result of altered gene expression and signaling of some specific biomolecules and inflammation as described above (Papadopoulos et al., 2020). However, these changes do not culminate into any pathological phenotypes, thereby allowing the aging organism to continue to survive, but with some limitations or difficulties (Gorgoulis et al., 2019). Concentrating on normal aging in the CNS of animals, studies show that the growing brain encompasses structural and functional changes ranging from an increase in neuronal and glial cells population (Yamaguchi et al., 2016) as well as size, to increase in neuronal connections between and within brain regions (Gorgoulis et al., 2019). Functionally, these changes during development and maturation of the brain enable it to function efficiently regarding learning and memory along with the regulation of other organs of the body. For example, the matured hippocampus and cortex function in memory acquisition and storage (Brod et al., 2013; Takehara-Nishiuchi, 2020) whereas the hypothalamus influences the endocrine and cardiovascular functions like heart rate and blood pressure (Rahmouni, 2016). However, once the brain advances with age, that is post adulthood, certain changes in brain cells and their microenvironment decrease the efficiency of the brain, and some of these changes will be discussed in the following sections.

### 1.3.2 *Learning and memory in normal aging*

In the brain, aging stimulates a gradual loss of ability to learn, keep as well as recall important information and this is one of the earliest effects of aging (Bergado and Almaguer, 2002). Learning and memory follow two stages, namely the initial acquisition of short-term memory followed by the consolidation and storage of long-term memory (Alberini et al., 2013; Roesler and McGaugh, 2010). Memory acquisition, also referred to as learning, requires structural modifications of the brain, specifically with neurons by sensory stimulus (Puzzo et al., 2016) resulting in short-term memory (Cowan, 2008). This phase of memory formation involves the retention of limited information over a short period that can be in a matter of seconds and minutes (Vallar, 2017), and this strongly correlates with synaptic plasticity, LTP and LTD. Here, synapses triggered by memory acquisition undergo long-lasting potentiation through NMDAR activation (Roesler and McGaugh, 2010). The transition of sensory information from short- to long-term storage depends on a critical step called memory consolidation (Bisaz et al., 2014; Fiebig and Lansner, 2014). The neural basis of memory consolidation includes synaptic consolidation which is the fastest form of memory consolidation lasting more than 24 hours (Dudai, 2004). This involves protein synthesis, trafficking of new AMPAR to synaptic membrane as well as structural stabilization of changes at the dendritic spines (Malenka and Bear, 2004). Different brain regions are involved in varying aspects of learning and memory together with the hippocampus, for example, encoding and storing short-term memories, in addition to, consolidating information from short-term memory to long-term memories which are then stored in the cortical regions (Preston and Eichenbaum, 2013).

Age-dependent impairments or decrease in the efficiency of the various aspects of learning and memory in several brain regions including the hippocampus, prefrontal cortex (PFC) and anterior cingulate cortex (ACC) in both humans and rodents (Gallagher and Burwell, 1989; Mizoguchi et al., 2009) have been reported. Age-dependent changes in hippocampal neuronal transmission and reduced volume influence memory impairments in aging population of rodents and humans (Gould and Feiro, 2005). In humans, decreased performance in spatial navigation using virtual maze have been reported (Marutle et al., 1998) as well as impaired memory acquisition (Squire and Wixted, 2011). Aged-dependent cognitive effects observed in rodents include impairment of spatial learning and memory retention from different behavioral strategies (Feiro and Gould, 2005) such as the Barnes maze, water- and T-maze. One study by Vegh in 2014 reported impairment of hippocampus-dependent spatial memory using the Barnes maze. With this maze, mice are placed on a circular platform with holes and trained to locate the escape hole within a target region. From their work, they found that animals from 1 year-old struggled to locate the escape holes

compared to 5-months-old controls (Vegh et al., 2014). This finding corroborates with previous work performed in young and 18-month-old wild-type mice (Barreto et al., 2010). Another study in 20-month-old mice show a progressive loss of memory in 3-behavioral paradigms namely spontaneous object recognition and alternation as well as spatial navigation using the Barnes maze (Yang et al., 2021). Other brain regions like amygdala and PFC are also affected by aging and studies show similar cognitive impairments in these regions. Impairment of spatial working memory as the result of decreased dopamine expression in cortical cells in aged rats, reduced long-term retention of contextual and cued fear conditioning memories, which are known to involve amygdala, have all been reported in multiple studies (Gould and Feiro, 2005; Mizoguchi et al., 2009). In humans as well, non-pathological aging impairs working memory which has been associated with reduced dopamine release in the PFC (Bimonte et al., 2003) and in the Anterior cingulate cortex (Ota et al., 2006). This has also been reported in PFC of monkeys together with a reduction of neuronal population (Smith et al., 2004).

### *1.3.3 Aging and impaired synaptic plasticity*

Many researchers suggest that alterations in the number and function of synapses are a critical physiological substrate for memory formation and retention (Ashby et al., 2021; Bliss and Collingridge, 1993). Therefore, synaptic loss in areas necessary for learning and memory such as the hippocampus and the cortex as a result of aging (Bergado and Almaguer, 2002; Kumar et al., 2012; Morrison and Baxter, 2012) culminates in age-dependent cognitive impairments. One major change due to aging is alterations of dendritic branching and spine density of excitatory neurons (Burke and Barnes, 2006; Torres and Cardenas, 2020) as observed in humans (Honer et al., 1992) and animal models (Adams et al., 2008). Also, there is decreased expression of glutamate in the hippocampus of aged mice and rats, but the total number of Schaffer collaterals-CA1 connections are somehow constant between young and aged animals (Bear et al., 1987). The decreased glutamate expression in aged hippocampus is coupled with decreased presynaptic glutamate release (Deak and Sonntag, 2012a). In addition, increase in nonfunctional and immature synapses in aged hippocampus has been reported (Burke and Barnes, 2010), all indicating an age-dependent changes in the synaptic density.

In the aging brain, a decrease in the ability to induce LTP as a result of changes in expression or function of AMPAR and NMDAR at excitatory synapses has been reported to impair synaptic plasticity (Temido-Ferreira et al., 2019). The reduced AMPAR and NMDARs functions (Deak and Sonntag, 2012a) as well as increased internalization of AMPARs in aged hippocampus correlates with impaired LTP and behaviorally-

dependent plasticity, and this depends on changes in  $\text{Ca}^{2+}$  signaling (Burke and Barnes, 2010). One major finding of the age-dependent modification of NMDAR is with its subunits and this accounts for the reduction in excitatory postsynaptic potentials (EPSPs) in hippocampal CA1 (Temido-Ferreira et al., 2019). During development, GluN2B and GluN2D are highly expressed which decreases after birth whereas GluN2A and GluN2C increase and persist even at adulthood (Paoletti et al., 2013b). Meanwhile, during aging, there is a shift in the distribution of specific subunits of NMDAR of which GluN2B containing NMDARs diffuses laterally to extra-synaptic sites of dendritic spines (Avila et al., 2017). This movement and signaling of extra-synaptic NMDAR impairs or dephosphorylates transcription factor cAMP response element-binding protein (CREB), and inactivates the ERK1/2 and the MAP kinase (Avila et al., 2017; Hardingham and Bading, 2010). A shift in synaptic and extra-synaptic NMDAR correlates with cognitive impairments found in the aged brain (Avila et al., 2017; Hardingham and Bading, 2010). Aging also increases GluN2B subunits of NMDAR in cortical and hippocampal neurons as compared to GluN1 (reduced) and GluN2A (unaltered) subunits (Biello et al., 2018; Magnusson, 2012) (**Figure 1.17**). An interesting study demonstrated that the reduction in LTP observed in 24-month-old mice was rescued by stimulating GluN2A or inhibition of GluN2B receptors, suggesting that LTP depends on the appropriate balance between GluN2A and GluN2B signaling (Kochlamazashvili et al., 2012).

Interestingly, in aged hippocampal neurons, L-type voltage-gated  $\text{Ca}^{2+}$  channels (LTCC) are highly expressed thereby altering  $\text{Ca}^{2+}$  (Navakkode et al., 2018; Thibault and Landfield, 1996) conductance. The altered calcium conductance, therefore, impairs LTP whereas enhancing LTD sensitivity along with the increase in the slow after-hyperpolarization in aged animals (Navakkode et al., 2018). Also, studies report an age-dependent increase in the LTP threshold compared to reduced LTD threshold, potentially explaining the difficulties in memory acquisition in aged animals (Barnes et al., 2000). Furthermore, a strong relationship has been established between dysregulated  $\text{Ca}^{2+}$  signaling and impairment of learning and memory (Koh et al., 2021). Hence, the increased entry of  $\text{Ca}^{2+}$  into aged synapses through L-type voltage-gated  $\text{Ca}^{2+}$  channels stimulates extensive release of  $\text{Ca}^{2+}$  from the ER and this further increases calcineurin functions as well as reduces both protein kinase-A and CREB activity (Koh et al., 2021; Singh et al., 2012). Regarding CREB, the phosphorylated species related to learning and memory, and more importantly with neuronal excitability (Guzowski and McGaugh, 1997), are significantly reduced in aged animals compared to young ones, especially, right after behavioral tests (Porte et al., 2008). This is because the late phase of LTP depends on protein synthesis, and CREB activation is essential for protein synthesis but this signaling is impaired in aged brain (Deak and Sonntag, 2012a). Also, CaMKII- $\alpha$  is decreased in aged rats which

correlates with decreased spatial memory and presynaptic releases probabilities as it is essential for the phosphorylation of major vesicular proteins like, SNARE complex; SNAP25 and synaptobrevin 2 (Deak and Sonntag, 2012a; VanGuilder et al., 2011).

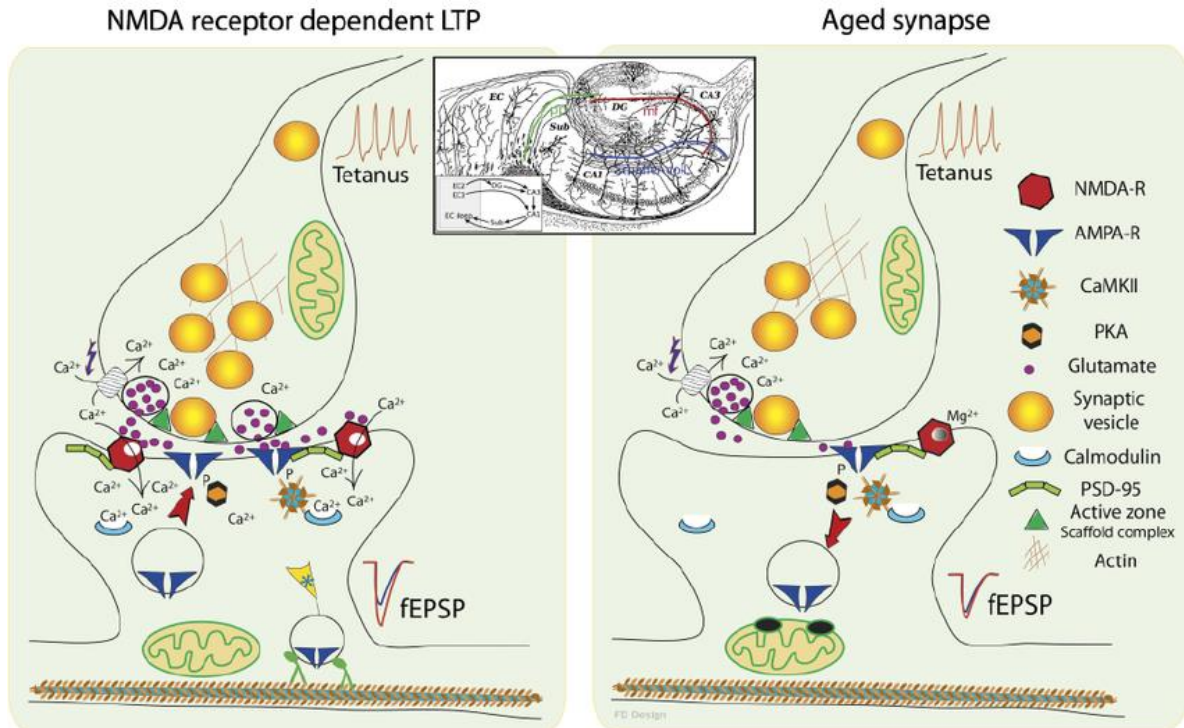


**Figure 1.17 Effect of Aging on hippocampal synaptic plasticity**

Aging compromises synaptic transmission by reducing the number of NMDAR as well as AMPAR in the postsynaptic compartment. In addition, the presynaptic compartment is plighted with reduced glutamate content and synaptic vesicles due to altered Ca<sup>2+</sup> signaling in both compartments (Deak and Sonntag, 2012a).

### 1.3.4 Aging and ECM

The fact that aging affects synaptic plasticity and cognitive performance, it is, therefore, interesting to know the effect of aging on ECM expression, and how they are all connected. However, this puzzle is not fully unraveled. Thus far, accumulating evidence indicates that both perisynaptic and PNNs also called perisomatic ECM can influence synaptic plasticity in several brain regions including the hippocampus and cortex (Senkov et al., 2014). For instance, PNNs alter AMPAR trafficking and neuronal excitability thereby

impairing LTP and LTD, molecular substrates of learning and memory (Wingert and Sorg, 2021). Interestingly, the digestion of PNNs with chABC relieves the burden of elevated ECM on synaptic plasticity together with cognitive performance (Bosiacki et al., 2019; Dityatev et al., 2010).

Cognitive functions throughout the lifespan of animals are associated with ECM load which peaks at adulthood. The ECM during the 1<sup>st</sup> week of postnatal development is mostly juvenile, which is immature, highly dynamic and very diffuse (Richard and Lu, 2019). At this point, ECM are mostly CSPG clusters that are lost by the end of the 2<sup>nd</sup> week, and studies highlights the onset of PNN formation at this period (Nakamura et al., 2009). Adulthood ECM including PNNs and perisynaptic ECM, on the other hand, are rich in CSPGs and they coincide with climaxed cognitive performance as there is a slow turnover of ECM which is essential for several processes such as memory stabilization (Dityatev and Fellin, 2008). However, during post adulthood, cognitive performance in animals gradually declines with normal aging (Richard and Lu, 2019) as well as in models of age-dependent pathologies like depression (Dityatev and Fellin, 2008; Koskinen et al., 2020), but ECM content steadily increases (Richard and Lu, 2019) (**Figure 1.18**). The relationship between ECM and aging, as reviewed by Richard in 2018, shows that age-dependent accumulation of both PNNs and diffuse CSPGs, results in a decline in cognitive functions specifically in motor learning. They also show that removal of ECM with chABC rescues the age-dependent cognitive impairments, indicating that indeed ECM accumulation creates a restrictive environment for both structural and functional synaptic plasticity (Richard et al., 2018). Similar relationship was also reported in rats following social-defeat-stress (depression), and here, an overlap between hippocampus time-dependent cognitive impairment and ECM imbalance (Koskinen et al., 2020) was observed. Another study reports a strong relationship between ECM and cognitive performance in aged mice. Here, they show that CSPGs BCAN and NCAN together with the link protein HAPLN1 in hippocampus increases with age, correlating with the decrease in hippocampus-dependent spatial memory (Vegh et al., 2014).

Furthermore, the role played by the sulfation patterns of CSPGs in learning and memory has been studied using enzymatic digestion or knockout models. From these approaches, it has been known that the sugar chains as well as the sulfation patterns might affect cognitive performance in animals. For example, removal of CSPGs with chABC rescues the negative effect of elevated ECM on LTP and this was studied in both wild-type aged mice as well as in models of disease (Vegh et al., 2014). More recently, age-dependent impairment of hippocampal cognitive performance and increased ECM amount in aged animals were shown to depend on a loss of 6-O-sulfation of CSPGs (Yang et al., 2021). From this study, the removal of CSPGs with chABC as well as overexpression of chondroitin 6-sulphotransferase 1 rescued the aging-dependent

cognitive impairments. This means the switch from 6-O-sulfated CSPGs as found in the juvenile brain to 4-O-sulfated CSPGs during brain development maturation results in the said phenotypes, that is 4-O-sulfated CSPGs negatively affects cognitive functions in the aged brain.

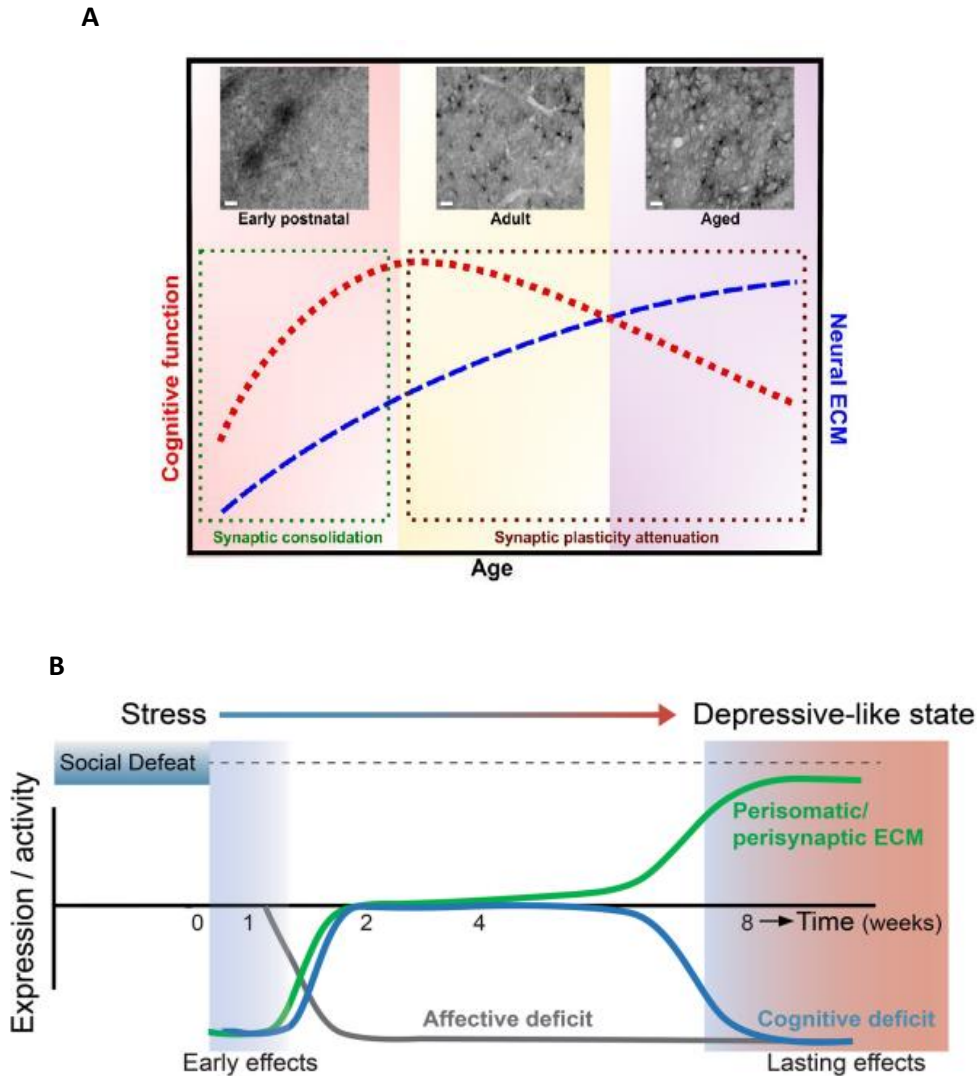


**Figure 1.18 Relationship between Aging and ECM**

(A) Role of ECM in synaptic plasticity and cognitive functions under normal aging (Richard and Lu, 2019)  
 (B) Interaction between ECM expression and cognitive functions in depressed animals, i.e. during pathological aging (Koskinen et al., 2020).

## 2 AIMS AND OBJECTIVES

From this introduction, it follows that ECM molecules are significantly increased at the protein level with aging, and a strong association has been established between ECM expression and decline in cognitive performance in normal aging and diseased conditions. However, the mechanism behind these alterations is not clear. The primary aim of this study, therefore, was to identify the age-dependent changes in the expression of ECM and related genes - namely the ECM-degrading and modifying enzymes - in the hippocampus of wild-type mice.

Therefore, this thesis work includes the following objectives:

1. To investigate the expression of neural ECM molecules and related genes including the sulfotransferases and proteases using q-PCR.
2. To rejuvenate the hippocampal ECM of aged mice by enhancing ECM proteolysis in order to potentially abrogate age-dependent cognitive impairments.
3. To study both cognitive and synaptic changes after ECM remodeling using hippocampus-dependent cognitive tasks and electrophysiological methods.
4. To unravel the possible cellular and molecular mechanism(s) behind ECM changes.

### 3 MATERIALS AND METHODS

In this thesis, the chemicals used for all experiments were from the following manufacturers: Invitrogen, Sigma-Aldrich, ThermoFisher, Abcam, Roche, Merck, and Gibco. In addition, buffers for RT-qPCR were prepared with deionized-double distilled water whereas, for immunohistochemistry, I used ultra-pure water. Details and composition of buffers are described below.

#### 3.1 Animals

All animals used in this thesis were from the Deutsches Zentrum für Neurodegenerative Erkrankungen e.V. (DZNE) animal facility (Pawlow Haus) and all animal experiments were performed in strict accordance with the ethical animal research standards defined by German law and approved by the Ethical Committee on Animal Health and Care of the State of Saxony-Anhalt, Germany (license 42502-2-1343 DZNE). Overall, a total of 94 male C57BL/6J mice were used in this thesis work. They include thirty-nine 2-3 months-old, four 10 months-old, forty-two 22-24 months-old and nine >30 months-old mice.

#### Tissue isolation, RNA extraction and RT-qPCR

Table 3.1 Probes used for qPCR

Gene	Species	Reference Sequence		Sequence (5' to 3')
<i>Acan</i>	<i>Mus musculus</i>	NM_007424.2	Fw	CTTACCCTGAGGCTGGTGTG
			Rv	ACATTGCTCCTGGTCTGCAA
<i>Vcan</i>	<i>Mus musculus</i>	NM_001081249.1	Fw	CTAGGAAACGGGAGATGGGC
			Rv	AGGCGCTTCGTGTAAGTGAA
<i>Ncan</i>	<i>Mus musculus</i>	NM_007789.3	Fw	CAGGCCACAGCAATCATCCT
			Rv	GATGTGGAAACAGAAGTGGGG
<i>Bcan</i>	<i>Mus musculus</i>	NM_001109758.1	Fw	TGCCCTCGTTCCTTTTCTG
			Rv	CTGTGTGGCCAGTGAGATGT
<i>Hapln1</i>	<i>Mus musculus</i>	NM_013500.4	Fw	AGTCTCCTGGTGACGCTTTG
			Rv	GGGGCCATTTTCTGCTTGA
<i>Tnr</i>	<i>Mus musculus</i>	NM_022312.3	Fw	TTCACGTCAGAGGCAGGAAC

			Rv	GAGCAGAGAGCTAGAGCAGC
<i>Chsy1</i>	<i>Mus musculus</i>	NM_001081163.1	Fw	GGAGATCCTGGAGTGGGAGT
			Rv	TCCGCTGTAAACACCAGGTC
<i>Chsy3</i>	<i>Mus musculus</i>	NM_001081328.1	Fw	CCTCATATCGGCGAATGCCT
			Rv	GAGTAAAGCAGCTTCCCCGT
<i>Chpf2</i>	<i>Mus musculus</i>	NM_133913.2	Fw	AGGGTGAGGGAGAAGATCCC
			Rv	ATACCGAGTCCTGAGCACCT
<i>Chst3</i>	<i>Mus musculus</i>	NM_016803.3	Fw	GATCGGAGTCGTGGGTAGGA
			Rv	GCTGCTGTGGGAAAGTTGTG
<i>Chst7</i>	<i>Mus musculus</i>	NM_021715.1	Fw	CCCAACATTGAGGGAGACCC
			Rv	GTCTCGGAAGAGTTGCACCA
<i>Chst11</i>	<i>Mus musculus</i>	NM_021439.2	Fw	TTCCAAAGTATGTTGCACCCAG
			Rv	GCGTGAACCTTGTTGCGGTAG
<i>Chst13</i>	<i>Mus musculus</i>	NM_027928.1	Fw	CATGGGAAGACGCTCCTGTT
			Rv	TTTTCAAATGCGGGACGCAG
<i>Gapdh</i>	<i>Mus musculus</i>	NM_001289726.1	Fw	CCCTTAAGAGGGATGCTGCC
			Rv	ACTGTGCCGTTGAATTTGCC
<i>Timp-1</i>	<i>Mus musculus</i>	NM_001044384.1	Fw	CACACCAGAGCAGATACCAT
			Rv	CCCTTATGACCAGGTCCGAG
<i>Timp-2</i>	<i>Mus musculus</i>	NM_011594.3	Fw	CTCGGAGCGCAATAAAACGG
			Rv	CCTCTTGATGGGGTTGCCAT
<i>Timp-3</i>	<i>Mus musculus</i>	NM_011595.2	Fw	CCCTTGGCCACTTAGTCCTG
			Rv	ATGCAGGCGTAGTGTTTGGGA
<i>Timp-4</i>	<i>Mus musculus</i>	NM_080639	Fw	GGAGGAGTCCTGGAGGGGCT
			Rv	AAGC ATTTTCCCTC CAGGTT
<i>Mmp-2</i>	<i>Mus musculus</i>	NM_008610.2	Fw	ACAACAGCTGTACCACCGAG
			Rv	AGCTCCTGGATCCCCTTGAT
<i>Mmp-9</i>	<i>Mus musculus</i>	NM_013599.3	Fw	TCTAGGCCAGAGGTAACCC
			Rv	GTGCCTGTCACAAAAGCCAG
<i>Mmp-12</i>	<i>Mus musculus</i>	NM_008605.3	Fw	TTGTGTTCTTACAGGTATCTGCC
			Rv	TCTTGACAAGTACCATTACAGCAAAT

<i>Mmp-14</i>	<i>Mus musculus</i>	NM_008608.3	Fw	CGCGCTCTAGGAATCCACAT
			Rv	TTTCATGTCCCTCCCGGAT
<i>Adamts-1</i>	<i>Mus musculus</i>	NM_009621	Fw	TTGCACTCGC TAGAAAGCAG
			Rv	TATTTACAAA AACAAA
<i>Adamts-4</i>	<i>Mus musculus</i>	NM_172845.2	Fw	CATCCTACGCCGGAAGAGTC
			Rv	AAGGTGAGTGCTTCGTCTGG
<i>Adamts-5</i>	<i>Mus musculus</i>	NM_011782.2	Fw	AAGAAGGTCGCACACGCTTA
			Rv	AAGACCAGGCTGTGAGAAGC

### 3.1.1 Tissue isolation

I isolated brain tissue in ice-cold phosphate-buffered saline (PBS) after quickly decapitating the animals. Then, I dissected and quickly froze specific brain regions on dry ice and stored them at -80°C until further use. I isolated and stored the right hippocampi of all animals for RNA extraction and downstream processing.

### 3.1.2 RNA extraction, cDNA conversion, and qPCR

I extracted total RNA from the frozen right hippocampi by using the EURx GeneMatrix DNA/RNA Extracol kit (Roboklon Cat. No. E3750) according to the manufacturer's recommendations (Ventura Ferreira *et al.*, 2018). Then, I checked the yield, purity, and integrity of RNA products with Nano-drop and gel electrophoresis respectively, to confirm the absence of genomic DNA. Furthermore, I converted 1.5 µg of RNA to cDNA by using the High-Capacity cDNA Reverse Transcription Kit (Cat.4368814). For qPCR analysis of cDNA products, I used the TaqMan gene expression array (Cat. 4331182) from Thermo-Fisher Scientific and the Quant-Studio-5 device from Applied Biosystems (Table 3.1). Overall, I analyzed twenty-four genes comprising five CSPG genes namely *Acan*, *Bcan*, *Ncan*, *Vcan*, and *Pcan*, two genes coding for the link proteins *Hapln1* and *Tnr*, and eight genes coding for the enzymes necessary for glycosylation and sulfation of CSPG GAGs that are *Chpf2*, *Chsy1*, *Chsy3*, *Chst3*, *Chst7*, *Chst11*, and *Chst13*. Furthermore, seven genes for major metalloproteases degrading neural ECM proteins, namely; *Mmp-2*, *Mmp-9*, *Mmp-12*, *Mmp-14*, *Adamts-1*, *Adamts-4*, and *Adamts-5*, in addition to four genes coding for the tissue metalloprotease inhibitors *Timp-1*, *Timp-2*, *Timp-3* and *Timp-4* were also analyzed. All gene targets were

analyzed relative to the expression of glyceraldehyde 3-phosphate dehydrogenase (*Gapdh*) (Meldgaard *et al.*, 2006). I did not find any difference in the mRNA levels of *Gapdh* between 2-3M, 24-26M, and >30M mice, making it a suitable candidate for the normalization of other genes.

### 3.2 3.2.3 FACS technology

Table 3.2 Buffers and solutions for FACS technology

Buffer	Composition
Low-sucrose buffer (LSB)	5mM CaCl <sub>2</sub> -Applichem A3652,0500, 320mM sucrose-Applichem A4737,5000, 0.1mM EDTA-Invitrogen AM9260G, 5mM MgAc <sub>2</sub> - Sigma M5661-250G, 10mM HEPES pH 8 - Gibco 15630-056, 1mM DTT – Roth 6908.2, 0.1% Triton X-100 – Sigma T8787, 1x EDTA free Roche protease inhibitor cocktail - Sigma 5056489001, RNase inhibitor (Promega N2615)
High-sucrose buffer (HSB)	3mM MgAc <sub>2</sub> , 1mM DTT, 1000mM Sucrose, 10mM HEPES pH 8, protease inhibitor, RNase inhibitor (Promega N2615)
Resuspension buffer; PBS containing Tween-20 and BSA (PBTB)	1% BSA, 0.2% Tween-20, EDTA-free protease inhibitor dissolved in 1X PBS, RNase inhibitor (Promega N2615)

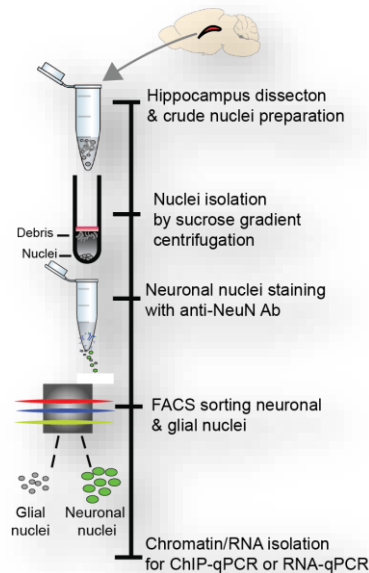


Figure 3.1: FACS Strategy

### 3.2.1 FACS sorting for neuronal and glial nuclei extraction

Next, I collaborated with Sadman Sakib from DZNE Goettingen to use fluorescence-activated cell sorting (FACS) technology to sort hippocampal cells with the nuclei extraction protocol (NeuN antibodies) into neurons and glia. For this experiment, I dissected hippocampi from four 2-3M and four 22-24M mice, flash froze and kept them at  $-80^{\circ}\text{C}$  until further use. Sakib adopted the nuclei extraction protocol from (Halder et al., 2016) with slight modifications. He homogenized the right frozen hippocampi in Low-sucrose buffer (Table 3.2). He then spun down nuclei by centrifuging at  $2000 \times g$  for 3 minutes at  $4^{\circ}\text{C}$ . The remaining crude nuclear pellet was re-suspended into Low-sucrose buffer and homogenized with a mechanical homogenizer (IKA Ultraturax T10). He layered the suspension on 6mL High-sucrose buffer (Table 3.2) in oak-ridge tubes and centrifuged for 10 minutes at  $3220 \times g$  at  $4^{\circ}\text{C}$ . After removing the upper phase containing myelin debris, he re-suspended the resulting nuclear pellet into the leftover buffer, then transferred it into microfuge tubes (Eppendorf DNA-low bind, 022431021) and centrifuged at  $2000 \times g$  for 3 minutes to recover the nuclear pellet. Before staining, the nuclei pellet was re-suspended into PBS containing Tween-20 and BSA (Table 3.2) and anti-NeuN-Alexa488 conjugated antibody (MAB377X) was added at 1:1000 dilution. After 1-hour incubation at  $4^{\circ}\text{C}$ , the samples were washed twice with PBS and proceeded with the sorting in BD FACS Aria III. Sorted nuclei were collected into Falcon tubes, pelleted with brief centrifugation, and pellets were used for RNA extraction by using the Trizol reagent (Sigma T9424) and RNA was kept at  $-80^{\circ}\text{C}$  until further processing.

**Table 3.3** Probes used for sorted nuclei qPCR

Gene	Species	Reference Sequence		Sequence (5' to 3')
<i>Chst3</i>	<i>Mus musculus</i>	NM_007424.2	Fw	CCACAGCAGCCAGATCTTC
			Rv	TGGGGGACACTCTGATCCT
<i>Adamts-5</i>	<i>Mus musculus</i>	NM_011782.2	Fw	CCTGGATGATGGTCATGGTA
			Rv	AGTTCCTCGGGACCCAAA
<i>Top1</i>	<i>Mus musculus</i>	NM_009408.2	Fw	TGCCTCCATCACACTACAGC
			Rv	CGCTGGTACATTCTCATCAGG

### 3.2.3.2 cDNA preparation from sorted nuclear RNA and qPCR

Next, RNA concentrations were measured from the sorted nuclei in Qubit 2.0 (Invitrogen) using an RNA high sensitivity kit. Three ng of RNA were used to prepare cDNA using SMART-Seq v4 Ultra Low Input Kit (Takara). Following cDNA preparation, equal amounts of cDNA were subjected to qPCR using primers (designed by Roche universal probe library tool) for *Chst3* and *Adamts-5* mRNA. A standard curve was generated to calculate primer efficiency, which was used to obtain normalized expression value (delta-delta Ct method), using DNA topoisomerase I (*Top1*) as housekeeping gene (Penna *et al.*, 2011).

### 3.3 Immunohistochemistry (IHC) and Immunocytochemistry (ICC)

**Table 3.4** Primary antibodies and their dilutions

Antibody/Reagent	Dilution	Species	Provider
Aggrecan (ACAN)	1:300	Rabbit	Millipore; AB1031
Brevican (BCAN)	1:500	Guinea pig	LIN, Magdeburg (Prof. C.Seidenbecher)
Neurocan (NCAN)	1:500	Guinea pig	Synaptic System; 453 004
Versican (VCAN)	1:200	Mouse	The Developmental Studies Hybridoma Bank, 12C5
Phosphacan (PCAN)	1:200	Mouse	The Developmental Studies Hybridoma Bank, 3F8
Parvalbumin	1:500	Chicken	Synaptic System; 195006
MAP2	1:500	Chicken	Abcam; ab5543
MAP2	1:200	Mouse	Millipore; MAB3418
vGLUT1	1:1000	Guinea pig	Synaptic Systems; 135304
vGAT	1:500	Rabbit	Synaptic Systems; 131002
GFP	1:100	Sheep	BioRAD; 4745-1051
pCREB	1:500	Rabbit	LIFE Technologies; MA511192
C-FOS	1:500	Rabbit	Santa Cruz; sc-52
CaMKII	1:300	Mouse	Abcam; ab22609
mADAMTS-5	1:100	Rabbit	Abcam; ab231595
hADAMTS-5	1:200	Rabbit	OriGene Technologies; TA321798
CHST3	1:200	Rabbit	Proteintech; 18242-1-AP
C6S	1:200	Mouse	Seikagaku; 270423
GFAP	1:500	Chicken	Millipore; AB5541
IBA1	1:500	Guinea pig	Synaptic Systems; 234004
CD68	1:500	Rat	AbD Serotec; MCA1957
C1q	1:1000	Rabbit	Abcam; ab182451
NeuN	1:500	Mouse	Chemicon; MAB377
OLIG2	1:200	Rabbit	Millipore; AB9610
DAPI	1:300		Life Technologies; D1306

**Table 3.5** Secondary antibodies and their dilutions

Antibody (Alexa Fluor)	Dilution	Species	Company
Anti-Rabbit	1:1000	Goat	Invitrogen
Anti-Guinea pig	1:1000	Goat	Invitrogen
Anti-Sheep	1:1000	Donkey	Invitrogen
Anti-Mouse	1:1000	Goat	Invitrogen
Anti-Chicken	1:1000	Goat	Invitrogen
Anti-Rat	1:1000	Goat	Invitrogen

**Table 3.6** Buffers and solutions for IHC

Buffer	Composition
4% paraformaldehyde (PFA) (w/v)	4 % PFA in PBS, pH 7.4
Phosphate buffer (PB)	0.1 M sodium phosphate dibasic; 0.1 M sodium phosphate monobasic
Permeabilization solution	0.4 % Triton-X 100 in PB
Blocking Solution	10 % normal goat serum (NGS) in PB, 0.4 % Glycine, 0.4 % Triton-X 100
Floating solution	Ethylene glycol, glycerin, PBS in the ratio 1:1:2

**Table 3.7** Buffer composition for ICC

Buffer	Composition
4% PFA (w/v)	4 % PFA in PBS, pH 7.4
Permeabilization solution	0.1 % Triton-X 100 in PBS
Blocking Solution	10 % normal goat serum in PBS, 0.1 % Glycine, 0.4 % Tween 20

### 3.3.1 Immunohistochemistry

Deeply anesthetized mice were perfused with ice-cold PBS, and fixed with 4% PFA in PBS. Then, I extracted mice brains and kept them immersed in 4% PFA overnight before cryoprotecting in 30% sucrose for 48 hours. Finally, I chilled the brains in 100% 2-methyl butane at -80°C before sectioning into 50- $\mu$ m thick coronal sections. I maintained the sections in a floating solution at 4°C (Table 3.6). Using one section per animal for each staining, I washed the sections 3 times in 120 mM PB at a pH of 7.2 for 10 minutes and then permeabilized the sections in a permeabilization solution for 10 minutes at room temperature. I blocked the sections with a blocking solution for 1 hour at room temperature (Table 3.6). After blocking, I incubated the sections with primary antibodies (Table 3.4) at 37°C for 20 hours, washed 3 times in PB for 10 minutes,

followed by secondary antibodies (Table 3.5) at room temperature for 3 hours, and afterward also washed 3 times in PB for 10 minutes. Finally, I mounted the sections on Superfrost glasses with Fluoromount (Sigma, F4680), and then confocal images were taken.

### 3.3.2 Immunocytochemistry

I fixed cultured hippocampal neurons by incubating them in 4% paraformaldehyde (PFA) for 10 minutes, then permeabilized them in a permeabilization solution for 10 minutes, washed them 3 times, and blocked them for 60 minutes at room temperature (Table 3.4). Next, the blocked cells were then stained with primary antibodies (Table 3.4) at 4°C overnight, washed 3 times with PBS for 10 minutes, and incubated with secondary antibodies (Table 3.5) at room temperature for 1.5 hours. After secondary antibody staining, coverslips were finally mounted for imaging.

## 3.4 Generation, characterization and stereotaxic injection of hADAMTS-5 AAVs

**Table 3.9** Buffer composition for AAV production

Buffer	Composition
Wash buffer 1	20 mM Tris, 100 mM NaCl, pH 8.0; sterile filtered
Wash buffer 2	20 mM Tris, 250 mM NaCl, pH 8.0; sterile filtered
Elution buffer	20 mM Tris, 500 mM NaCl, pH 8.0; sterile filtered

### 3.4.1 Generation of pAAV\_hPGK\_hADAMTS5\_T2A\_eGFP and pAAV\_hPGK\_eGFP

With the help of Dr. R. Kaushik in the lab of Prof. A. Dityatev at the DZNE, constructs to overexpress hADAMTS-5 were designed and plasmids were produced by a company (VectorBuilder Inc. USA). I produced, purified, and titrated viral particles together with Mrs. Katrin Boehm at the DZNE. In brief, the human ADAMTS-5 (GeneID: NM\_007038.5) sequences under the human phosphoglycerate kinase (hPGK) promoter tagged with the enhanced green fluorescent protein (EGFP) was inserted into the mammalian gene expression AAV vector (VB191122) (pAAV[Exp]-hPGK\_hADAMTS5[NM\_007038.5]/T2A/EGFP, hereafter referred to as pAAV\_hPGK\_hADAMTS5\_T2A\_EGFP) (VB191122-1897eux). Furthermore, the control vector which included the hPGK and the EGFP tag inserted into the mammalian gene expression AAV vector (VB191122) (pAAV[Exp]-

hPGK>EGFP, hereafter referred to as pAAV\_hPGK\_EGFP) (VB191122-1902dpv) were developed. These vectors were delivered in *Escherichia coli* (E. coli) stocks and I used them for the production of recombinant adeno-associated particles as described previously (McClure et al., 2011). Here, I transfected HEK 293T cells using PEI (1ng/ $\mu$ l) with an equimolar mixture of the pAAV\_hPGK\_hADAMTS5\_T2A\_EGFP or pAAV\_hPGK\_EGFP, pHelper (Cell Biolabs Inc., San Diego, CA, USA). Then, 48-72 hours after transfection, I implemented the freeze-thaw cycles to lyse cells and treated them with benzonase (50 U/mL; Merck Millipore, Burlington, MA, USA) for 1 hour at 37 °C. I centrifuged the lysates at 8000 $\times$  g at 4 °C, then collected the supernatants, and filtered with a 0.2-micron filter. I then purified the filtrates using the pre-equilibrated HiTrap Heparin HP affinity columns (GE HealthCare, Chicago, IL, USA), followed by washing with the following buffers in sequence; wash buffer 1 followed by wash buffer 2 and then eluted viral particles with the elution buffer. Finally, I used the Amicon Ultra-4 centrifugal filters with 100,000 Da molecular weight cutoff (Merck Millipore, Burlington, MA, USA) along with 0.22  $\mu$ M Nalgene® syringe filter units (sterile, PSE, Sigma-Aldrich, St. Louis, MO, USA) to further purify viral particles before being aliquoted and stored at -80 °C.

### 3.4.2 Cell culture and characterization of pAAV\_hPGK\_hADAMTS5\_T2A\_EGFP and pAAV\_hPGK\_EGFP

**Table 3.8** Chemicals for Cell Cultures

Name	Company	Catalog number
Polyethyleneimine solution	Sigma-Aldrich	408727-100ml
Neurobasal medium	Life Technologies	21103049
Dulbecco's Modified Eagle's Medium (DMEM)	Life Technologies	41965062
B27	Life Technologies	17504044
L-glutamine	Life Technologies	25030-81
Pen-Strep	Sigma-Aldrich	P4333-20ML

Hippocampal neurons were isolated from embryonic C57BL6/J mice (E18), as described previously (Minge et al., 2017). After harvesting, I used polyethyleneimine-coated 18 mm coverslips (Thermo Scientific) in 12 well plates with a cell density of 150,000 per well for plating. Firstly, I plated neurons in a 1ml DMEM+, which included DMEM supplemented with 2% B27 and 1% L-glutamine and 1% Pen-Strep, for 4 hours. After 4 hours, DMEM+ was then changed to NB+ media which had the same composition as DMEM+, except for Neurobasal medium used instead of DMEM. Cultured neurons were maintained by feeding cells

with 250 $\mu$ l NB+ medium at 14 and 17 days *in vitro* (DIV). At DIV 17, I infected neurons with pAAV\_hPGK\_hADAMTS5\_T2A\_EGFP and pAAV\_hPGK\_EGFP vectors ( $4.96 \times 10^{11}$  and  $4.9 \times 10^{11}$ , respectively) and they were fixed and stained on DIV 21 (Figure 3.2A). I then investigated the proteolytic activity of hADAMTS-5 protease by staining for ACAN and BCAN around CaMKII-immunopositive or negative (CaMKII+/CaMKII-) neurons (Figure 3.2B).

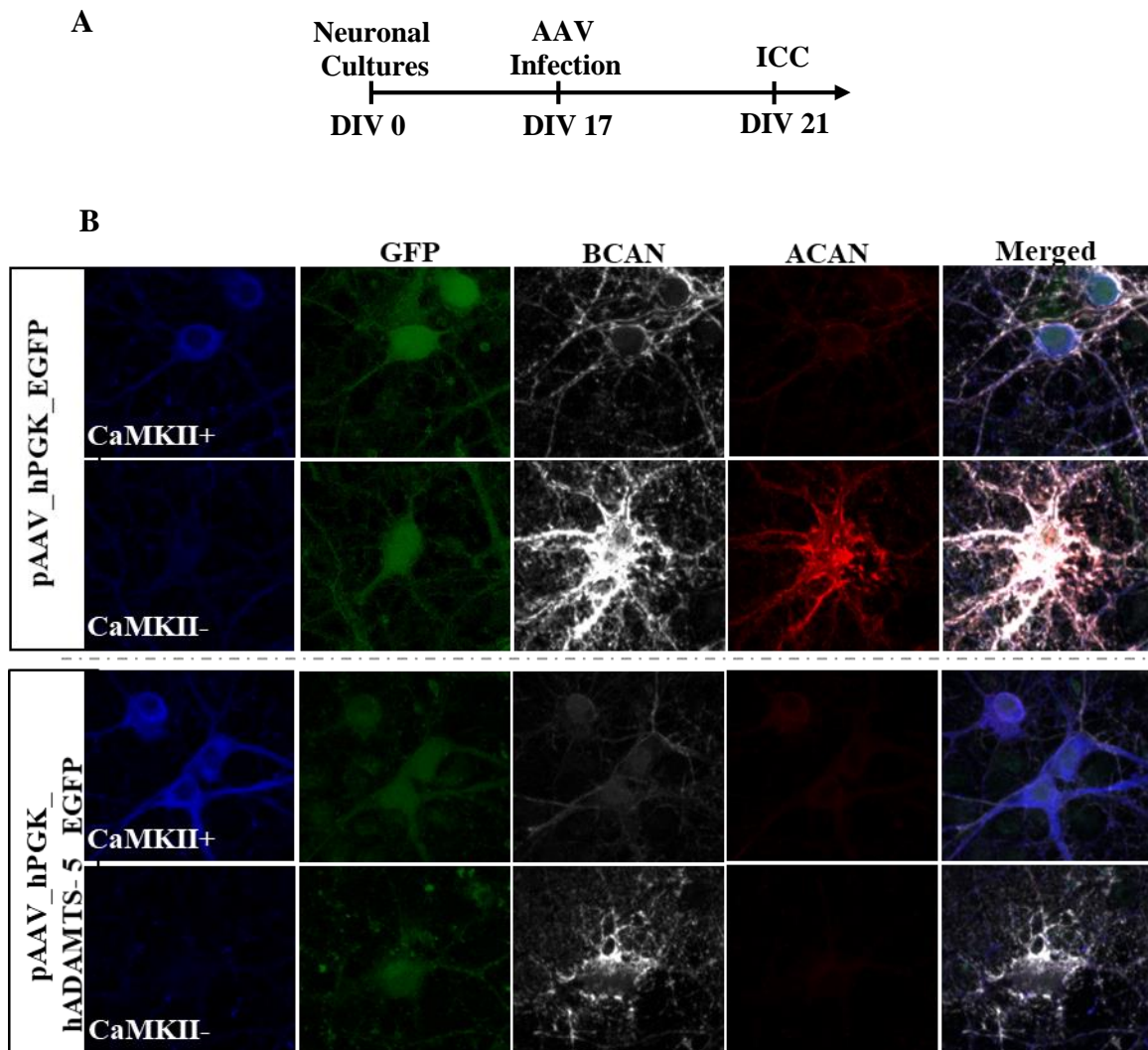


**Figure 3.2: *In vitro* proteolytic activity of hADAMTS-5 in hippocampal cultured neurons**

*In vitro* characterization of the proteolytic activity of hADAMTS-5 expressed in hippocampal neurons was performed. (A) Hippocampal neurons were infected from DIV 17 to 21, fixed and stained for major neural CSPGs. (B) Proteolytic activity of hADAMTS-5 on ACAN and BCAN was examined around CaMKII+/CaMKII- cells.

### 3.4.3 Stereotaxic injection of pAAV\_hPGK\_hADAMTS5\_T2A\_EGFP and pAAV\_hPGK\_EGFP into the hippocampal CA1

I briefly sedated fifteen 2-3M, and twenty-nine 22-24M mice with isoflurane in a chamber and fixed them in a stereotaxic frame (SR-6M, Narishige Scientific Instrument Lab, Japan). I anesthetized mice with isoflurane and adjusted its concentration to 4% for induction and then reduced to 1.5-2%, with oxygen levels set to 0.4 L/min (Baxter 250ml Ch.-B.: 17L13A31). I also maintained the body temperature of mice at 37°C by using a heating pad (ATC1000 from World Precision Instrument, USA). I applied an ophthalmic ointment (BAUSCH and LOMB) to protect the eyes during surgery after which the skin was cleaned with 70% ethanol and hair shaved. I injected viral particles at a volume of 1000 nl by using a 10 µl NanoFil syringe (World Precision Instrument, USA) and calibrated glass microelectrodes connected to an Ultra microinfusion pump (UMP3, World Precision Instrument, USA) at a rate of 3 nl/sec. The coordinates for injection were dorso-ventral (DV) from the brain surface, anterior-posterior (AP) from bregma, and medio-lateral (ML) from the midline (in mm): AP, -1.94; ML, -/+ 1.50; DV, -1.0. I injected pAAV\_hPGK\_hADAMTS5\_T2A\_EGFP ( $4.96 \times 10^{11}$ ) and pAAV\_hPGK\_EGFP ( $4.9 \times 10^{11}$ ) bilaterally into the hippocampal CA1. After all procedures, I placed the animals in a recovery chamber under red light for 15 minutes.

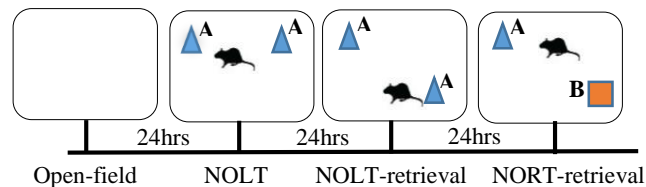


**Figure 3.3: Time-line for NOLT & NORT tests**

### 3.5 Behavioral experiments

In my thesis work, I used for behavioral experiments 27 male C57BL6/J mice in total, which included nine 2-3-month-old and eighteen 22-24-month-old mice. I have described the numbers of mice used in each experiment in the text and figure legends. All mice I used were transferred to the DZNE research facility from the DZNE animal breeding house and were housed individually with food and water available *ad libitum* for at least 72 hours before experiments under a reversed 12/12 light/dark cycle (light on 9 P.M.). I

performed all behavioral experiments during the dark phase of the cycle, i.e. when mice are active, under constant temperature and humidity. I used the Anymaze 4.99 (Stoelting Co., Wood Dale, IL, USA) to capture and analyze animals' performance during behavioral tests. Animals were subsequently tested using the open field test, the novel object location test (NOLT), and the novel object recognition test (NORT). All behavior experiments, especially after injection, were performed by a trained observer who was blinded to treatment conditions. Also, objects used for NOLT and NORT experiments as well as entry-paths used in the labyrinth test were counterbalanced for all groups of mice.

### 3.5.1 *Open field*

I put animals from each experimental group into an open field arena (50 x 50 x 30 cm) (Holter *et al.*, 2015; Kaushik *et al.*, 2018) and allowed them to freely move for 10 minutes while recording with an overhead camera. The arena was predefined into two parts, the central area (30 x 30 cm) and a peripheral area (the 10 cm area adjacent to the wall of the recording chamber). I used the total distance moved and time spent in the central/peripheral area to estimate the animal's general activity and anxiety.

### 3.5.2 *Novel object location and recognition tests*

I carried out the novel object location test in the same open-field arena. This test includes two phases: the encoding phase and the retrieval phase (Vogel-Ciernia & Wood, 2014). In the encoding phase, I permitted animals to explore the arena with a pair of identical objects for 10 minutes. Twenty-four hours later, in the retrieval phase, I gave the animals 10 minutes to explore the arena again with the same objects, except that one of them was placed in a novel position. I used the time spent exploring the objects located at familiar (F) and novel (N) positions as well as the discrimination ratio  $[(N-F)/(N+F)] \times 100\%$  to analyze animals' behavior. Next, twenty-four hours after the NOLT retrieval phase, I conducted the NORT in the open field arena containing the encoding phase and retrieval phase as described previously (Antunes & Biala, 2012; Kaushik *et al.*, 2018). In the encoding phase, I allowed animals to explore the arena with a pair of identical objects whereas, in the retrieval phase, one of the objects was replaced by a novel object that the animal had not seen before. Both the encoding and retrieval phase lasted 10 minutes. I used a similar method of analysis as described earlier to measure animals' recognition memory.

3.5.3 Labyrinth (dry maze)

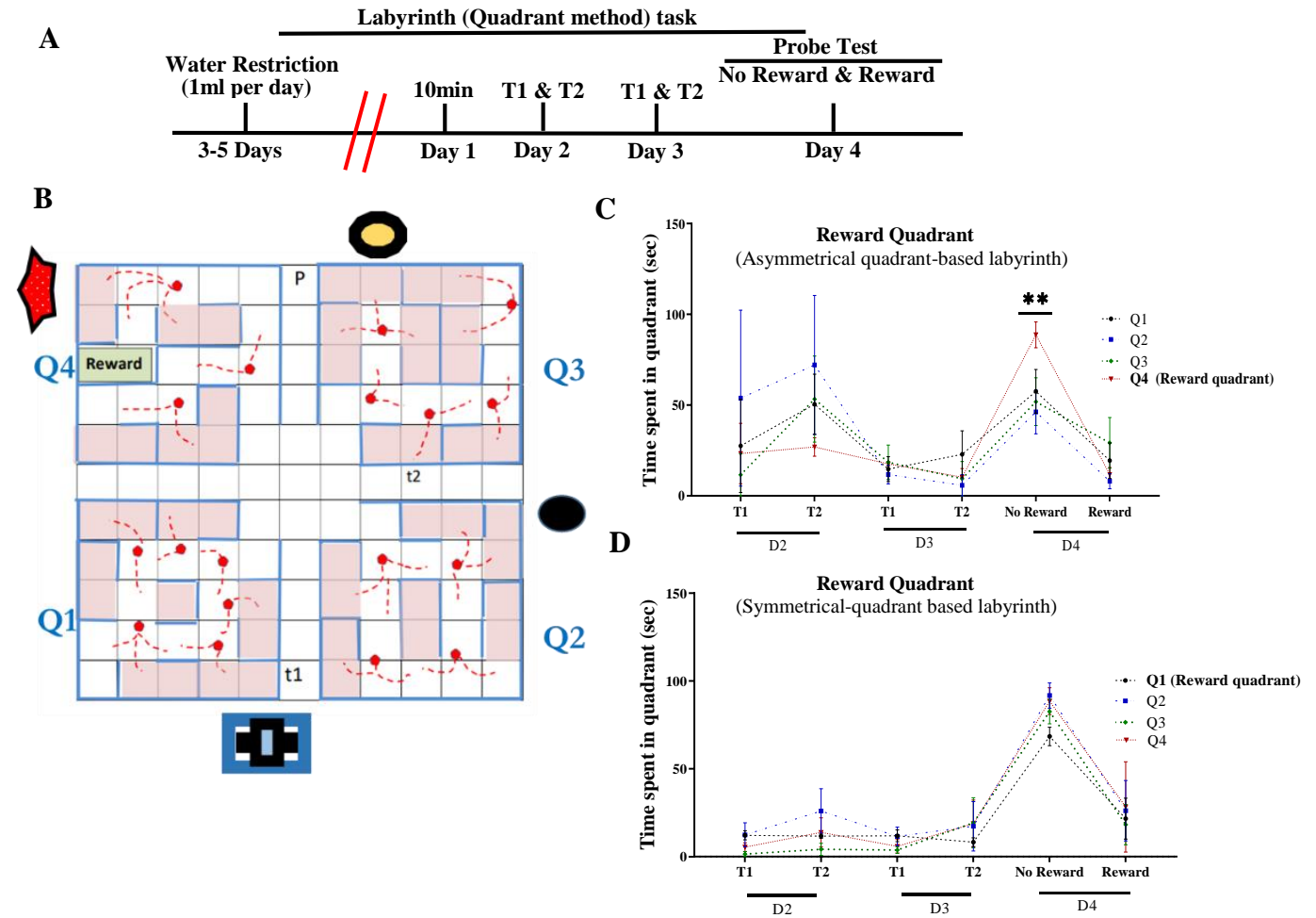


**Figure 3.4. Optimization of the quadrant-based labyrinth** **A.** Time-line for all cognitive tests **B.** Layout of asymmetrical quadrant-based labyrinth with distal cues **C.** Time spent in the asymmetrical quadrant-based labyrinth **D.** Time spent in the symmetrical quadrant-based labyrinth. All data in the graph represent mean  $\pm$  SEM values, \*\*\*P<0.001.

3.5.4 Optimization of the quadrant-based labyrinth task (dry maze)

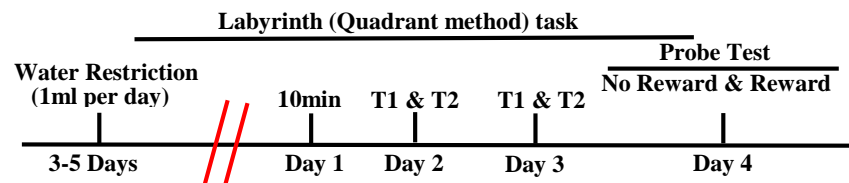
I designed a quadrant-based labyrinth task with the objective of measuring spatial learning and memory as well as spatial navigational strategies in aged mice. This task was designed and implemented as an alternative to Morris water maze (MWM) task that uses imaginary quadrants (software) compared to actual quadrants. Comparatively, the dry maze is less stressful and capable of distinguishing between navigational

strategies used by mice, namely egocentric (route) and allocentric (place) (Harrison and Feldman, 2009; Rich and Shapiro, 2007). Recent studies recommend the use of navigational errors as a more effective measure of spatial learning and memory instead of latency to reward (Maei et al., 2009a). Here I used the asymmetrical-quadrant-based labyrinth to quantify percentage errors. Initially, I made 2 different quadrants-based labyrinth configurations, namely, the symmetrical and asymmetrical configurations. I then implemented these configurations to optimize them. Therefore, I used four 10M mice to test both quadrants-based labyrinths at different time points and, surprisingly, I found the asymmetrical quadrant-based labyrinth to better measure spatial navigation (learning and memory) than the symmetrical quadrant-based labyrinth. The symmetrical quadrant-based labyrinth failed to differentiate between time spent in the reward quadrant relative to other quadrants, especially during the probe test without reward (Figure 3.4D). For both symmetrical and asymmetrical quadrants-based labyrinth, I restricted mice to 1ml of water per day (for a maximum of 5 days), which I dispensed in the labyrinth room. I designed the labyrinth with three entry-paths and divided the maze into quadrants of equal size but with different intra-quadrant configurations (for asymmetrical quadrant) and similar intra-quadrant configurations (for symmetrical quadrant) (Figure 3.4A&B).

In each quadrant configuration, I defined the zones to quantify errors (shown by pink highlights). As outlined above, I carried out the quadrants-based labyrinth task with distal cues placed on curtains to enclose the maze and the reward (water) placed in a particular quadrant (which can be changed for the reversal-learning task). This is because studies show that distal cues are essential for the allocentric form of spatial navigation in mice (Vorhees and Williams, 2014). The quadrants-based labyrinth experiment was categorized into two phases of memory tests: the memory acquisition phase and the probe phase. With the memory acquisition phase, I used two entry-paths (E1 and E2) for all daily training sessions from day 1 (D1) to day3 (D3), whereas the probe path (P) was used for the probe phase on day 4 (D4) (Figure 3.4A&B). On D1, I allowed mice to explore the maze for 10 minutes with a reward. From subsequent training sessions, I performed 2 trails per day for 2 days (T1 & T2 for day2 & day3), and each trial ended once each mouse entered into the reward zone. I implemented an inter-trial delay of 1 hour for each daily training session. On the fourth day (D4), I performed the 2-phase probe test sequentially, namely; 1<sup>st</sup> probe test without reward followed by an hour delay, and finally 2<sup>nd</sup> probe test with reward. For both probe tests, I allowed mice to explore the maze for 5 minutes (this time can be changed without significant changes in results), but I quantified mice performance with the first approach of the reward. Using an overhead camera with animal tracking software (Anymaze 4.99: Stoelting Co., Wood Dale, IL, USA), I recorded and quantified

parameters such as the distance travelled and errors made. However, to compare the sensitivity of symmetrical to asymmetrical quadrants-based labyrinth, I used the time spent in each quadrant during both the memory acquisition phase and the probe phase. Interestingly, during the probe test, I found the asymmetrical quadrant-based labyrinth to be more efficient in quantifying the cognitive performance of mice (Figure 3.4C&D).

**A**



**B**

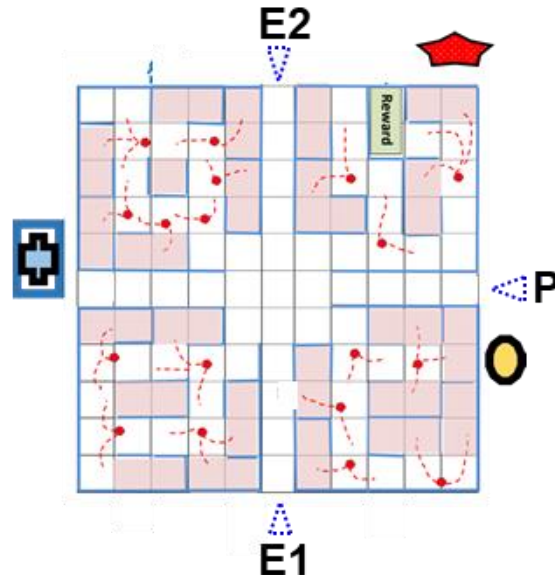


**Figure 3.5. Asymmetrical quadrant-based labyrinth**

**A.** Time-line for all cognitive tests **B.** Layout of asymmetrical quadrant-based labyrinth with distal cues.

### 3.5.5 Asymmetrical-quadrant-based labyrinth task

Next, I used the asymmetrical-quadrant-based labyrinth to study hippocampus-dependent spatial learning and memory in mice injected with AAV. Here, I followed the behavioral paradigm described above with minor modifications to further complicate the learning process and promote the use of allocentric strategy.

Such modifications include alternation between the entry-paths and trial sessions for each mouse during the memory acquisition phase. That is, the entry-path used by each mouse during a particular training session was changed in subsequent training sessions. I implemented the alternation of entry-paths from the 1<sup>st</sup> training session on D2 to the last training session on D3. Additionally, during the memory acquisition phase, I counterbalanced the entry-paths for all groups. All measurement for each session was limited to the first entry into the reward location for both the memory acquisition phase and the probe phase. Therefore, I used two measures, the errors made and distance travelled by each mouse to estimate the spatial navigational learning and memory performance of each mouse as they explored the maze locate the reward (water). I also measured the level of familiarity of mice to the maze after their first encounter with the maze, by comparing the total number of errors made on day 1 and the first training session on day 2.

Finally, from the 2-phase probe test, I estimated the degree of memory stabilization by matching the performance of each mouse between the 1<sup>st</sup> and 2<sup>nd</sup> probe tests. The percentage difference (Memory stabilization (%)) was then calculated. The following formulas were then used:

$$1. \text{ Memory Stabilization (\%)} = \frac{\left( \frac{(\text{Er}_{nR} - \text{Er}_R)}{(\text{Er}_{nR} + \text{Er}_R)} \right)}{\text{(Errors made)}} \times 100$$

$\text{Er}$  = errors made

$\text{Er}_{nR}$  = errors made in probe test without reward

$\text{Er}_R$  = errors made in probe test with reward

$$2. \text{ Memory Stabilization (\%)} = \frac{\left( \frac{(\text{Dt}_{nR} - \text{Dt}_R)}{(\text{Dt}_{nR} + \text{Dt}_R)} \right)}{\text{(Distance travelled)}} \times 100$$

$\text{Dt}$  = Distance travelled

$\text{Dt}_{nR}$  = Distance travelled in probe test without reward

$\text{Dt}_R$  = Distance travelled in probe test with reward

### 3.6 Microscopy and image analysis

#### 3.6.1 Confocal microscopy, High-resolution imaging, image acquisition, processing, and analysis

Confocal images in this thesis were obtained with the Zeiss LSM 700 microscope (1024x1024 pixels display resolution, 8-bit dynamic range, 63X (NA 1.40) and 40X (NA 1.30) oil objectives, 0.5 X optical zoom, pixel size app. 60 nm). I took images with the 63X or 40X objective as z-stacks. Usually, 20-25 optical sections were taken with an average depth of 25  $\mu\text{m}$  and a two-time line average. I used maximum intensity projections from each fluorescence channel from the image stack for image analysis. I also used the open software Image J (NIH, <http://rsb.info.nih.gov/ij/>) to further process and analyze images. I implemented a novel semi-automatic open-source Fiji-script co-developed in DZNE by me and Dr. Rahul Kaushik to perform individual quantifications. Overall, 12 and 18 sections from 2-3M and 22-24M mice respectively, were used for the IHC analysis. Sections from six 2-3M and seven 22-24M mice were used for CHST3, mADAMTS-5, and C6S staining. Furthermore, six and five respective sections from 2-3M and 22-24M mice injected with pAAV\_hPGK\_GFP, together with six sections from pAAV\_hPGK\_hADAMTS-5\_GFP injected mice were used for hADAMTS-5, ACAN, BCAN, NCAN, VCAN, and PCAN staining. They were also used for the glial fibrillary acidic protein (GFAP), allograft inflammatory factor 1 (IBA1), oligodendrocyte transcription factor (OLIG2), pCREB, c-FOS, and presynaptic: vesicular glutamate transporter (vGLUT1) and vesicular GABA transporter (vGAT)) staining. I maintained the acquiring conditions throughout all imaging sessions to compare the fluorescence intensity between samples for each staining.

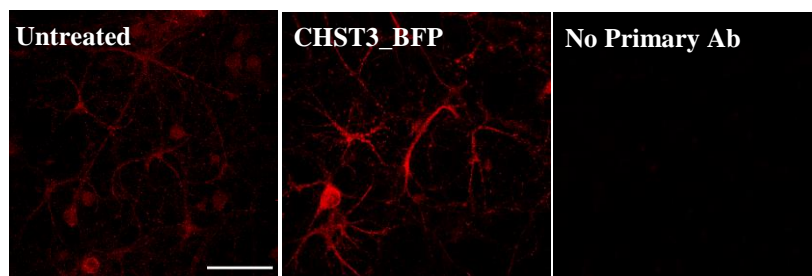


**Figure 3.6. Validation of CHST3 antibody specificity**

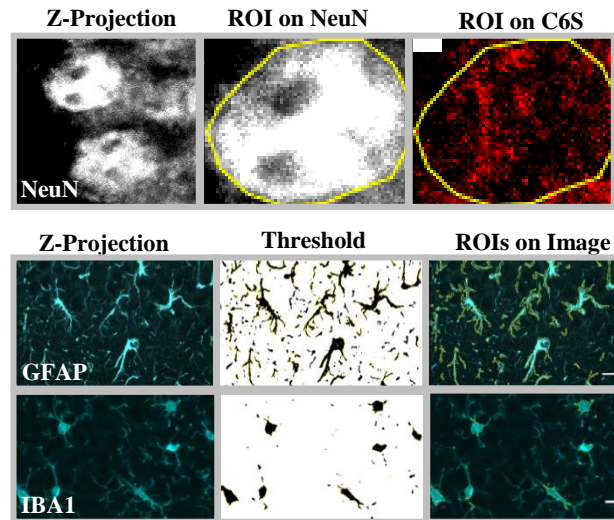


**Figure 3.7. Cell-type-specific quantifications**

### 3.6.2 Cell-type specific analysis

For CHST3 staining, I first confirmed the specificity of the antibody in hippocampal neuronal and astrocytes cultures infected with CHST3 overexpressing vectors, which showed a stronger immunolabelling than control cultures (Figure 3.6). Then, I processed and analyzed images by using a modified version of previously developed Fiji-scripts (Strackeljan et al., 2021). For cell-type-specific quantification of the expression of specific molecules (CHST3 and mADAMTS-5), I thresholded, identified, and outlined astrocytes and microglia by using the GFAP and IBA1 channels, respectively. This approach was also used for all GFAP and IBA1 measurements. However, for neuronal expression using NeuN antibody, a manual outlining of cell approach was used (Figure 3.7).

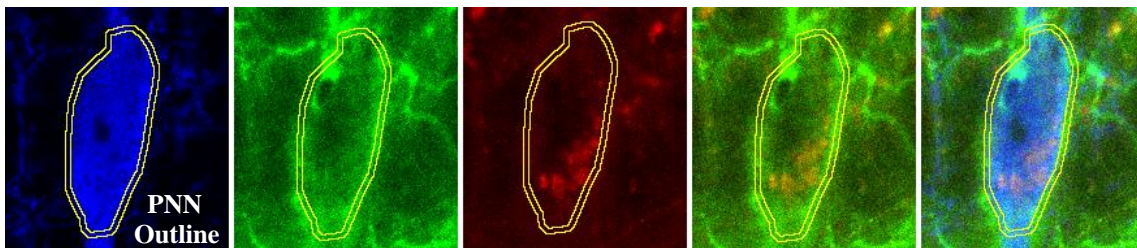


**Figure 3.8. Perineuronal net measurements**

### 3.6.3 *Perineuronal and synaptic puncta analysis*

Analysis of images with C6S, ACAN, BCAN, NCAN, VCAN, and PCAN immunostainings was done by measuring the perineuronal expression of ECM. With this measurement, I manually outlined the soma of PV- and PV+ cells, and a band of 0.6  $\mu\text{m}$  was then created as the region of interest (ROI) to measure protein levels of the aforementioned ECM targets (Figure 3.8). For the quantification of the perisomatic expression of vGLUT1+ and vGAT+ puncta on PV+ cells, I outlined manually the profiles of the cell somata and created a band of 1.5  $\mu\text{m}$  as the region of interest (ROI). The bands were duplicated, cleared outside, background-subtracted with the rolling value of 50, and filtered using Gaussian blur with s-value of 1. Synaptic puncta were detected using “find maxima” plugin in Fiji with a prominence of 5, the size of 0.3 to 1.0  $\mu\text{m}^2$  and the circularity between 0.5 and 1.0. I measured the mean intensity along with the number of synaptic puncta.

### 3.6.4 *Analysis of PV-network configuration*

Analysis of PV expression in PV+ cells was performed using z-maximum projection of 5 confocal images collected using the 40x objective with 1  $\mu\text{m}$  interval, in which PV+ cells were manually outlined. Then, I measured the mean intensity of PV signals and normalized it to soma size. Next, I studied the PV-network configurations by following the “operational” definitions of 4 classes of PV+ cells previously described by Donato and colleagues (Donato et al., 2013). Following these definitions, I categorized the PV intensity of PV+ cells, after normalizing to soma size, into approximately 0-5% (low), 5-30% (interlow), 30-80% (interhigh), and from 80% (high) for young mice and then applied the same thresholds to measurements performed in aged ADAMTS-5 and control mice.

### 3.6.5 *GluN2B staining and image analysis*

Slice fixation was performed using 4% PFA in PBS (137 mM NaCl, 2 mM  $\text{KH}_2\text{PO}_4$ , 10 mM  $\text{Na}_2\text{HPO}_4$ , 2.7 mM KCl, pH 7.4), for 40 minutes at room temperature, followed by quenching for 30 minutes using 100 mM  $\text{NH}_4\text{Cl}$  (dissolved in PBS). Permeabilization was performed using 0.3% Triton X (#9005-64-5, Merck, Germany) for 15 minutes, in presence of 2.5% bovine serum albumin (BSA; #A1391-0250; Applichem, Germany), as a blocking reagent. Primary antibodies were then added overnight, in the same buffer (against GluN2B, Neuromab, 75-101). Two additional labels were used, a nanobody for PSD95

(FluoTag-X2 anti-PSD95 conjugated to AZDye™ 568, Nanotag Biotechnologies GmbH, Germany) and phalloidin (conjugated to iFluor 488, ab176753, Abcam, USA). Secondary nanobodies were also added, to reveal the primary antibodies (FluoTag®-X2 anti-Mouse Immunoglobulin kappa light chain, conjugated to Abberior STAR 635P, Nanotag Biotechnologies GmbH, Germany). The samples were then washed, 3 times for 5 minutes in the same buffer, followed by high-salt PBS (same as above, but with 500 mM NaCl), and finally by a normal PBS wash. The samples were then embedded in Mowiol (Calbiochem, USA). Stimulated emission depletion (STED) microscopy was performed using the Leica TCS SP5 microscope (Leica Microsystems, Wetzlar, Germany) and a  $\times 100$  1.4 NA HCX PL APO CS oil-immersion objective (Leica). Phalloidin was excited using an Argon laser line at 488 nm and PSD95 was excited using a helium-neon laser line at 543 nm. The appropriate emission windows were obtained using acousto-optic tunable filters, and detection was performed using hybrid detectors (Leica). Abberior STAR 635P was excited using diode laser at 635 nm. Stimulated emission depletion was obtained using a 750 nm beam (Spectra-Physics MaiTai multiphoton laser, Newport Spectra-Physics, USA), and the photons were detected using an avalanche photodiode (Leica). Data analysis for GluN2B staining was performed by identifying the synapses in the PSD95 channel, using an empirically set threshold, and analyzing the fluorescence in the vicinity of the PSD95 spots, using macros written in Matlab (version R2017b, The Mathworks, Natick, MA, USA).

### 3.7 Electrophysiological experiments

**Table 3.9** Solutions for in vitro electrophysiology

<b>Solution</b>	<b>Composition (in mM)</b>
Slice cutting solution	240 sucrose, 2 KCl, 2 MgSO <sub>4</sub> , 1.25 NaH <sub>2</sub> PO <sub>4</sub> , 26 NaHCO <sub>3</sub> , 1 CaCl <sub>2</sub> , 1. MgCl <sub>2</sub> , and 10 D-glucose.
Storage solution	113 NaCl, 2.38 KCl, 1.24 MgSO <sub>4</sub> , 0.95 NaH <sub>2</sub> PO <sub>4</sub> , 24.9 NaHCO <sub>3</sub> , 1 CaCl <sub>2</sub> , 1.6 MgCl <sub>2</sub> , 27.8 D-glucose
Artificial cerebrospinal fluid (ACSF)	120 NaCl, 2.5 KCl, 1.5 MgCl <sub>2</sub> , 1.25 NaH <sub>2</sub> PO <sub>4</sub> , 24 NaHCO <sub>3</sub> , 2 CaCl <sub>2</sub> and 25 D-Glucose

LTP recordings were carried out in collaboration with Hadi Mirzapourdelavar (DZNE Magdeburg). Acute hippocampal slices were prepared from mice with AAV injected into the hippocampal CA1 area, as described before (Kochlamazashvili et al., 2010b). After killing mice by cervical dislocation and decapitation, hippocampal transverse 350  $\mu\text{m}$ -thick slices were prepared in sucrose-based ice-cold cutting solution (Table 3.9) using the vibrating microtome (VT1200S, Leica). Slices then were transferred and incubated in a submerged chamber containing storage solution (Table 3.9) for at least 2 hours at room temperature before recording. Next, slices were transferred to a recording chamber and were continuously perfused with the ACSF (2-3 ml/min) (Table 3.9). All solutions were saturated with 95%  $\text{O}_2$  and 5%  $\text{CO}_2$  with osmolality maintained at  $300 \pm 5$  mOsm. Thin glass electrodes filled with ACSF were used for stimulation and recording of fEPSPs. CA1 pyramidal neurons were identified with an infrared differential interference contrast microscope (Slicescope, Scientica, UK). The stimulation intensity was determined based on the input-output curve and was set to give fEPSPs with a slope of  $\sim 30\%$  and  $\sim 50\%$  of the supramaximal fEPSP for the paired-pulse facilitation (PPF) and LTP induction, respectively. In the CA3-CA1 pathway, single stimuli were repeated every 20 seconds for at least 10 minutes for baseline recording before and for 60 minutes after LTP induction. Theta-burst stimulation (TBS) was applied two times with 20 seconds interval as 8 bursts of four pulses delivered at 100 Hz repeated with 200 ms inter-burst-intervals to induce LTP. The paired-pulse ratio (PPR) was evaluated at different time intervals under the same conditions. All recordings were obtained at room temperature using an EPC-10 amplifier (HEKA Elektronik). The recordings were filtered at 1–3 kHz and digitized at 10-20 kHz. For pharmacological analysis, 3  $\mu\text{M}$  RO25 (Ro 25-6981) was added to the recording solution (ACSF).

### 3.8 Statistical analysis

I used RStudio 1.4.1106 software for data management and statistical analysis along with GraphPad Prism 7.0 (GraphPad Software Inc., La Jolla, USA). All data are shown as mean  $\pm$  SEM with  $n$  being the number of samples per each mouse and  $N$  being the number of mice. Asterisks in figures indicate statistical significance (with details in the figure legends or results). The hypothesis that experimental distributions follow the Gaussian law was verified using Kolmogorov-Smirnov, Shapiro-Wilk, or D'Agostiniov tests. For pairwise comparisons, I performed the Students t-test where the samples qualify for the normality test; otherwise, the Mann-Whitney test was employed. Additionally, Wilcoxon matched-pairs test was used for paired comparisons that did not pass the normality test. The Holm-Sidak's t-test and Dunn's test were used to correct for multiple comparisons. As indicated, one- and two-way ANOVA with uncorrected Fisher's

LSD as well as Brown-Forsythe with Welch ANOVA tests were also used, when appropriate. For skewed data, the Kruskal-Wallis test was implemented. Additionally, cumulative frequency distribution analysis was used once the p-value for one-way ANOVA showed a tendency toward. The Kolmogorov-Smirnov test was used to compare cumulative frequency distributions. The p-values represent the level of significance as indicated in figures by asterisks (\* $p < 0.05$ , \*\* $p < 0.01$ , \*\*\* $p < 0.001$  and \*\*\*\* $p < 0.0001$ ) unless stated otherwise.

## 4 RESULTS

The results of my thesis are in two parts, that is, an exploratory side and an intervention side. The exploratory aspects address the mechanism behind aged-dependent ECM protein accumulation in the hippocampus and identify potential targets to reverse this accumulation associated with aging. The intervention side reports on the structural changes after the hippocampal ECM remodelling of the aged mice and their functional correlates.

### 4.1 Increased ECM protein levels in the aged brains do not correlate with mRNA levels of CSPG core-proteins

#### 4.1.1 *Expression of CSPG core-proteins and enzymes regulating synthesis and sulfation of GAG chains in the hippocampus of 22-24 and >30M old mice*

In the aged brain, several major neural ECM proteins have been reported to be upregulated (Vegh et al., 2014), and this has been associated with an age-dependent cognitive decline as well as reduced synaptic plasticity (Koskinen et al., 2020; Richard et al., 2018). However, as the mechanism behind the reported ECM upregulation in the aged brain is still not clear, I aimed at investigating the relationship between the reported ECM protein expression and transcription of ECM-related genes using RT-qPCR. Therefore, I studied the mRNA changes of ECM-related genes including CSPG core-proteins and modifying enzymes in three age groups, namely, the 2-3 months (M), 22-24M, and the > 30M old mice. Surprisingly, I observed a downregulation in the mRNA levels of the CSPG core-proteins *Acan*, *Bcan*, *Vcan*, and *Ncan* in >30M mice by more than 30% compared to 2-3M old mice (37%, 35%, 32%, and 48%, respectively), alternatively, this was not the case in 22-24M old mice. Additionally, the gene for the link protein *Hapln1* was equally reduced in >30M old mice to about 38%, with no difference observed for the glycoprotein gene *Tnr* (Figure 4.1.1A). Similar to the CSPG core-protein expression, I found a reduction in mRNA levels of glycosylation and sulfation genes, with *Chsy3*, *Chst3*, and *Chst11* reduced to about 41%, 50%, and 33%, respectively. However, no significant reduction was observed for *Chsy1*, *Chpf2*, *Chst7*, and *Chst13* (Figure 4.1.1B). Furthermore, the mRNA levels of *Acan*, *Bcan*, *Vcan*, *Ncan*, *Hapln1*, and *Tnr* did not change in 22-24M old mice compared to 2-3M old mice (Figure 4.1.1C).

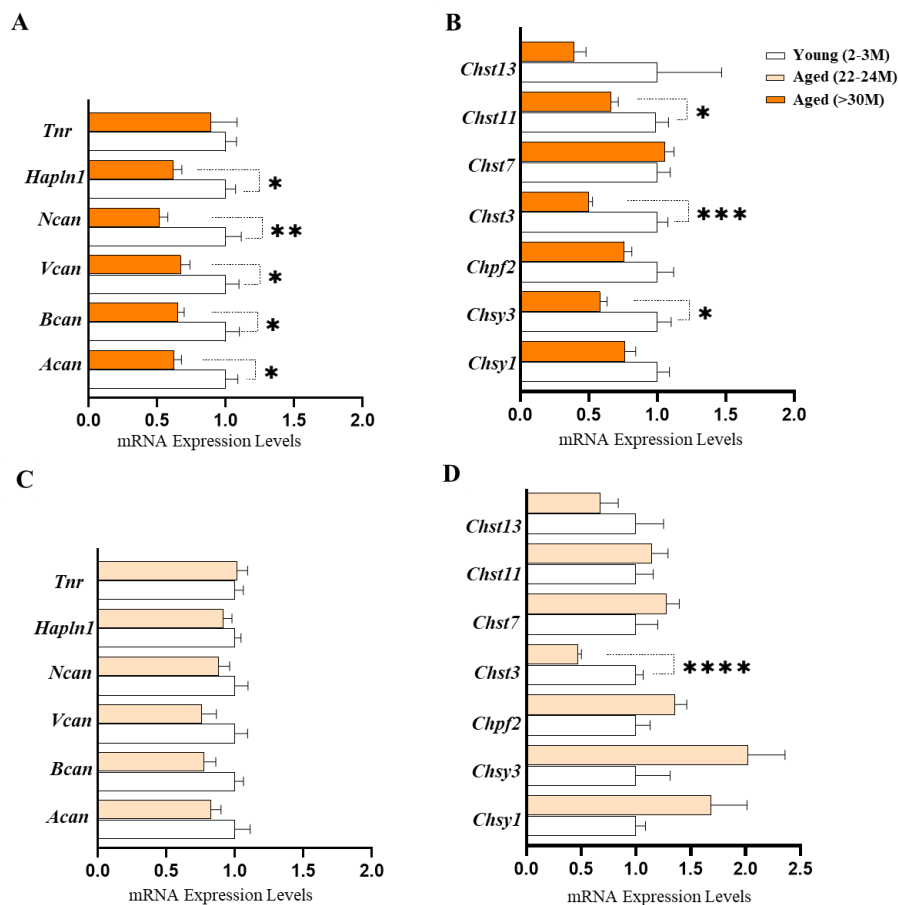


**Figure 4.1.1 Expression of CSPG core-proteins and enzymes regulating synthesis and sulfation of GAG chains in the hippocampus of 22-24 and >30M old mice.**

(A) The mRNA expression of the core proteins of major components of PNNs except for *Tnr* were downregulated in >30M old mice compared to 2-3M old mice. Bar graph shows mean  $\pm$  SEM values; Holm-Sidak's multiple comparisons t-test \* $p < 0.05$ , \*\* $p < 0.01$ , and \*\*\* $p < 0.001$  (2-3M old mice: N=10 and >30M old mice: N=9).

(B) The glycosylation enzyme *Chsy3* along with *Chst3* and *Chst11* were downregulated in >30M old mice relative to 2-3M old mice. Bar graph shows mean  $\pm$  SEM values; Holm-Sidak's multiple comparisons t-test \* $p < 0.05$  and \*\*\* $p < 0.001$  (2-3M old mice: N=10 and >30M old mice: N=9).

(C) The gene expression of PNN components was not different between 22-24M old mice and 2-3M old mice. Bar graph shows mean  $\pm$  SEM values; Holm-Sidak's multiple comparisons t-test (2-3M old mice: N=10 and 22-24M old mice: N=10).

(D) Furthermore, the gene expression of glycosylation and sulfation enzymes, except for *Chst3*, were not different between 22-24M old mice and 2-3M old mice. Bar graph shows mean  $\pm$  SEM values; Holm-Sidak's multiple comparisons t-test \*\*\*\* $p < 0.0001$  (2-3M old mice: N=10 and 22-24M old mice: N=10).

Furthermore, I detected no difference in the mRNA levels of *Chsy1*, *Chsy3*, *Chst7*, *Chst11*, and *Chst13*. Surprisingly, *Chst3* that encodes for the chondroitin 6-O-sulfotransferase-1, which catalyzes 6-sulfation of CSPG GAGs in the hippocampus (Mikami and Kitagawa, 2013b), was reduced to about 52% in 22-24M old mice, similar to levels found in >30M old mice (Figure 4.1.1D). This was the only ECM-related gene whose expression profile was consistent between 22-24M and >30M old mice, suggesting *Chst3* might be an interesting candidate to better understand the aged-dependent changes in ECM protein levels. Collectively, the data suggest that the age-associated negative feedback mechanisms might be involved in regulating the expression levels of CSPG core-proteins and glycosylating and sulfating enzymes to counteract their accumulation.

#### 4.1.2 Reduced *Adamts-5* expression in the hippocampus of 22-24 and >30M old mice

Since there was no correspondence between the mRNA levels of ECM-synthesizing genes and the reported ECM protein levels in 22-24 and >30M old mice, I then checked the mRNA levels of major ECM-degrading enzymes. I observed no difference in the mRNA levels of matrix metalloproteinases *Mmp-2*, *Mmp-9*, *Mmp-14*, *Adamts-1*, and *-4* in >30M old mice. However, compared to 2-3M old mice *Mmp-12* was upregulated by 80-fold in the hippocampus of >30M old mice (Figure 4.1.2A). This protease, in particular, has a unique substrate preference, which is mostly elastin and is highly active during inflammation (Liu et al., 2013). In contrast to the mRNA pattern of *Mmp-12*, the major CSPG protease in the hippocampus, *Adamts-5*, was downregulated to about 30% in >30M old mice (Figure 4.1.2A). I explored further to see if aging might have an impact on other regulatory factors of ECM degrading enzymes. Therefore, I checked the mRNA levels of tissue inhibitors of metalloproteinases (TIMPs) because it is known that a disturbance in the balance of TIMP/MMP and TIMP/ADAMTS results in a number of pathologies (Brew and Nagase, 2010). I found that the *Timp-1* gene, a major inhibitor of MMP-9, was upregulated to about 4.5-fold whereas *Timp-3* was downregulated by about 45% in >30M old mice (Figure 4.1.2B). Similar outcomes were observed in 22-24M old mice regarding MMPs, ADAMTS, and TIMPs gene expression with *Adamts-5* reduced by about 29%. One exception, however, was that *Timp-2* and *-3* were upregulated with *Timp-3*, a major inhibitor of ADAMTS-5, increased by about 38% (Figure 4.1.2C and 4.1.2D). These findings together suggest that the reported age-dependent increase in ECM-protein levels might be due to the accumulation of CSPGs due to reduced expression and activity of degrading enzymes. This is as a result of the age-dependent dysregulation in the mRNA levels of *Adamts-5* coupled with a potential increase in the inhibition of its proteolytic activity via increased expression of *Timp-3*. Therefore, I selected 22-24M old mice to be the appropriate age to further elucidate the compromised ECM proteolysis.

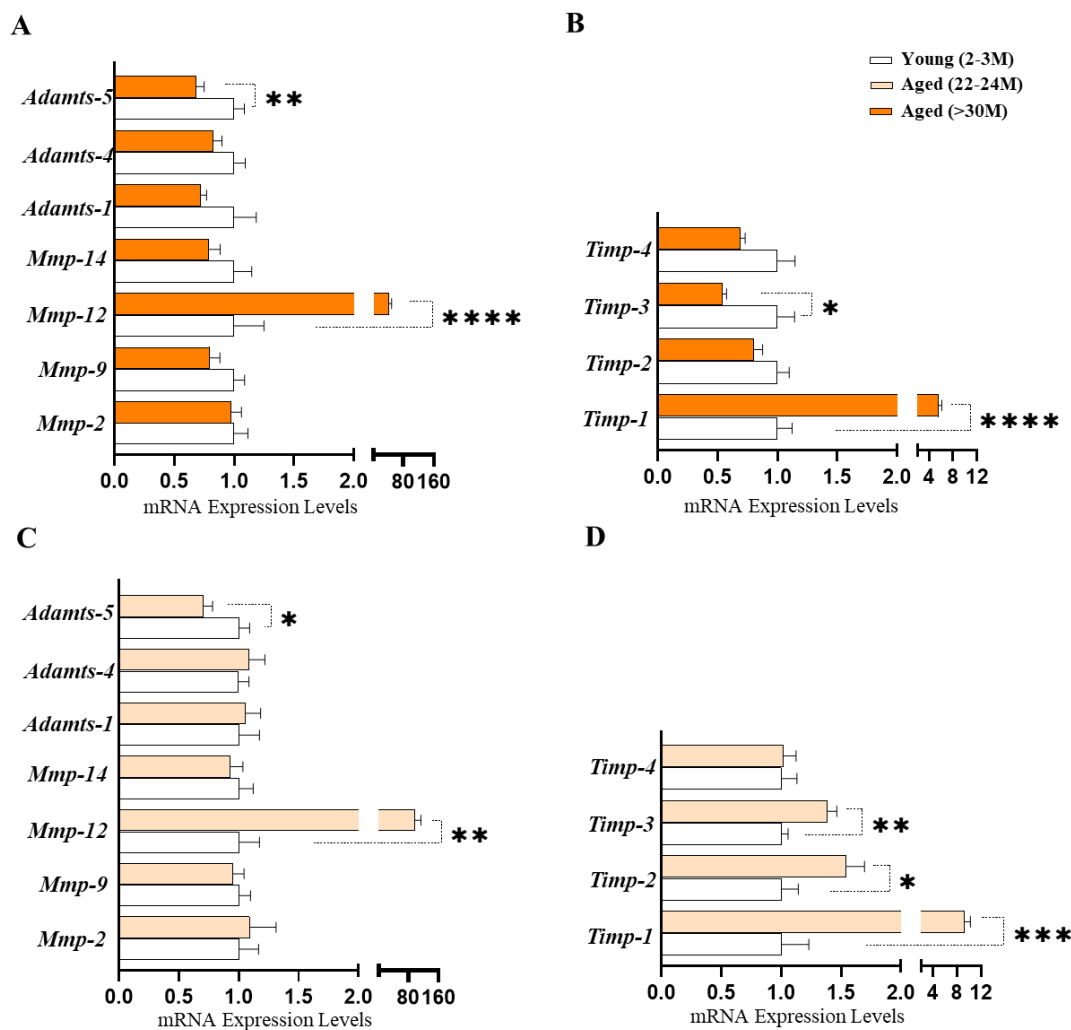


**Figure 4.1.2 Reduced *Adamts-5* expression in the hippocampus of 22-24 and >30M old mice.**

(A) The mRNA expression levels of major ECM proteases, *Mmps* and *Adamts*, were not different between >30M old mice and 2-3M old mice baring *Mmp-12* (upregulated) and *Adamts-5* (downregulated). Bar graph shows mean  $\pm$  SEM values; Holm-Sidak's multiple comparisons t-test \*\* $p < 0.01$  and \*\*\* $p < 0.001$  (2-3M old mice: N=10 and >30M old mice: N=9).

(B) Further analysis shows that *Timp-1* and -3 were upregulated and downregulated respectively, in >30M old mice relative to 2-3M old mice. Bar graph shows mean  $\pm$  SEM values; Holm-Sidak's multiple comparisons t-test \* $p < 0.05$  and \*\*\*\* $p < 0.0001$  (2-3M old mice: N=10 and >30M old mice: N=9).

(C) Similar expression profiles for both *Mmps-12* and *Adamts-5* were found in 22-24M old mice compared to 2-3M old mice. Bar graph shows mean  $\pm$  SEM values; Holm-Sidak's multiple comparisons t-test \* $p < 0.05$  and \*\* $p < 0.01$  (2-3M old mice: N=10 and 22-24M old mice: N=10).

(D) Regarding *Timp* gene expression in 22-24M old mice, all *Timps* were upregulated except for *Timp-4*. Bar graph shows mean  $\pm$  SEM values; Holm-Sidak's multiple comparisons t-test; \* $p < 0.05$ , \*\* $p < 0.01$ , and \*\*\* $p < 0.001$  (2-3M old mice: N=10 and 22-24M old mice: N=10).

### 4.1.3 Cell-specific reduction of *Adamts-5* and *Chst3* in the hippocampus of 22-24M old mice

Next, I dissected the effect of aging on the cell-specific expression of *Adamts-5* in the hippocampus of 22-24M old mice. I collaborated with Sadman Sakib from DZNE Goettingen to use FACS technology to sort hippocampal cells with the nuclei extraction protocol (NeuN antibodies) into neurons and glia. With this approach, I found that NeuN+ cells were reduced in 22-24M old mice compared to 2-3M old mice contrary to the glia proportion (Figure 4.1.3B). Furthermore, using the chromatin immunoprecipitation (ChIP) technique, we discovered that the reduced *Adamts-5* mRNA levels in 22-24M old mice came from both neurons and glia. Here, about a 50% reduction of *Adamts-5* was observed in both neurons and glial cells (Figure 4.1.3C). Further analysis of the sorted samples revealed that the aforementioned downregulation of *Chst3* in 22-24M old mice is glia-specific (Figure 4.1.3D).

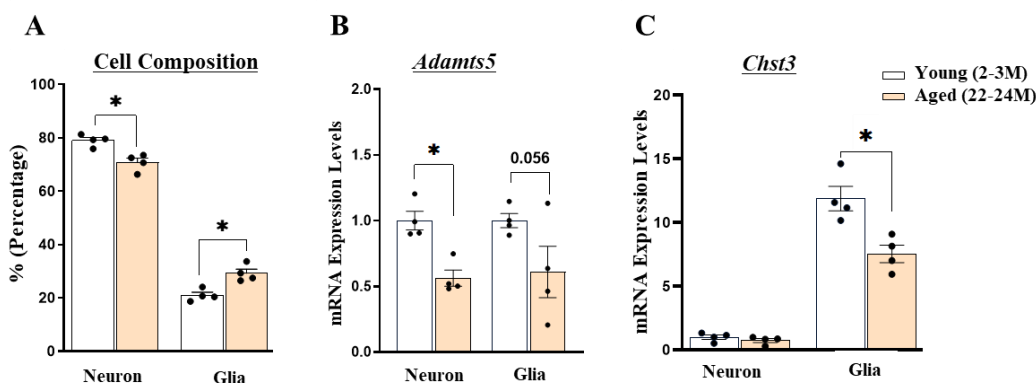


**Figure 4.1.3 Cell-specific reduction of *Adamts-5* and *Chst3* in the hippocampus of 22-24M old mice.**

Using FACS techniques with neuron-specific NeuN-antibody conjugated to Alexa Fluor 488, the cell-specific changes of *Adamts-5* and *Chst3* during aging were investigated in neurons and glia of the hippocampus of 22-24M old mice and 2-3M old mice. (A) Therefore, the percentages of neurons and non-neuronal cells (mostly glia) within 22-24M old mice and 2-3M old mice were compared. Bar graph shows mean  $\pm$  SEM values; Holm-Sidak's multiple comparisons t-test; \* $p < 0.05$  (2-3M old mice:  $N=4$  and 22-24M old mice:  $N=4$ ).

(B) *Adamts-5* mRNA levels were significantly and modestly reduced in neurons and glia, respectively in 22-24M old mice compared to 2-3M old mice. Bar graph shows mean  $\pm$  SEM values; Two-way mixed ANOVA (Age:  $F=13.74$ ,  $p=0.003$ ); Holm-Sidak's post hoc test, \* $p < 0.05$  (2-3M old mice:  $N=4$  and 22-24M old mice:  $N=4$ ).

(C) Meanwhile, *Chst3* was downregulated only in glia of 22-24M old mice. Bar graph shows mean  $\pm$  SEM values; Due to difference in variability between cell types, Holm-Sidak's multiple comparisons t-test was used instead of two-way ANOVA; \* $p < 0.05$  (2-3M old mice:  $N=4$  and 22-24M old mice:  $N=4$ ).

#### 4.1.4 Cell-specific increase in ADAMTS-5 and CHST3 expression in the hippocampus of 22-24M mice

To prove that the reduced *Adamts-5* expression and the increased mRNA levels of its inhibitor, *Timp-3*, in the hippocampus are the potential causes of the age-dependent increase in ECM protein levels, I used IHC to elucidate the cell-specific expression of ADAMTS-5 proteins. Therefore, I stained for mouse ADAMTS-5 and checked for the cell-specific expression in neurons, astrocytes, and microglia by using MAP2, GFAP, and IBA1 antibodies (Figure 4.1.4.1A, 4.1.4.1B and 4.1.4.1C, respectively). I quantified ADAMTS-5 expression by using masks generated from MAP2, GFAP+, and IBA+ cells to measure the mean intensity of ADAMTS-5 signals. Surprisingly, I found an increase in the protein levels of mouse ADAMTS-5 in neurons, astrocytes, and microglia cells in the hippocampus of 22-24M old mice compared to 2-3M old mice. Then, I also used IHC to quantify the protein levels of CHST3 in neurons, astrocytes, and microglia in the hippocampus of 22-24M old mice. In glia, CHST3 levels were measured using masks created from GFAP+ and IBA1+ cells, whereas neurons in the pyramidal layer were manually outlined using NeuN signals (Figure 4.1.4.2A, 4.1.4.2B and 4.1.4.2C). Similar to the ADAMTS-5 protein expression pattern, especially in glia, there was an increase in the protein levels of CHST3 in GFAP+ and IBA+ cells. However, no difference in neurons was detected (Figure 4.1.4.2D). This finding was contrary to the observed mRNA levels.

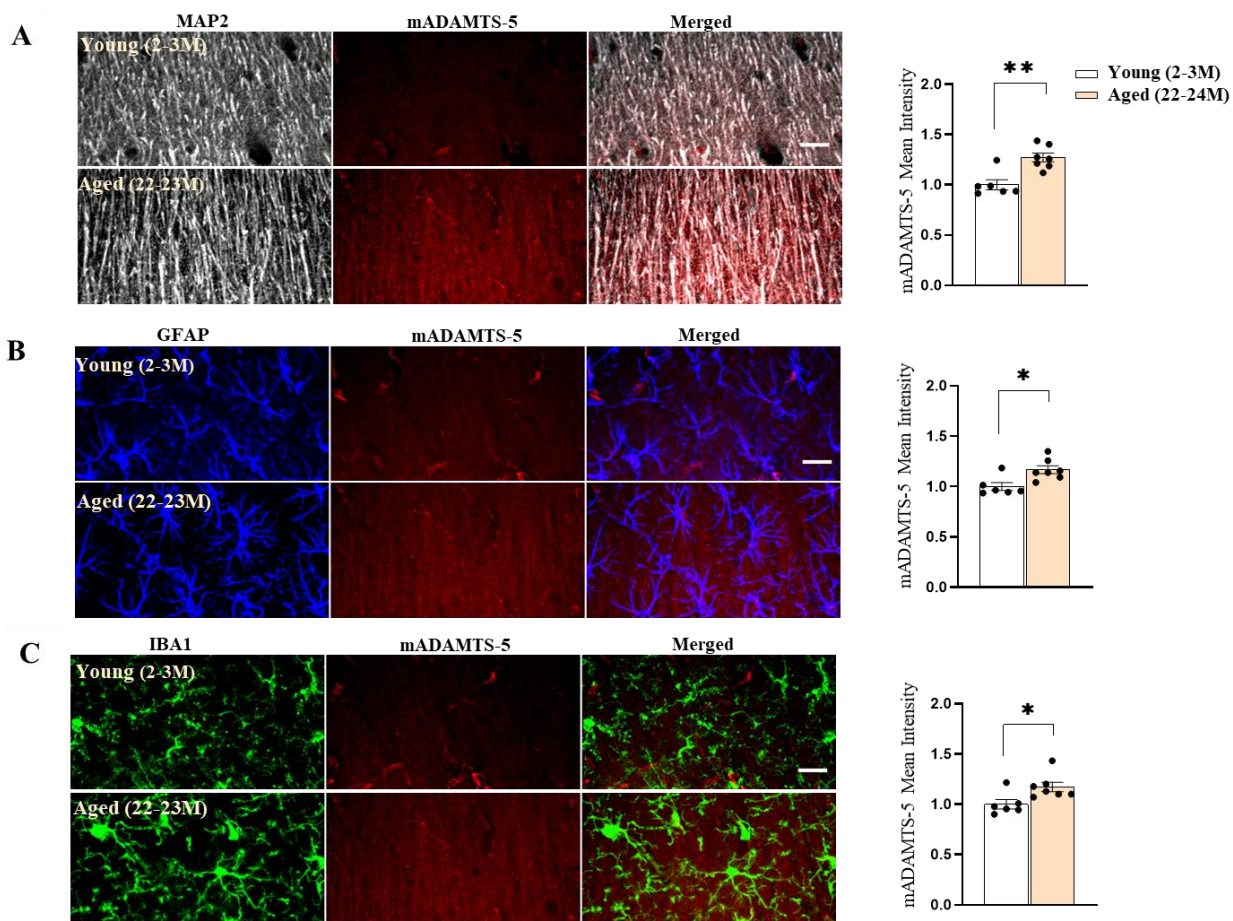


**Figure 4.1.4.1 Cell-specific increase in ADAMTS-5 protein levels in the hippocampus of 22-24M mice.**

ADAMTS5 protein levels were quantified in the hippocampus of 2-3M old mice and 22-24M old mice using IHC. **(A)** Using MAP2, mouse ADAMTS-5 (mADAMTS-5) protein was upregulated in neurons of 22-24M old mice relative to 2-3M old mice (Scale bar 20 $\mu$ m). Bar graph shows mean  $\pm$  SEM values; Unpaired t-test; Welch's correction  $**p < 0.01$  (2-3M old mice: N=6 and 22-24M old mice: N=7).

**(B)** Additionally, mADAMTS-5 protein was upregulated in astrocytes of 22-24M old mice compared to 2-3M old mice (Scale bar 20 $\mu$ m). Bar graph shows mean  $\pm$  SEM values; Unpaired t-test with Welch's correction,  $*p < 0.05$  (2-3M old mice: N=6 and 22-24M old mice: N=7).

**(C)** Analysis of IBA1+ cells showed that mADAMTS-5 protein was also upregulated in microglia of 22-24M old mice relative to 2-3M old mice (Scale bar 20 $\mu$ m). Bar graph shows mean  $\pm$  SEM values; Unpaired t-test with Welch's correction,  $*p < 0.05$  (2-3M old mice: N=6 and 22-24M old mice: N=7).

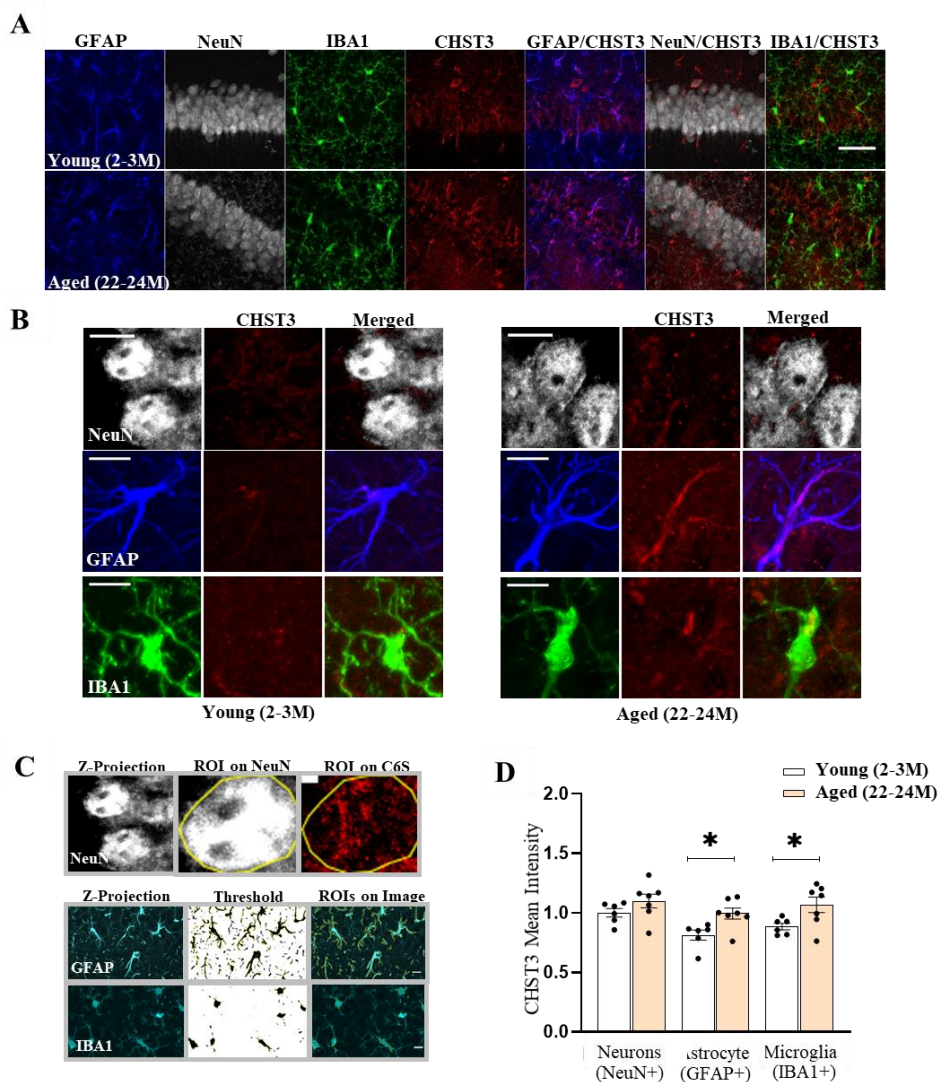


**Figure 4.1.4.2 Cell-specific increase in CHST3 protein levels in the hippocampus of 22-24M mice.**

(A) CHST3 protein levels were quantified in neurons, astrocytes, and microglia by using NeuN, GFAP, and IBA1 antibodies respectively; in the hippocampus of 2-3M old mice and 22-24M old mice (scale bar, 50 $\mu$ m).

(B) Zoomed confocal images CHST3 staining (Scale bar 50  $\mu$ m)

(C) Method of selecting cells.

(D) The mean intensity of CHST3 was increased in astrocytes and microglia but not in neurons of 22-24M old mice compared to 2-3M old mice. Bar graph shows mean  $\pm$  SEM values; Holm-Sidak's multiple comparisons t-test; \* $p < 0.05$  (2-3M old mice: N=6 and 22-24M old mice: N=7).

#### 4.1.5 Reduced activity of CHST3 and ADAMTS-5 in the hippocampus of 22-24M old mice

Since CHST3 and ADAMTS-5 protein levels were in direct contrast to their mRNA levels, I then checked for their functionality in aged animals by labelling the core proteins of the CSPG, VCAN, and the chondroitin 6 sulfates with the VCAN and C6S antibodies (Figure 4.1.5A). This is because recent data suggest that VCAN is the major carrier of 6-O-sulfates (Chelini et al., 2021) as well as having unique ADAMTS-5 cleavage sites (Demircan et al., 2014). Having quantified VCAN protein levels in a 0.6µm proximity around PV+ cells, I observed a significant increase in VCAN levels in 22-24M old mice. This finding confirmed the reports of increased ECM protein levels in the hippocampus of aged mice. Additionally, the increase in VCAN core-proteins, as reported for the first time by this study, suggests potential impairment of ADAMTS-5 activity in aged mice. Furthermore, when C6S protein levels were normalized to VCAN core-proteins, I found a reduction in C6S intensity in 22-24M old mice, indicating a reduced functionality of CHST3 in these animals (Figure 4.1.5B).

To better understand the potential targets for the abrogation of the age-dependent changes in ECM-related genes in the hippocampus, I summarized the mRNA and protein expression patterns. As shown in Figure 4.1.5C, a picture that includes no change in the expression of CSPG core-proteins and modifying enzymes, except for *Chst3*, was observed. Also, no difference was found for the ECM proteases, with the exception of the major ECM protease, *Adamts-5*. Both *Chst3* and *Adamts-5* were reduced in 22-24M old mice. Interestingly, a relationship between these two enzymes has been reported earlier by Miyata and Kitagawa, where they show that high 6-O-sulfated CSPGs are readily cleaved by ADAMTS-5 (S. Miyata and Kitagawa, 2016). Summarizing my IHC findings, I found that in the hippocampus of 22-24M old mice, both CHST3 and ADAMTS-5 protein levels are contradictory to their mRNA levels. However, it is likely that these enzymes have reduced functionality since I detected no increase in 6-O sulfation and increased levels of VCAN core-proteins in 22-24M old mice. Therefore, both major changes in gene and protein expression of CHST3 and ADAMTS-5 point to impaired ECM proteolysis in the aged hippocampus.

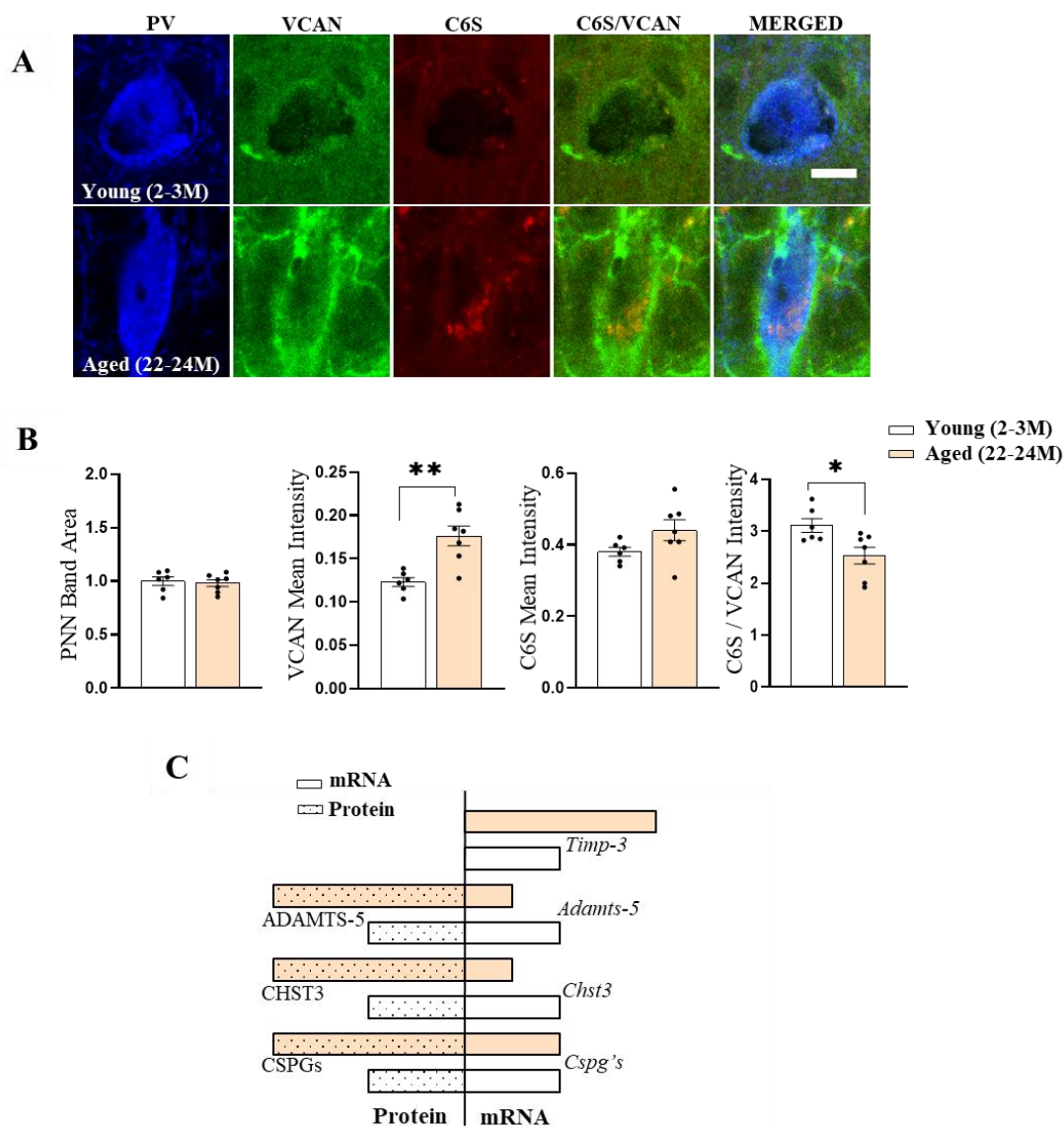


**Figure 4.1.5 Reduced activity of CHST3 and ADAMTS-5 in the hippocampus of 22-24M old mice.**

(A) Using C6S (red) and VCAN (green) antibodies, the perineuronal content of 6-O sulfated GAGs around PV+ cells (blue) in the hippocampus of 2-3M old mice and 22-24M old mice were investigated (Scale bar 20  $\mu$ m).

(B) VCAN core-proteins increased with the respective reduction of 6-O sulfated GAGs in 22-24M old mice relative to 2-3M old mice. Bar graphs show mean  $\pm$  SEM values; Unpaired t-test with Welch's correction, \* $p < 0.05$  and \*\* $p < 0.01$  (2-3M old mice: N=6 and 22-24M old mice: N=7).

(C) Summary of mRNA and protein expression patterns.

## 4.2 ECM remodelling by overexpressing hADAMTS-5 in the hippocampus of 22-24M old mice

### 4.2.1 Increased ECM cleavage by hADAMTS-5 in the hippocampus of 22-24M old mice and in hippocampal cultures

Having identified an age-dependent reduction in the expression of ECM-related genes and increased protein levels of ADAMTS-5 along with its compromised functionality, I overexpressed the human ADAMTS-5 in the hippocampus of 22-24M old mice. This approach was adopted to potentially override the existing age-dependent brakes due to neural ECM accumulation. Before delivering AAV *in vivo*, I first characterized the efficiency of the developed pAAV\_hPGK\_hADAMTS-5\_EGFP vectors in hippocampal neuronal cultures. I infected hippocampal cells with the pAAV\_hPGK\_hADAMTS-5\_EGFP on DIV 17, for 3 days. Then, the cells were fixed and stained with antibodies against the major known substrates of ADAMTS-5, that is, ACAN and BCAN. I found that after 3 days of infection, ACAN and BCAN were extensively cleaved by the hADAMTS-5 protease, indicating a promising proteolytic efficiency (Figure 3.2). Then, I injected the pAAV\_hPGK\_hADAMTS-5\_EGFP vectors into the hippocampal CA1 of 22-24M old mice (hereafter referred to as aged ADAMTS-5) and the control vectors, pAAV\_hPGK\_EGFP into aged-matched mice as well as into 2-3M old mice (hereafter referred to as aged control and young, respectively). I studied these mice using IHC, hippocampus-dependent cognitive tests, and electrophysiological experiments to characterize the structural and functional changes after long-term expression of hADAMTS-5 and continuous cleavage of CSPGs (Figure 4.2.1A). Using a human ADAMTS-5 specific antibody, I evaluated the levels of hADAMTS-5 expression two weeks and ten weeks after AAV injection. The time-dependent expression of the pAAV\_hADAMTS-5 vectors was quantified in the targeted CA1 region. There was a significant upregulation of hADAMTS-5 in aged ADAMTS-5 mice compared to aged control and young mice (Figure 4.2.1B and 4.2.1C). There was no difference in hADAMTS-5 expression between two weeks and ten weeks after injection in aged ADAMTS-5 mice. Additionally, I monitored the bodyweight of injected animals and observed no change in body weight between two weeks and ten weeks after injection, indicating no systemic detrimental effects of AAV delivery (Figure 4.2.1D). Therefore, I studied the structural and physiological effects of acutely cleaving ECM in the hippocampus of 22-24M old mice.

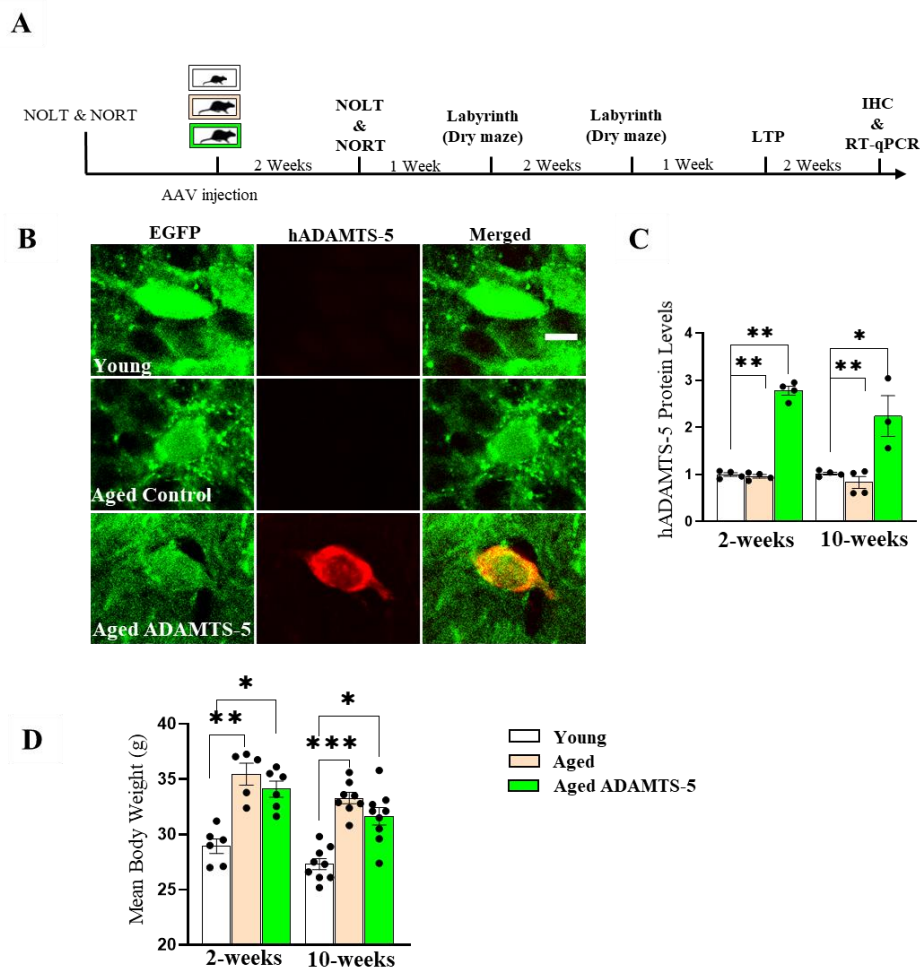


**Figure 4.2.1 Validation of hADAMTS-5 expression in the hippocampus of 22-24M old mice injected with the pAAV\_hPGK\_hADAMTS-5\_EGFP and pAAV\_hPGK\_EGFP.**

**(A)** Timeline for remodelling ECM in the hippocampus of 22-24M old mice.

**(B)** Maximum protection of confocal images of hippocampal sections of test groups labelled with the human ADAMTS-5 antibody (red) (Scale bar 10  $\mu$ m).

**(C)** Comparison of the time-dependent expression (2 weeks and 10 weeks) show no difference ( $p=0.226$ ) in the protein levels of hADAMTS-5 in aged ADAMTS-5 mice. Bar graph shows mean  $\pm$  SEM values; Two-way mixed ANOVA (*Group*:  $F=88.60$ ,  $p<0.0001$ ); Holm-Sidak's post hoc test, \* $p < 0.05$  and \*\* $p < 0.01$  (Young mice:  $N=4$  and  $4$  for 2 and 10 weeks, respectively; Aged mice:  $N=4$  and  $4$ ; Aged ADAMTS-5 mice:  $N=4$  and  $3$ ).

**(D)** Analysis of body weight shows no detrimental effects of AAV delivery in all test groups. Bar graph shows mean  $\pm$  SEM values; Two-way mixed ANOVA (*Group*:  $F=42.97$ ,  $p<0.0001$ ); Holm-Sidak's post hoc test, \* $p < 0.05$ , \*\* $p < 0.01$ , and \*\*\* $p < 0.001$  (Young mice:  $N=6$  and  $9$  for 2 and 10 weeks, respectively; Aged mice:  $N=5$  and  $8$ ; Aged ADAMTS-5 mice:  $N=6$  and  $9$ ).

#### 4.2.2 Removal of Aggrecan and Brevican in CA1, CA2, and CA3 of 22-24M old mice injected with pAAV\_hPGK\_hADAMTS5\_EGFP

To evaluate the proteolytic properties of the pAAV\_hADAMTS-5 vectors *in vivo*, I used IHC to study the expression of BCAN and ACAN core proteins in the hippocampal sections. The overexpression of hADAMTS-5 in the CA1 of aged ADAMTS-5 resulted in extensive loss of BCAN and ACAN compared to aged and young control mice. As BCAN and ACAN are major components of PNN, I then, quantified the fluorescent intensity of BCAN and ACAN in a 0.5 $\mu$ m band created around PV positive and negative neurons (PV- and PV+). As shown in Figure 4.2.2.1A, the mean intensity of BCAN around PV- cells was decreased by 54% between aged ADAMTS-5 and aged control mice, whereas I observed no difference in the mean intensity between young and aged control mice. Similarly, around PV+ neurons BCAN was significantly reduced by about 52% and 60% in aged ADAMTS-5 mice compared to young and aged control mice, respectively. Around PV- neurons, about a 52% reduction of ACAN core-proteins was observed in aged ADAMTS-5 mice compared to aged control mice. Moreover, about an 11-fold reduction of ACAN was observed around PV+ neurons in aged ADAMTS-5 mice compared to aged control mice. This confirms previous findings that ACAN is extensively cleaved by ADAMTS-5 compared to other CSPGs, as this is due to a high number of ADAMTS-5 cleavage sites (Durigova et al., 2011; Gendron et al., 2007) (Figure 4.2.2.1B). In the neuropil of CA1, I found similar results as above which includes about a 38% and 37% reduction of BCAN core-proteins at the *stratum radiatum* and *oriens*, respectively, in aged ADAMTS-5 mice compared to aged control mice. With ACAN, on the other hand, about a 28% and 39% reduction was observed in the *stratum radiatum* and *oriens*, respectively, in aged ADAMTS-5 mice compared to aged control mice (Figure 4.2.2.1C). In the CA2, BCAN expression was reduced by approximately 52.4% and 52.1% around PV- and PV+ neurons, respectively, in aged ADAMTS-5 mice, compared to the aged control mice. On the other hand, ACAN was reduced in CA2 10- and 11-fold around PV- and PV+ neurons respectively in aged ADAMTS-5 mice compared to aged control mice (Figure 4.2.2.2A and 4.2.2.2B). Furthermore, BCAN was reduced to about 41% and 49% whereas ACAN was reduced by 26.5% and 7-fold around PV- and PV+ neurons respectively, in the CA3 of aged ADAMTS-5 mice compared to aged control mice (Figure 4.2.2.3A and 4.2.2.3B).

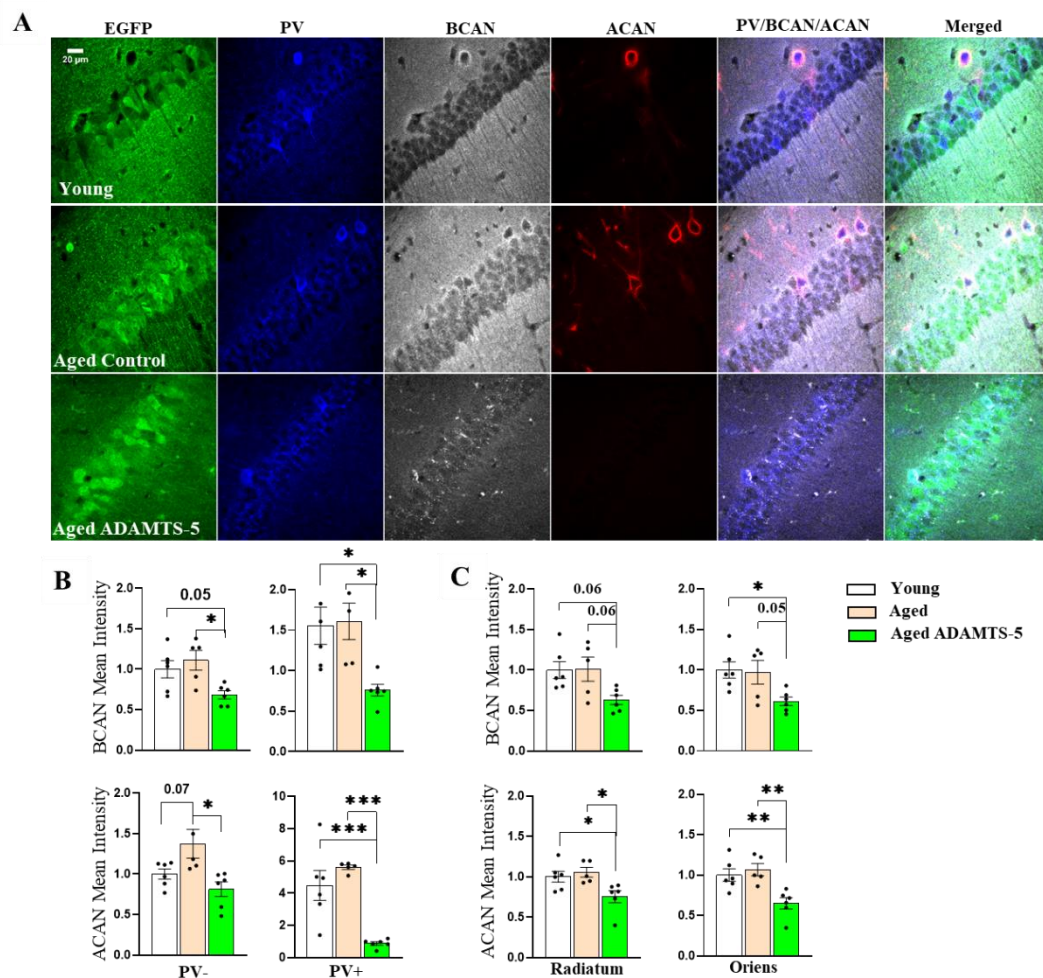


**Figure 4.2.2.1 Removal of Aggrecan and Brevican in CA1 of 22-24M old mice injected with pAAV\_hPGK\_hADAMTS5\_EGFP or pAAV\_hPGK\_EGFP.**

(A) Maximum projection of high-magnification confocal images (63x) of hippocampal CA1 of 2-3M old mice and 22-24M old mice two weeks after hADAMTS-5 injection. EGFP (green), parvalbumin (PV; blue), brevican (BCAN; grey), and aggrecan (ACAN; red) (Scale bar 20 $\mu$ m).

(B) Quantification of perineuronal expression of ECM shows that BCAN and ACAN were reduced in aged ADAMTS-5 mice relative to aged mice and young mice. Bar graphs show mean  $\pm$  SEM values. One-way ANOVA (BCAN  $p=0.0187$  and  $0.0092$  for PV- and PV+ cells, respectively; ACAN  $p=0.034$  and  $0.003$  for PV- and PV+ cells, respectively); Holm-Sidak's post hoc test,  $*p < 0.05$  and  $***p < 0.001$  (Young mice:  $N=6$ ,  $n=46$  PV- and  $82$  PV+ cells; Aged mice:  $N=5$ ,  $n=47$  PV- and  $76$  PV+ cells; Aged ADAMTS-5 mice:  $N=6$ ,  $n=49$  PV- and  $99$  PV+ cells).

(C) Similarly, analysis of neuropil ECM expression shows reduced levels of BCAN and ACAN core-protein levels in aged ADAMTS-5 mice compared to control groups. Bar graphs show mean  $\pm$  SEM values; One-way ANOVA (*str. radiatum*: BCAN  $p=0.0334$ , ACAN  $p=0.0178$ ; *str. orien*: BCAN  $p=0.0268$ , ACAN  $p=0.0028$ ); Holm-Sidak's post hoc test,  $*p < 0.05$  and  $**p < 0.01$  (Young mice:  $N=6$  and  $n=57$  ROIs; Aged mice:  $N=5$  and  $n=51$  ROIs; Aged ADAMTS-5 mice:  $N=6$  and  $n=50$  ROIs).

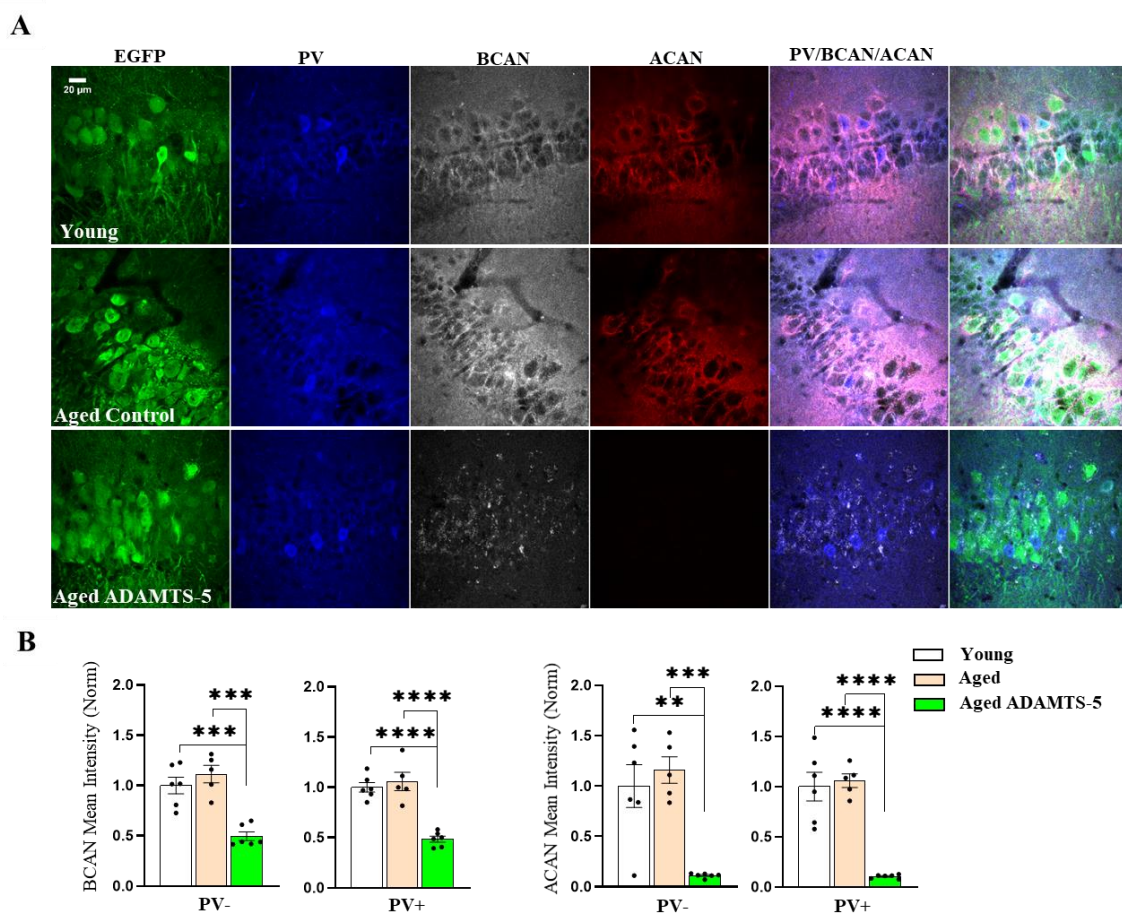


**Figure 4.2.2.2 Removal of Aggrecan and Brevican in CA2 of 22-24M old mice injected with pAAV\_hPGK\_hADAMTS5\_EGFP.**

(A) Maximum projection of high magnification of confocal images (63x) of hippocampal CA2 of 2-3M old mice and 22-24M old mice two weeks after hADAMTS-5 injection. EGFP (green), Parvablumin (PV; blue), Brevican (BCAN; grey), and Aggrecan (ACAN; red) (Scale bar 20µm).

(B) Quantification of perineuronal expression of ECM shows that BCAN and ACAN were reduced in aged ADAMTS-5 mice relative to aged mice and young mice. Bar graphs show mean  $\pm$  SEM values; One-way ANOVA (BCAN  $p < 0.0001$  for both PV- and PV+ cells; ACAN  $p = 0.0003$  and  $p < 0.0001$  for PV- and PV+ cells, respectively); Holm-Sidak's post hoc test, \*\* $p < 0.01$ , \*\*\* $p < 0.001$  and \*\*\*\* $p < 0.0001$  (Young mice:  $N = 6$ ,  $n = 16$  PV- and 16 PV+ cells; Aged mice:  $N = 5$ ,  $n = 16$  PV- and 15 PV+ cells; Aged ADAMTS-5 mice:  $N = 6$ ,  $n = 18$  PV- and 25 PV+ cells).

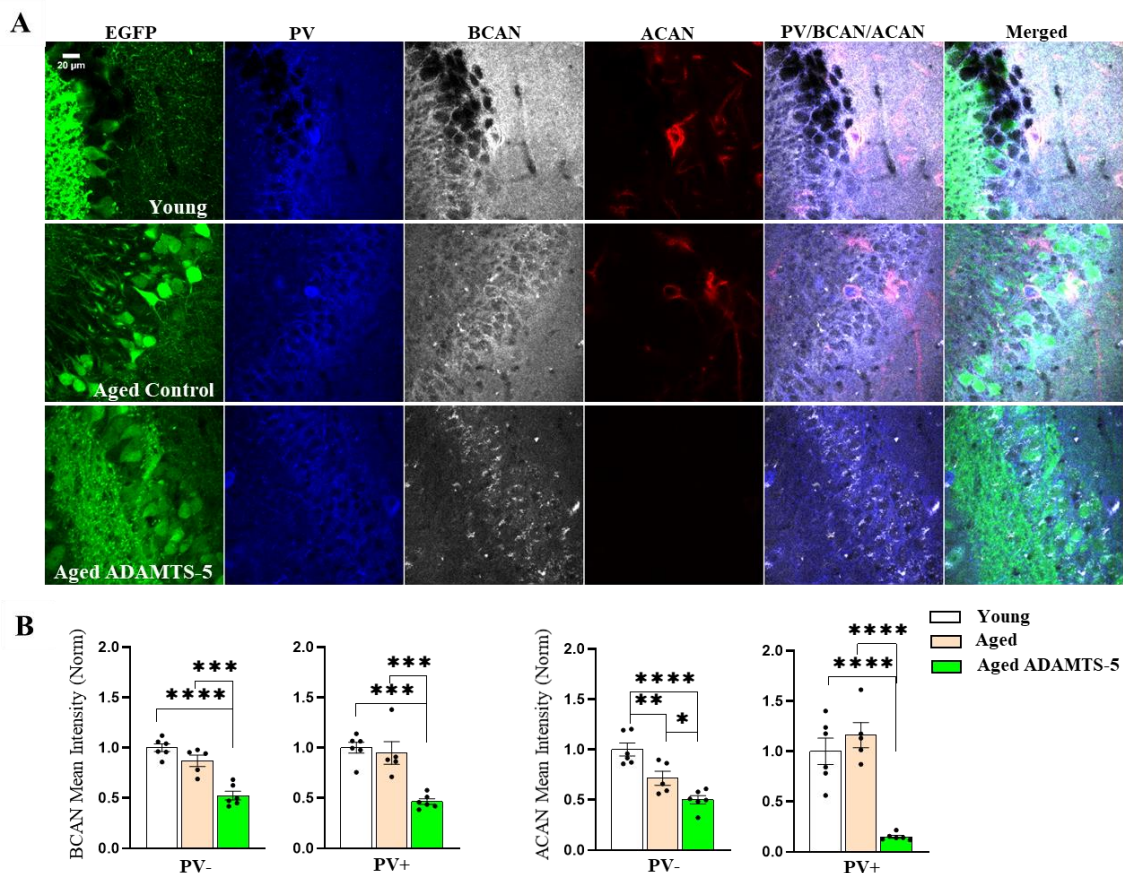


**Figure 4.2.2.3 Removal of Aggrecan and Brevican in CA3 of 22-24M old mice injected with pAAV\_hPGK\_hADAMTS5\_EGFP.**

(A) Maximum projection of high magnification of confocal images (63x) of hippocampal CA3 of 2-3M old mice and 22-24M old mice two weeks after hADAMTS-5 injection. EGFP (green), Parvablumin (PV; blue), Brevican (BCAN; grey), and Aggrecan (ACAN; red) (Scale bar 20µm).

(B) Quantification of perineuronal expression of ECM shows reduced levels of BCAN and ACAN core-proteins in aged ADAMTS-5 mice relative to control aged mice and young mice. Bar graphs show mean  $\pm$  SEM values; One-way ANOVA (BCAN  $p < 0.0001$  for both PV- and PV+ cells; ACAN  $p < 0.0001$  for both PV- and PV+ cells); Holm-Sidak's post hoc test, \* $p < 0.05$ , \*\* $p < 0.01$ , \*\*\* $p < 0.001$ , and \*\*\*\* $p < 0.0001$  (Young mice: N=6, n=19 PV- and 15 PV+ cells; Aged mice: N=5, n=7 PV- and 12 PV+ cells; Aged ADAMTS-5 mice: N=6, n=16 PV- and 18 PV+ cells).

#### 4.2.3 *pAAV\_hPGK\_hADAMTS-5\_EGFP* cleaved other CSPGs in the hippocampus of 22-24M old mice

Previous studies showed that CSPGs other than ACAN and BCAN, such as VCAN, also have ADAMTS-5 cleavage sites, therefore, I checked the degree of activity of hADAMTS-5 on the other CSPGs (Demircan et al., 2014). Using IHC, further investigation revealed that the hADAMTS-5 has a mild proteolytic effect on three other CSPGs, namely VCAN, NCAN, and PCAN. I stained hippocampal slices of young, aged control, and aged ADAMTS-5 mice with antibodies raised against PV (blue) and the three CSPG core-proteins, namely, VCAN (grey), NCAN (grey), and PCAN (red), as shown in Figure 4.2.3A, 4.2.3C and 4.2.3E, and quantified their levels of enrichment around PV+ neurons. Using a similar method of analysis as used for ACAN and BCAN, and additionally computing the cumulative frequency distributions, I measured the intensity of VCAN, NCAN, and PCAN around PV+ neurons in all three groups of mice. I found that the mean intensity of VCAN per cell was reduced by about 27% in aged ADAMTS-5 compared to aged control mice, whereas approximately 17% reductions were observed for NCAN and PCAN (Figure 4.2.3B, 4.2.3D, and 4.2.3F). Overall, the IHC results show that the hADAMTS-5 is proteolytically active against all CSPGs, albeit in varying order of sensitivity. ACAN was extensively cleaved, followed by BCAN, then VCAN, PCAN, and finally, NCAN, being the least sensitive. These findings corroborate with the following studies (Demircan et al., 2014; Durigova et al., 2011).

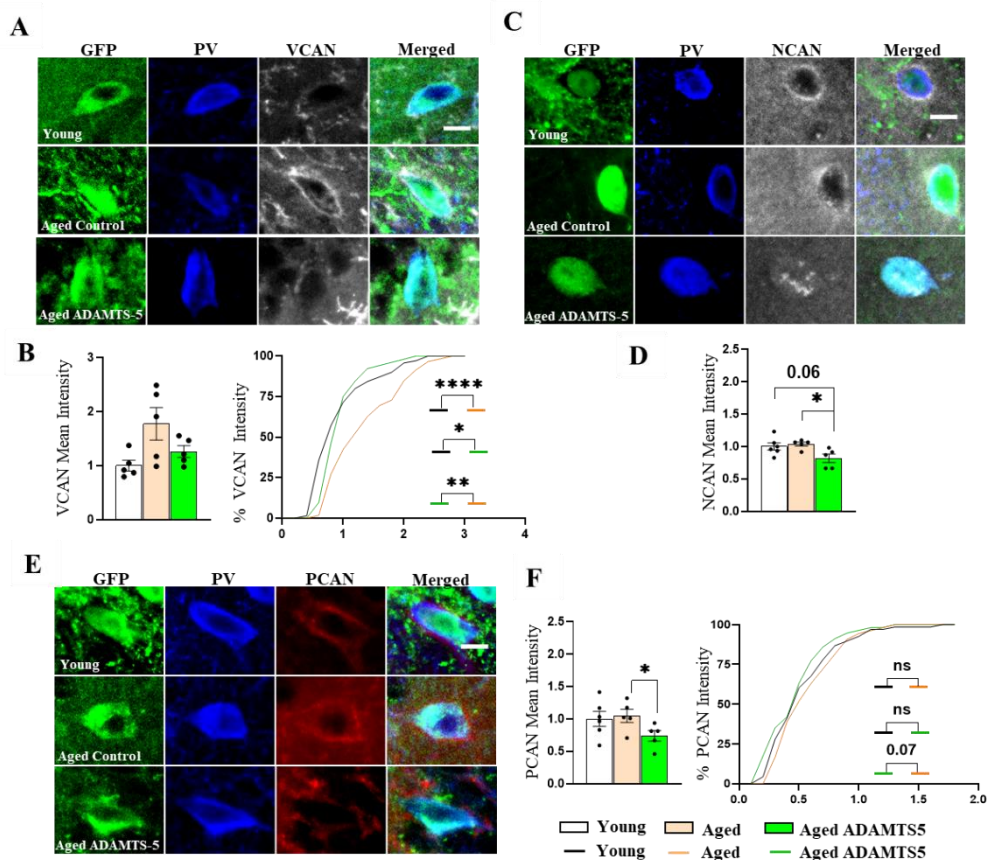


**Figure 4.2.3 pAAV\_hPGK\_hADAMTS5\_GFP cleaved other CSPGs in the hippocampus of 22-24M old mice.**

Representative confocal images of other CSPGs cleaved by hADAMTS-5 in the hippocampus of 22-24M old mice. These include, (A) Versican; VCAN (grey), (C) Neurocan; NCAN (grey) and (E) Phosphacan; PCAN (red) in addition to EGFP (green) and Parvalbumin (PV; blue) staining of the hippocampus of 22-24M old mice (Scale bar 10 $\mu$ m).

(B) Comparison by group means shows a tendency in the proteolysis of VCAN by hADAMTS-5 protease and this was observed to be significant from the cumulative frequency distribution. Bar graph shows mean  $\pm$  SEM values; For comparison of group means: One-way ANOVA with Welch's correction (p=0.0878). For cumulative frequency analysis: Kolmogorov-Smirnov's test, \*p < 0.05, \*\*p < 0.01, and \*\*\*\* p < 0.0001 (Young mice: N=6, n=70 PV+ cells; Aged mice: N=5, n= 60; Aged ADAMTS-5 mice: N=5, n= 52).

(D) Analysis of NCAN mean intensity showed a significant reduction in aged ADAMTS-5 mice compared to aged mice indicating proteolysis by hADAMTS-5 protease. Bar graph shows mean  $\pm$  SEM values; One-way ANOVA (p=0.0323); Holm-Sidak's post hoc test, \*p < 0.05 (Young mice: N=6, n=68 PV+ cells; Aged mice: N=5, n= 54; Aged ADAMTS-5 mice: N=5, n= 57).

(F) Additionally, PCAN was cleaved by hADAMTS-5 protease from the comparison of group means. Bar graph shows mean  $\pm$  SEM values; For comparison of group means: One-way ANOVA with Welch's correction (p=0.0955); Unpaired t-test with Welch's correction, \*p < 0.05. For cumulative frequency analysis: Kolmogorov-Smirnov's test (Young mice: N=6, n= 68 PV+ cells; Aged mice: N=5, n= 54; Aged ADAMTS-5 mice: N=5, n= 57). Measurements from one animal were excluded from the VCAN analysis after applying the identify outlier function in Graphpad with ROUT (Q=1%).

#### 4.2.4 *Effect of overexpressing hADAMTS-5 on neuroinflammation in hippocampal CA1 of 22-24-month-old mice*

Following up on the aforementioned structural changes in CSPGs in hADAMTS-5 overexpressing mice, I investigated the effects of cleaving CSPGs on astroglial and microglial activation. Using GFAP and IBA1 as markers for astrogliosis and microglia, respectively (Figure 4.2.4.1A, 4.2.4.1C), I discovered that the removal of CSPGs did not alter the density of GFAP+ cells in the CA1 area of the hippocampus in the aged ADAMTS-5 mice compared to young and aged control mice. However, I detected a reduction in the area of GFAP+ cells in aged control mice compared to young mice but no difference between young and aged ADAMTS-5 mice. Regarding the mean intensity of GFAP, I found that though aging increased the mean intensity of GFAP in astrocytes, this was, however, reduced in the aged ADAMTS-5 mice using cumulative frequency distribution (Figure 4.2.4.1B). Furthermore, using a similar approach as described earlier (Kaushik *et al.*, 2018), I characterized the morphometric properties of microglia after cleaving CSPGs. Two weeks after injection, I observed that microglia branching was slightly higher in young mice compared to aged control and aged ADAMTS-5 mice. Additionally, I detected an increase in the soma area of IBA1+ cells in aged control and aged ADAMTS-5 mice compared to young mice. Compared to young mice, the IBA1+ cells density was higher in aged control and aged ADAMTS-5 mice, by about 18% and 33%, respectively (Figure 4.2.4.1D). This initial measurement suggested that microglia in aged control and aged ADAMTS-5 mice were activated, as it is known that increased soma area with a respective decrease in branching area of microglia is a major morphological indicator of microglial activation (Davis *et al.*, 2017; Kaushik *et al.*, 2018). Then, I investigated the changes in microglia 10 weeks after injection, and interestingly, I detected similar outcomes for both the branching area and the soma area of IBA1+ cells in aged control and aged ADAMTS-5 mice compared to young mice. Furthermore, the density of IBA1+ cells was increased in aged control and aged ADAMTS-5 mice (Figure 4.2.4.1E).

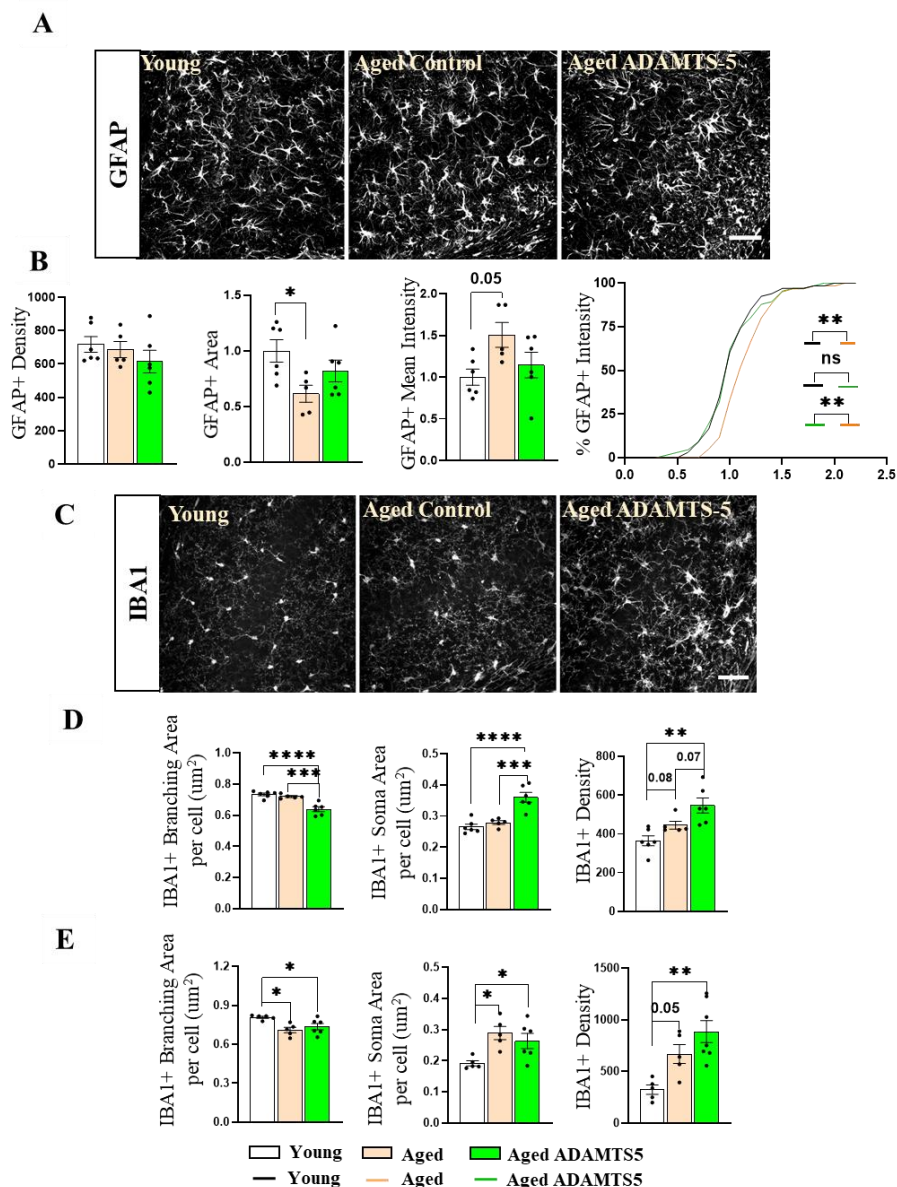


**Figure 4.2.4.1 Effect of overexpressing hADAMTS-5 on neuroinflammation in hippocampal CA1 of 22-24-month-old mice.**

(A&C) Using GFAP and IBA1 antibodies as markers for astrocytes and microglia respectively, the effects of cleaving CSPGs on astroglial and microglial activation were investigated (Scale bar 50 $\mu$ m).

(B) There were no changes in the density or area of GFAP+ cells, while a decrease in GFAP signal intensity was indicated by cumulative frequency distributions, suggesting reduced astroglial activation in hADAMTS-5 injected mice. Bar graphs show mean  $\pm$  SEM values; For comparison of group means: One-way ANOVA (Area,  $p=0.0415$ ; intensity,  $p=0.0550$ ); Holm-Sidak's post hoc test,  $*p < 0.05$ . For cumulative frequency analysis: Kolmogorov-Smirnov's test,  $**p < 0.01$  (Young mice:  $N=6$ ,  $n=1417$  GFAP+ cells; Aged mice:  $N=5$ ,  $n=971$ ; Aged ADAMTS-5 mice:  $N=6$ ,  $n=1374$ ).

**(D)** Analysis of IBA1+ cells, 2 weeks after injection, showed enhanced microglial activation due to reduced branching area together with increased soma area in aged ADAMTS-5 mice but surprisingly not in aged mice. A higher density of IBA1+ cells was found in aged ADAMTS-5 mice and aged mice compared to young mice. Bar graphs show mean  $\pm$  SEM values; One-way ANOVA (Branching area,  $p < 0.0001$ ; soma area,  $p < 0.0001$ ; density,  $p = 0.0024$ ); Holm-Sidak's post hoc test,  $**p < 0.01$ ,  $***p < 0.001$ , and  $****p < 0.0001$  (Young mice:  $N=6$ ,  $n=911$  IBA1+ cells; Aged mice:  $N=5$ ,  $n=717$ ; Aged ADAMTS-5 mice:  $N=6$ ,  $n=1538$ ).

**(E)** Therefore, 10 weeks after injection showed as expected increased microglial activation and density of IBA+ cells in aged mice compared to young mice. Regarding aged ADAMTS-5 mice, microglial activation was still present. Bar graphs show mean  $\pm$  SEM values; One-way ANOVA (Branching area,  $p = 0.0148$ ; soma area,  $p = 0.0148$ ; density,  $p = 0.0026$ ); Holm-Sidak's post hoc test,  $*p < 0.05$  and  $**p < 0.01$  (Young mice:  $N=6$ ,  $n=291$  IBA1+ cells; Aged mice:  $N=5$ ,  $n=552$ ; Aged ADAMTS-5 mice:  $N=6$ ,  $n=786$ ).

The above analysis suggests that the cleavage of CSPGs did not reduce microglial activation, therefore, I analyzed the functional state of activated microglia by using IL1beta, CD68, and C1q markers. The expression of IL1beta, produced predominantly by microglia and astrocytes, have a number of age-dependent effects such as inducing the release of other inflammatory cytokines (Gee et al., 2006), and have a beneficial effect on learning and memory in young mice but not in adult mice (Takemiya et al., 2017). CD68 and C1q are essential for the phagocytic phenotype of activated microglia in the context of ECM removal and synaptic pruning, respectively (Presumey et al., 2017; Vainchtein et al., 2018). From IL1beta analysis, I detected an age-dependent downregulation in pyramidal cells, GFAP+ cells, and IBA1+ cells of aged control mice compared to young mice. However, IL1beta expression increased in aged ADAMTS-5 mice compared to aged control mice in the aforementioned cell types except for IBA1+ cells (Figure 4.2.4.2). Additionally, I found a decreased density of CD68+ puncta in activated microglia of aged ADAMTS-5 mice compared to aged control mice (Figure 4.2.4.3B). On the other hand, I detected an increase in the area and intensity of CD68+ puncta along in activated microglia of aged ADAMTS-5 mice compared to aged control mice (Figure 4.2.4.3B). I found an increase in C1q intensity in both activated microglia and in the neuropil area of the hippocampus of aged control mice compared to young mice. However, C1q intensity in the soma and branches of microglia of aged ADAMTS-5 mice was reduced to the levels of young mice. From the neuropil analysis, C1q intensity was also reduced in aged ADAMTS-5 mice to the levels of young mice compared to aged control mice (Figure 4.2.4.3C).

Putting together, these data indicate the increased activation of microglia in aged ADAMTS-5 mice is possibly due to the increased phagocytosis of ECM from the extracellular space.

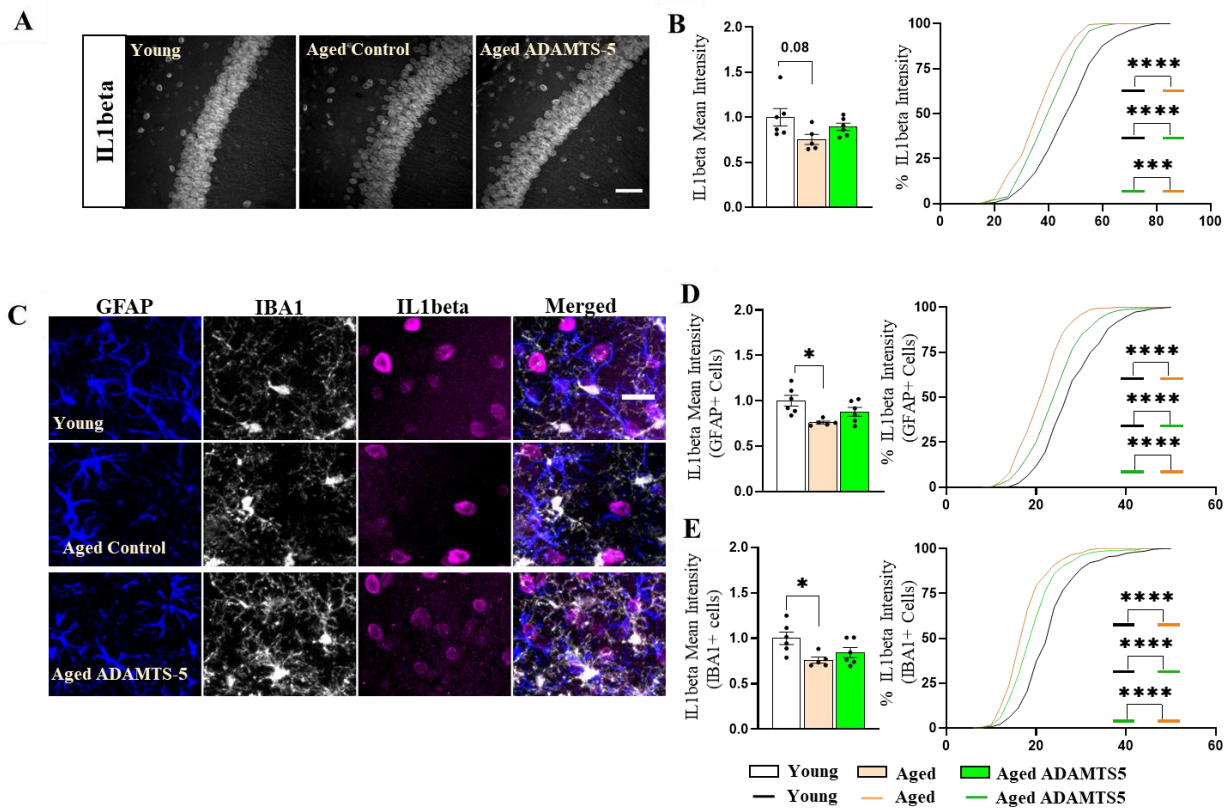


**Figure 4.2.4.2 Effect of overexpressing hADAMTS-5 on IL1beta signalling in 22-24-month-old mice injected.**

(A&C) Using IL1beta antibody, additional inflammatory status after cleaving CSPGs were investigated in pyramidal cells, astrocytes, and microglia (Scale bar; 50  $\mu$ m and 20 $\mu$ m, respectively).

(B) Quantification of IL1beta intensity at the pyramidal area revealed a slight increase in the mean intensity which was confirmed by cumulative frequency distribution in aged ADAMTS-5 mice relative to aged mice. The bar graph shows mean  $\pm$  SEM values; One-way ANOVA with Welch's correction ( $p=0.0944$ ). For cumulative frequency distribution: Kolmogorov-Smirnov's test, \*\*\* $p < 0.001$  and \*\*\*\* $p < 0.0001$  (Young mice: N=6, n=270 cells in *stratum pyramidale*; Aged mice: N=5, n=225; Aged ADAMTS-5 mice: N=6, n=270).

(D) Additionally, IL1beta was upregulated in astrocytes of aged ADAMTS-5 mice compared to aged mice. Bar graph shows mean  $\pm$  SEM values; One-way ANOVA ( $p=0.0126$ ); Holm-Sidak's post hoc test, \* $p < 0.05$  (Young mice: N=6, n=270 GFAP+ cells; Aged mice: N=5, n=225; Aged ADAMTS-5 mice: N=6, n=262).

(E) IL1beta expression in microglia was increased in aged ADAMTS-5 mice relative to aged mice. Bar graph shows mean  $\pm$  SEM values; One-way ANOVA ( $p=0.0286$ ); Holm-Sidak's post hoc test, \* $p < 0.05$  (Young mice: N=6, n=270 IBA1+ cells; Aged mice: N=5, n=210; Aged ADAMTS-5 mice: N=6, n=263).

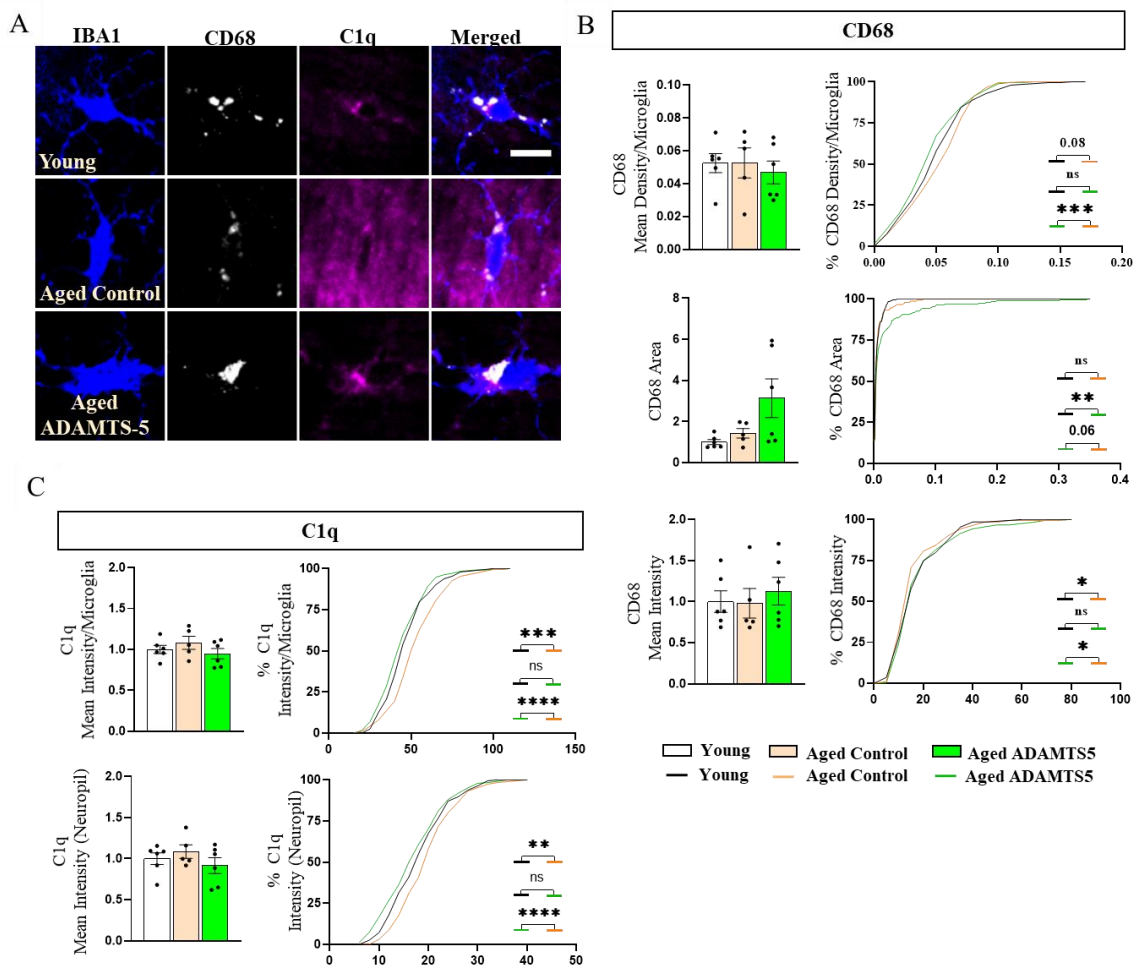


**Figure 4.2.4.3** Effect of overexpressing hADAMTS-5 on microglia functionality in 22-24-month-old mice.

(A) Using CD68 and C1q antibodies, the functional properties of the activated microglia after cleaving CSPGs were investigated (Scale bar; 10  $\mu$ m).

(B) The density of CD68+ puncta reduced whereas area and intensity increased in aged ADAMTS-5 mice relative to aged mice. Bar graphs show mean  $\pm$  SEM values; One-way ANOVA (density,  $p=0.8051$ ; intensity,  $p=0.7733$ ); One-way ANOVA with Welch's correction (area, 0.0778). For cumulative frequency distribution: Kolmogorov-Smirnov's test,  $*p < 0.05$ ,  $**p < 0.01$  and  $***p < 0.001$  (Young mice:  $N=6$ ,  $n=194$  IBA1+ cells; Aged mice:  $N=5$ ,  $n=191$ ; Aged ADAMTS-5 mice:  $N=6$ ,  $n=245$ ).

(C) Quantification of C1q showed reduced intensity in microglia as well as at the neuropil area in aged ADAMTS-5 mice compared to aged mice. Bar graphs show mean  $\pm$  SEM values; One-way ANOVA (Intensity/microglia,  $p=0.3688$ ; intensity/neuropil,  $p=0.3963$ ). For cumulative frequency distribution: Kolmogorov-Smirnov's test,  $**p < 0.01$ ,  $***p < 0.001$ , and  $****p < 0.0001$  (Young mice:  $N=6$ ,  $n=194$  IBA1+ cells; Aged mice:  $N=5$ ,  $n=191$ ; Aged ADAMTS-5 mice:  $N=6$ ,  $n=245$ ).

#### 4.2.5 Effect of overexpressing hADAMTS-5 on myelination in the hippocampus of 22-24M mice

Next, I studied the effect of removing CSPGs on the migration of oligodendrocytes as previous studies showed that CSPGs like BCAN, NCAN, and VCAN inhibit the functions and distribution of oligodendrocytes (Andrews et al., 2012). This inhibitory effect of CSPGs on oligodendrocytes, especially during injury, prevents the remyelination of demyelinated axons (Harlow and Macklin, 2014). As such, the digestion of CSPGs by chABC has been shown to rescue the inhibitory effects of CSPGs on oligodendrocytes (Harlow and Macklin, 2014; Pendleton et al., 2013b).

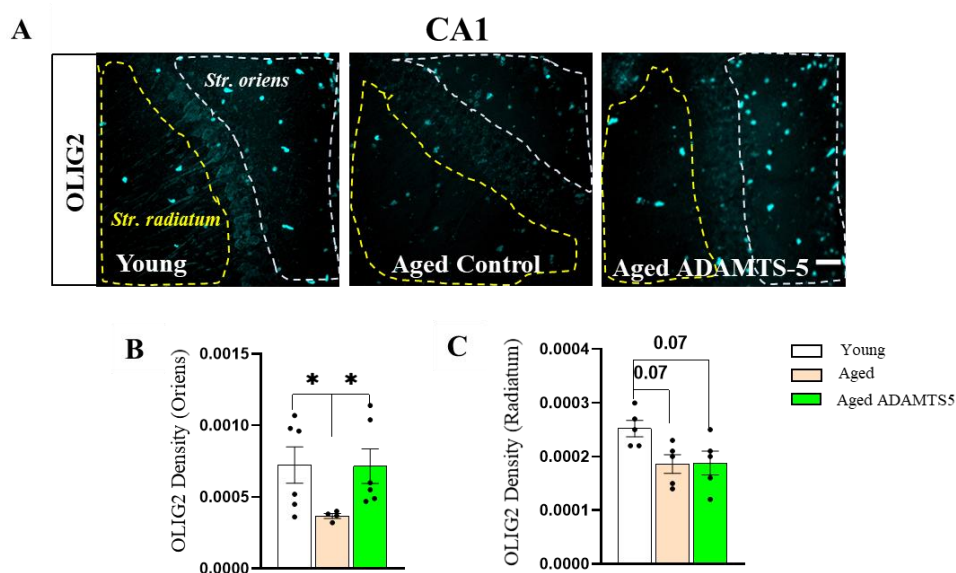


**Figure 4.2.5 Effect of overexpressing hADAMTS-5 on oligodendrocytes in the hippocampus of 22-24M mice.**

(A) Using the OLIG2 antibody, the effect of cleaving CSPGs on the migration of oligodendrocytes into the hippocampal CA1 was examined (Scale bar; 50  $\mu$ m).

(B) The density of OLIG2+ cells was restored in aged ADAMTS-5 mice to the level measured in young mice in the *stratum oriens* (white dashed ROI). Bar graphs show mean  $\pm$  SEM values; One-way ANOVA with Welch's correction ( $p=0.0215$ ); Unpaired t-test with Welch's correction,  $*p < 0.05$  (Young mice: N=6; Aged mice: N=4; Aged ADAMTS-5 mice: N=6).

(C) However, only a tendency was detected in the *stratum radiatum* (yellow dashed ROI). Bar graphs show mean  $\pm$  SEM values; One-way ANOVA ( $p=0.0442$ ); Holm-Sidak's post hoc test,  $p=0.07$  (Young mice: N=6; Aged mice: N=4; Aged ADAMTS-5 mice: N=6).

Then, I used IHC to check if the continuous removal of CSPGs in aged ADAMTS-5 mice could improve oligodendrocytes distribution and functions. I labelled oligodendrocytes with the known marker OLIG2 and I observed an increase in the density of OLIG2+ cells in the *stratum oriens* of aged ADAMTS-5 mice to the level of young mice. However, I did not see any difference in the density of OLIG2+ cells in the *stratum radiatum* between aged control and aged ADAMTS-5 mice, which were reduced for both groups compared to the young mice (Figure 4.2.5A and 4.2.5B).

#### 4.2.6 Overexpression of ADAMTS5 improved long-term memory of NOLT in 22-24M mice

Having confirmed the proteolytic activity of hADAMTS-5 and the effects of the continuous removal of CSPGs on neuroinflammation and myelination, I then studied the cognitive functions of aged ADAMTS-5 mice. I used the novel object location task (NOLT) together with the novel object recognition task (NORT) to study spatial memory and discrimination, and recognition memory before and after removing ECM (Figure 4.2.6.1A and 4.2.6.1B). I initially checked mice for any motor or emotional changes before injection by using the open field test. In this test, both aged control and aged ADAMTS-5 mice covered less distance compared to young mice. Additionally, I did not see any difference in time spent in peripheral or central areas between all groups, indicating no anxiogenic effects of aging and ADAMTS-5 overexpression (Figure 4.2.6.1C). Before injection, both aged control and aged ADAMTS-5 mice had equal performance regarding time spent exploring familiar and novel objects in the NOLT task, which was significantly different from young controls, indicating cognitive impairments (Figure 4.2.6.1D). However, 2 weeks after injection, there was an improvement in the performance of aged ADAMTS-5 mice regarding their ability to discriminate between objects at familiar and novel locations (Figure 4.2.6.1E). Then, I compared the discrimination ratio for all groups before and after injection and noticed a significant improvement in the aged ADAMTS-5 mice compared to aged control mice (Figure 4.2.6.1F). This suggests that the removal of ECM by hADAMTS-5 rather enhances hippocampus-dependent spatial discrimination and memory.

Next, I performed the NORT test before and after injection and observed no differences in time spent exploring both familiar and novel objects between all study groups. A similar outcome was also observed 2 weeks after the injection whereby the discrimination ratios for all groups did not show any difference either (Figure 4.2.6.2D). However, comparing the discrimination ratios before and after AAV injection, I found that with the aged ADAMTS-5 mice, there was an enhancement of recognition memory, whereas no change occurred for both young and aged controls (Figure 4.2.6.2E).

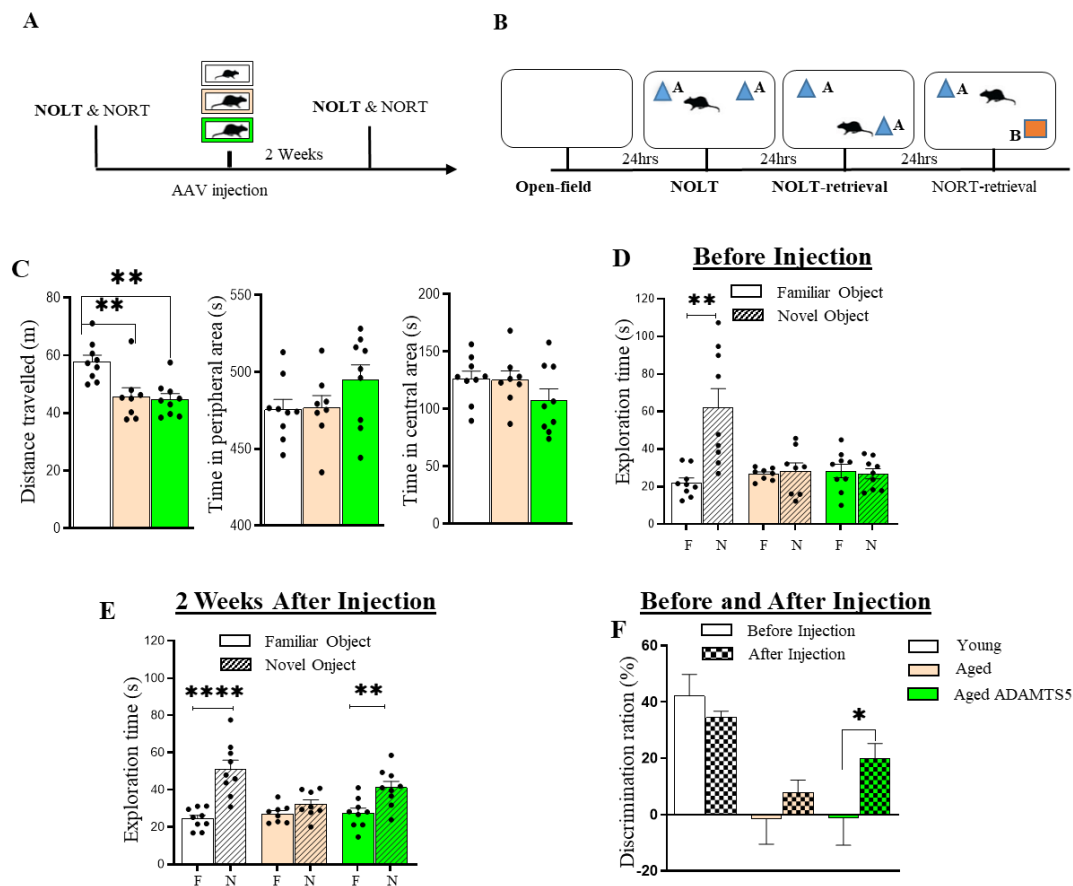


**Figure 4.2.6.1** Overexpression of ADAMTS5 improved long-term memory of NOLT in 22-24M mice.

Hippocampus-dependent long-term NOLT memory was tested in all test groups.

**(A&B)** Timeline of experiments and behavioral paradigm.

**(C)** Before injecting mice with AAV vectors into the CA1, a baseline cognitive test was performed. From the open field test, both groups of aged mice travelled shorter distances compared to young mice, in addition to, no difference in time spent at both peripheral and central areas. Bar graphs show mean  $\pm$  SEM values; One-way ANOVA (Distance travelled,  $p=0.0012$ ; Time in peripheral and central areas,  $p=0.1957$  and  $0.2281$ , respectively); Holm-Sidak's post hoc test,  $**p < 0.01$  (Young mice:  $N=9$ ; Aged mice:  $N=8$ ; Aged ADAMTS-5 mice:  $N=9$ ).

**(D)** With the NOLT test before injection, aged mice spent equal time exploring the objects at familiar (F) and novel (N) locations, which was different from young mice. Bar graph shows mean  $\pm$  SEM values; Paired t-test,  $**p < 0.01$  (Young mice:  $N=9$ ; Aged mice:  $N=8$ ; Aged ADAMTS-5 mice:  $N=9$ ).

**(E)** Two weeks after AAV injection, aged ADAMTS5 mice spent a significant amount of time exploring the displaced object whereas aged mice spent a similar amount of time exploring the familiar and the displaced objects. Bar graph shows mean  $\pm$  SEM values; Paired t-test,  $**p < 0.01$ , and  $***p < 0.001$  (Young mice:  $N=9$ ; Aged mice:  $N=8$ ; Aged ADAMTS-5 mice:  $N=9$ ).

**(F)** Comparing the discrimination ratios before and after injection, a significant improvement in NOLT memory was observed in aged ADAMTS5 mice. Bar graph shows mean  $\pm$  SEM values; Two-way mixed ANOVA (*Group*:  $F=15.03$ ,  $p<0.0001$ ); Fisher's LSD test,  $*p < 0.05$  (Young mice:  $N=9$ ; Aged mice:  $N=8$ ; Aged ADAMTS-5 mice:  $N=9$ ).

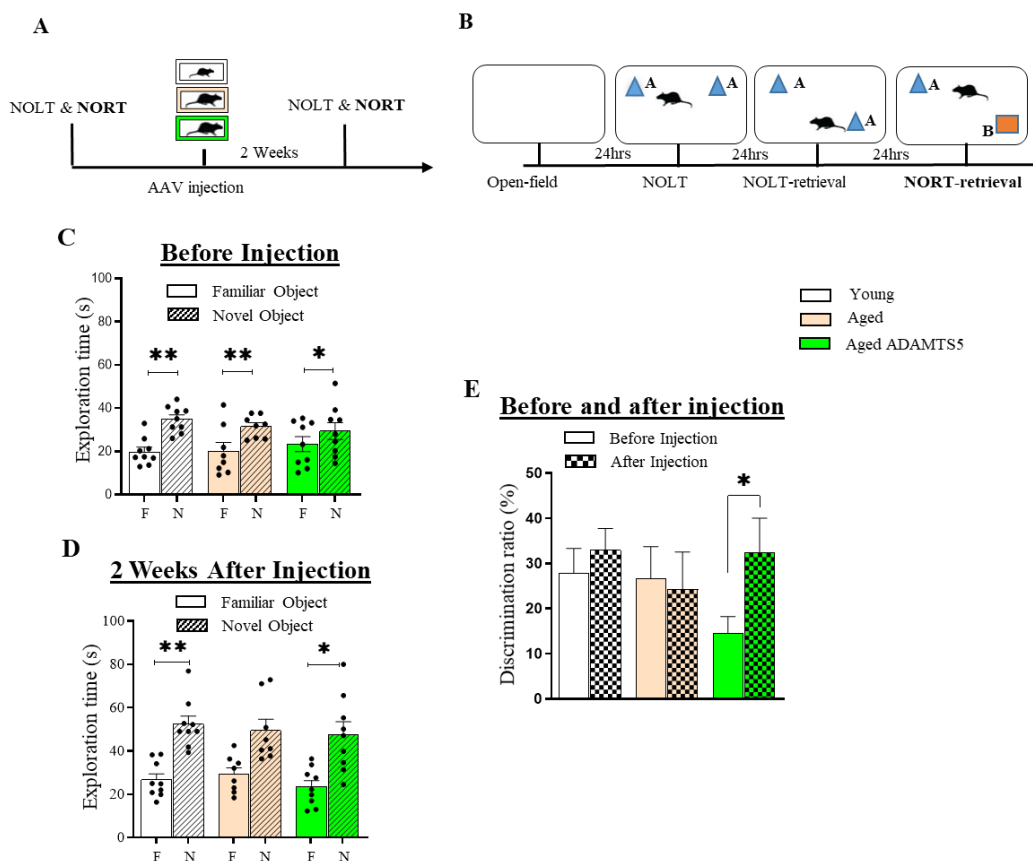


**Figure 4.2.6.2** Overexpression of ADAMTS5 has a tendency to improve long-term NORT memory in 22-24M mice.

Long-term NORT memory was tested in all test groups. **(A&B)** Timeline of experiments and behavioral paradigm.

**(C)** NORT test before injection showed all test groups spent significantly more time exploring the novel object relative to the familiar object. Bar graph shows mean  $\pm$  SEM values; Paired t-test,  $*p < 0.05$  and  $**p < 0.01$  (Young mice:  $N=9$ ; Aged mice:  $N=8$ ; Aged ADAMTS-5 mice:  $N=9$ ).

**(D)** Two weeks after AAV injection, all test groups spent a significant amount of time exploring the novel objects compared to familiar objects. Bar graph shows mean  $\pm$  SEM values; Paired t-test,  $*p < 0.05$  and  $**p < 0.01$  (Young mice:  $N=9$ ; Aged mice:  $N=8$ ; Aged ADAMTS-5 mice:  $N=9$ ).

**(E)** Interestingly, comparing the discrimination ratios before and after injection, an improvement in NORT memory was observed in aged ADAMTS5 mice. Bar graph shows mean  $\pm$  SEM values; Wilcoxon matched-pairs test,  $*p < 0.05$  (Young mice:  $N=9$ ; Aged mice:  $N=8$ ; Aged ADAMTS-5 mice:  $N=9$ ).

#### 4.2.7 *Overexpression of ADAMTS-5 improved spatial learning and memory in 22-24M mice*

After observing the enhancement of hippocampus-dependent memory in the aged ADAMTS-5 mice in the NOLT test, I then used another hippocampus-dependent cognitive function test to confirm the observed cognitive improvement. Therefore, I employed the labyrinth or dry maze task, which has been shown to be highly sensitive in measuring hippocampus-dependent spatial navigation learning and memory (Peters et al., 2013). Additionally, this behavioral task is known to be much less stressful compared to the water maze task (Harrison and Feldman, 2009; Rich and Shapiro, 2007). Here, I designed an asymmetrical quadrant-based dry maze experiment with two phases of memory tests: the memory acquisition phase and the probe phase. The asymmetrical quadrant-based dry maze had three entry-paths, and two of these entry-paths were used for the memory acquisition phase, which lasted three days. The 3<sup>rd</sup> entry-path was used for the 2-phase probe test on the 4<sup>th</sup> day with an hour delay. The entry-paths for the memory acquisition phase were counterbalanced for all groups. Additionally, I included distal cues, which studies show are essential for the allocentric form of spatial navigation in mice (Vorhees and Williams, 2014) (Figure 4.2.7A and 4.2.7B). Using two measures, the errors made and the distance travelled, I estimated the spatial navigational learning and memory performance of each mouse as they explored the maze to locate the reward (water) during both the acquisition and probe phases. The first parameter I measured was the level of familiarity of mice with the maze, that is, how well each mouse knew the reward location after their first encounter with the maze. With this metric, I compared the total number of errors made on day 1 (as mice explored the maze for 10 min) and the first trial on day 2, with both measurements limited to the first entry into the reward location. This is because, during the first session on day 2, each mouse used the same entry-path as on day 1. Using the level of familiarity metric, I observed that the aged control mice, despite some cognitive impairments, were able to familiarize themselves with the maze. Similarly, aged ADAMTS-5 and young control mice all showed a satisfactory degree of familiarity with the maze. However, as the entry-paths from subsequent training sessions, that is, from the 1<sup>st</sup> trial on day 2 to the 2<sup>nd</sup> trial on day 3, were alternated, I noticed a unique learning pattern in the aged ADAMTS-5 mice which was consistent with that of young controls. Thus, by the last training session on day 3 (T2 on day 3), aged ADAMTS-5 mice eventually became consistent in reducing the number of errors together with covering shorter distances in their quest to locate the reward. This was not the case with aged control, as they consistently increased the number of errors and travelled long distances to locate the reward (Figure 4.2.7C, 4.2.7D, 4.2.7F, and 4.2.7G).

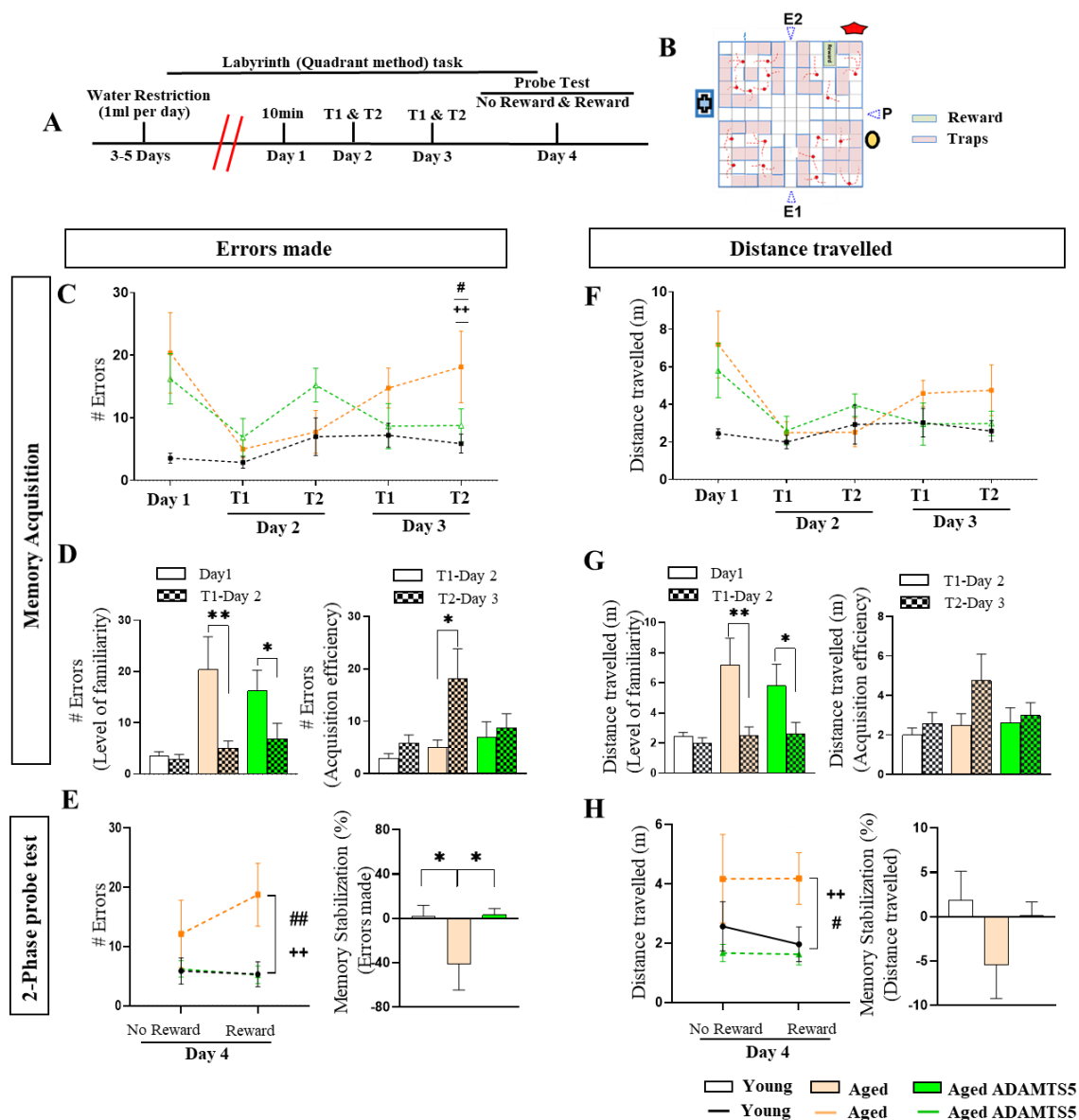


**Figure 4.2.7 Overexpression of ADAMTS5 improved spatial learning and memory in 22-24M mice.**

Hippocampal-dependent spatial learning and memory were investigated in all tests by using the asymmetrical quadrant-based Labyrinth.

(A&B) Timeline of labyrinth test and design.

(C&F) Two measures, errors made and distance traveled, were used to estimate the cognitive performance of each mouse during the acquisition phase. Plots show mean  $\pm$  SEM values; Two-way mixed ANOVA (Errors made, *Group*:  $F=7.991$ ,  $p=0.0006$ ; distance travelled, *Group*:  $F=4.314$ ,  $p=0.0156$ ); Fisher's LSD test, \* $p < 0.05$  and \*\* $p < 0.01$  (+ aged ADAMTS-5 mice vs aged mice; # young mice vs aged mice; Young mice:  $N=9$ ; Aged mice:  $N=8$ ; Aged ADAMTS-5 mice:  $N=9$ ).

(D&G) Although aged mice are cognitively challenged, however, they displayed, together with young mice, a satisfactory level of familiarity with the maze. Aged ADAMTS-5 mice on the other hand showed

an enhanced efficiency in memory acquisition relative to aged mice. Bar graphs show mean  $\pm$  SEM values; Two-way mixed ANOVA (Level of familiarity: errors made, *Group*:  $F=4.961$ ,  $p=0.0112$ ; distance travelled, *Group*:  $F=3.699$ ,  $p=0.0324$ ; acquisition efficiency: errors made, *Group\*Training session*:  $F=4.504$ ,  $p=0.0309$ ); Fisher's LSD test, \* $p < 0.05$  and \*\* $p < 0.01$  (Young mice:  $N=9$ ; Aged mice:  $N=8$ ; Aged ADAMTS-5 mice:  $N=9$ ).

**(E&H)** From the 2-phase probe test, aged ADAMTS-5 mice showed an enhanced memory stabilization contrary to aged mice. Bar graphs show mean  $\pm$  SEM values; For probe tests: Two-way mixed ANOVA (Errors made: *Group*:  $F=5.566$ ,  $p=0.0068$ ; Distance travelled, *Group*:  $F=5.198$ ,  $p=0.0092$ ); Fisher's LSD test, \* $p < 0.05$  and \*\* $p < 0.01$ . For memory stabilization: One-way ANOVA (Errors made,  $p=0.0614$ ; Distance travelled,  $p=0.2284$ ), Fisher's LSD test, \* $p < 0.05$  (+ aged ADAMTS-5 mice vs aged mice; # young mice vs aged mice; Young mice:  $N=9$ ; Aged mice:  $N=8$ ; Aged ADAMTS-5 mice:  $N=9$ ).

Next, using the 2-phase probe test, which includes the 1<sup>st</sup> probe test without reward and the 2<sup>nd</sup> probe test with reward with an hour delay, I observed a trend in the mean number of errors and distance travelled for both aged ADAMTS-5 and young mice. Here, both groups made fewer errors compared to aged control mice; however, they were not statistically different. Meanwhile, after the hour interval, I observed that both aged ADAMTS-5 and young mice made significantly fewer errors along with travelling shorter distances to the reward. Then, I matched the performance between the 1<sup>st</sup> and 2<sup>nd</sup> probe tests to estimate the degree of memory stabilization. Thus, when computing the effect of mice entering the reward location but not finding water on memory stabilization, I found that both aged ADAMTS-5 and young mice were able to maintain their memory of the reward location, which was, however, modified in aged controls (Figure 4.2.7E and 4.2.7F). It appears from both NOLT and dry maze studies that the continuous removal of CSPG from the hippocampus restores spatial learning and memory, spatial discrimination memory, and navigation memory.

#### 4.2.8 Overexpression of ADAMTS5 improved synaptic plasticity in 22-24M mice

LTP in the hippocampus of aged mice has been shown to be impaired due to a host of structural and physiological factors. Such factors include changes in the expression and function of both AMPAR and NMDAR in excitatory neurons (Burke and Barnes, 2010; Temido-Ferreira et al., 2019). Aging is known to increase the internalization of AMPARs from synaptic sites as well as alter the expression and distribution of NMDARs (Deak and Sonntag, 2012b). With NMDARs, aging increases GluN2B-containing NMDARs that are mostly located at the extrasynaptic sites, thereby reducing synaptic NMDARs (Hardingham and Bading, 2010). Activation of the extrasynaptic GluN2B-containing NMDARs in the hippocampus of aged

mice may impair CREB signaling and this correlates with cognitive impairments (Avila et al., 2017; Morrison and Baxter, 2012). Therefore, prompted by the cognitive enhancements seen in NOLT and in the spatial learning and memory of aged ADAMTS-5 mice, I analyzed the possible cellular and molecular mechanisms by using electrophysiological and pharmacological experiments in collaboration with Hadi Mirzapourdelavar (DZNE Magdeburg). We detected no difference between the three compared groups in terms of the basal excitatory synaptic transmission, measured using the stimulus-response curves (Figure 4.2.8B).

I found that the basal synaptic transmission was not different in aged control mice relative to young mice or aged ADAMTS-5 mice. However, there was a reduction in the stimulus-response curves of aged ADAMTS-5 mice compared to young mice. Then, I studied the effect of cleaving CSPGs on the induction and maintenance of LTP. I found that the percentage of short-term potentiation (STP) within the first 3 minutes of LTP induction was reduced in both aged control mice and aged ADAMTS-5 mice compared to young mice. I did not see any difference between aged ADAMTS-5 mice and aged control mice. From the analysis of the last 10 minutes of LTP, I found that LTP reduced to about 20% in aged control mice whereas a 12% reduction was observed in aged ADAMTS-5 mice, compared to young mice. This 8% difference in LTP levels observed between aged ADAMTS-5 mice and aged control mice was statistically significant (Figure 4.2.8C, 4.2.8D, and 4.2.8E). Furthermore, I investigated if the removal of CSPGs increased LTP by inhibiting signaling via the extrasynaptic GluN2B-containing NMDARs. signaling by blocking their activation with RO25 (Ro 25-6981). Application of GluN2B antagonist Ro 25-6981 (RO25) at the concentration of 3  $\mu$ M enhanced LTP in the aged control mice to the level seen in aged ADAMTS-5 mice without RO25. Blocking the GluN2B NMDARs in aged ADAMTS-5 mice with RO25 did not alter the level of LTP, suggesting that overexpression of ADAMTS-5 and removal of perisynaptic ECM might inactivate signaling via extrasynaptic GluN2B or increase signaling via synaptic GluN2B to counterbalance activity of extrasynaptic GluN2B-containing receptors (Figure 4.2.8C and 4.2.8D).

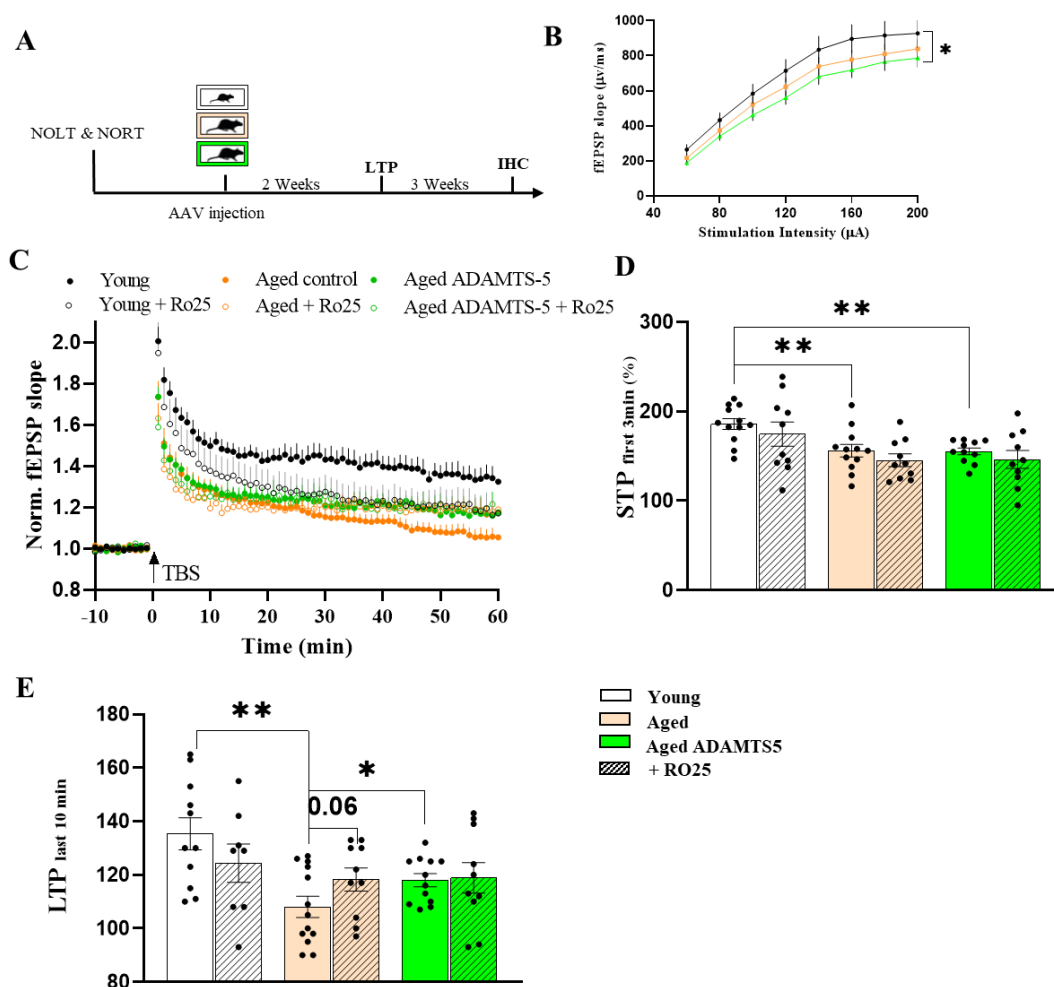


**Figure 4.2.8** Overexpression of ADAMTS5 improved synaptic transmission in 22-24M mice.

(A) Timeline for AAV injection into hippocampal CA1 and experiment.

(B) The basal synaptic transmission was not different in aged mice relative to young mice and to aged ADAMTS-5 mice. This was, however, reduced in aged ADAMTS-5 mice compared to young mice. Plot shows mean  $\pm$  SEM values; Two-way mixed ANOVA (*Group*:  $F=2.167$ ,  $p=0.1348$ ); Fisher's LSD test,  $*p < 0.05$  (Young mice:  $N=9$ ,  $n=11$  slices; Aged mice:  $N=8$ ,  $n=13$ ; Aged ADAMTS-5 mice:  $N=9$ ,  $n=12$ ).

(C) The mean slope of fEPSPs recorded 10 minutes before TBS was used as the baseline and subsequent trace which is the average of fEPSPs recorded 60 minutes after TBS.

(D) The short-term potentiation (STP) was computed using the first 3 minutes after TBS. Here, both aged mice and aged ADAMTS-5 mice showed a reduced percentage of STP. Bar graph shows mean  $\pm$  SEM values; Two-way mixed ANOVA (*Group*:  $F=8.402$ ,  $p=0.0019$ ); Fisher's LSD test,  $**p < 0.01$  (Young mice:  $N=9$ ,  $n=11$  slices; Aged mice:  $N=8$ ,  $n=13$ ; Aged ADAMTS-5 mice:  $N=9$ ,  $n=12$ ).

(E) Impaired LTP in aged mice, as estimated using the last 10 minutes of a 60-minute LTP time course, was improved after cleaving CSPGs in aged ADAMTS-5 mice. Pharmacological inhibition of the extrasynaptic GluN2B-containing NMDAR by RO25, slightly enhanced LTP in aged mice but had no effect in aged ADAMTS-5 mice. Bar graph shows mean  $\pm$  SEM values; For LTP without RO25, One-way

ANOVA ( $p=0.010$ ), Fisher's LSD test,  $*p < 0.05$  and  $**p < 0.01$  and comparison of aged mice with and without RO25, Unpaired t-test, (Young mice:  $N=9$ ,  $n=11$ , [8] slices; Aged mice:  $N=8$ ,  $n=13$ , [10]; Aged ADAMTS-5 mice:  $N=9$ ,  $n=12$ , [10]); [RO25].

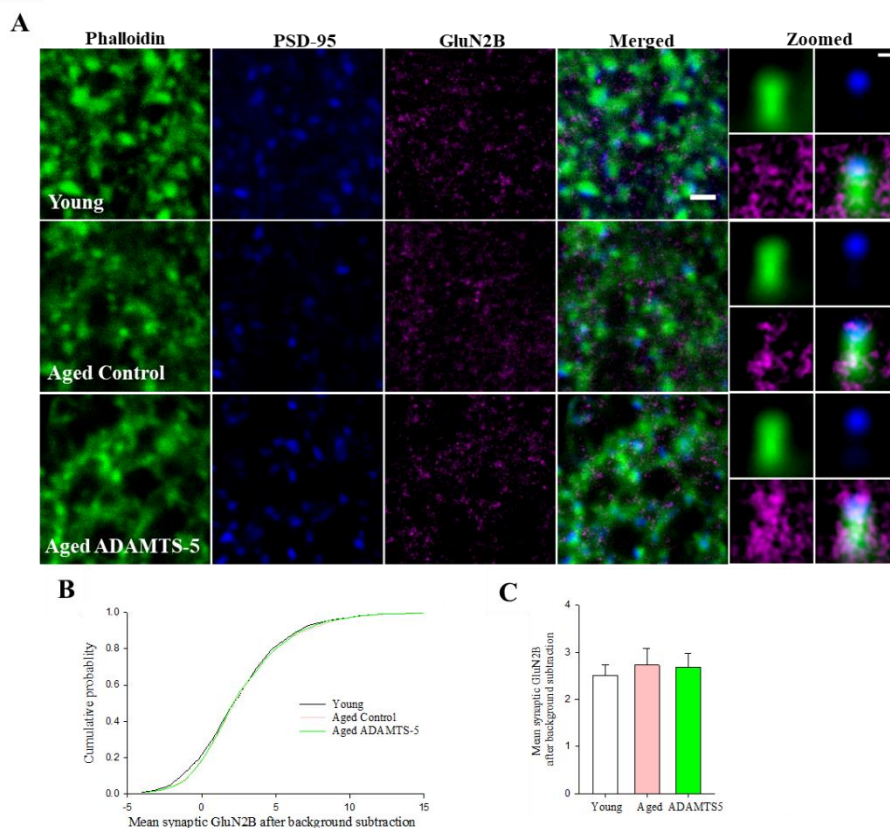


**Figure 4.2.9 ECM remodeling did not affect synaptic GluN2B expression in 22-24M mice.**

(A) STED imaging of hippocampal sections from all groups immunostained with antibodies to GluN2B (magenta) and PSD-95 (blue) with dendritic spines labelled with phalloidin (green). (Scale bar; 1  $\mu$ m and zoomed images 250nm). (B&C) No difference between synaptic GluN2B expression in all test groups was observed in cumulative distribution as well as comparison of group means. One-way ANOVA ( $p=0.900$ ). Bar graph shows mean  $\pm$  SEM values (Young mice:  $N=4$ ,  $n=1521$  spines; Aged mice:  $N=5$ ,  $n=1882$ ; Aged ADAMTS-5 mice:  $N=6$ ,  $n=2680$ ).

#### 4.2.9 *CSPG remodelling does not change expression of synaptic GluN2B expression in 22-24M mice*

To further investigate if the enhanced LTP in aged ADAMTS-5 mice was due to accumulation of synaptic or dispersal of extrasynaptic GluN2B-containing NMDAR receptors, STED imaging of hippocampal sections from all groups immunostained with antibodies to GluN2B and PSD-95 was performed in collaboration with Prof. Dr. Silvio Rizzoli from the Georg-August-Universität, Göttingen. Since the GFP signals were weak to identify synapses, phalloidin which stains F-actin structures in all dendritic spines (Bär et al., 2016), was used for spine detection (Figure 4.2.9A, 4.2.9B and 4.2.9C). From this experiment, I observed no changes in cumulative distributions of GluN2B at synaptic (PSD-95+ area) between all test groups. There was no difference in the mean intensity of GluN2B signals per animal. Overall, these data suggest that the removal of CSPGs did not affect GluN2B expression at synaptic sites, but influenced the perisynaptic GluN2B signaling.

#### 4.2.10 *CSPG remodelling enhanced pCREB signaling in aged ADAMTS-5 mice*

Next, I investigated the mechanism downstream of the extrasynaptic GluN2B-containing NMDAR signaling in aged ADAMTS-5 mice. In the aging postsynaptic compartment, activation of the extrasynaptic GluN2B-containing NMDARs shuts-off the CREB pathway (Grochowska et al., 2021). In detail, activation of the extrasynaptic GluN2B-containing NMDARs prevents the phosphorylation of ERK1/2 or the synaptonuclear messenger, Jacob. The phosphorylation of Jacob is essential for transducing NMDAR signals to the nucleus (Karpova et al., 2013), nevertheless, once the non-phosphorylated Jacob translocates to the nucleus it activates protein phosphatase 1 which then dephosphorylates CREB thereby displacing CREB (Dieterich et al., 2008; Spilker et al., 2016). However, recent evidence indicates that aging decreases the expression and phosphorylation of CREB which affects the expression of some synaptic genes like c-FOS and brain-derived neurotrophic factor (BDNF) (Miranda et al., 2019). Meanwhile, both c-FOS and brain-derived neurotrophic factor are essential for the maintenance of LTP and synaptic plasticity (Gandolfi et al., 2017; Loebrich and Nedivi, 2009). Therefore, I used IHC to study the effects of removing CSPGs on pCREB signaling in the hippocampal sections of all test groups (Figure 4.2.10A and 4.2.10C). Image analysis revealed that pCREB mean intensity increased in aged ADAMTS-5 mice compared to aged control mice in both the distal and proximal CA1 regions that are known to influence spatial and recognition memory, respectively (Beer et al., 2018; Nakazawa et al., 2016) (Figure 4.2.10B and 4.2.10D).

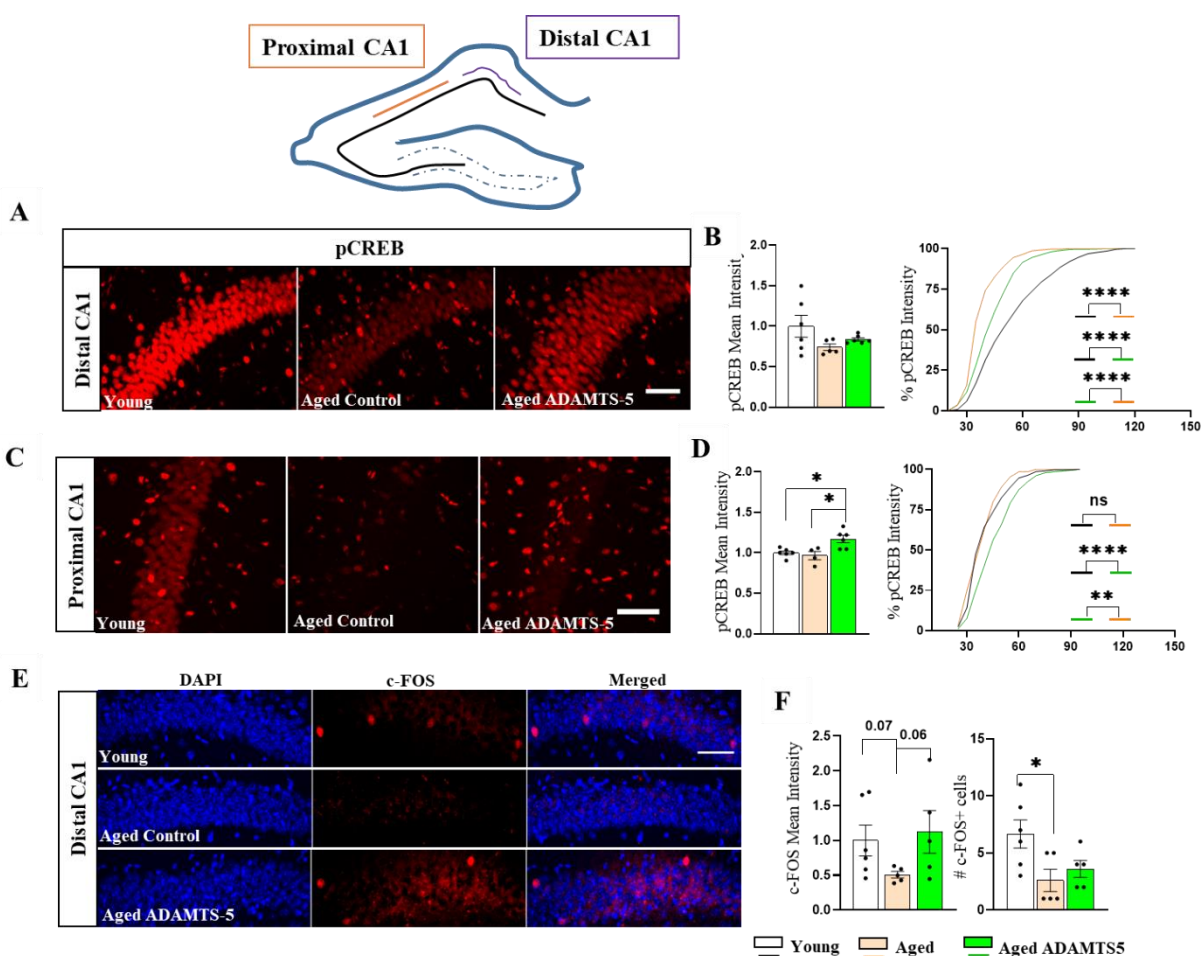


**Figure 4.2.10 ECM remodelling enhanced pCREB signaling in aged ADAMTS-5 mice.**

(A&C) Representative 40 $\times$  images of pCREB in the distal and proximal CA1 of young mice, aged ADAMTS-5 mice, and aged mice (Scale bar; 50 $\mu$ m).

(B&D) Quantification of mean intensity as well as cumulative frequency analysis show that pCREB levels increases in aged ADAMTS-5 mice relative to aged mice. Bar graphs show mean  $\pm$  SEM values; For distal CA1: One-way ANOVA with Welch's correction ( $p=0.1069$ ). For cumulative frequency distribution: Kolmogorov-Smirnov's test, \*\* $p < 0.01$  and \*\*\*\*  $p < 0.0001$ . For proximal CA1: One-way ANOVA ( $p=0.0061$ ); Holm-Sidak's post hoc test, \* $p < 0.05$ . For cumulative frequency distribution: Kolmogorov-Smirnov's test, \*\* $p < 0.01$  and \*\*\*\*  $p < 0.0001$  (Young mice:  $N=6$ ,  $n= [128$  and  $69]$  pCREB+ cells; Aged mice:  $N=5$ ,  $n= [134$  and  $19]$ ; Aged ADAMTS-5 mice:  $N=6$ ,  $n= [198$  and  $52]$ ).

(E&F) Using c-FOS staining which is downstream of pCREB signaling revealed that in aged ADAMTS-5 mice the removal of CSPGs slightly increased the mean intensity of c-FOS signal without affecting the density (Scale bar; 50 $\mu$ m). Bar graphs show mean  $\pm$  SEM values; For c-FOS intensity: Kruskal-Wallis test with uncorrected Dunn's test. For the number of c-FOS+ cells: One-way ANOVA ( $p=0.0367$ ); Holm-Sidak's post hoc test, \* $p < 0.05$  (Young mice:  $N=6$ ; Aged mice:  $N=5$ ; Aged ADAMTS-5 mice:  $N=6$ ). Measurements from one animal were excluded from aged ADAMTS-5 mice for both intensity and number of c-FOS+ cells as outliers detected by Graphpad with ROUT ( $Q=1\%$ ).

Then, I decided to confirm the functionality of the increased pCREB, especially in the distal CA1, by staining for c-FOS, which expression is downstream of pCREB. I noticed that c-FOS intensity slightly increased in aged ADAMTS-5 mice compared to aged control mice to the level found in young mice. However, no difference was observed in the density of c-FOS<sup>+</sup> cells in the distal CA1 between aged mice and aged ADAMTS-5 mice (Figure 4.2.10E and 4.2.10F).

#### *4.2.11 CSPG remodelling partially restored both excitatory and inhibitory synaptic inputs in aged ADAMTS-5 mice to young controls*

In the brain, although synaptic connections are stabilized by ECM, aging increases the ECM protein molecules that negatively affects the excitatory and inhibitory synapses, thereby disrupting the excitatory and inhibitory balance (E/I) (Morrison and Baxter, 2012). Available evidence suggests that aging reduces the number of functional synapses (Deak and Sonntag, 2012b) and this strongly correlates with LTP and cognitive impairments (Bergado and Almaguer, 2002; Kumar et al., 2012). Therefore, I investigated the extent to which the continuous removal of CSPG core proteins alters the expression of both excitatory and inhibitory contacts on PV<sup>+</sup> cells. Here, I used vGLUT1 and vGAT antibodies to study the perisomatic glutamatergic and GABAergic innervation of PV<sup>+</sup> neurons (Figure 4.2.11.1A) and in the *stratum radiatum* (Figure 4.2.11.2A and 4.2.11.2C) in all groups. Using both mean intensity and density together with cumulative frequency analysis, I observed an overall trend for possible restoration of both perisomatic glutamatergic and GABAergic innervations in aged ADAMTS-5 mice to the levels of young mice. In detail, I found an increase in both the density and intensity of vGLUT1<sup>+</sup> puncta in aged ADAMTS-5 mice compared to aged control mice. Cumulative frequency analysis confirmed this trend (Figure 4.2.11.1B). Regarding changes to vGAT expression, I found no difference in the mean intensity and density of vGAT<sup>+</sup> puncta in aged ADAMTS-5 mice relative to aged control mice. However, using the more powerful cumulative frequency analysis with PV<sup>+</sup> cell rather than animal as an observation unit, I observed that the aging reduced intensity and density of vGAT<sup>+</sup> puncta, which were rescued in aged ADAMTS-5 mice as I observed no difference between young mice and aged ADAMTS-5 mice (Figure 4.2.11.1C).

Further analysis in the *stratum radiatum* showed no difference in the mean density of vGLUT1+ puncta between aged ADAMTS-5 mice and aged control mice, which was further confirmed by cumulative frequency analysis. The mean intensity of vGLUT1+ puncta in the *stratum radiatum*, although reduced in aged control mice relative to young mice, did not change between aged ADAMTS-5 mice and young mice. However, I observed a slight increase in the intensity of vGLUT1 by the cumulative frequency analysis in aged ADAMTS-5 mice compared to aged control mice (Figure 4.2.11.2B). In the context of vGAT in the *stratum radiatum*, I found no difference in the mean density and intensity of vGAT+ puncta in aged ADAMTS-5 mice relative to aged control mice. Interestingly, from the cumulative frequency analysis, I noticed that the increase in the intensity but not the density of vGAT+ puncta was highly significant between aged ADAMTS-5 mice and aged control mice (Figure 4.2.11.2D). Putting all together, both excitatory and inhibitory perisomatic synaptic inputs to PV+ cells and synaptic densities in the *stratum radiatum* are slightly improved but not restored in aged mice after ECM remodeling.

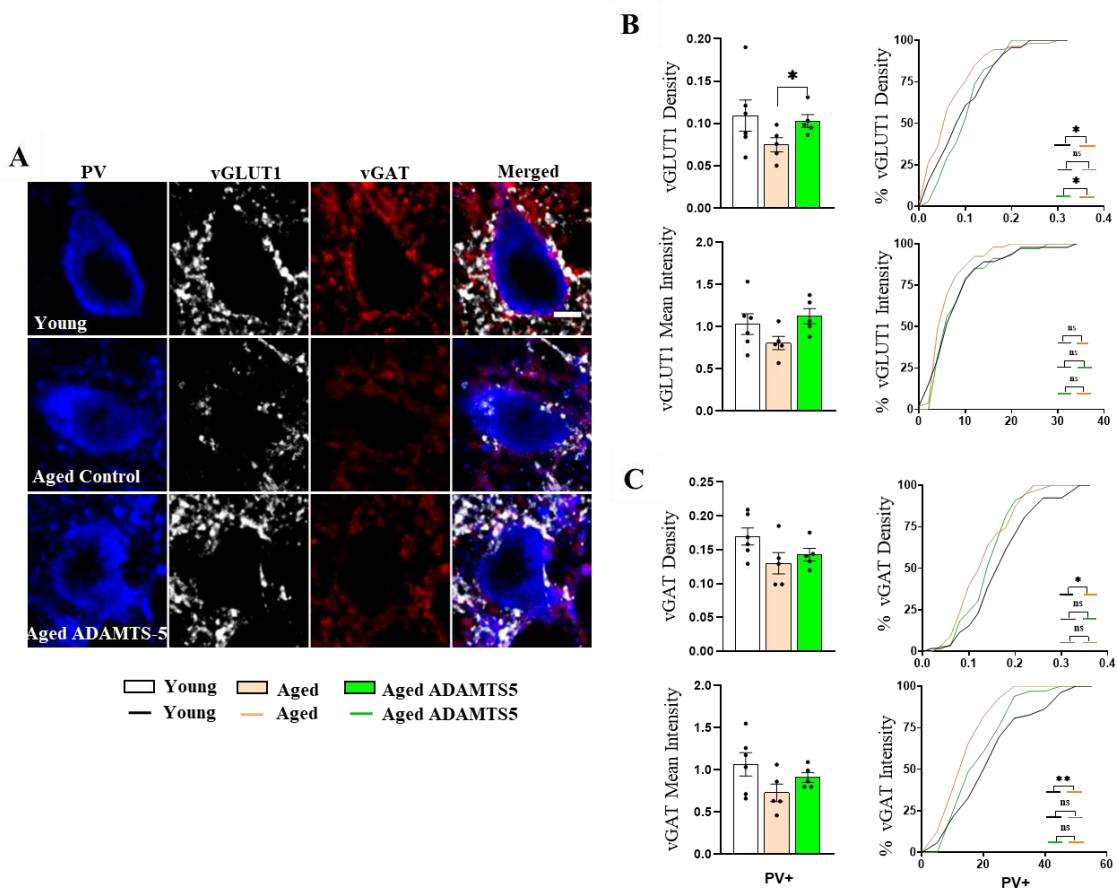


**Figure 4.2.11.1** CSPG remodeling restored both excitatory and inhibitory synaptic inputs to PV+ cells in aged ADAMTS-5 mice to young controls.

(A) Representative 63 $\times$  images of PV+ cells innervated by excitatory (vGLUT1) and inhibitory (vGAT) synapses in the hippocampal CA1 of young mice, aged ADAMTS-5 mice and aged mice (Scale bar; 5 $\mu$ m). (B) Quantification of vGLUT1+ puncta around PV+ cells shows an overall increase in the density in aged ADAMTS-5 mice compared to aged mice. Bar graphs show mean  $\pm$  SEM values; For density: One-way ANOVA with Welch's correction ( $p=0.0861$ ). For cumulative frequency distribution: Kolmogorov-Smirnov's test,  $*p < 0.05$ . For vGLUT1 intensity: One-way ANOVA ( $p=0.1371$ ); For cumulative frequency distribution: Kolmogorov-Smirnov's test (Young mice:  $N=6$ ,  $n=52$  PV+ cells; Aged mice:  $N=5$ ,  $n=55$ ; Aged ADAMTS-5 mice:  $N=6$ ,  $n=33$ ).

(C) However, the age-dependent reduction of the density and intensity of vGAT+ puncta were not the case in aged ADAMTS-5 mice relative to young mice. Bar graphs show mean  $\pm$  SEM values; One-way ANOVA (Density,  $p=0.1150$ ; intensity,  $p=0.1356$ ). For cumulative frequency distribution: Kolmogorov-Smirnov's test,  $*p < 0.05$  and  $**p < 0.01$  (Young mice:  $N=6$ ,  $n=52$  PV+ cells; Aged mice:  $N=5$ ,  $n=55$ ; Aged ADAMTS-5 mice:  $N=6$ ,  $n=33$ ).

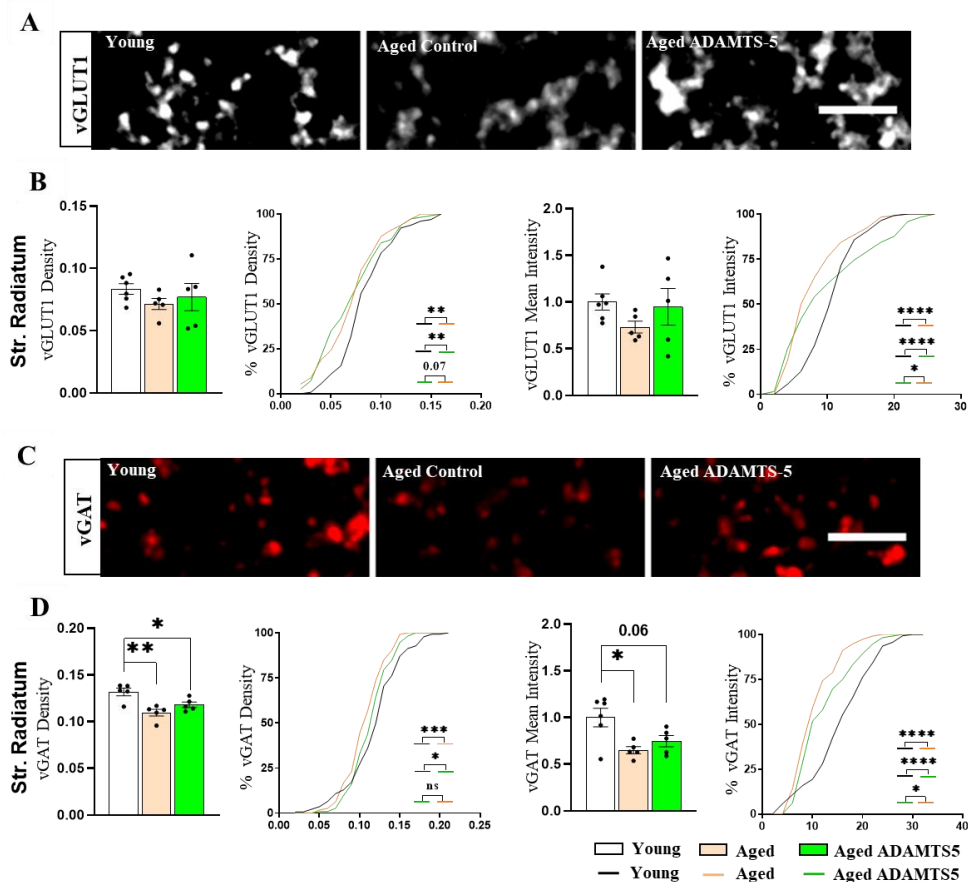


**Figure 4.2.11.2 CSPG remodeling restored neither excitatory nor inhibitory synaptic inputs in aged ADAMTS-5 mice to young controls.**

(A&C) Representative 63 $\times$  images of excitatory (vGLUT1-grey) and inhibitory (vGAT-red) synapses in the hippocampal *stratum radiatum* of young mice, aged ADAMTS-5 mice and aged mice (Scale bar; 5 $\mu$ m). (B) Quantification of the density and intensity of vGLUT1+ puncta within *stratum radiatum* was reduced in aged mice and aged ADAMTS-5 mice relative to young mice. Bar graphs show mean  $\pm$  SEM values; One-way ANOVA with Welch's correction (Density,  $p=0.2337$ ; intensity,  $p=0.1059$ ). For cumulative frequency distribution: Kolmogorov-Smirnov's test, \* $p < 0.05$ , \*\* $p < 0.01$ , and \*\*\*\* $p < 0.0001$  (Young mice:  $N=6$ ,  $n=1764$  vGLUT+ synapses; Aged mice:  $N=5$ ,  $n=1307$ ; Aged ADAMTS-5 mice:  $N=6$ ,  $n=1348$ ). (D) Furthermore, from the cumulative frequency analysis, the intensity of vGAT+ puncta increased in the *stratum radiatum* of aged ADAMTS-5 mice compared to aged mice. Bar graphs show mean  $\pm$  SEM values; One-way ANOVA (Density,  $p=0.0033$ ; intensity,  $p=0.0143$ ); Holm-Sidak's post hoc test, \* $p < 0.05$  and \*\* $p < 0.01$ . For cumulative frequency distribution: Kolmogorov-Smirnov's test, \* $p < 0.05$ , \*\*\* $p < 0.001$ , and \*\*\*\* $p < 0.0001$  (Young mice:  $N=6$ ,  $n=2786$  vGAT+ synapses; Aged mice:  $N=5$ ,  $n=1307$ ; Aged ADAMTS-5 mice:  $N=6$ ,  $n=2149$ ).

Next, I used IHC in addition to following the “operational” definitions of previously defined 4 classes of PV expression which includes high, interhigh, interlow, and low (Donato et al., 2013) to investigate the effect of removing CSPGs on the expression of PV proteins in PV+ cells. Studies have shown that learning and memory processes in the hippocampus, for example, follow a unique PV-network configuration in adult mice, which is reversible (Donato et al., 2015, 2013; Huang et al., 1999). From these studies, it is known that hippocampus-dependent behavioral tasks like fear conditioning can induce large fractions of PV+ cells with a high amount of PV proteins. Interestingly, this finding was further supported by an increased fraction of PV+ cells with high PV content after pharmacogenetic activation of these neurons (Donato et al., 2013). In this study, I found that the age-dependent reduction of the intensity of PV proteins in PV+ cells was rescued in aged ADAMTS-5 mice. This was further confirmed by cumulative frequency analysis (Figure 4.2.11.3B and 4.2.11.3C). Furthermore, I observed that the intensity of PV proteins positively correlated with the soma size of PV+ cells in all test groups (Figure 4.2.11.3D). Meanwhile, from this study, I discovered that the proportion of PV+ cells with a high PV content in their soma increased in aged ADAMTS-5 mice compared to aged control mice. No difference was seen in the proportion of the other classes of PV in PV+ cells (Figure 4.2.11.3E and Figure 4.2.11.3F). This suggests that CSPG remodeling is essential in the reconfiguration of the expression of PV proteins in PV+ cells, especially in high PV+ cells.

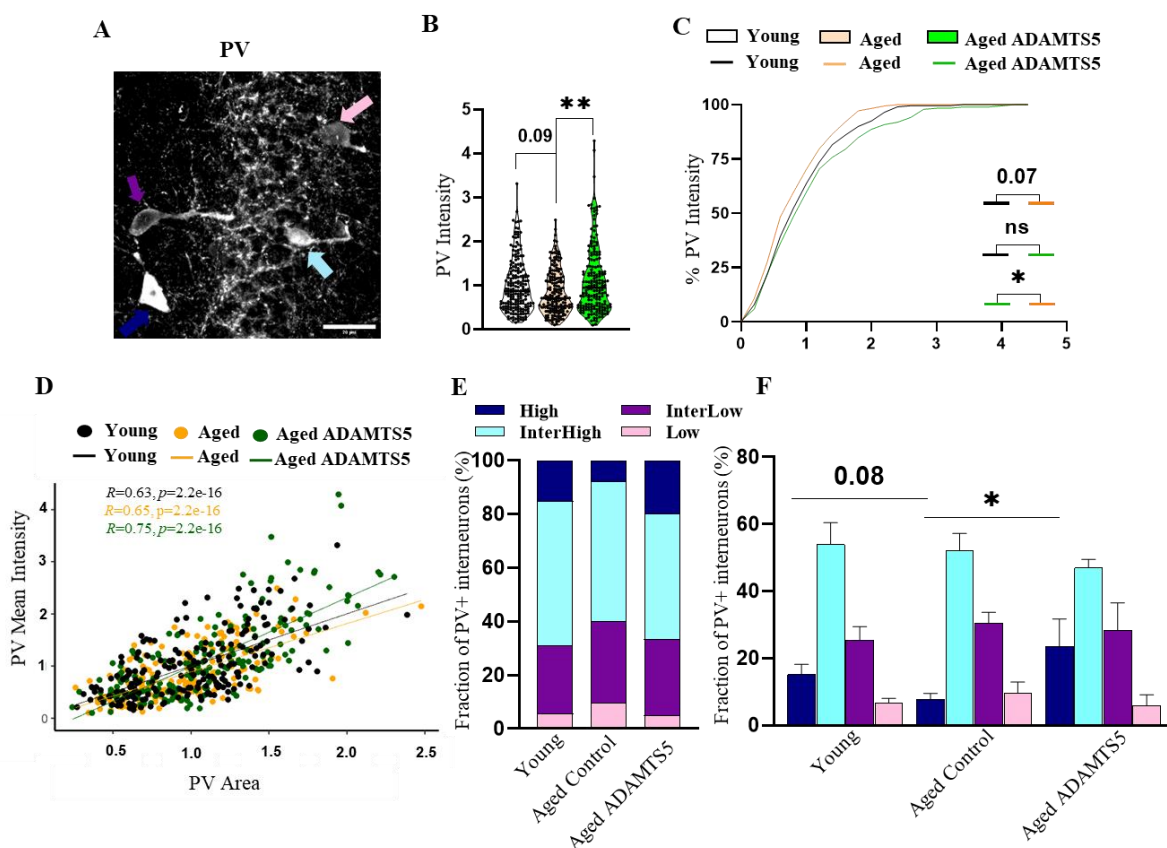


**Figure 4.2.11.3 CSPG remodeling modified the PV expression in PV+ cells in the hippocampus of aged ADAMATS-5 mice compared to aged control mice.**

(A) Representative 40 $\times$  images of parvalbumin-expressing inhibitory neurons (PV+ cells -grey) in the hippocampus of mice (Scale bar; 20 $\mu$ m).

(B&C) PV intensity increased in aged ADAMTS-5 mice compared to aged mice. Plots shows mean  $\pm$  SEM values; Kruskal-Wallis test ( $p=0.0076$ ); Dunn's post hoc test,  $**p < 0.01$ . For cumulative frequency distribution: Kolmogorov-Smirnov's test,  $*p < 0.05$  (Young mice,  $N=6$ ,  $n=201$  PV+ cells; Aged mice,  $N=5$ ,  $n=178$ ; Aged ADAMTS-5 mice,  $N=6$ ,  $n=186$ ).

(D) A positive relationship was observed between PV intensity and soma size for all test groups. Correlation plot and values of Spearman's coefficient of correlation.

(E&F) From the PV-network configuration analysis, the removal of CSPGs in aged ADAMTS-5 mice increased the proportion of high-intensity PV+ cells compared to aged mice. Bar graphs show mean  $\pm$  SEM values. As frequencies of PV classes are not independent measure (the sum=100%), multiple comparison t-test was used instead of two-way ANOVA,  $*p < 0.05$  (Young mice:  $N=6$ ,  $n=201$  PV+ cells; Aged mice:  $N=5$ ,  $n=178$ ; Aged ADAMTS-5 mice:  $N=6$ ,  $n=186$ ).

## 5 DISCUSSION

Studies over the past years have indicated that CSPGs are essential at every stage of brain development, including the embryonic, postnatal, and adult stages (Dityatev and Schachner, 2003; Williams et al., 2010). The expression of CSPG core-proteins as well as their GAG chains in the brain has been shown to influence cell migration, differentiation, and maturation during early development (Urbán and Guillemot, 2014). However, recent evidence suggests that aging increases the protein content of CSPGs and, as such, they are strongly associated with quite a number of age-dependent structural and physiological changes (Vegh et al., 2014). These changes include the reduction in synaptogenesis, synaptic transmission, and plasticity, which correspond to cognitive impairment in multiple brain regions such as the hippocampus and PFC (Mencio et al., 2021). It is noteworthy that little or no information exists regarding the mechanisms behind the age-dependent changes in CSPG protein content, as this could be through the parallel increase in transcription and translation of CSPG genes or the disruption of the regulatory mechanisms. Furthermore, several studies have investigated the role played by CSPGs in age-dependent cognitive impairment, especially in disease models (Végh et al., 2014), however, using less clinically-related approaches. Such approaches include the application of chABC enzymes, which originate from bacteria, and whose function is global, crude, and limited to removing only the sugar chains. This approach is further limited by the short recovery time of CSPG GAGs, and this recovery is accompanied by negative effects (Carceller et al., 2020). Therefore, it is essential to have a better approach to control CSPG remodeling in the aged brain.

Therefore, in my thesis, I set out to investigate the aforementioned potential mechanisms in the hippocampus of aged mice by using both RT-qPCR and IHC. Here, I first checked the mRNA levels of CSPG core-proteins followed by the expression analysis of enzymes necessary for GAG synthesis and modifications in aged mice from 30-months-old and compared them to 2-3 months-old young mice. Then, I followed up these findings by investigating the said genes at the earlier stage of aging, in 22-24 month-old mice. Afterward, I monitored if aging altered the gene expression of proteases and their tissue inhibitors that regulate the CSPG turnover. This thesis work, therefore, illuminates the mechanisms underlying the observed age-dependent increase in CSPG protein content, as well as abrogation of the aged-dependent effects by promoting ECM proteolysis in the hippocampus of 22-24 month-old mice.

## 5.1 mRNA levels of CSPGs core-proteins and glycosylation enzymes do not correlate with PNN protein levels in aged mice

In a proteomics study, Vegh and colleagues showed a time-dependent increase in the expression of some ECM molecules such as HAPLN1, BCAN, and NCAN. Further analysis with immunoblotting confirmed the age-dependent upregulation of these molecules in the hippocampus and increased expression of the more specialized form of ECM, that is, PNN, using the WFA labelling (Vegh et al., 2014). However, they failed to elucidate the mechanism behind these alterations. This thesis, according to my knowledge, is the first study to provide a significant foundation to further understand the mechanisms behind the age-dependent increase in neural ECM. I show here that the high protein levels of PNN components as reported are not due to the direct increase in the transcription of CSPG core proteins. This is because, from the RT-qPCR analysis, it follows that the gene expression of the CSPG core proteins was not upregulated in 22-24M and > 30M old mice when compared to young controls. Additionally, the fact that there was no difference between aged and young mice regarding the expression of enzymes necessary for glycosylation indicates that the reported high WFA intensity in aged animals might not be due to increased synthesis of GAGs. This is because WFA binds to the terminal N-acetylgalactosamine residues of the GAG chains of CSPGs (Ajmo et al., 2008; Miyata et al., 2018; Young and Williams, 1985), and its intensity reflects the amount and maturity of PNNs (Slaker et al., 2016). Therefore, it is possible that the high WFA intensity reported might be due to the accumulation of GAGs through reduced degradation of CSPGs. The reported low correlation of about 0.40 between mRNA and protein expressions in mammals (Kosti et al., 2016) is in line with our finding that the gene expression of PNN components is not parallel to the reported protein levels in the hippocampus of aged mice. Previously, the researchers suggested that proteins are mostly conserved once formed, whereas mRNAs are subject to post-transcriptional modifications which can alter protein levels (Perl et al., 2017; Vogel and Marcotte, 2012). Meanwhile, one interesting finding in the present study was the consistent downregulation of *Chst3* in both 22-24M and > 30M old mice. The *Chst3* gene is transcribed and translated into the CHST3 enzyme, which catalyzes the sulfation of carbon at the 6<sup>th</sup> position in the GAGs of CSPG, which is known to be low from previous studies (Shinji Miyata and Kitagawa, 2016).

## 5.2 mRNA levels of CSPGs proteases did not change in aged mice compared to young controls except for *Adamts-5* and *MMP-12*

Studies have shown that CSPGs are remodeled by MMPs and ADAMTS with the latter having higher activity, especially ADAMTS-5. In the brain, MMP-2 and MMP-9 also known as the gelatinases have been shown to cleave CSPGs in an activity-dependent manner thereby influencing processes such as brain development (Verslegers et al., 2013), synaptogenesis (Dityatev et al., 2004), and synaptic plasticity (Bozdagi et al., 2007). Similarly, ADAMTS-4 and -5, which are expressed in multiple brain regions including the hippocampus (Lemarchant et al., 2013), also degrade CSPGs and are essential for some physiological processes such as axonal regeneration during injury (Tauchi et al., 2012) as well as anti-inflammatory effects (Lemarchant et al., 2016). Protein levels of ADAMTS-5, which has higher aggrecanase activity compared to ADAMTS-4 and MMPs (Gendron et al., 2007), are reduced in AD mice (Ferrer-Ferrer and Dityatev, 2018) and this may result in the accumulation of CSPGs in these models. Studies have shown that both MMPs and ADAMTS activities in the brain are tightly controlled by TIMPs (Zhai et al., 2018).

Therefore, since I did not observe any direct relationship between mRNA and protein levels of PNN core proteins and GAG synthesis, I investigated the effect of aging on CSPG proteases and their regulators. Surprisingly, I did see a striking upregulation of *Mmp-12* in aged mice, and previous studies showed that it is essential for microglia migration during neuroinflammation. In an *Mmp-12* KO study, an age-dependent relationship between microglia recruitment and migration into the brain with increased levels of MMP-12 was established (Liu et al., 2013). They also show that lack of MMP-12 reduces neuroinflammation in aged mice. Further studies have shown that MMP-12 cleaves fibrin and extracellular actin, as well as elastin which facilitates microglia migration (Bellac et al., 2014; Liu et al., 2013). Thus, this makes MMP-12 an interesting target in the context of neuroinflammation in the aged brain but it appeared to be beyond my focus on the regulation of neural ECM.

Strikingly, almost all *Mmps* and *Adamts* that cleave CSPGs were not changed in the hippocampus of 22-24M and > 30M old mice relative to young controls, except for *Adamts-5*. Here, *Adamts-5* reduction suggested CSPGs proteolysis might be compromised in the aged brain, and, further analysis of the regulators of ADAMTS-5 activity showed that *Timp-1-3* were upregulated in 22-24M old mice, but only *Timp-1* was unregulated, with *Timp-3* downregulated in > 30M old mice. ADAMTS-5 is a major CSPG protease and the fact that it was downregulated at the mRNA level coupled with increased *Timp-3* expression prompted further analysis, especially in 22-24M old mice. Moreover, cell-specific analysis

confirmed the downregulation of *Adamts-5* in neurons and glia compared to *Chst-3* downregulated only in glia. Therefore, I checked for the protein levels of these two targets, considering a strong relationship between the activity of ADAMTS-5 on 6-sulfated CSGPs as previously suggested (Shinji Miyata and Kitagawa, 2016). In that study, they reported that 6-sulfated CSPGs are susceptible to ADAMTS-5 cleavage, and since the mRNA levels of both molecules are affected in the aged hippocampus, this might explain the reported increased expression of CSPG protein molecules.

### 5.3 CHST-3 and ADAMTS-5 are upregulated in 22-24M old mice

ADAMTS-5 is known to be expressed in neurons, astrocytes, and microglia in the hippocampus of mice (Krstic et al., 2012b) and humans (Cross et al., 2006). Using IHC, I found that the expression of ADAMTS-5 in 22-24M old mice was upregulated in neurons, astrocytes, and microglia. Furthermore, the expression of CHST-3 was also upregulated in glia but not in neurons of the hippocampus of 22-24M old mice. This thesis work, to my knowledge, is the first to specifically quantify the cell-specific expression of CHST3 and ADAMTS-5 in the hippocampus of aged mice. The high content of CHST3 and ADAMTS-5 could mean that: 1. increased post-transcriptional modification and translation of mRNA species and/or 2. decreased degradation of these proteins. These findings are robust since the specificity of antibodies was confirmed, with that of CHST3 validated in hippocampal neurons and astrocytes cultures infected with CHST3 overexpressing vectors (shown in Materials and Methods). The mouse ADAMTS-5 antibody used in this study has already been validated in an ADAMTS-5 knockdown study by ICC and western blot analysis (Mitlöhner et al., 2020). The increased levels of CHST-3 and ADAMTS-5, therefore, raise questions about their functionality, as previous studies have shown that there is an age-dependent reduction of 6-sulfated GAGs as well as increased PNN content (Mikami and Kitagawa, 2013b; Vegh et al., 2014). By staining hippocampal slices for VCAN and C6S, I discovered a high amount of VCAN core proteins in aged mice and a lower ratio of 6-sulfated GAGs relative to versican expression levels. The fact that recent finding indicates VCAN as the major carrier of 6-sulfated GAGs (Chelini et al., 2021), which has a unique ADAMTS-5 cleavage sensitivity as it is protected from proteolysis in ADAMTS-5 knockout mice unlike other lecticans (Demircan et al., 2014), making VCAN the ideal CSPG to estimate the functionality of both CHST3 and ADAMTS-5. This finding also supports previous studies that examined the ratio of 6-sulfated to 4-sulfated GAGs and showed this ratio decreases with aging (Mikami and Kitagawa, 2013b; Uyama et al., 2006). Moreover, it has already been established that the onset of 4-sulfation of GAGs coincides with PNN formation as 4-sulfated GAGs are more resistant to proteolysis (Fawcett, Oohashi and Pizzorusso,

2019). Therefore, from this first part of my thesis, I selected ADAMTS-5 as the major target to stimulate the rejuvenation of neural ECM and ameliorate the effects of aging on the hippocampus of 22-24M old mice. Here, I overexpressed the human ADAMTS-5 in the hippocampal CA1 of 22-24M old mice, and the findings will be discussed in the following sections.

#### **5.4 Effects of overexpressing hADAMTS-5 on CSPGs cleavage, neuroinflammation and distribution of oligodendrocytes**

In the brain, ADAMTS-5 cleaves several lecticans, including ACAN, BCAN, NCAN, VCAN and PCAN (Hong et al., 2020; Krstic et al., 2012b; Nakada et al., 2005). This function of ADAMTS-5, as shown above, is compromised by aging, leading to the accumulation of lecticans and hence resulting in age-dependent synaptic and cognitive impairments. Therefore, attempting to abrogate these effects of aging and considering possible medical applications, I overexpressed the human ADAMTS-5 under the human phosphoglycerate kinase promoter (hPGK) by injecting these vectors into the CA1 of 22-24M old mice. In 2 weeks, I checked and confirmed the expression of hADAMTS-5 in the hippocampus using IHC with an antibody already validated. Using body weight as an indicator of general condition of infected mice, it appeared that overexpressing ADAMTS-5 did not affect the mouse health for both acute (2-weeks) and long-term treatments (10-weeks). From further IHC analysis of proteolytic properties, I found that the hADAMTS-5 was proteolytically active as evidenced by a significant reduction in the amount of ACAN, BCAN, VCAN, NCAN, and PCAN around PV+ cells. As it is already known that PV+ cells are the major hosts of PNNs in the CA1, it was reasonable to focus on these cells to quantify the degree of hADAMTS-5 activity. Although the AAVs were injected into the CA1, I did observe some GFP+ cells in CA2 and CA3, which might be due to the retrograde diffusion of vectors (Cearley and Wolfe, 2007). The degree of substrate cleavage by hADAMTS-5 in this study follows previous reports of ADAMTS-5. The mADAMTS-5 has been reported to have the strongest effect on ACAN due to the multiple cleavage sites compared to the other CSPGs. My findings also follow the reports from these studies, with the highest degree of cleavage occurring for ACAN, followed by BCAN, and the least seen for NCAN.

Although overexpressing hADAMTS-5 cleaved all CSPGs found in PNNs, it was, therefore, necessary to check the burden of having excessive CSPG fragments in the extracellular space on the innate immune system in the hippocampus. In the context of this study, it is noteworthy that non-pathological aging results in neuroinflammation, which includes activated microglia and astrocytes (Norden and Godbout, 2013). Activated microglia and astrocytes are known to release pro-inflammatory and anti-inflammatory factors that aid in maintaining the integrity of the microenvironment (Cleeland et al., 2019). Some studies have

estimated astroglial activation using the GFAP marker (Abdelhak et al., 2019), which in this study was reduced in the hADAMTS-5 injected mice compared to age-matched controls, supporting the notion that CSPG cleavage reduces astrogliosis. A similar observation was made in a study where removal of GAGs of CSPGs with chABC in reactive astrocytes restored their resting phenotype associated with reduced GFAP mRNA levels (Rocha et al., 2015). Regarding the microglial activation, although the mean intensity of IBA1 is not recommended for the analysis of microglia activation (Kaushik et al., 2018), IBA1 is ideal for studying the morphological changes, which is the useful metric of microglia activation (Hovens et al., 2014). Surprisingly, the cleavage of CSPGs did not restore microglia to their resting state like in astrocytes but rather increased their soma and reduced their branches, which is indicative of microglial activation. This, therefore, prompted the need to further study microglia activation using the IL1beta, CD68, and C1q makers to analyze the functional state of microglia. This was essential because activated microglia are bidirectional and can either enhance synaptogenesis and plasticity or prune and eliminate synapses (Szepesi et al., 2018). For instance, the release of IL1beta, a proinflammatory cytokine, by activated microglia has been shown to enhance learning and memory in young mice but not in adult mice (Takemiya et al., 2017). The expression of IL1beta has also been shown to provide neuroprotection once its receptor (IL1-receptor1) is expressed in astrocytes (Todd et al., 2019). This might explain why from the cumulative frequency analysis I observed increased expression of IL1beta in pyramidal cells, GFAP+ and IBA1+ cells of aged ADAMTS-5 mice relative to aged control mice. This, therefore, suggests that the removal of CSPGs facilitates neuroprotection through IL1beta and activated microglia mediation, as proposed earlier (Todd et al., 2019). To further test for the neuroprotection phenotype of microglial activation, I used both CD68 and C1q markers to study the phagocytic and synaptic pruning phenotypes of activated microglia, respectively. Studies have shown that the removal of PNN fragments from the extracellular space by microglia after activity-dependent proteolysis is impaired in the aged hippocampus due to reduced neuronal expression of IL-33 (Nguyen et al., 2020). Furthermore, the phagocytosis of PNN fragments is CD68 dependent and this is vital for experience-dependent synapse remodelling which promotes memory consolidation (Nguyen et al., 2020). Reduced expression of CD68 has been shown to result in enhanced perisynaptic accumulation of ECM thereby restricting synaptic plasticity (Crapser et al., 2021). The activity of microglia has also been shown to depend on C1q expression. C1q, a member of the immune complement system (Györfy et al., 2018), tags synapses that are subsequently pruned by phagocytic microglia (Presumey et al., 2017). The activated microglia in hADAMTS-5 injected mice appeared to be beneficial for removing the excessive CSPG fragments in the extracellular space whilst be less active to eliminate synapses. This is because

CD68+ puncta were bigger in size, while C1q expression was decreased in both microglia and in the neuropil of aged ADAMTS-5 mice compared to aged control mice.

Evidence suggests that aging, as well as overexpression of CSPGs, affect the distribution and function of oligodendrocytes (Andrews et al., 2012; Harlow and Macklin, 2014; Hayakawa et al., 2007). Studies have shown that the removal of CSPGs with chABC abrogated the inhibitory effects of CSPGs on oligodendrocyte functions (Pendleton et al., 2013b). Functionally, oligodendrocytes, aside from myelinating axons of neurons that enhance the conduction velocity of action potentials, control action potentials conduction in neurons via mechanisms other than myelination (Yamazaki et al., 2010). Such mechanisms include oligodendrocyte depolarization by responding to neurotransmitters through glutamate receptors (Salter and Fern, 2005). Additionally, depolarization of oligodendrocytes has been demonstrated in a recent study to enhance LTP and learning in adult mice (Yamazaki et al., 2021). In the present study, I show by IHC analysis with the OLIG2 antibody that the removal of CSPGs enhanced the migration/differentiation of the cells of the oligodendrocyte lineage which includes oligodendrocyte progenitor cells (OPCs), pre and myelinating oligodendrocytes (Pepper et al., 2018), into the *stratum oriens*. In the CA1, axonal projections from the somata of pyramidal neurons to distant brain areas pass through the *stratum oriens* (Arszovszki et al., 2014), and this might explain why I observed increased migration of oligodendrocyte to this region but not to the *stratum radiatum*. Previous studies showed that there are myelinated axons passing the *stratum oriens* (Yamazaki et al., 2021, 2010). In summary, these data suggest that overexpression of ADAMTS-5 affected all types of glial cells by reducing astrogliosis and synaptic phagocytosis by microglia, and promoting microglial clearance of degraded ECM/cell debris and long-range neuronal communication via myelinated axons.

### **5.5 CSPG remodeling improved long-term NOLT memory and spatial learning and memory in 22-24-month-old mice**

It is noteworthy from previous studies that increased expression of CSPGs results in cognitive impairment (Koskinen et al., 2020). For example, a study by Vegh and colleagues observed reduced spontaneous object recognition as well as spatial learning and memory in the hippocampus of aged mice using several behavioral strategies like the Barnes maze test (Vegh et al., 2014; Yang et al., 2021). Some studies have also shown that ECM remodeling might have a positive or negative impact on cognitive functions, especially in the hippocampus. For instance, cognitive and LTP impairments have been reported in TnC

KO mice (Evers et al., 2002) and after digestion of neural ECM by hyaluronidase or ChABC (Senkov et al., 2012), whereas only LTP impairment has been observed in BCAN KO mice (Brakebusch et al., 2002). However, cognitive enhancement, on the other hand, has been seen in TNR KO mice in the context of reversal learning (Morellini et al., 2010) along with enhanced object recognition memory after depleting PNNs using chABC (Romberg et al., 2013).

In this study, using the hippocampus-dependent NOLT test, cognitive impairment was first confirmed in 22-24-month-old mice. Here, the 22-24-month-old mice failed to discriminate between the stably located and displaced objects. However, two weeks after overexpressing hADAMTS-5 in aged mice, the long-term NOLT memory was enhanced, together with a partial improvement in NORT memory. Additionally, CSPG remodeling in the hippocampus enhanced spatial learning and memory in an asymmetrical quadrant-based dry maze test. With this behavioral strategy, both errors made and the distance travelled were used to measure cognitive performance, and hADAMTS-5-injected mice made fewer errors and covered shorter distances in locating the reward. The use of errors has been shown to be an ideal metric for quantifying cognitive performance in maze experiments compared to latency to reward (Maei et al., 2009b). From the additional analysis, I concluded that the removal of CSPGs also stabilized memory of reward location during the 2-phase probe test, which was impaired in aged control mice. Although some studies showed that CSPGs are essential for memory consolidation (Shi et al., 2019), in this study, however, memory consolidation was not affected in the aged ADAMTS-5 mice.

## **5.6 Molecular and cellular mechanisms behind cognitive enhancement in hADAMTS-5 injected mice**

Changes in synaptic strength have been strongly associated with learning and memory through LTP and LTD. Induction and maintenance of LTP are dependent on the activity of AMPA and NMDA subtypes of glutamate receptors in addition to  $\text{Ca}^{2+}$ -dependent downstream signaling (Mango et al., 2019). Noteworthy, the ADAMTS-5 activity towards perisynaptic CSPGs and intracellular  $\text{Ca}^{2+}$  signaling has been demonstrated to be NMDA receptor- and CaMKII-dependent (Mitlöhner et al., 2020). Aging has been shown to affect the expression of LTP via reducing AMPAR and NMDAR expression and functions (Temido-Ferreira et al., 2019). Interestingly, aging also increases the expression of GluN2B-containing NMDARs, which are mostly located at extrasynaptic sites (Hardingham and Bading, 2010). The imbalance in activation of these extrasynaptic GluN2B-containing NMDARs relative to synaptic NMDARs has been

associated with reduced LTP as well as memory impairments (Avila et al., 2017; Kochlamazashvili et al., 2012). Therefore, since the removal of CSPGs in ADAMTS-5 injected mice enhanced cognitive performance, I studied synaptic plasticity and observed enhanced LTP. Moreover, inhibiting the extrasynaptic GluN2B-containing NMDARs with GluN2B antagonist Ro25 improved LTP in aged control mice but not in ADAMTS-5 injected mice, showing occlusion of GluN2B inhibition and cleavage of ECM. This implies that the LTP enhancement observed in ADAMTS-5 injected mice is due to the inhibition of signaling via extrasynaptic NMDARs.

Another reason might be that the increased GluN2B signaling at synaptic sites overrides the inhibitory contribution from the extrasynaptic NMDARs in ADAMTS-5 injected mice. Therefore, the interaction between CSPG and the expression of GluN2B-containing NMDARs has been studied. One study by Schweitzer in 2017 found that the enzymatic remodeling of ECM with hyaluronidase, for example, increased the surface expression of GluN2B-NMDARs without altering the total GluN2B protein. Schweitzer also demonstrated that the surface GluN2B-NMDARs were further phosphorylated, thereby preventing lateral diffusion to extrasynaptic sites (Chen et al., 2012) and endocytosis (Cheung and Gurd, 2001; Prybylowski et al., 2005; Sanz-Clemente et al., 2010), which enhances LTP (Schweitzer *et al.*, 2017). Therefore, using super-resolution imaging, the effect of CSPG remodeling on GluN2B-containing NMDARs was analyzed in this study to better elucidate the mechanism behind the aforementioned enhancement of synaptic transmission in hADAMTS-5 injected mice. However, our STED analysis revealed no changes in expression of synaptic GluN2B in PSD95+ domains, suggesting that the rescue of plasticity by ADAMTS-5 overexpression is due to functional inactivation of extrasynaptic GluN2B signaling. Using an antibody widely used to study phosphorylated CREB, I showed that the removal of CSPGs resulted in increased phosphorylation of CREB. Interestingly, c-Fos, which is downstream of pCREB, was also upregulated in hADAMTS-5 injected mice, confirming the effect of CSPG remodeling on the pCREB and c-Fos axis, which is critical for LTP induction and maintenance.

Lastly, CSPG expression has been shown to affect synaptic strength and abundance in the aged hippocampus (Wingert and Sorg, 2021). Aging has been shown, by overwhelming evidence, to reduce the expression of proteins that regulate neurotransmission in the hippocampal synaptosomal proteome (VanGuilder et al., 2010). Additionally, decreased expression of the neurotransmitter, glutamate, has been reported in the hippocampus of aged mice together with decreased presynaptic glutamate release probability (Deak and Sonntag, 2012a). However, in this study, I show that the proteolytic removal of CSPG core proteins may at least partially restore the synaptic density and the level of vGAT/vGLUT1 expression for

both vGAT+ and in particular vGLUT1+ synapses on PV+ cells to the level of young mice. Also, the expression of PV proteins was normalized to the soma size of PV+ cells and using the established classes of PV-network configurations which included the high, interhigh, interlow and low PV content (Donato et al., 2013), I discovered that the removal of CSPGs affected PV-network configurations. CSPG remodelling promoted an increase in the fraction of high PV-containing PV+ cells in aged mice. Interestingly, studies show that the switch of PV configurations in PV+ cells to high-PV-network configurations is essential for learning and memory processes in mice (Donato et al., 2015, 2013). Furthermore, as PV expression is activity-dependent, this finding suggests normalization of PV+ cell activity, which is crucial to synchronize the activity of principal cells. Hippocampal rhythms are important for proper memory formation and the activity of PV+ inhibitory neurons (Bartos et al., 2007; Colgin and Moser, 2010) is important for gamma-oscillations (Colgin, 2016). Moreover, PNNs have been shown to modulate gamma-oscillations (Wingert and Sorg, 2021). Strikingly, PNN attenuation increased gamma activity in the visual cortex (Lensjø et al., 2017) as well as in the hippocampus (Lorenzo Bozzelli et al., 2018; Sun et al., 2018). Thus, some of the effects on cognitive functions may be due to PNN remodeling and changes in synaptic innervation of PV+ neurons in addition to facilitation of the induction of LTP. Finally, as from this study the removal of CSPGs by hADAMTS-5 in the hippocampus of aged mice resulted in a lot of essential changes or effects, I have, therefore, summarized the age-dependent changes and the degree of restoration in the following table (Table 5.1).

**Table 5.1** Summary of age-dependent changes and degree of restoration after removing CSPGs in the hippocampus of aged mice

<b>Parameter</b>	<b>Aging Effect</b>	<b>ADAMTS-5 effect</b>
<b>ECM (CSPGs)</b>	Increased ACAN, BCAN and VCAN	ACAN and BCAN are strongly cleaved, VCAN, NCAN and PCAN are less cleaved
<b>Astrogliosis</b>	Increased	Restored to resting state
<b>Microglia activation</b>	Increased	Enhanced phagocytosis (CD68)
<b>Oligodendrocytic migration/differentiation</b>	Decreased in <i>str. oriens</i>	Increased in <i>str. oriens</i>
<b>vGLUT1+ synapses on PV+ cells</b>	Decreased	Fully rescued
<b>vGAT+ synapses on PV+ cells</b>	Decreased	Fully rescued
<b>Overall PV expression</b>	Decreased	Fully rescued
<b>High PV fraction</b>	Decreased	Fully rescued
<b>GluN2B at synaptic sites</b>	Normal	Not changed
<b>pCREB signaling</b>	Decreased	Fully rescued
<b>LTP</b>	Impaired	Partially rescued
<b>NOLT memory</b>	Impaired	Fully rescued
<b>NORT memory</b>	No change	Improved
<b>Spatial learning and memory</b>	Impaired	Fully rescued

## 6 CONCLUSIONS

- The age-dependent accumulation of ECM proteins may be due to the dysregulated proteolysis of ECM by ADAMTS-5.
- The degradation of CSPGs in the hippocampus of aged mice overexpressing hADAMTS-5 reduced activation of astrocytes whereas microglial phagocytosis was increased to critically deal with the burden of having excessive proteolytic CSPG fragments in the extracellular space.
- The removal of CSPGs partially restored both excitatory and inhibitory synaptic contacts on PV+ cells to the level seen in young mice. Additionally, this treatment promoted the switch of PV-network configurations to high PV content in PV+ interneurons.
- The removal of CSPGs partially abrogated the age-associated LTP impairment and this rescue effect was presumably via the inactivation of GluN2B-containing NMDARs at the extrasynaptic sites and enhanced CREB-mediated signaling.
- Impaired NOLT memory, as well as spatial learning and memory in aged mice, were fully rescued by overexpression of hADAMTS-5.

## OUTLOOK

To gain better control over the timing and levels of activity-dependent remodeling of ECM in the aged hippocampus, it will be instrumental in the future to use an inducible form of hADAMTS-5. Further analysis to unravel the mechanism by which proteolytic degradation of CSPGs affects both synaptic and extrasynaptic signaling via NMDARs may guide us in the development of new treatments for cognitive enhancement in aging.

---

## 7 REFERENCES

- Abbaszade, I., Liu, R.-Q., Yang, F., Rosenfeld, S.A., Ross, O.H., Link, J.R., Ellis, D.M., Tortorella, M.D., Pratta, M.A., Hollist, J.M., Wynn, R., Duke, J.L., George, H.J., Hillman Jr., M.C., Murphy, K., Wiswall, B.H., Copeland, R.A., Decicco, C.P., Bruckner, R., Nagase, H., Itoh, Y., Newton, R.C., Magolda, R.L., Trzaskos, J.M., Hollis, G.F., Arner, E.C., Burn, T.C., 1999. Cloning and characterization of ADAMTS11, an aggrecanase from the ADAMTS family. *J. Biol. Chem.* 274, 23443–23450. <https://doi.org/10.1074/jbc.274.33.23443>
- Abdelhak, A., Hottenrott, T., Morenas-Rodríguez, E., Suárez-Calvet, M., Zettl, U.K., Haass, C., Meuth, S.G., Rauer, S., Otto, M., Tumani, H., Huss, A., 2019. Glial Activation Markers in CSF and Serum From Patients With Primary Progressive Multiple Sclerosis: Potential of Serum GFAP as Disease Severity Marker? *Front. Neurol.* 10, 280. <https://doi.org/10.3389/fneur.2019.00280>
- Abraham, W.C., Jones, O.D., Glanzman, D.L., 2019. Is plasticity of synapses the mechanism of long-term memory storage? *Npj Sci. Learn.* 4, 1–10. <https://doi.org/10.1038/s41539-019-0048-y>
- Adams, M.M., Shi, L., Linville, M.C., Forbes, M.E., Long, A.B., Bennett, C., Newton, I.G., Carter, C.S., Sonntag, W.E., Riddle, D.R., Brunso-Bechtold, J.K., 2008. Caloric restriction and age affect synaptic proteins in hippocampal CA3 and spatial learning ability. *Exp. Neurol.* 211, 141–149. <https://doi.org/10.1016/j.expneurol.2008.01.016>
- Ajmo, J.M., Eakin, A.K., Hamel, M.G., Gottschall, P.E., 2008. Discordant localization of WFA reactivity and brevican/ADAMTS-derived fragment in rodent brain. *BMC Neurosci.* 9, 14. <https://doi.org/10.1186/1471-2202-9-14>
- Alberini, C.M., Johnson, S.A., Ye, X., 2013. Chapter five - Memory Reconsolidation: Lingering Consolidation and the Dynamic Memory Trace, in: Alberini, C.M. (Ed.), *Memory Reconsolidation*. Academic Press, San Diego, pp. 81–117. <https://doi.org/10.1016/B978-0-12-386892-3.00005-6>
- Andrews, E.M., Richards, R.J., Yin, F.Q., Viapiano, M.S., Jakeman, L.B., 2012. Alterations in chondroitin sulfate proteoglycan expression occur both at and far from the site of spinal contusion injury. *Exp. Neurol.* 235, 174–187. <https://doi.org/10.1016/j.expneurol.2011.09.008>
- Apte, S.S., Hayashi, K., Seldin, M.F., Mattei, M.G., Hayashi, M., Olsen, B.R., 1994. Gene encoding a novel murine tissue inhibitor of metalloproteinases (TIMP), TIMP-3, is expressed in developing mouse epithelia, cartilage, and muscle, and is located on mouse chromosome 10. *Dev. Dyn. Off. Publ. Am. Assoc. Anat.* 200, 177–197. <https://doi.org/10.1002/aja.1002000302>
- Aranapakam, V., Grosu, G.T., Davis, J.M., Hu, B., Ellingboe, J., Baker, J.L., Skotnicki, J.S., Zask, A., DiJoseph, J.F., Sung, A., Sharr, M.A., Killar, L.M., Walter, T., Jin, G., Cowling, R., 2003. Synthesis and structure - Activity relationship of  $\alpha$ -sulfonylhydroxamic acids as novel, orally active matrix metalloproteinase inhibitors for the treatment of osteoarthritis. *J. Med. Chem.* 46, 2361–2375. <https://doi.org/10.1021/jm0205548>
- Arszovszki, A., Borhegyi, Z., Klausberger, T., 2014. Three axonal projection routes of individual pyramidal cells in the ventral CA1 hippocampus. *Front. Neuroanat.* 8.
- Ashby, D.M., Floresco, S.B., Phillips, A.G., McGirr, A., Seamans, J.K., Wang, Y.T., 2021. LTD is involved in the formation and maintenance of rat hippocampal CA1 place-cell fields. *Nat. Commun.* 12, 100. <https://doi.org/10.1038/s41467-020-20317-7>
- Asher, R.A., Morgenstern, D.A., Shearer, M.C., Adcock, K.H., Pesheva, P., Fawcett, J.W., 2002. Versican Is Upregulated in CNS Injury and Is a Product of Oligodendrocyte Lineage Cells. *J. Neurosci.* 22, 2225–2236. <https://doi.org/10.1523/JNEUROSCI.22-06-02225.2002>
- Avila, J., Llorens-Martín, M., Pallas-Bazarrá, N., Bolós, M., Perea, J.R., Rodríguez-Matellán, A., Hernández, F., 2017. Cognitive Decline in Neuronal Aging and Alzheimer’s Disease: Role of NMDA Receptors and Associated Proteins. *Front. Neurosci.* 11, 626. <https://doi.org/10.3389/fnins.2017.00626>

- 
- Ayoub, A.E., Cai, T.-Q., Kaplan, R.A., Luo, J., 2005. Developmental expression of matrix metalloproteinases 2 and 9 and their potential role in the histogenesis of the cerebellar cortex. *J. Comp. Neurol.* 481, 403–415. <https://doi.org/10.1002/cne.20375>
- Back, S.A., Tuohy, T.M.F., Chen, H., Wallingford, N., Craig, A., Struve, J., Luo, N.L., Banine, F., Liu, Y., Chang, A., Trapp, B.D., Bebo, Rao, M.S., Sherman, L.S., 2005. Hyaluronan accumulates in demyelinated lesions and inhibits oligodendrocyte progenitor maturation. *Nat. Med.* 11, 966–972. <https://doi.org/10.1038/nm1279>
- Bai, X., Wei, G., Sinha, A., Esko, J.D., 1999. Chinese Hamster Ovary Cell Mutants Defective in Glycosaminoglycan Assembly and Glucuronosyltransferase I\*. *J. Biol. Chem.* 274, 13017–13024. <https://doi.org/10.1074/jbc.274.19.13017>
- Bai, X., Zhou, D., Brown, J.R., Crawford, B.E., Hennet, T., Esko, J.D., 2001. Biosynthesis of the Linkage Region of Glycosaminoglycans: CLONING AND ACTIVITY OF GALACTOSYLTRANSFERASE II, THE SIXTH MEMBER OF THE  $\beta$ 1,3-GALACTOSYLTRANSFERASE FAMILY ( $\beta$ 3GalT6)\*. *J. Biol. Chem.* 276, 48189–48195. <https://doi.org/10.1074/jbc.M107339200>
- Bär, J., Kobler, O., van Bommel, B., Mikhaylova, M., 2016. Periodic F-actin structures shape the neck of dendritic spines. *Sci. Rep.* 6, 37136. <https://doi.org/10.1038/srep37136>
- Barnes, C.A., Rao, G., Houston, F.P., 2000. LTP induction threshold change in old rats at the perforant path–granule cell synapse. *Neurobiol. Aging* 21, 613–620. [https://doi.org/10.1016/S0197-4580\(00\)00163-9](https://doi.org/10.1016/S0197-4580(00)00163-9)
- Barreto, G., Huang, T.-T., Giffard, R.G., 2010. Age-related defects in sensorimotor activity, spatial learning and memory in C57BL/6 mice. *J. Neurosurg. Anesthesiol.* 22, 214–219. <https://doi.org/10.1097/ANA.0b013e3181d56c98>
- Bartos, M., Vida, I., Jonas, P., 2007. Synaptic mechanisms of synchronized gamma oscillations in inhibitory interneuron networks. *Nat. Rev. Neurosci.* 8, 45–56. <https://doi.org/10.1038/nrn2044>
- Bear, M.F., Cooper, L.N., Ebner, F.F., 1987. A Physiological Basis for a Theory of Synapse Modification. *Science* 237, 42–48. <https://doi.org/10.1126/science.3037696>
- Beer, Z., Vavra, P., Atucha, E., Rentzing, K., Heinze, H.-J., Sauvage, M.M., 2018. The memory for time and space differentially engages the proximal and distal parts of the hippocampal subfields CA1 and CA3. *PLoS Biol.* 16, e2006100. <https://doi.org/10.1371/journal.pbio.2006100>
- Bekku, Y., Rauch, U., Ninomiya, Y., Oohashi, T., 2009. Brevican distinctively assembles extracellular components at the large diameter nodes of Ranvier in the CNS. *J. Neurochem.* 108, 1266–1276. <https://doi.org/10.1111/j.1471-4159.2009.05873.x>
- Bellac, C.L., Dufour, A., Krisinger, M.J., Loonchanta, A., Starr, A.E., auf dem Keller, U., Lange, P.F., Goebeler, V., Kappelhoff, R., Butler, G.S., Burtnick, L.D., Conway, E.M., Roberts, C.R., Overall, C.M., 2014. Macrophage Matrix Metalloproteinase-12 Dampens Inflammation and Neutrophil Influx in Arthritis. *Cell Rep.* 9, 618–632. <https://doi.org/10.1016/j.celrep.2014.09.006>
- Bergado, J.A., Almaguer, W., 2002. Aging and Synaptic Plasticity: A Review. *Neural Plast.* 9, 217–232. <https://doi.org/10.1155/NP.2002.217>
- Bernard, C., Prochiantz, A., 2016. Otx2-PNN Interaction to Regulate Cortical Plasticity. *Neural Plast.* 2016, 1–7. <https://doi.org/10.1155/2016/7931693>
- Beurden, P.A.M.S., Hoff, J.W.V. den, 2018. Zymographic techniques for the analysis of matrix metalloproteinases and their inhibitors [WWW Document]. <https://doi.org/10.2144/05381RV01>. <https://doi.org/10.2144/05381RV01>
- Biello, S.M., Bonsall, D.R., Atkinson, L.A., Molyneux, P.C., Harrington, M.E., Lall, G.S., 2018. Alterations in glutamatergic signaling contribute to the decline of circadian photoentrainment in aged mice. *Neurobiol. Aging* 66, 75–84. <https://doi.org/10.1016/j.neurobiolaging.2018.02.013>

- 
- Bikbaev, A., Frischknecht, R., Heine, M., 2015. Brain extracellular matrix retains connectivity in neuronal networks. *Sci. Rep.* 5, 14527. <https://doi.org/10.1038/srep14527>
- Bimonte, H.A., Nelson, M.E., Granholm, A.-C.E., 2003. Age-related deficits as working memory load increases: relationships with growth factors. *Neurobiol. Aging* 24, 37–48. [https://doi.org/10.1016/S0197-4580\(02\)00015-5](https://doi.org/10.1016/S0197-4580(02)00015-5)
- Bisaz, R., Travaglia, A., Alberini, C.M., 2014. The neurobiological bases of memory formation: from physiological conditions to psychopathology. *Psychopathology* 47, 347–356. <https://doi.org/10.1159/000363702>
- Bitanhirwe, B.K.Y., Woo, T.-U.W., 2014. Perineuronal Nets and Schizophrenia: The Importance of Neuronal Coatings. *Neurosci. Biobehav. Rev.* 45, 85–99. <https://doi.org/10.1016/j.neubiorev.2014.03.018>
- Blanke, M.L., VanDongen, A.M.J., 2009. Activation Mechanisms of the NMDA Receptor, in: Van Dongen, A.M. (Ed.), *Biology of the NMDA Receptor*, *Frontiers in Neuroscience*. CRC Press/Taylor & Francis, Boca Raton (FL).
- Bliss, T.V., Collingridge, G.L., 1993. A synaptic model of memory: long-term potentiation in the hippocampus. *Nature* 361, 31–39. <https://doi.org/10.1038/361031a0>
- Blumberg, M., Freeman, J., Robinson, S., 2009. *Oxford Handbook of Developmental Behavioral Neuroscience*. Oxford University Press.
- Boggio, E.M., Ehlert, E.M., Lupori, L., Moloney, E.B., De Winter, F., Vander Kooi, C.W., Baroncelli, L., Mecollari, V., Blits, B., Fawcett, J.W., Verhaagen, J., Pizzorusso, T., 2019. Inhibition of Semaphorin3A Promotes Ocular Dominance Plasticity in the Adult Rat Visual Cortex. *Mol. Neurobiol.* 56, 5987–5997. <https://doi.org/10.1007/s12035-019-1499-0>
- Bonnans, C., Chou, J., Werb, Z., 2014. Remodelling the extracellular matrix in development and disease. *Nat Rev Mol Cell Biol* 15, 786–801. <https://doi.org/10.1038/nrm3904>
- Bonneh-Barkay, D., Wiley, C.A., 2009. Brain Extracellular Matrix in Neurodegeneration. *Brain Pathol.* 19, 573–585. <https://doi.org/10.1111/j.1750-3639.2008.00195.x>
- Bosiacki, M., Gąssowska-Dobrowolska, M., Kojder, K., Fabiańska, M., Jeżewski, D., Gutowska, I., Lubkowska, A., 2019. Perineuronal Nets and Their Role in Synaptic Homeostasis. *Int. J. Mol. Sci.* 20, 4108. <https://doi.org/10.3390/ijms20174108>
- Bozdagi, O., Nagy, V., Kwei, K.T., Huntley, G.W., 2007. In Vivo Roles for Matrix Metalloproteinase-9 in Mature Hippocampal Synaptic Physiology and Plasticity. *J. Neurophysiol.* 98, 334–344. <https://doi.org/10.1152/jn.00202.2007>
- Brakebusch, C., Seidenbecher, C.I., Asztely, F., Rauch, U., Matthies, H., Meyer, H., Krug, M., Böckers, T.M., Zhou, X., Kreutz, M.R., Montag, D., Gundelfinger, E.D., Fässler, R., 2002. Brevican-deficient mice display impaired hippocampal CA1 long-term potentiation but show no obvious deficits in learning and memory. *Mol. Cell. Biol.* 22, 7417–7427. <https://doi.org/10.1128/MCB.22.21.7417-7427.2002>
- Brauer, P.R., 2006. MMPs--role in cardiovascular development and disease. *Front. Biosci. J. Virtual Libr.* 11, 447–478. <https://doi.org/10.2741/1810>
- Brauer, R., Beck, I.M., Roderfeld, M., Roeb, E., Sedlacek, R., 2011. Matrix metalloproteinase-19 inhibits growth of endothelial cells by generating angiostatin-like fragments from plasminogen. *BMC Biochem.* 12, 38. <https://doi.org/10.1186/1471-2091-12-38>
- Brew, K., Nagase, H., 2010. The tissue inhibitors of metalloproteinases (TIMPs): An ancient family with structural and functional diversity. *Biochim. Biophys. Acta* 1803, 55–71. <https://doi.org/10.1016/j.bbamcr.2010.01.003>
- Brinckerhoff, C.E., Matrisian, L.M., 2002. Matrix metalloproteinases: a tail of a frog that became a prince. *Nat. Rev. Mol. Cell Biol.* 3, 207–214. <https://doi.org/10.1038/nrm763>

- 
- Brod, G., Werkle-Bergner, M., Shing, Y.L., 2013. The Influence of Prior Knowledge on Memory: A Developmental Cognitive Neuroscience Perspective. *Front. Behav. Neurosci.* 7, 139. <https://doi.org/10.3389/fnbeh.2013.00139>
- Brömme, D., Nallaseth, F.S., Turk, B., 2004. Production and activation of recombinant papain-like cysteine proteases. *Methods San Diego Calif* 32, 199–206. [https://doi.org/10.1016/s1046-2023\(03\)00212-3](https://doi.org/10.1016/s1046-2023(03)00212-3)
- Brömme, D., Wilson, S., 2011. Role of Cysteine Cathepsins in Extracellular Proteolysis, in: Parks, W.C., Mecham, R.P. (Eds.), *Extracellular Matrix Degradation, Biology of Extracellular Matrix*. Springer, Berlin, Heidelberg, pp. 23–51. [https://doi.org/10.1007/978-3-642-16861-1\\_2](https://doi.org/10.1007/978-3-642-16861-1_2)
- Buck, M.R., Karustis, D.G., Day, N.A., Honn, K.V., Sloane, B.F., 1992. Degradation of extracellular-matrix proteins by human cathepsin B from normal and tumour tissues. *Biochem. J.* 282 ( Pt 1), 273–278. <https://doi.org/10.1042/bj2820273>
- Bukalo, O., Schachner, M., Dityatev, A., 2001. Modification of extracellular matrix by enzymatic removal of chondroitin sulfate and by lack of tenascin-R differentially affects several forms of synaptic plasticity in the hippocampus. *Neuroscience* 104, 359–369. [https://doi.org/10.1016/S0306-4522\(01\)00082-3](https://doi.org/10.1016/S0306-4522(01)00082-3)
- Burke, S.N., Barnes, C.A., 2010. Senescent synapses and hippocampal circuit dynamics. *Trends Neurosci.* 33, 153–161. <https://doi.org/10.1016/j.tins.2009.12.003>
- Burke, S.N., Barnes, C.A., 2006. Neural plasticity in the ageing brain. *Nat Rev Neurosci* 7, 30–40. <https://doi.org/10.1038/nrn1809>
- Butler, D., Hwang, J., Estick, C., Nishiyama, A., Kumar, S.S., Baveghems, C., Young-Oxendine, H.B., Wisniewski, M.L., Charalambides, A., Bahr, B.A., 2011. Protective Effects of Positive Lysosomal Modulation in Alzheimer’s Disease Transgenic Mouse Models. *PLoS ONE* 6, e20501. <https://doi.org/10.1371/journal.pone.0020501>
- Caglič, D., Pungerčar, J.R., Pejler, G., Turk, V., Turk, B., 2007. Glycosaminoglycans Facilitate Procathepsin B Activation through Disruption of Propeptide-Mature Enzyme Interactions \*. *J. Biol. Chem.* 282, 33076–33085. <https://doi.org/10.1074/jbc.M705761200>
- Cao, M., Huang, H., He, Y., 2017. Developmental Connectomics from Infancy through Early Childhood. *Trends Neurosci.* 40, 494–506. <https://doi.org/10.1016/j.tins.2017.06.003>
- Carceller, H., Guirado, R., Ripolles-Campos, E., Teruel-Marti, V., Nacher, J., 2020. Perineuronal Nets Regulate the Inhibitory Perisomatic Input onto Parvalbumin Interneurons and  $\gamma$  Activity in the Prefrontal Cortex. *J. Neurosci.* 40, 5008–5018. <https://doi.org/10.1523/JNEUROSCI.0291-20.2020>
- Carulli, D., Pizzorusso, T., Kwok, J.C.F., Putignano, E., Poli, A., Forostyak, S., Andrews, M.R., Deepa, S.S., Glant, T.T., Fawcett, J.W., 2010. Animals lacking link protein have attenuated perineuronal nets and persistent plasticity. *Brain* 133, 2331–2347. <https://doi.org/10.1093/brain/awq145>
- Carulli, D., Verhaagen, J., 2021. An Extracellular Perspective on CNS Maturation: Perineuronal Nets and the Control of Plasticity. *Int. J. Mol. Sci.* 22, 2434. <https://doi.org/10.3390/ijms22052434>
- Cearley, C.N., Wolfe, J.H., 2007. A Single Injection of an Adeno-Associated Virus Vector into Nuclei with Divergent Connections Results in Widespread Vector Distribution in the Brain and Global Correction of a Neurogenetic Disease. *J. Neurosci.* 27, 9928–9940. <https://doi.org/10.1523/JNEUROSCI.2185-07.2007>
- Cermak, S., Kosicek, M., Mladenovic-Djordjevic, A., Smiljanic, K., Kanazir, S., Hecimovic, S., 2016. Loss of Cathepsin B and L Leads to Lysosomal Dysfunction, NPC-Like Cholesterol Sequestration and Accumulation of the Key Alzheimer’s Proteins. *PloS One* 11, e0167428. <https://doi.org/10.1371/journal.pone.0167428>
- Cerofolini, L., Amar, S., Lauer, J.L., Martelli, T., Fragai, M., Luchinat, C., Fields, G.B., 2016. Bilayer Membrane Modulation of Membrane Type 1 Matrix Metalloproteinase (MT1-MMP) Structure and Proteolytic Activity. *Sci. Rep.* 6, 29511. <https://doi.org/10.1038/srep29511>

- 
- Chakraborti, S., Mandal, M., Das, S., Mandal, A., Chakraborti, T., 2003. Regulation of matrix metalloproteinases. An overview. *Mol. Cell. Biochem.* 253, 269–285. <https://doi.org/10.1023/A:1026028303196>
- Chan, C.C.M., Roberts, C.R., Steeves, J.D., Tetzlaff, W., 2008. Aggrecan components differentially modulate nerve growth factor-responsive and neurotrophin-3-responsive dorsal root ganglion neurite growth. *J. Neurosci. Res.* 86, 581–592. <https://doi.org/10.1002/jnr.21522>
- Chan, W.Y., Lorke, D.E., Tiu, S.C., Yew, D.T., 2002. Proliferation and apoptosis in the developing human neocortex. *Anat. Rec.* 267, 261–276. <https://doi.org/10.1002/ar.10100>
- Chee, S.E.J., Solito, E., 2021. The Impact of Ageing on the CNS Immune Response in Alzheimer’s Disease. *Front. Immunol.* 12, 3818. <https://doi.org/10.3389/fimmu.2021.738511>
- Chen, B.-S., Gray, J.A., Sanz-Clemente, A., Wei, Z., Thomas, E.V., Nicoll, R.A., Roche, K.W., 2012. SAP102 mediates synaptic clearance of NMDA receptors. *Cell Rep.* 2, 1120–1128. <https://doi.org/10.1016/j.celrep.2012.09.024>
- Cheng, X.W., Shi, G.-P., Kuzuya, M., Sasaki, T., Okumura, K., Murohara, T., 2012. Role for Cysteine Protease Cathepsins in Heart Disease: Focus on Biology and Mechanisms With Clinical Implication. *Circulation* 125, 1551–1562. <https://doi.org/10.1161/CIRCULATIONAHA.111.066712>
- Cheung, H.H., Gurd, J.W., 2001. Tyrosine phosphorylation of the N-methyl-d-aspartate receptor by exogenous and postsynaptic density-associated Src-family kinases. *J. Neurochem.* 78, 524–534. <https://doi.org/10.1046/j.1471-4159.2001.00433.x>
- Chini, M., Hanganu-Opatz, I.L., 2021. Prefrontal Cortex Development in Health and Disease: Lessons from Rodents and Humans. *Trends Neurosci.* 44, 227–240. <https://doi.org/10.1016/j.tins.2020.10.017>
- Cleeland, C., Pipingas, A., Scholey, A., White, D., 2019. Neurochemical changes in the aging brain: A systematic review. *Neurosci. Biobehav. Rev.* 98, 306–319. <https://doi.org/10.1016/j.neubiorev.2019.01.003>
- Coles, C.H., Shen, Y., Tenney, A.P., Siebold, C., Sutton, G.C., Lu, W., Gallagher, J.T., Jones, E.Y., Flanagan, J.G., Aricescu, A.R., 2011. Proteoglycan-Specific Molecular Switch for RPTP $\sigma$  Clustering and Neuronal Extension. *Science* 332, 484–488. <https://doi.org/10.1126/science.1200840>
- Colgin, L.L., 2016. Rhythms of the hippocampal network. *Nat. Rev. Neurosci.* 17, 239–249. <https://doi.org/10.1038/nrn.2016.21>
- Colgin, L.L., Moser, E.I., 2010. Gamma oscillations in the hippocampus. *Physiol. Bethesda Md* 25, 319–329. <https://doi.org/10.1152/physiol.00021.2010>
- Collingridge, G.L., Peineau, S., Howland, J.G., Wang, Y.T., 2010. Long-term depression in the CNS. *Nat. Rev. Neurosci.* 11, 459–473. <https://doi.org/10.1038/nrn2867>
- Collins-Racie, L.A., Flannery, C.R., Zeng, W., Corcoran, C., Annis-Freeman, B., Agostino, M.J., Arai, M., DiBlasio-Smith, E., Dorner, A.J., Georgiadis, K.E., Jin, M., Tan, X.-Y., Morris, E.A., LaVallie, E.R., 2004. ADAMTS-8 exhibits aggrecanase activity and is expressed in human articular cartilage. *Matrix Biol.* 23, 219–230. <https://doi.org/10.1016/j.matbio.2004.05.004>
- Colognato, H., French-Constant, C., Feltri, M.L., 2005. Human diseases reveal novel roles for neural laminins. *Trends Neurosci.* 28, 480–486. <https://doi.org/10.1016/j.tins.2005.07.004>
- Cooke, S.F., Bliss, T.V.P., 2006. Plasticity in the human central nervous system. *Brain* 129, 1659–1673. <https://doi.org/10.1093/brain/awl082>
- Cowan, N., 2008. What are the differences between long-term, short-term, and working memory? *Prog. Brain Res.* 169, 323–338. [https://doi.org/10.1016/S0079-6123\(07\)00020-9](https://doi.org/10.1016/S0079-6123(07)00020-9)
- Cox, T.R., Erler, J.T., 2011. Remodeling and homeostasis of the extracellular matrix: implications for fibrotic diseases and cancer. *Dis. Model. Mech.* 4, 165–178. <https://doi.org/10.1242/dmm.004077>

- 
- Crapser, J.D., Arreola, M.A., Tsourmas, K.I., Green, K.N., 2021. Microglia as hackers of the matrix: sculpting synapses and the extracellular space. *Cell. Mol. Immunol.* 18, 2472–2488. <https://doi.org/10.1038/s41423-021-00751-3>
- Cross, A.K., Haddock, G., Stock, C.J., Allan, S., Surr, J., Bunning, R. a. D., Buttle, D.J., Woodroffe, M.N., 2006. ADAMTS-1 and -4 are up-regulated following transient middle cerebral artery occlusion in the rat and their expression is modulated by TNF in cultured astrocytes. *Brain Res.* 1088, 19–30. <https://doi.org/10.1016/j.brainres.2006.02.136>
- Cua, R.C., Lau, L.W., Keough, M.B., Midha, R., Apte, S.S., Yong, V.W., 2013. Overcoming neurite-inhibitory chondroitin sulfate proteoglycans in the astrocyte matrix. *Glia* 61, 972–984. <https://doi.org/10.1002/glia.22489>
- Dalziel, M., Crispin, M., Scanlan, C.N., Zitzmann, N., Dwek, R.A., 2014. Emerging Principles for the Therapeutic Exploitation of Glycosylation. *Science* 343, 1235681. <https://doi.org/10.1126/science.1235681>
- Davis, B.M., Salinas-Navarro, M., Cordeiro, M.F., Moons, L., De Groef, L., 2017. Characterizing microglia activation: a spatial statistics approach to maximize information extraction. *Sci. Rep.* 7, 1576. <https://doi.org/10.1038/s41598-017-01747-8>
- de Groot, R., Bardhan, A., Ramroop, N., Lane, D.A., Crawley, J.T.B., 2009. Essential role of the disintegrin-like domain in ADAMTS13 function. *Blood* 113, 5609–5616. <https://doi.org/10.1182/blood-2008-11-187914>
- Deak, F., Sonntag, W.E., 2012a. Aging, Synaptic Dysfunction, and Insulin-Like Growth Factor (IGF)-1. *J. Gerontol. Ser. A* 67A, 611–625. <https://doi.org/10.1093/gerona/gls118>
- Deak, F., Sonntag, W.E., 2012b. Aging, Synaptic Dysfunction, and Insulin-Like Growth Factor (IGF)-1. *J. Gerontol. A Biol. Sci. Med. Sci.* 67A, 611–625. <https://doi.org/10.1093/gerona/gls118>
- Demircan, K., Topcu, V., Takigawa, T., Akyol, S., Yonezawa, T., Ozturk, G., Ugurcu, V., Hasgul, R., Yigitoglu, M.R., Akyol, O., McCulloch, D.R., Hirohata, S., 2014. ADAMTS4 and ADAMTS5 Knockout Mice Are Protected from Versican but Not Aggrecan or Brevican Proteolysis during Spinal Cord Injury. *BioMed Res. Int.* 2014, e693746. <https://doi.org/10.1155/2014/693746>
- Demircan, K., Yonezawa, T., Takigawa, T., Topcu, V., Erdogan, S., Ucar, F., Armutcu, F., Yigitoglu, M.R., Ninomiya, Y., Hirohata, S., 2013. ADAMTS1, ADAMTS5, ADAMTS9 and aggrecanase-generated proteoglycan fragments are induced following spinal cord injury in mouse. *Neurosci. Lett.* 544, 25–30. <https://doi.org/10.1016/j.neulet.2013.02.064>
- Didangelos, A., Mayr, U., Monaco, C., Mayr, M., 2012. Novel role of ADAMTS-5 protein in proteoglycan turnover and lipoprotein retention in atherosclerosis. *J. Biol. Chem.* 287, 19341–19345. <https://doi.org/10.1074/jbc.C112.350785>
- Dieterich, D.C., Karpova, A., Mikhaylova, M., Zdobnova, I., König, I., Landwehr, M., Kreutz, M., Smalla, K.-H., Richter, K., Landgraf, P., Reissner, C., Boeckers, T.M., Zuschratter, W., Spilker, C., Seidenbecher, C.I., Garner, C.C., Gundelfinger, E.D., Kreutz, M.R., 2008. Caldendrin-Jacob: a protein liaison that couples NMDA receptor signalling to the nucleus. *PLoS Biol.* 6, e34. <https://doi.org/10.1371/journal.pbio.0060034>
- Dityatev, A., Brückner, G., Dityateva, G., Grosche, J., Kleene, R., Schachner, M., 2007. Activity-dependent formation and functions of chondroitin sulfate-rich extracellular matrix of perineuronal nets. *Dev. Neurobiol.* 67, 570–588. <https://doi.org/10.1002/dneu.20361>
- Dityatev, A., Dityateva, G., Sytnyk, V., Delling, M., Toni, N., Nikonenko, I., Muller, D., Schachner, M., 2004. Polysialylated neural cell adhesion molecule promotes remodeling and formation of hippocampal synapses. *J. Neurosci. Off. J. Soc. Neurosci.* 24, 9372–9382. <https://doi.org/10.1523/JNEUROSCI.1702-04.2004>
- Dityatev, A., Fellin, T., 2008. Extracellular matrix in plasticity and epileptogenesis. *Neuron Glia Biol.* 4, 235–247. <https://doi.org/10.1017/S1740925X09000118>

- 
- Dityatev, A., Rusakov, D.A., 2011. Molecular signals of plasticity at the tetrapartite synapse. *Curr Opin Neurobiol* 21, 353–9. <https://doi.org/10.1016/j.conb.2010.12.006>
- Dityatev, A., Schachner, M., 2003. Extracellular matrix molecules and synaptic plasticity. *Nat. Rev. Neurosci.* 4, 456–468. <https://doi.org/10.1038/nrn1115>
- Dityatev, A., Schachner, M., Sonderegger, P., 2010. The dual role of the extracellular matrix in synaptic plasticity and homeostasis. *Nat Rev Neurosci* 11, 735–46. <https://doi.org/10.1038/nrn2898>
- Doehner, J., Knuesel, I., 2010. Reelin-mediated Signaling during Normal and Pathological Forms of Aging. *Aging Dis.* 1, 12–29.
- Donato, F., Chowdhury, A., Lahr, M., Caroni, P., 2015. Early- and Late-Born Parvalbumin Basket Cell Subpopulations Exhibiting Distinct Regulation and Roles in Learning. *Neuron* 85, 770–786. <https://doi.org/10.1016/j.neuron.2015.01.011>
- Donato, F., Rompani, S.B., Caroni, P., 2013. Parvalbumin-expressing basket-cell network plasticity induced by experience regulates adult learning. *Nature* 504, 272–276. <https://doi.org/10.1038/nature12866>
- Dong, Z., Gong, B., Li, H., Bai, Y., Wu, X., Huang, Y., He, W., Li, T., Wang, Y.T., 2012. Mechanisms of hippocampal long-term depression are required for memory enhancement by novelty exploration. *J. Neurosci. Off. J. Soc. Neurosci.* 32, 11980–11990. <https://doi.org/10.1523/JNEUROSCI.0984-12.2012>
- Dours-Zimmermann, M.T., Maurer, K., Rauch, U., Stoffel, W., Fässler, R., Zimmermann, D.R., 2009. Versican V2 Assembles the Extracellular Matrix Surrounding the Nodes of Ranvier in the CNS. *J. Neurosci.* 29, 7731–7742. <https://doi.org/10.1523/JNEUROSCI.4158-08.2009>
- Dubey, D., McRae, P.A., Rankin-Gee, E.K., Baranov, E., Wandrey, L., Rogers, S., Porter, B.E., 2017. Increased metalloproteinase activity in the hippocampus following status epilepticus. *Epilepsy Res.* 132, 50–58. <https://doi.org/10.1016/j.epilepsyres.2017.02.021>
- Dudai, Y., 2004. The Neurobiology of Consolidations, Or, How Stable is the Engram? *Annu. Rev. Psychol.* 55, 51–86. <https://doi.org/10.1146/annurev.psych.55.090902.142050>
- Durigova, M., Nagase, H., Mort, J.S., Roughley, P.J., 2011. MMPs are less efficient than ADAMTS5 in cleaving aggrecan core protein. *Matrix Biol. J. Int. Soc. Matrix Biol.* 30, 145–153. <https://doi.org/10.1016/j.matbio.2010.10.007>
- El-Tabbal, M., Niekisch, H., Henschke, J.U., Budinger, E., Frischknecht, R., Deliano, M., Happel, M.F.K., 2021. The extracellular matrix regulates cortical layer dynamics and cross-columnar frequency integration in the auditory cortex. *Commun. Biol.* 4, 1–13. <https://doi.org/10.1038/s42003-021-01837-4>
- Embury, C.M., Dyavarshetty, B., Lu, Y., Wiederin, J.L., Ciborowski, P., Gendelman, H.E., Kiyota, T., 2017. Cathepsin B Improves  $\beta$ -Amyloidosis and Learning and Memory in Models of Alzheimer's Disease. *J. Neuroimmune Pharmacol.* 12, 340–352. <https://doi.org/10.1007/s11481-016-9721-6>
- Evers, M.R., Salmen, B., Bukalo, O., Rollenhagen, A., Bösl, M.R., Morellini, F., Bartsch, U., Dityatev, A., Schachner, M., 2002. Impairment of L-type  $\text{Ca}^{2+}$  channel-dependent forms of hippocampal synaptic plasticity in mice deficient in the extracellular matrix glycoprotein tenascin-C. *J. Neurosci. Off. J. Soc. Neurosci.* 22, 7177–7194. <https://doi.org/20026735>
- Farizatto, K.L.G., Ikonne, U.S., Almeida, M.F., Ferrari, M.F.R., Bahr, B.A., 2017. A $\beta$ 42-mediated proteasome inhibition and associated tau pathology in hippocampus are governed by a lysosomal response involving cathepsin B: Evidence for protective crosstalk between protein clearance pathways. *PloS One* 12, e0182895. <https://doi.org/10.1371/journal.pone.0182895>
- Fawcett, J.W., Oohashi, T., Pizzorusso, T., 2019. The roles of perineuronal nets and the perinodal extracellular matrix in neuronal function. *Nat. Rev. Neurosci.* 20, 451–465. <https://doi.org/10.1038/s41583-019-0196-3>

- 
- Feiro, O., Gould, T.J., 2005. The interactive effects of nicotinic and muscarinic cholinergic receptor inhibition on fear conditioning in young and aged C57BL/6 mice. *Pharmacol. Biochem. Behav.* 80, 251–262. <https://doi.org/10.1016/j.pbb.2004.11.005>
- Ferrer-Ferrer, M., Dityatev, A., 2018. Shaping Synapses by the Neural Extracellular Matrix. *Front. Neuroanat.* 12, 40. <https://doi.org/10.3389/fnana.2018.00040>
- Fiebig, F., Lansner, A., 2014. Memory consolidation from seconds to weeks: a three-stage neural network model with autonomous reinstatement dynamics. *Front. Comput. Neurosci.* 8, 64. <https://doi.org/10.3389/fncom.2014.00064>
- Fisher, D., Xing, B., Dill, J., Li, H., Hoang, H.H., Zhao, Z., Yang, X.-L., Bachoo, R., Cannon, S., Longo, F.M., Sheng, M., Silver, J., Li, S., 2011. Leukocyte Common Antigen-Related Phosphatase Is a Functional Receptor for Chondroitin Sulfate Proteoglycan Axon Growth Inhibitors. *J. Neurosci.* 31, 14051–14066. <https://doi.org/10.1523/JNEUROSCI.1737-11.2011>
- Flannery, C.R., Zeng, W., Corcoran, C., Collins-Racie, L.A., Chockalingam, P.S., Hebert, T., Mackie, S.A., McDonagh, T., Crawford, T.K., Tomkinson, K.N., LaVallie, E.R., Morris, E.A., 2002. Autocatalytic cleavage of ADAMTS-4 (Aggrecanase-1) reveals multiple glycosaminoglycan-binding sites. *J. Biol. Chem.* 277, 42775–42780. <https://doi.org/10.1074/jbc.M205309200>
- Flurkey, K., M. Curren, J., Harrison, D.E., 2007. Chapter 20 - Mouse Models in Aging Research, in: Fox, J.G., Davisson, M.T., Quimby, F.W., Barthold, S.W., Newcomer, C.E., Smith, A.L. (Eds.), *The Mouse in Biomedical Research (Second Edition)*, American College of Laboratory Animal Medicine. Academic Press, Burlington, pp. 637–672. <https://doi.org/10.1016/B978-012369454-6/50074-1>
- Fosang, A.J., Rogerson, F.M., East, C.J., Stanton, H., 2008. ADAMTS-5: the story so far. *Eur. Cell. Mater.* 15, 11–26. <https://doi.org/10.22203/ecm.v015a02>
- Frantz, C., Stewart, K.M., Weaver, V.M., 2010. The extracellular matrix at a glance. *J. Cell Sci.* 123, 4195–4200. <https://doi.org/10.1242/jcs.023820>
- Friedlander, D.R., Milev, P., Karthikeyan, L., Margolis, R.K., Margolis, R.U., Grumet, M., 1994. The neuronal chondroitin sulfate proteoglycan neurocan binds to the neural cell adhesion molecules Ng-CAM/L1/NILE and N-CAM, and inhibits neuronal adhesion and neurite outgrowth. *J. Cell Biol.* 125, 669–680. <https://doi.org/10.1083/jcb.125.3.669>
- Frischknecht, R., Chang, K.-J., Rasband, M.N., Seidenbecher, C.I., 2014. Chapter 4 - Neural ECM molecules in axonal and synaptic homeostatic plasticity, in: Dityatev, A., Wehrle-Haller, B., Pitkänen, A. (Eds.), *Progress in Brain Research, Brain Extracellular Matrix in Health and Disease*. Elsevier, pp. 81–100. <https://doi.org/10.1016/B978-0-444-63486-3.00004-9>
- Gagliano, 2019. EXTRACELLULAR MATRIX REMODELING. MDPI AG, Place of publication not identified.
- Gallagher, M., Burwell, R.D., 1989. Relationship of age-related decline across several behavioral domains. *Neurobiol. Aging* 10, 691–708. [https://doi.org/10.1016/0197-4580\(89\)90006-7](https://doi.org/10.1016/0197-4580(89)90006-7)
- Gandolfi, D., Cerri, S., Mapelli, J., Polimeni, M., Tritto, S., Fuzzati-Armentero, M.-T., Bigiani, A., Blandini, F., Mapelli, L., D'Angelo, E., 2017. Activation of the CREB/c-Fos Pathway during Long-Term Synaptic Plasticity in the Cerebellum Granular Layer. *Front. Cell. Neurosci.* 11, 184. <https://doi.org/10.3389/fncel.2017.00184>
- Gao, G., Plaas, A., Thompson, V.P., Jin, S., Zuo, F., Sandy, J.D., 2004. ADAMTS4 (Aggrecanase-1) Activation of the Cell Surface Involves C-terminal Cleavage by Glycosylphosphatidyl Inositol-anchored Membrane Type 4-Matrix Metalloproteinase and Binding of the Activated Proteinase to Chondroitin Sulfate and Heparan Sulfate on Syndecan-1 \*. *J. Biol. Chem.* 279, 10042–10051. <https://doi.org/10.1074/jbc.M312100200>

- 
- Gao, G., Westling, J., Thompson, V.P., Howell, T.D., Gottschall, P.E., Sandy, J.D., 2002. Activation of the Proteolytic Activity of ADAMTS4 (Aggrecanase-1) by C-terminal Truncation\*. *J. Biol. Chem.* 277, 11034–11041. <https://doi.org/10.1074/jbc.M107443200>
- Gawlak, M., Górkiewicz, T., Gorlewicz, A., Konopacki, F.A., Kaczmarek, L., Wilczynski, G.M., 2009. High resolution in situ zymography reveals matrix metalloproteinase activity at glutamatergic synapses. *Neuroscience, Protein trafficking, targeting, and interaction at the glutamate synapse* 158, 167–176. <https://doi.org/10.1016/j.neuroscience.2008.05.045>
- Gee, J.R., Ding, Q., Keller, J.N., 2006. Age-related Alterations of Apolipoprotein E and Interleukin-1 $\beta$  in the Aging Brain. *Biogerontology* 7, 69–79. <https://doi.org/10.1007/s10522-005-6039-9>
- Gendron, C., Kashiwagi, M., Lim, N.H., Enghild, J.J., Thøgersen, I.B., Hughes, C., Caterson, B., Nagase, H., 2007. Proteolytic Activities of Human ADAMTS-5: COMPARATIVE STUDIES WITH ADAMTS-4\*. *J. Biol. Chem.* 282, 18294–18306. <https://doi.org/10.1074/jbc.M701523200>
- Glasson, S.S., Askew, R., Sheppard, B., Carito, B., Blanchet, T., Ma, H.-L., Flannery, C.R., Peluso, D., Kanki, K., Yang, Z., Majumdar, M.K., Morris, E.A., 2005. Deletion of active ADAMTS5 prevents cartilage degradation in a murine model of osteoarthritis. *Nature* 434, 644–648. <https://doi.org/10.1038/nature03369>
- Gomis-Rüth, F.X., 2009. Catalytic Domain Architecture of Metzincin Metalloproteases. *J. Biol. Chem.* 284, 15353–15357. <https://doi.org/10.1074/jbc.R800069200>
- Gorgoulis, V., Adams, P.D., Alimonti, A., Bennett, D.C., Bischof, O., Bishop, C., Campisi, J., Collado, M., Evangelou, K., Ferbeyre, G., Gil, J., Hara, E., Krizhanovsky, V., Jurk, D., Maier, A.B., Narita, M., Niedernhofer, L., Passos, J.F., Robbins, P.D., Schmitt, C.A., Sedivy, J., Vougas, K., von Zglinicki, T., Zhou, D., Serrano, M., Demaria, M., 2019. Cellular Senescence: Defining a Path Forward. *Cell* 179, 813–827. <https://doi.org/10.1016/j.cell.2019.10.005>
- Gotoh, M., Sato, T., Akashima, T., Iwasaki, H., Kameyama, A., Mochizuki, H., Yada, T., Inaba, N., Zhang, Y., Kikuchi, N., Kwon, Y.-D., Togayachi, A., Kudo, T., Nishihara, S., Watanabe, H., Kimata, K., Narimatsu, H., 2002. Enzymatic Synthesis of Chondroitin with a Novel Chondroitin Sulfate N-Acetylgalactosaminyltransferase That Transfers N-Acetylgalactosamine to Glucuronic Acid in Initiation and Elongation of Chondroitin Sulfate Synthesis\*. *J. Biol. Chem.* 277, 38189–38196. <https://doi.org/10.1074/jbc.M203619200>
- Gottschall, P.E., Howell, M.D., 2015. ADAMTS expression and function in central nervous system injury and disorders. *Matrix Biol. J. Int. Soc. Matrix Biol.* 44–46, 70–76. <https://doi.org/10.1016/j.matbio.2015.01.014>
- Gottschall, P.E., Yu, X., 1995. Cytokines regulate gelatinase A and B (matrix metalloproteinase 2 and 9) activity in cultured rat astrocytes. *J. Neurochem.* 64, 1513–1520. <https://doi.org/10.1046/j.1471-4159.1995.64041513.x>
- Gould, T.J., Feiro, O.R., 2005. Age-related deficits in the retention of memories for cued fear conditioning are reversed by galantamine treatment. *Behav. Brain Res.* 165, 160–171. <https://doi.org/10.1016/j.bbr.2005.06.040>
- Graber, S., Maiti, S., Halpain, S., 2004. Cathepsin B-like proteolysis and MARCKS degradation in sublethal NMDA-induced collapse of dendritic spines. *Neuropharmacology* 47, 706–713. <https://doi.org/10.1016/j.neuropharm.2004.08.004>
- Greger, I.H., Ziff, E.B., Penn, A.C., 2007. Molecular determinants of AMPA receptor subunit assembly. *Trends Neurosci.* 30, 407–416. <https://doi.org/10.1016/j.tins.2007.06.005>
- Groblewska, M., Siewko, M., Mroczko, B., Szmitkowski, M., 2012. The role of matrix metalloproteinases (MMPs) and their inhibitors (TIMPs) in the development of esophageal cancer. *Folia Histochem. Cytobiol.* 50, 12–19. <https://doi.org/10.2478/18691>

- 
- Grochowska, K.M., Bär, J., Gomes, G.M., Kreutz, M.R., Karpova, A., 2021. Jacob, a Synapto-Nuclear Protein Messenger Linking N-methyl-D-aspartate Receptor Activation to Nuclear Gene Expression. *Front. Synaptic Neurosci.* 13, 787494. <https://doi.org/10.3389/fnsyn.2021.787494>
- Grumet, M., Milev, P., Sakurai, T., Karthikeyan, L., Bourdon, M., Margolis, R.K., Margolis, R.U., 1994. Interactions with tenascin and differential effects on cell adhesion of neurocan and phosphacan, two major chondroitin sulfate proteoglycans of nervous tissue. *J. Biol. Chem.* 269, 12142–12146. [https://doi.org/10.1016/S0021-9258\(17\)32692-3](https://doi.org/10.1016/S0021-9258(17)32692-3)
- Guzowski, J.F., McGaugh, J.L., 1997. Antisense oligodeoxynucleotide-mediated disruption of hippocampal cAMP response element binding protein levels impairs consolidation of memory for water maze training. *Proc. Natl. Acad. Sci.* 94, 2693–2698. <https://doi.org/10.1073/pnas.94.6.2693>
- Györfy, B.A., Kun, J., Török, G., Bulyáki, É., Borhegyi, Z., Gulyássi, P., Kis, V., Szocsics, P., Micsonai, A., Matkó, J., Drahos, L., Juhász, G., Kékesi, K.A., Kardos, J., 2018. Local apoptotic-like mechanisms underlie complement-mediated synaptic pruning. *Proc. Natl. Acad. Sci. U. S. A.* 115, 6303–6308. <https://doi.org/10.1073/pnas.1722613115>
- Haddock, G., Cross, A.K., Plumb, J., Surr, J., Buttle, D.J., Bunning, R.A., Woodroffe, M.N., 2006. Expression of ADAMTS-1, -4, -5 and TIMP-3 in normal and multiple sclerosis CNS white matter. *Mult. Scler. J.* 12, 386–396. <https://doi.org/10.1191/135248506ms1300oa>
- Halder, R., Hennion, M., Vidal, R.O., Shomroni, O., Rahman, R.U., Rajput, A., Centeno, T.P., van Bebber, F., Capece, V., Garcia Vizcaino, J.C., Schuetz, A.L., Burkhardt, S., Benito, E., Navarro Sala, M., Javan, S.B., Haass, C., Schmid, B., Fischer, A., Bonn, S., 2016. DNA methylation changes in plasticity genes accompany the formation and maintenance of memory. *Nat Neurosci* 19, 102–10. <https://doi.org/10.1038/nn.4194>
- Hamel, M.G., Mayer, J., Gottschall, P.E., 2005. Altered production and proteolytic processing of brevicin by transforming growth factor beta in cultured astrocytes. *J. Neurochem.* 93, 1533–1541. <https://doi.org/10.1111/j.1471-4159.2005.03144.x>
- Hamel, M.G., Mayer, J., Leonardo, C.C., Zuo, F., Sandy, J.D., Gottschall, P.E., 2008. Multimodal Signaling by the ADAMTSs (a disintegrin and metalloproteinase with thrombospondin motifs) Promote Neurite Extension. *Exp. Neurol.* 210, 428–440. <https://doi.org/10.1016/j.expneurol.2007.11.014>
- Hardingham, G.E., Bading, H., 2010. Synaptic versus extrasynaptic NMDA receptor signalling: implications for neurodegenerative disorders. *Nat. Rev. Neurosci.* 11, 682–696. <https://doi.org/10.1038/nrn2911>
- Harlow, D.E., Macklin, W.B., 2014. Inhibitors of myelination: ECM changes, CSPGs and PTPs. *Exp. Neurol.* 251, 39–46. <https://doi.org/10.1016/j.expneurol.2013.10.017>
- Harrison, S.J., Feldman, J., 2009. Perceptual comparison of features within and between objects: A new look. *Vision Res.* 49, 2790–2799. <https://doi.org/10.1016/j.visres.2009.08.014>
- Hatsuzawa, K., Nagahama, M., Takahashi, S., Takada, K., Murakami, K., Nakayama, K., 1992. Purification and characterization of furin, a Kex2-like processing endoprotease, produced in Chinese hamster ovary cells. *J. Biol. Chem.* 267, 16094–16099.
- Hatton, C.J., Paoletti, P., 2005. Modulation of Triheteromeric NMDA Receptors by N-Terminal Domain Ligands. *Neuron* 46, 261–274. <https://doi.org/10.1016/j.neuron.2005.03.005>
- Hayakawa, N., Kato, H., Araki, T., 2007. Age-related changes of astrocytes, oligodendrocytes and microglia in the mouse hippocampal CA1 sector. *Mech. Ageing Dev.* 128, 311–316. <https://doi.org/10.1016/j.mad.2007.01.005>
- Hayashi, Y., Koyanagi, S., Kusunose, N., Okada, R., Wu, Z., Tozaki-Saitoh, H., Ukai, K., Kohsaka, S., Inoue, K., Ohdo, S., Nakanishi, H., 2013. The intrinsic microglial molecular clock controls synaptic strength via the circadian expression of cathepsin S. *Sci. Rep.* 3, 2744. <https://doi.org/10.1038/srep02744>

- 
- Hedstrom, K.L., Xu, X., Ogawa, Y., Frischknecht, R., Seidenbecher, C.I., Shrager, P., Rasband, M.N., 2007. Neurofascin assembles a specialized extracellular matrix at the axon initial segment. *J. Cell Biol.* 178, 875–886. <https://doi.org/10.1083/jcb.200705119>
- Hering, H., Sheng, M., 2001. DENDRITIC SPINES: STRUCTURE, DYNAMICS AND REGULATION 9.
- Herszényi, L., Hritz, I., Lakatos, G., Varga, M.Z., Tulassay, Z., 2012. The behavior of matrix metalloproteinases and their inhibitors in colorectal cancer. *Int. J. Mol. Sci.* 13, 13240–13263. <https://doi.org/10.3390/ijms131013240>
- Higgins, S., Wong, S.H.X., Richner, M., Rowe, C.L., Newgreen, D.F., Werther, G.A., Russo, V.C., 2009. Fibroblast Growth Factor 2 Reactivates G1 Checkpoint in SK-N-MC Cells via Regulation of p21, Inhibitor of Differentiation Genes (Id1-3), and Epithelium-Mesenchyme Transition-Like Events. *Endocrinology* 150, 4044–4055. <https://doi.org/10.1210/en.2008-1797>
- Himmelstein, B.P., Canete-Soler, R., Bernhard, E.J., Dilks, D.W., Muschel, R.J., 1994. Metalloproteinases in tumor progression: The contribution of MMP-9. *Invasion Metastasis* 14, 246–258.
- Hinton, R.B., Yutzey, K.E., 2011. Heart Valve Structure and Function in Development and Disease. *Annu. Rev. Physiol.* 73, 29–46. <https://doi.org/10.1146/annurev-physiol-012110-142145>
- Honer, W.G., Dickson, D.W., Gleeson, J., Davies, P., 1992. Regional synaptic pathology in Alzheimer's disease. *Neurobiol. Aging* 13, 375–382. [https://doi.org/10.1016/0197-4580\(92\)90111-a](https://doi.org/10.1016/0197-4580(92)90111-a)
- Hong, C.C., Tang, A.T., Detter, M.R., Choi, J.P., Wang, R., Yang, X., Guerrero, A.A., Wittig, C.F., Hobson, N., Girard, R., Lightle, R., Moore, T., Shenkar, R., Polster, S.P., Goddard, L.M., Ren, A.A., Leu, N.A., Sterling, S., Yang, J., Li, L., Chen, M., Mericko-Ishizuka, P., Dow, L.E., Watanabe, H., Schwaninger, M., Min, W., Marchuk, D.A., Zheng, X., Awad, I.A., Kahn, M.L., 2020. Cerebral cavernous malformations are driven by ADAMTS5 proteolysis of versican. *J. Exp. Med.* 217. <https://doi.org/10.1084/jem.20200140>
- Hornik, T.C., Vilalta, A., Brown, G.C., 2016. Activated microglia cause reversible apoptosis of pheochromocytoma cells, inducing their cell death by phagocytosis. *J. Cell Sci.* 129, 65–79. <https://doi.org/10.1242/jcs.174631>
- Hou, W.-S., Li, Z., Büttner, F.H., Bartnik, E., Brömme, D., 2003. Cleavage Site Specificity of Cathepsin K toward Cartilage Proteoglycans and Protease Complex Formation 384, 891–897. <https://doi.org/10.1515/BC.2003.100>
- Hovens, I.B., Nyakas, C., Schoemaker, R.G., 2014. A novel method for evaluating microglial activation using ionized calcium-binding adaptor protein-1 staining: cell body to cell size ratio. *Neuroimmunol. Neuroinflammation* 1, 82–88. <https://doi.org/10.4103/2347-8659.139719>
- Howell, M.D., Torres-Collado, A.X., Iruela-Arispe, M.L., Gottschall, P.E., 2012. Selective Decline of Synaptic Protein Levels in the Frontal Cortex of Female Mice Deficient in the Extracellular Metalloproteinase ADAMTS1. *PLOS ONE* 7, e47226. <https://doi.org/10.1371/journal.pone.0047226>
- Huang, Z.J., Kirkwood, A., Pizzorusso, T., Porciatti, V., Morales, B., Bear, M.F., Maffei, L., Tonegawa, S., 1999. BDNF Regulates the Maturation of Inhibition and the Critical Period of Plasticity in Mouse Visual Cortex. *Cell* 98, 739–755. [https://doi.org/10.1016/S0092-8674\(00\)81509-3](https://doi.org/10.1016/S0092-8674(00)81509-3)
- Ibata, K., Kono, M., Narumi, S., Motohashi, J., Kakegawa, W., Kohda, K., Yuzaki, M., 2019. Activity-Dependent Secretion of Synaptic Organizer Cbln1 from Lysosomes in Granule Cell Axons. *Neuron* 102, 1184–1198.e10. <https://doi.org/10.1016/j.neuron.2019.03.044>
- Ingraham, C.A., Park, G.C., Makarenkova, H.P., Crossin, K.L., 2011. Matrix Metalloproteinase (MMP)-9 Induced by Wnt Signaling Increases the Proliferation and Migration of Embryonic Neural Stem Cells at Low O<sub>2</sub> Levels. *J. Biol. Chem.* 286, 17649–17657. <https://doi.org/10.1074/jbc.M111.229427>

- 
- Ishidoh, K., Kominami, E., 1995. Procathepsin L Degrades Extracellular Matrix Proteins in the Presence of Glycosaminoglycans in Vitro. *Biochem. Biophys. Res. Commun.* 217, 624–631. <https://doi.org/10.1006/bbrc.1995.2820>
- Itoh, T., Tanioka, M., Matsuda, H., Nishimoto, H., Yoshioka, T., Suzuki, R., Uehira, M., 1999. Experimental metastasis is suppressed in MMP-9-deficient mice. *Clin. Exp. Metastasis* 17, 177–181. <https://doi.org/10.1023/A:1006603723759>
- Itoh, Y., 2021. Modulation of Microenvironment Signals by Proteolytic Shedding of Cell Surface Extracellular Matrix Receptors. *Front. Cell Dev. Biol.* 9, 2831. <https://doi.org/10.3389/fcell.2021.736735>
- Izumikawa, T., Koike, T., Shiozawa, S., Sugahara, K., Tamura, J., Kitagawa, H., 2008. Identification of Chondroitin Sulfate Glucuronyltransferase as Chondroitin Synthase-3 Involved in Chondroitin Polymerization: CHONDROITIN POLYMERIZATION IS ACHIEVED BY MULTIPLE ENZYME COMPLEXES CONSISTING OF CHONDROITIN SYNTHASE FAMILY MEMBERS. *J. Biol. Chem.* 283, 11396–11406. <https://doi.org/10.1074/jbc.M707549200>
- Jakoš, T., Pišlar, A., Jewett, A., Kos, J., 2019. Cysteine Cathepsins in Tumor-Associated Immune Cells. *Front. Immunol.* 10, 2037. <https://doi.org/10.3389/fimmu.2019.02037>
- Jang, D.G., Sim, H.J., Song, E.K., Kwon, T., Park, T.J., 2020. Extracellular matrixes and neuroinflammation. *BMB Rep.* 53, 491–499. <https://doi.org/10.5483/BMBRep.2020.53.10.156>
- Jones, L.L., Margolis, R.U., Tuszynski, M.H., 2003. The chondroitin sulfate proteoglycans neurocan, brevican, phosphacan, and versican are differentially regulated following spinal cord injury. *Exp. Neurol.* 182, 399–411. [https://doi.org/10.1016/S0014-4886\(03\)00087-6](https://doi.org/10.1016/S0014-4886(03)00087-6)
- Jones, S.A., 2006. Ageing to arrhythmias: conundrums of connections in the ageing heart. *J. Pharm. Pharmacol.* 58, 1571–1576. <https://doi.org/10.1211/jpp.58.12.0002>
- Jungers, K.A., Le Goff, C., Somerville, R.P.T., Apte, S.S., 2005. Adamts9 is widely expressed during mouse embryo development. *Gene Expr. Patterns GEP* 5, 609–617. <https://doi.org/10.1016/j.modgep.2005.03.004>
- Jurga, A.M., Paleczna, M., Kuter, K.Z., 2020. Overview of General and Discriminating Markers of Differential Microglia Phenotypes. *Front. Cell. Neurosci.* 14, 198. <https://doi.org/10.3389/fncel.2020.00198>
- Kappler, J., Junghans, U., Koops, A., Stichel, C.C., Hausser, H.-J., Kresse, H., Müller, H.W., 1997. Chondroitin/Dermatan Sulphate Promotes the Survival of Neurons from Rat Embryonic Neocortex. *Eur. J. Neurosci.* 9, 306–318. <https://doi.org/10.1111/j.1460-9568.1997.tb01401.x>
- Karpova, A., Mikhaylova, M., Bera, S., Bär, J., Reddy, P.P., Behnisch, T., Rankovic, V., Spilker, C., Bethge, P., Sahin, J., Kaushik, R., Zuschratter, W., Kähne, T., Naumann, M., Gundelfinger, E.D., Kreutz, M.R., 2013. Encoding and transducing the synaptic or extrasynaptic origin of NMDA receptor signals to the nucleus. *Cell* 152, 1119–1133. <https://doi.org/10.1016/j.cell.2013.02.002>
- Kashiwagi, M., Enghild, J.J., Gendron, C., Hughes, C., Caterson, B., Itoh, Y., Nagase, H., 2004. Altered Proteolytic Activities of ADAMTS-4 Expressed by C-terminal Processing\*. *J. Biol. Chem.* 279, 10109–10119. <https://doi.org/10.1074/jbc.M312123200>
- Kashiwagi, M., Tortorella, M., Nagase, H., Brew, K., 2001. TIMP-3 is a potent inhibitor of aggrecanase 1 (ADAM-TS4) and aggrecanase 2 (ADAM-TS5). *J. Biol. Chem.* 276, 12501–12504. <https://doi.org/10.1074/jbc.C000848200>
- Katoh-Semba, R., Matsuda, M., Kato, K., Oohira, A., 1995. Chondroitin sulphate proteoglycans in the rat brain: candidates for axon barriers of sensory neurons and the possible modification by laminin of their actions. *Eur. J. Neurosci.* 7, 613–621. <https://doi.org/10.1111/j.1460-9568.1995.tb00665.x>
- Kaushik, R., Morkovin, E., Schneeberg, J., Confettura, A.D., Kreutz, M.R., Senkov, O., Dityatev, A., 2018. Traditional Japanese Herbal Medicine Yokukansan Targets Distinct but Overlapping Mechanisms in Aged Mice and in the 5xFAD Mouse Model of Alzheimer’s Disease. *Front. Aging Neurosci.* 10.

- 
- Keller, K.M., Howlett, S.E., 2016. Sex Differences in the Biology and Pathology of the Aging Heart. *Can. J. Cardiol.* 32, 1065–1073. <https://doi.org/10.1016/j.cjca.2016.03.017>
- Kelwick, R., Desanlis, I., Wheeler, G.N., Edwards, D.R., 2015. The ADAMTS (A Disintegrin and Metalloproteinase with Thrombospondin motifs) family. *Genome Biol.* 16, 113. <https://doi.org/10.1186/s13059-015-0676-3>
- Keough, M.B., Rogers, J.A., Zhang, P., Jensen, S.K., Stephenson, E.L., Chen, T., Hurlbert, M.G., Lau, L.W., Rawji, K.S., Plemel, J.R., Koch, M., Ling, C.-C., Yong, V.W., 2016. An inhibitor of chondroitin sulfate proteoglycan synthesis promotes central nervous system remyelination. *Nat. Commun.* 7, 11312. <https://doi.org/10.1038/ncomms11312>
- Khundrakpam, B.S., Lewis, J.D., Zhao, L., Chouinard-Decorte, F., Evans, A.C., 2016. Brain connectivity in normally developing children and adolescents. *NeuroImage* 134, 192–203. <https://doi.org/10.1016/j.neuroimage.2016.03.062>
- Kimata, K., Habuchi, O., Habuchi, H., Watanabe, H., 2007. 4.10 - Knockout Mice and Proteoglycans, in: Kamerling, H. (Ed.), *Comprehensive Glycoscience*. Elsevier, Oxford, pp. 159–191. <https://doi.org/10.1016/B978-044451967-2/00087-8>
- Kitagawa, H., Izumikawa, T., Uyama, T., Sugahara, K., 2003. Molecular Cloning of a Chondroitin Polymerizing Factor That Cooperates with Chondroitin Synthase for Chondroitin Polymerization\*. *J. Biol. Chem.* 278, 23666–23671. <https://doi.org/10.1074/jbc.M302493200>
- Kitagawa, H., Tone, Y., Tamura, J., Neumann, K.W., Ogawa, T., Oka, S., Kawasaki, T., Sugahara, K., 1998. Molecular Cloning and Expression of Glucuronyltransferase I Involved in the Biosynthesis of the Glycosaminoglycan-Protein Linkage Region of Proteoglycans\*. *J. Biol. Chem.* 273, 6615–6618. <https://doi.org/10.1074/jbc.273.12.6615>
- Kleiser, S., Nyström, A., 2020. Interplay between Cell-Surface Receptors and Extracellular Matrix in Skin. *Biomolecules* 10, 1170. <https://doi.org/10.3390/biom10081170>
- Kochlamazashvili, G., Bukalo, O., Senkov, O., Salmen, B., Gerardy-Schahn, R., Engel, A.K., Schachner, M., Dityatev, A., 2012. Restoration of Synaptic Plasticity and Learning in Young and Aged NCAM-Deficient Mice by Enhancing Neurotransmission Mediated by GluN2A-Containing NMDA Receptors. *J. Neurosci.* 32, 2263–2275. <https://doi.org/10.1523/JNEUROSCI.5103-11.2012>
- Kochlamazashvili, G., Henneberger, C., Bukalo, O., Dvoretzkova, E., Senkov, O., Lievens, P.M.-J., Westenbroek, R., Engel, A.K., Catterall, W.A., Rusakov, D.A., Schachner, M., Dityatev, A., 2010a. The extracellular matrix molecule hyaluronic acid regulates hippocampal synaptic plasticity by modulating postsynaptic L-type Ca(2+) channels. *Neuron* 67, 116–128. <https://doi.org/10.1016/j.neuron.2010.05.030>
- Kochlamazashvili, G., Senkov, O., Grebenyuk, S., Robinson, C., Xiao, M.-F., Stummeyer, K., Gerardy-Schahn, R., Engel, A.K., Feig, L., Semyanov, A., Suppiramaniam, V., Schachner, M., Dityatev, A., 2010b. Neural Cell Adhesion Molecule-Associated Polysialic Acid Regulates Synaptic Plasticity and Learning by Restraining the Signaling through GluN2B-Containing NMDA Receptors. *J. Neurosci.* 30, 4171–4183. <https://doi.org/10.1523/JNEUROSCI.5806-09.2010>
- Koh, J., Navakkode, S., Zhai, J., Soong, T.W., 2021. Chapter 19 - Neuronal L-type calcium channels in aging, in: Martin, C.R., Preedy, V.R., Rajendram, R. (Eds.), *Factors Affecting Neurological Aging*. Academic Press, pp. 213–225. <https://doi.org/10.1016/B978-0-12-817990-1.00019-6>
- Koike, T., Izumikawa, T., Sato, B., Kitagawa, H., 2014. Identification of Phosphatase That Dephosphorylates Xylose in the Glycosaminoglycan-Protein Linkage Region of Proteoglycans\*. *J. Biol. Chem.* 289, 6695–6708. <https://doi.org/10.1074/jbc.M113.520536>
- Koike, T., Izumikawa, T., Tamura, J.-I., Kitagawa, H., 2009. FAM20B is a kinase that phosphorylates xylose in the glycosaminoglycan-protein linkage region. *Biochem. J.* 421, 157–162. <https://doi.org/10.1042/BJ20090474>

- 
- Kolb, B., Gibb, R., 2011. Brain Plasticity and Behaviour in the Developing Brain. *J. Can. Acad. Child Adolesc. Psychiatry* 20, 265–276.
- Kondapaka, S.B., Fridman, R., Reddy, K.B., 1997. Epidermal growth factor and amphiregulin up-regulate matrix metalloproteinase-9 (MMP-9) in human breast cancer cells. *Int. J. Cancer* 70, 722–726. [https://doi.org/10.1002/\(SICI\)1097-0215\(19970317\)70:6<722::AID-IJC15>3.0.CO;2-B](https://doi.org/10.1002/(SICI)1097-0215(19970317)70:6<722::AID-IJC15>3.0.CO;2-B)
- Koo, B.-H., Longpré, J.-M., Somerville, R.P.T., Alexander, J.P., Leduc, R., Apte, S.S., 2007. Regulation of ADAMTS9 secretion and enzymatic activity by its propeptide. *J. Biol. Chem.* 282, 16146–16154. <https://doi.org/10.1074/jbc.M610161200>
- Korotchenko, S., Zanicchi, F.C., Diaspro, A., Dityatev, A., 2014. Zooming in on the (Peri)synaptic Extracellular Matrix, in: Nägerl, U.V., Triller, A. (Eds.), *Nanoscale Imaging of Synapses: New Concepts and Opportunities*, *NeuroMethods*. Springer, New York, NY, pp. 187–203. [https://doi.org/10.1007/978-1-4614-9179-8\\_10](https://doi.org/10.1007/978-1-4614-9179-8_10)
- Koskinen, M.-K., van Mourik, Y., Smit, A.B., Riga, D., Spijker, S., 2020. From stress to depression: development of extracellular matrix-dependent cognitive impairment following social stress. *Sci. Rep.* 10, 17308. <https://doi.org/10.1038/s41598-020-73173-2>
- Kosti, I., Jain, N., Aran, D., Butte, A.J., Sirota, M., 2016. Cross-tissue Analysis of Gene and Protein Expression in Normal and Cancer Tissues. *Sci. Rep.* 6, 24799. <https://doi.org/10.1038/srep24799>
- Krishnaswamy, V.R., Benbenishty, A., Blinder, P., Sagi, I., 2019. Demystifying the extracellular matrix and its proteolytic remodeling in the brain: structural and functional insights. *Cell. Mol. Life Sci.* 76, 3229–3248. <https://doi.org/10.1007/s00018-019-03182-6>
- Krstic, D., Rodriguez, M., Knuesel, I., 2012a. Regulated Proteolytic Processing of Reelin through Interplay of Tissue Plasminogen Activator (tPA), ADAMTS-4, ADAMTS-5, and Their Modulators. *PLoS ONE* 7, e47793. <https://doi.org/10.1371/journal.pone.0047793>
- Krstic, D., Rodriguez, M., Knuesel, I., 2012b. Regulated Proteolytic Processing of Reelin through Interplay of Tissue Plasminogen Activator (tPA), ADAMTS-4, ADAMTS-5, and Their Modulators. *PLoS ONE* 7, e47793. <https://doi.org/10.1371/journal.pone.0047793>
- Kumar, A., Rani, A., Tchigranova, O., Lee, W.-H., Foster, T.C., 2012. Influence of late-life exposure to environmental enrichment or exercise on hippocampal function and CA1 senescent physiology. *Neurobiol. Aging* 33, 828.e1-828.e17. <https://doi.org/10.1016/j.neurobiolaging.2011.06.023>
- Kuno, K., Okada, Y., Kawashima, H., Nakamura, H., Miyasaka, M., Ohno, H., Matsushima, K., 2000. ADAMTS-1 cleaves a cartilage proteoglycan, aggrecan. *FEBS Lett.* 478, 241–245. [https://doi.org/10.1016/S0014-5793\(00\)01854-8](https://doi.org/10.1016/S0014-5793(00)01854-8)
- Laezza, F., Doherty, J.J., Dingledine, R., 1999. Long-term depression in hippocampal interneurons: joint requirement for pre- and postsynaptic events. *Science* 285, 1411–1414. <https://doi.org/10.1126/science.285.5432.1411>
- Lah, T.T., Buck, M.R., Honn, K.V., Crissman, J.D., Rao, N.C., Liotta, L.A., Sloane, B.F., 1989. Degradation of laminin by human tumor cathepsin B. *Clin. Exp. Metastasis* 7, 461–468. <https://doi.org/10.1007/BF01753666>
- Lau, L.W., Cua, R., Keough, M.B., Haylock-Jacobs, S., Yong, V.W., 2013. Pathophysiology of the brain extracellular matrix: a new target for remyelination. *Nat. Rev. Neurosci.* 14, 722–729. <https://doi.org/10.1038/nrn3550>
- Lee, W.J., Shin, C.Y., Yoo, B.K., Ryu, J.R., Choi, E.Y., Cheong, J.H., Ryu, J.H., Ko, K.H., 2003. Induction of matrix metalloproteinase-9 (MMP-9) in lipopolysaccharide-stimulated primary astrocytes is mediated by extracellular signal-regulated protein kinase 1/2 (Erk1/2). *Glia* 41, 15–24. <https://doi.org/10.1002/glia.10131>
- Lemarchant, S., Dunghana, H., Pomeschik, Y., Leinonen, H., Kolosowska, N., Korhonen, P., Kanninen, K.M., García-Berrocó, T., Montaner, J., Malm, T., Koistinaho, J., 2016. Anti-inflammatory

- 
- effects of ADAMTS-4 in a mouse model of ischemic stroke. *Glia* 64, 1492–1507. <https://doi.org/10.1002/glia.23017>
- Lemarchant, S., Pruvost, M., Montaner, J., Emery, E., Vivien, D., Kanninen, K., Koistinaho, J., 2013. ADAMTS proteoglycanases in the physiological and pathological central nervous system. *J. Neuroinflammation* 10, 899. <https://doi.org/10.1186/1742-2094-10-133>
- Lemarchant, S., Wojciechowski, S., Vivien, D., Koistinaho, J., 2017. ADAMTS-4 in central nervous system pathologies. *J. Neurosci. Res.* 95, 1703–1711. <https://doi.org/10.1002/jnr.24021>
- Lemons, M.L., Sandy, J.D., Anderson, D.K., Howland, D.R., 2001. Intact Aggrecan and Fragments Generated by Both Aggrecanase and Metalloproteinase-Like Activities Are Present in the Developing and Adult Rat Spinal Cord and Their Relative Abundance Is Altered by Injury. *J. Neurosci.* 21, 4772–4781. <https://doi.org/10.1523/JNEUROSCI.21-13-04772.2001>
- Lensjø, K.K., Lepperød, M.E., Dick, G., Hafting, T., Fyhn, M., 2017. Removal of Perineuronal Nets Unlocks Juvenile Plasticity Through Network Mechanisms of Decreased Inhibition and Increased Gamma Activity. *J. Neurosci. Off. J. Soc. Neurosci.* 37, 1269–1283. <https://doi.org/10.1523/JNEUROSCI.2504-16.2016>
- Levy, A.D., Omar, M.H., Koleske, A.J., 2014. Extracellular matrix control of dendritic spine and synapse structure and plasticity in adulthood. *Front. Neuroanat.* 8, 116. <https://doi.org/10.3389/fnana.2014.00116>
- Levy, C., Brooks, J.M., Chen, J., Su, J., Fox, M.A., 2015. Cell-specific and developmental expression of lectican-cleaving proteases in mouse hippocampus and neocortex. *J. Comp. Neurol.* 523, 629–648. <https://doi.org/10.1002/cne.23701>
- Li, C., Wang, L.-X., 2016. Chapter Two - Endoglycosidases for the Synthesis of Polysaccharides and Glycoconjugates, in: Baker, D.C. (Ed.), *Advances in Carbohydrate Chemistry and Biochemistry*. Academic Press, pp. 73–116. <https://doi.org/10.1016/bs.accb.2016.07.001>
- Liddel, S.A., Guttenplan, K.A., Clarke, L.E., Bennett, F.C., Bohlen, C.J., Schirmer, L., Bennett, M.L., Münch, A.E., Chung, W.-S., Peterson, T.C., Wilton, D.K., Frouin, A., Napier, B.A., Panicker, N., Kumar, M., Buckwalter, M.S., Rowitch, D.H., Dawson, V.L., Dawson, T.M., Stevens, B., Barres, B.A., 2017. Neurotoxic reactive astrocytes are induced by activated microglia. *Nature* 541, 481–487. <https://doi.org/10.1038/nature21029>
- Lin, R., Rosahl, T.W., Whiting, P.J., Fawcett, J.W., Kwok, J.C.F., 2011. 6-Sulphated chondroitins have a positive influence on axonal regeneration. *PloS One* 6, e21499. <https://doi.org/10.1371/journal.pone.0021499>
- Liu, Y., Zhang, M., Hao, W., Mihaljevic, I., Liu, X., Xie, K., Walter, S., Fassbender, K., 2013. Matrix metalloproteinase-12 contributes to neuroinflammation in the aged brain. *Neurobiol. Aging* 34, 1231–1239. <https://doi.org/10.1016/j.neurobiolaging.2012.10.015>
- Lively, S., Schlichter, L.C., 2013. The microglial activation state regulates migration and roles of matrix-dissolving enzymes for invasion. *J. Neuroinflammation* 10, 843. <https://doi.org/10.1186/1742-2094-10-75>
- Lockhart, M., Wirrig, E., Phelps, A., Wessels, A., 2011. Extracellular Matrix and Heart Development. *Birt. Defects Res. A. Clin. Mol. Teratol.* 91, 535–550. <https://doi.org/10.1002/bdra.20810>
- Loeblich, S., Nedivi, E., 2009. The function of activity-regulated genes in the nervous system. *Physiol. Rev.* 89, 1079–1103. <https://doi.org/10.1152/physrev.00013.2009>
- Löffek, S., Schilling, O., Franzke, C.-W., 2011. Series “matrix metalloproteinases in lung health and disease”: Biological role of matrix metalloproteinases: a critical balance. *Eur. Respir. J.* 38, 191–208. <https://doi.org/10.1183/09031936.00146510>
- Longpré, J.-M., McCulloch, D.R., Koo, B.-H., Alexander, J.P., Apte, S.S., Leduc, R., 2009. Characterization of proADAMTS5 processing by proprotein convertases. *Int. J. Biochem. Cell Biol.* 41, 1116–1126. <https://doi.org/10.1016/j.biocel.2008.10.008>

- 
- Lorenzo Bozzelli, P., Alaiyed, S., Kim, E., Villapol, S., Conant, K., 2018. Proteolytic Remodeling of Perineuronal Nets: Effects on Synaptic Plasticity and Neuronal Population Dynamics. *Neural Plast.* 2018, e5735789. <https://doi.org/10.1155/2018/5735789>
- Lu, P., Takai, K., Weaver, V.M., Werb, Z., 2011. Extracellular Matrix Degradation and Remodeling in Development and Disease. *Cold Spring Harb. Perspect. Biol.* 3, a005058. <https://doi.org/10.1101/cshperspect.a005058>
- Luderman, L.N., Unlu, G., Knapik, E.W., 2017. Chapter Three - Zebrafish Developmental Models of Skeletal Diseases, in: Sadler, K.C. (Ed.), *Current Topics in Developmental Biology, Zebrafish at the Interface of Development and Disease Research*. Academic Press, pp. 81–124. <https://doi.org/10.1016/bs.ctdb.2016.11.004>
- Lundell, A., Olin, A.I., Mörgelin, M., al-Karadaghi, S., Aspberg, A., Logan, D.T., 2004. Structural Basis for Interactions between Tenascins and Lectican C-Type Lectin Domains: Evidence for a Crosslinking Role for Tenascins. *Structure* 12, 1495–1506. <https://doi.org/10.1016/j.str.2004.05.021>
- Maeda, N., Noda, M., 1996. 6B4 proteoglycan/phosphacan is a repulsive substratum but promotes morphological differentiation of cortical neurons. *Development* 122, 647–658. <https://doi.org/10.1242/dev.122.2.647>
- Maei, H., Zaslavsky, K., Teixeira, C., Frankland, P., 2009a. What is the most sensitive measure of water maze probe test performance? *Front. Integr. Neurosci.* 3.
- Maei, H., Zaslavsky, K., Wang, A., Yiu, A., Teixeira, C., Josselyn, S., Frankland, P., 2009b. Development and validation of a sensitive entropy-based measure for the water maze. *Front. Integr. Neurosci.* 3.
- Magnusson, K.R., 2012. Aging of the NMDA receptor: from a mouse's point of view. *Future Neurol.* 7, 627–637. <https://doi.org/10.2217/fnl.12.54>
- Malenka, R.C., Bear, M.F., 2004. LTP and LTD: An Embarrassment of Riches. *Neuron* 44, 5–21. <https://doi.org/10.1016/j.neuron.2004.09.012>
- Malfait, A.-M., Liu, R.-Q., Ijiri, K., Komiya, S., Tortorella, M.D., 2002. Inhibition of ADAM-TS4 and ADAM-TS5 prevents aggrecan degradation in osteoarthritic cartilage. *J. Biol. Chem.* 277, 22201–22208. <https://doi.org/10.1074/jbc.M200431200>
- Manahan-Vaughan, D., Braunewell, K.H., 1999. Novelty acquisition is associated with induction of hippocampal long-term depression. *Proc. Natl. Acad. Sci. U. S. A.* 96, 8739–8744. <https://doi.org/10.1073/pnas.96.15.8739>
- Mango, D., Saidi, A., Cisale, G.Y., Feligioni, M., Corbo, M., Nisticò, R., 2019. Targeting Synaptic Plasticity in Experimental Models of Alzheimer's Disease. *Front. Pharmacol.* 10, 778. <https://doi.org/10.3389/fphar.2019.00778>
- Margolis, R.K., Margolis, R.U., 1993. Nervous tissue proteoglycans. *Experientia* 49, 429–446. <https://doi.org/10.1007/BF01923587>
- Marutle, A., Warpman, U., Bogdanovic, N., Nordberg, A., 1998. Regional distribution of subtypes of nicotinic receptors in human brain and effect of aging studied by (±)-[3H]epibatidine. *Brain Res.* 801, 143–149. [https://doi.org/10.1016/S0006-8993\(98\)00558-7](https://doi.org/10.1016/S0006-8993(98)00558-7)
- Mason, R.W., 2008. Emerging Functions of Placental Cathepsins. *Placenta* 29, 385–390. <https://doi.org/10.1016/j.placenta.2008.02.006>
- Matthews, R.T., Gary, S.C., Zerillo, C., Pratta, M., Solomon, K., Arner, E.C., Hockfield, S., 2000. Brain-enriched hyaluronan binding (BEHAB)/brevican cleavage in a glioma cell line is mediated by a disintegrin and metalloproteinase with thrombospondin motifs (ADAMTS) family member. *J. Biol. Chem.* 275, 22695–22703. <https://doi.org/10.1074/jbc.M909764199>
- Mayer, M.L., 2005. Glutamate receptor ion channels. *Curr. Opin. Neurobiol., Signalling mechanisms* 15, 282–288. <https://doi.org/10.1016/j.conb.2005.05.004>

- 
- McClure, C., Cole, K.L.H., Wulff, P., Klugmann, M., Murray, A.J., 2011. Production and Titering of Recombinant Adeno-associated Viral Vectors. *J. Vis. Exp. JoVE* 3348. <https://doi.org/10.3791/3348>
- Mencio, C.P., Hussein, R.K., Yu, P., Geller, H.M., 2021. The Role of Chondroitin Sulfate Proteoglycans in Nervous System Development. *J. Histochem. Cytochem.* 69, 61–80. <https://doi.org/10.1369/0022155420959147>
- Michaluk, P., Mikasova, L., Groc, L., Frischknecht, R., Choquet, D., Kaczmarek, L., 2009. Matrix Metalloproteinase-9 Controls NMDA Receptor Surface Diffusion through Integrin 1 Signaling. *J. Neurosci.* 29, 6007–6012. <https://doi.org/10.1523/JNEUROSCI.5346-08.2009>
- Miguel, R.F., Pollak, A., Lubec, G., 2005. Metalloproteinase ADAMTS-1 but not ADAMTS-5 is manifold overexpressed in neurodegenerative disorders as Down syndrome, Alzheimer's and Pick's disease. *Brain Res. Mol. Brain Res.* 133, 1–5. <https://doi.org/10.1016/j.molbrainres.2004.09.008>
- Mikami, T., Kitagawa, H., 2013a. Biosynthesis and function of chondroitin sulfate. *Biochim. Biophys. Acta BBA - Gen. Subj.* 1830, 4719–4733. <https://doi.org/10.1016/j.bbagen.2013.06.006>
- Mikami, T., Kitagawa, H., 2013b. Biosynthesis and function of chondroitin sulfate. *Biochim. Biophys. Acta* 1830, 4719–4733. <https://doi.org/10.1016/j.bbagen.2013.06.006>
- Minge, D., Senkov, O., Kaushik, R., Herde, M.K., Tikhobrazova, O., Wulff, A.B., Mironov, A., van Kuppevelt, T.H., Oosterhof, A., Kochlamazashvili, G., Dityatev, A., Henneberger, C., 2017. Heparan Sulfates Support Pyramidal Cell Excitability, Synaptic Plasticity, and Context Discrimination. *Cereb. Cortex* 27, 903–918. <https://doi.org/10.1093/cercor/bhx003>
- Miranda, M., Morici, J.F., Zanoni, M.B., Bekinschtein, P., 2019. Brain-Derived Neurotrophic Factor: A Key Molecule for Memory in the Healthy and the Pathological Brain. *Front. Cell. Neurosci.* 13, 363. <https://doi.org/10.3389/fncel.2019.00363>
- Mitlöhner, J., Kaushik, R., Niekisch, H., Blondiaux, A., Gee, C.E., Happel, M.F.K., Gundelfinger, E., Dityatev, A., Frischknecht, R., Seidenbecher, C., 2020. Dopamine Receptor Activation Modulates the Integrity of the Perisynaptic Extracellular Matrix at Excitatory Synapses. *Cells* 9, 260. <https://doi.org/10.3390/cells9020260>
- Mitsui, S., Saito, M., Hayashi, K., Mori, K., Yoshihara, Y., 2005. A novel phenylalanine-based targeting signal directs telencephalin to neuronal dendrites. *J. Neurosci. Off. J. Soc. Neurosci.* 25, 1122–1131. <https://doi.org/10.1523/JNEUROSCI.3853-04.2005>
- Miyata, S., Kitagawa, H., 2017. Formation and remodeling of the brain extracellular matrix in neural plasticity: Roles of chondroitin sulfate and hyaluronan. *Biochim. Biophys. Acta Gen. Subj.* 1861, 2420–2434. <https://doi.org/10.1016/j.bbagen.2017.06.010>
- Miyata, Shinji, Kitagawa, H., 2016. Chondroitin 6-Sulfation Regulates Perineuronal Net Formation by Controlling the Stability of Aggrecan. *Neural Plast.* 2016, e1305801. <https://doi.org/10.1155/2016/1305801>
- Miyata, S., Kitagawa, H., 2016. Chondroitin 6-Sulfation Regulates Perineuronal Net Formation by Controlling the Stability of Aggrecan. *Neural Plast* 2016, 1305801. <https://doi.org/10.1155/2016/1305801>
- Miyata, S., Nadanaka, S., Igarashi, M., Kitagawa, H., 2018. Structural Variation of Chondroitin Sulfate Chains Contributes to the Molecular Heterogeneity of Perineuronal Nets. *Front. Integr. Neurosci.* 12, 3. <https://doi.org/10.3389/fnint.2018.00003>
- Mizoguchi, K., Shoji, H., Tanaka, Y., Maruyama, W., Tabira, T., 2009. Age-related spatial working memory impairment is caused by prefrontal cortical dopaminergic dysfunction in rats. *Neuroscience* 162, 1192–1201. <https://doi.org/10.1016/j.neuroscience.2009.05.023>
- Molloy, S.S., Bresnahan, P.A., Leppla, S.H., Klimpel, K.R., Thomas, G., 1992. Human furin is a calcium-dependent serine endoprotease that recognizes the sequence Arg-X-X-Arg and efficiently cleaves anthrax toxin protective antigen. *J. Biol. Chem.* 267, 16396–16402.

- 
- Moon, C., Lee, T.-K., Kim, H., Ahn, M., Lee, Y., Kim, M.D., Sim, K.-B., Shin, T., 2008. Immunohistochemical Study of Cathepsin D in the Spinal Cords of Rats with Clip Compression Injury. *J. Vet. Med. Sci.* 70, 937–941. <https://doi.org/10.1292/jvms.70.937>
- Morellini, F., Sivukhina, E., Stoenica, L., Oulianova, E., Bukalo, O., Jakovcevski, I., Dityatev, A., Irintchev, A., Schachner, M., 2010. Improved reversal learning and working memory and enhanced reactivity to novelty in mice with enhanced GABAergic innervation in the dentate gyrus. *Cereb. Cortex N. Y. N* 1991 20, 2712–2727. <https://doi.org/10.1093/cercor/bhq017>
- Morrison, J.H., Baxter, M.G., 2012. The ageing cortical synapse: hallmarks and implications for cognitive decline. *Nat. Rev. Neurosci.* 13, 240–250. <https://doi.org/10.1038/nrn3200>
- Mosyak, L., Georgiadis, K., Shane, T., Svenson, K., Hebert, T., McDonagh, T., Mackie, S., Olland, S., Lin, L., Zhong, X., Kriz, R., Reifenberg, E.L., Collins-Racie, L.A., Corcoran, C., Freeman, B., Zollner, R., Marvell, T., Vera, M., Sum, P.-E., Lavallie, E.R., Stahl, M., Somers, W., 2008. Crystal structures of the two major aggrecan degrading enzymes, ADAMTS4 and ADAMTS5. *Protein Sci. Publ. Protein Soc.* 17, 16–21. <https://doi.org/10.1110/ps.073287008>
- Murase, S., McKay, R.D., 2012. Matrix Metalloproteinase-9 Regulates Survival of Neurons in Newborn Hippocampus\*. *J. Biol. Chem.* 287, 12184–12194. <https://doi.org/10.1074/jbc.M111.297671>
- Murphy, G., 2011. Tissue inhibitors of metalloproteinases. *Genome Biol.* 12, 233. <https://doi.org/10.1186/gb-2011-12-11-233>
- Nagase, H., Fushimi, K., 2008. Elucidating the function of non catalytic domains of collagenases and aggrecanases. *Connect. Tissue Res.* 49, 169–174. <https://doi.org/10.1080/03008200802151698>
- Nagase, H., Kashiwagi, M., 2003. Aggrecanases and cartilage matrix degradation. *Arthritis Res. Ther.* 5, 94–103. <https://doi.org/10.1186/ar630>
- Nagase, H., Visse, R., Murphy, G., 2006. Structure and function of matrix metalloproteinases and TIMPs. *Cardiovasc. Res.* 69, 562–573. <https://doi.org/10.1016/j.cardiores.2005.12.002>
- Nagase, H., Woessner, J.F., 1999. Matrix Metalloproteinases\*. *J. Biol. Chem.* 274, 21491–21494. <https://doi.org/10.1074/jbc.274.31.21491>
- Nagy, V., Bozdagi, O., Matynia, A., Balcerzyk, M., Okulski, P., Dzwonek, J., Costa, R.M., Silva, A.J., Kaczmarek, L., Huntley, G.W., 2006. Matrix Metalloproteinase-9 Is Required for Hippocampal Late-Phase Long-Term Potentiation and Memory. *J. Neurosci.* 26, 1923–1934. <https://doi.org/10.1523/JNEUROSCI.4359-05.2006>
- Nakada, M., Miyamori, H., Kita, D., Takahashi, T., Yamashita, J., Sato, H., Miura, R., Yamaguchi, Y., Okada, Y., 2005. Human glioblastomas overexpress ADAMTS-5 that degrades brevican. *Acta Neuropathol. (Berl.)* 110, 239–246. <https://doi.org/10.1007/s00401-005-1032-6>
- Nakamura, K.C., Fujiyama, F., Furuta, T., Hioki, H., Kaneko, T., 2009. Afferent islands are larger than mu-opioid receptor patch in striatum of rat pups. *Neuroreport* 20, 584–588. <https://doi.org/10.1097/WNR.0b013e328329cbf9>
- Nakazawa, Y., Pevzner, A., Tanaka, K.Z., Wiltgen, B.J., 2016. Memory retrieval along the proximodistal axis of CA1. *Hippocampus* 26, 1140–1148. <https://doi.org/10.1002/hipo.22596>
- Navakkode, S., Liu, C., Soong, T.W., 2018. Altered function of neuronal L-type calcium channels in ageing and neuroinflammation: Implications in age-related synaptic dysfunction and cognitive decline. *Ageing Res. Rev.* 42, 86–99. <https://doi.org/10.1016/j.arr.2018.01.001>
- Navarro, S., Driscoll, B., 2017. Regeneration of the Aging Lung: A Mini-Review. *Gerontology* 63, 270–280. <https://doi.org/10.1159/000451081>
- Neveu, D., Zucker, R.S., 1996. Postsynaptic Levels of [Ca<sup>2+</sup>]<sub>i</sub> Needed to Trigger LTD and LTP. *Neuron* 16, 619–629. [https://doi.org/10.1016/S0896-6273\(00\)80081-1](https://doi.org/10.1016/S0896-6273(00)80081-1)
- New, S.E.P., Aikawa, E., 2011. Cardiovascular Calcification. *Circ. J.* 75, 1305–1313. <https://doi.org/10.1253/circj.CJ-11-0395>

- 
- Nguyen, P.T., Dorman, L.C., Pan, S., Vainchtein, I.D., Han, R.T., Nakao-Inoue, H., Taloma, S.E., Barron, J.J., Molofsky, A.B., Kheirbek, M.A., Molofsky, A.V., 2020. Microglial Remodeling of the Extracellular Matrix Promotes Synapse Plasticity. *Cell* 182, 388–403.e15. <https://doi.org/10.1016/j.cell.2020.05.050>
- Nguyen, Q., Mort, J.S., Roughley, P.J., 1990. Cartilage proteoglycan aggregate is degraded more extensively by cathepsin L than by cathepsin B. *Biochem. J.* 266, 569–573.
- Norden, D.M., Godbout, J.P., 2013. Microglia of the Aged Brain: Primed to be Activated and Resistant to Regulation. *Neuropathol. Appl. Neurobiol.* 39, 19–34. <https://doi.org/10.1111/j.1365-2990.2012.01306.x>
- Noti, C., Seeberger, P.H., 2005. Chapter 4 - Synthetic Approach to Define Structure-Activity Relationship of Heparin and Heparan Sulfate, in: Garg, H.G., Linhardt, R.J., Hales, C.A. (Eds.), *Chemistry and Biology of Heparin and Heparan Sulfate*. Elsevier Science, Amsterdam, pp. 79–142. <https://doi.org/10.1016/B978-008044859-6/50005-8>
- Ogawa, T., Hagihara, K., Suzuki, M., Yamaguchi, Y., 2001. Brevican in the developing hippocampal fimbria: Differential expression in myelinating oligodendrocytes and adult astrocytes suggests a dual role for brevican in central nervous system fiber tract development. *J. Comp. Neurol.* 432, 285–295. <https://doi.org/10.1002/cne.1103>
- Olson, O.C., Joyce, J.A., 2015. Cysteine cathepsin proteases: regulators of cancer progression and therapeutic response. *Nat. Rev. Cancer* 15, 712–729. <https://doi.org/10.1038/nrc4027>
- Olson, S.K., Esko, J.D., 2013. Proteoglycans, in: Lennarz, W.J., Lane, M.D. (Eds.), *Encyclopedia of Biological Chemistry (Second Edition)*. Academic Press, Waltham, pp. 654–660. <https://doi.org/10.1016/B978-0-12-378630-2.00113-4>
- Olson, S.K., Esko, J.D., 2004. Proteoglycans, in: Lennarz, W.J., Lane, M.D. (Eds.), *Encyclopedia of Biological Chemistry*. Elsevier, New York, pp. 549–555. <https://doi.org/10.1016/B0-12-443710-9/00556-1>
- Oohira, A., Matsui, F., Matsuda, M., Shoji, R., 1986. Developmental change in the glycosaminoglycan composition of the rat brain. *J. Neurochem.* 47, 588–593. <https://doi.org/10.1111/j.1471-4159.1986.tb04540.x>
- Orlando, C., Ster, J., Gerber, U., Fawcett, J.W., Raineteau, O., 2012. Perisynaptic Chondroitin Sulfate Proteoglycans Restrict Structural Plasticity in an Integrin-Dependent Manner. *J. Neurosci.* 32, 18009–18017. <https://doi.org/10.1523/JNEUROSCI.2406-12.2012>
- Ota, M., Yasuno, F., Ito, H., Seki, C., Nozaki, S., Asada, T., Suhara, T., 2006. Age-related decline of dopamine synthesis in the living human brain measured by positron emission tomography with  $l$ -[ $\beta$ - $^{11}\text{C}$ ]DOPA. *Life Sci.* 79, 730–736. <https://doi.org/10.1016/j.lfs.2006.02.017>
- Padamsey, Z., McGuinness, L., Bardo, S.J., Reinhart, M., Tong, R., Hedegaard, A., Hart, M.L., Emptage, N.J., 2017. Activity-Dependent Exocytosis of Lysosomes Regulates the Structural Plasticity of Dendritic Spines. *Neuron* 93, 132–146. <https://doi.org/10.1016/j.neuron.2016.11.013>
- Paoletti, P., Bellone, C., Zhou, Q., 2013a. NMDA receptor subunit diversity: impact on receptor properties, synaptic plasticity and disease. *Nat. Rev. Neurosci.* 14, 383–400. <https://doi.org/10.1038/nrn3504>
- Paoletti, P., Bellone, C., Zhou, Q., 2013b. NMDA receptor subunit diversity: impact on receptor properties, synaptic plasticity and disease. *Nat. Rev. Neurosci.* 14, 383–400. <https://doi.org/10.1038/nrn3504>
- Papadopoulos, D., Magliozzi, R., Mitsikostas, D.D., Gorgoulis, V.G., Nicholas, R.S., 2020. Aging, Cellular Senescence, and Progressive Multiple Sclerosis. *Front. Cell. Neurosci.* 14, 178. <https://doi.org/10.3389/fncel.2020.00178>
- Pehlivan, S., Fedakar, R., Eren, B., Akyol, S., Eren, F., Inanir, N.T., Gurses, M.S., Ural, M.N., Tagil, S.M., Demircan, K., 2016. ADAMTS4, 5, 9, and 15 Expressions in the Autopsied Brain of Patients with Alzheimer's Disease: A Preliminary Immunohistochemistry Study. *Klin. Psikofarmakol. Bül.-Bull. Clin. Psychopharmacol.* 26, 7–14. <https://doi.org/10.5455/bcp.20150706034008>

- 
- Pekny, M., Wilhelmsson, U., Pekna, M., 2014. The dual role of astrocyte activation and reactive gliosis. *Neurosci. Lett.* 565, 30–38. <https://doi.org/10.1016/j.neulet.2013.12.071>
- Pendleton, J.C., Shambloott, M.J., Gary, D.S., Belegu, V., Hurtado, A., Malone, M.L., McDonald, J.W., 2013a. Chondroitin sulfate proteoglycans inhibit oligodendrocyte myelination through PTP $\sigma$ . *Exp. Neurol.* 247, 113–121. <https://doi.org/10.1016/j.expneurol.2013.04.003>
- Pendleton, J.C., Shambloott, M.J., Gary, D.S., Belegu, V., Hurtado, A., Malone, M.L., McDonald, J.W., 2013b. Chondroitin sulfate proteoglycans inhibit oligodendrocyte myelination through PTP $\sigma$ . *Exp. Neurol.* 247, 113–121. <https://doi.org/10.1016/j.expneurol.2013.04.003>
- Pepper, R.E., Pitman, K.A., Cullen, C.L., Young, K.M., 2018. How Do Cells of the Oligodendrocyte Lineage Affect Neuronal Circuits to Influence Motor Function, Memory and Mood? *Front. Cell. Neurosci.* 12.
- Perl, K., Ushakov, K., Pozniak, Y., Yizhar-Barnea, O., Bhonker, Y., Shivatzki, S., Geiger, T., Avraham, K.B., Shamir, R., 2017. Reduced changes in protein compared to mRNA levels across non-proliferating tissues. *BMC Genomics* 18, 305. <https://doi.org/10.1186/s12864-017-3683-9>
- Peters, A., 2002. The effects of normal aging on myelin and nerve fibers: A review. *J. Neurocytol.* 31, 581–593. <https://doi.org/10.1023/A:1025731309829>
- Peters, G.J., David, C.N., Marcus, M.D., Smith, D.M., 2013. The medial prefrontal cortex is critical for memory retrieval and resolving interference. *Learn. Mem. Cold Spring Harb. N* 20, 201–209. <https://doi.org/10.1101/lm.029249.112>
- Pires-Neto, M.A., Braga-de-Souza, S., Lent, R., 1999. Extracellular matrix molecules play diverse roles in the growth and guidance of central nervous system axons. *Braz. J. Med. Biol. Res.* 32, 633–638. <https://doi.org/10.1590/S0100-879X1999000500017>
- Pizzorusso, T., Medini, P., Berardi, N., Chierzi, S., Fawcett, J.W., Maffei, L., 2002. Reactivation of ocular dominance plasticity in the adult visual cortex. *Science* 298, 1248–1251. <https://doi.org/10.1126/science.1072699>
- Plaas, A., Osborn, B., Yoshihara, Y., Bai, Y., Bloom, T., Nelson, F., Mikecz, K., Sandy, J.D., 2007. Aggrecanolytic in human osteoarthritis: confocal localization and biochemical characterization of ADAMTS5–hyaluronan complexes in articular cartilages. *Osteoarthritis Cartilage* 15, 719–734. <https://doi.org/10.1016/j.joca.2006.12.008>
- Porte, Y., Buhot, M.-C., Mons, N., 2008. Alteration of CREB phosphorylation and spatial memory deficits in aged 129T2/Sv mice. *Neurobiol. Aging* 29, 1533–1546. <https://doi.org/10.1016/j.neurobiolaging.2007.03.023>
- Porter, S., Clark, I.M., Kevorkian, L., Edwards, D.R., 2005. The ADAMTS metalloproteinases. *Biochem. J.* 386, 15–27. <https://doi.org/10.1042/BJ20040424>
- Preston, A.R., Eichenbaum, H., 2013. Interplay of hippocampus and prefrontal cortex in memory. *Curr. Biol. CB* 23, R764–R773. <https://doi.org/10.1016/j.cub.2013.05.041>
- Presumey, J., Bialas, A.R., Carroll, M.C., 2017. Complement System in Neural Synapse Elimination in Development and Disease. *Adv. Immunol.* 135, 53–79. <https://doi.org/10.1016/bs.ai.2017.06.004>
- Properzi, F., Asher, R.A., Fawcett, J.W., 2003. Chondroitin sulphate proteoglycans in the central nervous system: changes and synthesis after injury. *Biochem. Soc. Trans.* 31, 335–336. <https://doi.org/10.1042/bst0310335>
- Pruvost, M., Lépine, M., Leonetti, C., Etard, O., Naveau, M., Agin, V., Docagne, F., Maubert, E., Ali, C., Emery, E., Vivien, D., 2017. ADAMTS-4 in oligodendrocytes contributes to myelination with an impact on motor function. *Glia* 65, 1961–1975. <https://doi.org/10.1002/glia.23207>
- Prybylowski, K., Chang, K., Kan, L., Vicini, S., Wenthold, R.J., 2005. The synaptic localization of NR2B-containing NMDA receptors is controlled by interactions with PDZ proteins and AP-2. *Neuron* 47, 845–857. <https://doi.org/10.1016/j.neuron.2005.08.016>

- 
- Pujol, J., Blanco-Hinojo, L., Macia, D., Martínez-Vilavella, G., Deus, J., Pérez-Sola, V., Cardoner, N., Soriano-Mas, C., Sunyer, J., 2021. Differences between the child and adult brain in the local functional structure of the cerebral cortex. *NeuroImage* 237, 118150. <https://doi.org/10.1016/j.neuroimage.2021.118150>
- Puzzo, D., Fiorito, J., Purgatorio, R., Gulisano, W., Palmeri, A., Arancio, O., Nicholls, R., 2016. Chapter 1 - Molecular Mechanisms of Learning and Memory\*\*The authors declare no competing financial interests., in: Lazarov, O., Tesco, G. (Eds.), *Genes, Environment and Alzheimer's Disease*. Academic Press, San Diego, pp. 1–27. <https://doi.org/10.1016/B978-0-12-802851-3.00001-2>
- Rahmouni, K., 2016. Cardiovascular Regulation by the Arcuate Nucleus of the Hypothalamus: Neurocircuitry and Signaling Systems. *Hypertension* 67, 1064–1071. <https://doi.org/10.1161/HYPERTENSIONAHA.115.06425>
- Ramos-DeSimone, N., Hahn-Dantona, E., Siple, J., Nagase, H., French, D.L., Quigley, J.P., 1999. Activation of Matrix Metalloproteinase-9 (MMP-9) via a Converging Plasmin/Stromelysin-1 Cascade Enhances Tumor Cell Invasion\*. *J. Biol. Chem.* 274, 13066–13076. <https://doi.org/10.1074/jbc.274.19.13066>
- Rasband, M.N., Peles, E., 2021. Mechanisms of node of Ranvier assembly. *Nat. Rev. Neurosci.* 22, 7–20. <https://doi.org/10.1038/s41583-020-00406-8>
- Reid, M.J., Cross, A.K., Haddock, G., Allan, S.M., Stock, C.J., Woodroffe, M.N., Buttle, D.J., Bunning, R.A.D., 2009. ADAMTS-9 expression is up-regulated following transient middle cerebral artery occlusion (tMCAo) in the rat. *Neurosci. Lett.* 452, 252–257. <https://doi.org/10.1016/j.neulet.2009.01.058>
- Rich, E.L., Shapiro, M.L., 2007. Prelimbic/infralimbic inactivation impairs memory for multiple task switches, but not flexible selection of familiar tasks. *J. Neurosci. Off. J. Soc. Neurosci.* 27, 4747–4755. <https://doi.org/10.1523/JNEUROSCI.0369-07.2007>
- Richard, A.D., Lu, X.H., 2019. “Teaching old dogs new tricks”: targeting neural extracellular matrix for normal and pathological aging-related cognitive decline. *Neural Regen Res* 14, 578–581. <https://doi.org/10.4103/1673-5374.247459>
- Richard, A.D., Tian, X.-L., El-Saadi, M.W., Lu, X.-H., 2018. Erasure of striatal chondroitin sulfate proteoglycan-associated extracellular matrix rescues aging-dependent decline of motor learning. *Neurobiol. Aging* 71, 61–71. <https://doi.org/10.1016/j.neurobiolaging.2018.07.008>
- Ries, C., Egea, V., Karow, M., Kolb, H., Jochum, M., Neth, P., 2007. MMP-2, MT1-MMP, and TIMP-2 are essential for the invasive capacity of human mesenchymal stem cells: differential regulation by inflammatory cytokines. *Blood* 109, 4055–4063. <https://doi.org/10.1182/blood-2006-10-051060>
- Ritchie, M.D., Denny, J.C., Zuvich, R.L., Crawford, D.C., Schildcrout, J.S., Bastarache, L., Ramirez, A.H., Mosley, J.D., Pulley, J.M., Basford, M.A., Bradford, Y., Rasmussen, L.V., Pathak, J., Chute, C.G., Kullo, I.J., McCarty, C.A., Chisholm, R.L., Kho, A.N., Carlson, C.S., Larson, E.B., Jarvik, G.P., Sotoodehnia, N., Manolio, T.A., Li, R., Masys, D.R., Haines, J.L., Roden, D.M., 2013. Genome- and Phenome-Wide Analyses of Cardiac Conduction Identifies Markers of Arrhythmia Risk. *Circulation* 127, 1377–1385. <https://doi.org/10.1161/CIRCULATIONAHA.112.000604>
- Rocha, D.N., Ferraz-Nogueira, J.P., Barrias, C.C., Relvas, J.B., Pêgo, A.P., 2015. Extracellular environment contribution to astrogliosis—lessons learned from a tissue engineered 3D model of the glial scar. *Front. Cell. Neurosci.* 9.
- Rodríguez-Manzanique, J.C., Fernández-Rodríguez, R., Rodríguez-Baena, F.J., Iruela-Arispe, M.L., 2015. ADAMTS proteases in vascular biology. *Matrix Biol., Metalloproteinases in Extracellular Matrix Biology* 44–46, 38–45. <https://doi.org/10.1016/j.matbio.2015.02.004>
- Rodríguez-Manzanique, J.C., Milchanowski, A.B., Dufour, E.K., Leduc, R., Iruela-Arispe, M.L., 2000. Characterization of METH-1/ADAMTS1 processing reveals two distinct active forms. *J. Biol. Chem.* 275, 33471–33479. <https://doi.org/10.1074/jbc.M002599200>

- 
- Rodríguez-Manzaneque, J.C., Westling, J., Thai, S.N.-M., Luque, A., Knauper, V., Murphy, G., Sandy, J.D., Iruela-Arispe, M.L., 2002. ADAMTS1 cleaves aggrecan at multiple sites and is differentially inhibited by metalloproteinase inhibitors. *Biochem. Biophys. Res. Commun.* 293, 501–508. [https://doi.org/10.1016/S0006-291X\(02\)00254-1](https://doi.org/10.1016/S0006-291X(02)00254-1)
- Roesler, R., McGaugh, J.L., 2010. Memory Consolidation, in: Koob, G.F., Moal, M.L., Thompson, R.F. (Eds.), *Encyclopedia of Behavioral Neuroscience*. Academic Press, Oxford, pp. 206–214. <https://doi.org/10.1016/B978-0-08-045396-5.00147-0>
- Romberg, C., Yang, S., Melani, R., Andrews, M.R., Horner, A.E., Spillantini, M.G., Bussey, T.J., Fawcett, J.W., Pizzorusso, T., Saksida, L.M., 2013. Depletion of perineuronal nets enhances recognition memory and long-term depression in the perirhinal cortex. *J. Neurosci. Off. J. Soc. Neurosci.* 33, 7057–7065. <https://doi.org/10.1523/JNEUROSCI.6267-11.2013>
- Rossi, A., Deveraux, Q., Turk, B., Sali, A., 2004. Comprehensive search for cysteine cathepsins in the human genome. *Biol. Chem.* 385, 363–372. <https://doi.org/10.1515/BC.2004.040>
- Rosso, A.L., Studenski, S.A., Chen, W.G., Aizenstein, H.J., Alexander, N.B., Bennett, D.A., Black, S.E., Camicioli, R., Carlson, M.C., Ferrucci, L., Guralnik, J.M., Hausdorff, J.M., Kaye, J., Launer, L.J., Lipsitz, L.A., Verghese, J., Rosano, C., 2013. Aging, the Central Nervous System, and Mobility. *J. Gerontol. Ser. A* 68, 1379–1386. <https://doi.org/10.1093/gerona/glt089>
- Russell, D.L., Doyle, K.M.H., Ochsner, S.A., Sandy, J.D., Richards, J.S., 2003. Processing and Localization of ADAMTS-1 and Proteolytic Cleavage of Versican during Cumulus Matrix Expansion and Ovulation \*. *J. Biol. Chem.* 278, 42330–42339. <https://doi.org/10.1074/jbc.M300519200>
- Sage, J., Leblanc-Noblesse, E., Nizard, C., Sasaki, T., Schnebert, S., Perrier, E., Kurfurst, R., Brömme, D., Lalmanach, G., Lecaille, F., 2012. Cleavage of Nidogen-1 by Cathepsin S Impairs Its Binding to Basement Membrane Partners. *PLoS ONE* 7, e43494. <https://doi.org/10.1371/journal.pone.0043494>
- Saghatelyan, A.K., Gorissen, S., Albert, M., Hertlein, B., Schachner, M., Dityatev, A., 2000. The extracellular matrix molecule tenascin-R and its HNK-1 carbohydrate modulate perisomatic inhibition and long-term potentiation in the CA1 region of the hippocampus. *Eur. J. Neurosci.* 12, 3331–3342. <https://doi.org/10.1046/j.1460-9568.2000.00216.x>
- Salter, M.G., Fern, R., 2005. NMDA receptors are expressed in developing oligodendrocyte processes and mediate injury. *Nature* 438, 1167–1171. <https://doi.org/10.1038/nature04301>
- Sandy, J.D., Westling, J., Kenagy, R.D., Iruela-Arispe, M.L., Verscharen, C., Rodríguez-Manzaneque, J.C., Zimmermann, D.R., Lemire, J.M., Fischer, J.W., Wight, T.N., Clowes, A.W., 2001. Versican V1 Proteolysis in Human Aorta in Vivo Occurs at the Glu441-Ala442 Bond, a Site That Is Cleaved by Recombinant ADAMTS-1 and ADAMTS-4 \*. *J. Biol. Chem.* 276, 13372–13378. <https://doi.org/10.1074/jbc.M009737200>
- Santos, T.E., Schaffran, B., Broguière, N., Meyn, L., Zenobi-Wong, M., Bradke, F., 2020. Axon Growth of CNS Neurons in Three Dimensions Is Amoeboid and Independent of Adhesions. *Cell Rep.* 32, 107907. <https://doi.org/10.1016/j.celrep.2020.107907>
- Santos-Galindo, M., Acáz-Fonseca, E., Bellini, M.J., Garcia-Segura, L.M., 2011. Sex differences in the inflammatory response of primary astrocytes to lipopolysaccharide. *Biol. Sex Differ.* 2, 7. <https://doi.org/10.1186/2042-6410-2-7>
- Sanz-Clemente, A., Matta, J.A., Isaac, J.T.R., Roche, K.W., 2010. Casein kinase 2 regulates the NR2 subunit composition of synaptic NMDA receptors. *Neuron* 67, 984–996. <https://doi.org/10.1016/j.neuron.2010.08.011>
- Sato, T., Gotoh, M., Kiyohara, K., Akashima, T., Iwasaki, H., Kameyama, A., Mochizuki, H., Yada, T., Inaba, N., Togayachi, A., Kudo, T., Asada, M., Watanabe, H., Imamura, T., Kimata, K., Narimatsu, H., 2003. Differential Roles of Two N-Acetylgalactosaminyltransferases, CSGalNAcT-1, and a Novel Enzyme, CSGalNAcT-2: INITIATION AND ELONGATION IN SYNTHESIS OF

- 
- CHONDROITIN SULFATE\*. *J. Biol. Chem.* 278, 3063–3071. <https://doi.org/10.1074/jbc.M208886200>
- Schlatmann, T.J., Becker, A.E., 1977. Pathogenesis of dissecting aneurysm of aorta. Comparative histopathologic study of significance of medial changes. *Am. J. Cardiol.* 39, 21–26. [https://doi.org/10.1016/s0002-9149\(77\)80005-2](https://doi.org/10.1016/s0002-9149(77)80005-2)
- Schwab, C., Klegeris, A., McGeer, Patrick.L., 2010. Inflammation in transgenic mouse models of neurodegenerative disorders. *Biochim. Biophys. Acta BBA - Mol. Basis Dis., Mouse Models of Human Neurological Disorders* 1802, 889–902. <https://doi.org/10.1016/j.bbadis.2009.10.013>
- Schweitzer, B., Singh, J., Fejtova, A., Groc, L., Heine, M., Frischknecht, R., 2017. Hyaluronic acid based extracellular matrix regulates surface expression of GluN2B containing NMDA receptors. *Sci. Rep.* 7, 10991. <https://doi.org/10.1038/s41598-017-07003-3>
- Schweitzer, B.C., 2015. The effect of the extracellular environment on the composition and function of synapses. <https://doi.org/10.25673/4388>
- Semple, B.D., Blomgren, K., Gimlin, K., Ferriero, D.M., Noble-Haeusslein, L.J., 2013. Brain development in rodents and humans: Identifying benchmarks of maturation and vulnerability to injury across species. *Prog. Neurobiol.* 0, 1–16. <https://doi.org/10.1016/j.pneurobio.2013.04.001>
- Senkov, O., Andjus, P., Radenovic, L., Soriano, E., Dityatev, A., 2014. Neural ECM molecules in synaptic plasticity, learning, and memory. *Prog. Brain Res.* 214, 53–80. <https://doi.org/10.1016/B978-0-444-63486-3.00003-7>
- Sethi, M.K., Zaia, J., 2017. Extracellular Matrix Proteomics in Schizophrenia and Alzheimer’s Disease. *Anal. Bioanal. Chem.* 409, 379–394. <https://doi.org/10.1007/s00216-016-9900-6>
- Sevenich, L., Joyce, J.A., 2014. Pericellular proteolysis in cancer. *Genes Dev.* 28, 2331–2347. <https://doi.org/10.1101/gad.250647.114>
- Shabani, Z., Ghadiri, T., Karimipour, M., Sadigh-Eteghad, S., Mahmoudi, J., Mehrad, H., Farhoudi, M., 2021. Modulatory properties of extracellular matrix glycosaminoglycans and proteoglycans on neural stem cells behavior: Highlights on regenerative potential and bioactivity. *Int. J. Biol. Macromol.* 171, 366–381. <https://doi.org/10.1016/j.ijbiomac.2021.01.006>
- Sheng, M., 2001. The postsynaptic NMDA-receptor--PSD-95 signaling complex in excitatory synapses of the brain. *J. Cell Sci.* 114, 1251.
- Shi, J., Son, M.-Y., Yamada, S., Szabova, L., Kahan, S., Chrysovergis, K., Wolf, L., Surmak, A., Holmbeck, K., 2008. Membrane-type MMPs enable extracellular matrix permissiveness and mesenchymal cell proliferation during embryogenesis. *Dev. Biol.* 313, 196–209. <https://doi.org/10.1016/j.ydbio.2007.10.017>
- Shi, W., Wei, X., Wang, X., Du, S., Liu, W., Song, J., Wang, Y., 2019. Perineuronal nets protect long-term memory by limiting activity-dependent inhibition from parvalbumin interneurons. *Proc. Natl. Acad. Sci.* 116, 27063–27073. <https://doi.org/10.1073/pnas.1902680116>
- Shin, Y.H., Yoon, S.-H., Choe, E.-Y., Cho, S.-H., Woo, C.-H., Rho, J.-Y., Kim, J.-H., 2007. PMA-induced up-regulation of MMP-9 is regulated by a PKC $\alpha$ -NF- $\kappa$ B cascade in human lung epithelial cells. *Exp. Mol. Med.* 39, 97–105. <https://doi.org/10.1038/emm.2007.11>
- Silaghi, A., Piercecchi-Marti, M.-D., Grino, M., Leonetti, G., Alessi, M.C., Clement, K., Dadoun, F., Dutour, A., 2008. Epicardial Adipose Tissue Extent: Relationship With Age, Body Fat Distribution, and Coronaropathy. *Obesity* 16, 2424–2430. <https://doi.org/10.1038/oby.2008.379>
- Silver, J., Miller, J.H., 2004. Regeneration beyond the glial scar. *Nat. Rev. Neurosci.* 5, 146–156. <https://doi.org/10.1038/nrn1326>
- Sindhu, S., Al-Roub, A., Koshy, M., Thomas, R., Ahmad, R., 2016. Palmitate-Induced MMP-9 Expression in the Human Monocytic Cells is Mediated through the TLR4-MyD88 Dependent Mechanism. *Cell. Physiol. Biochem.* 39, 889–900. <https://doi.org/10.1159/000447798>

- 
- Singh, H., Stefani, E., Toro, L., 2012. Intracellular BKCa (iBKCa) channels. *J. Physiol.* 590, 5937–5947. <https://doi.org/10.1113/jphysiol.2011.215533>
- Sirko, S., von Holst, A., Wizenmann, A., Götz, M., Faissner, A., 2007. Chondroitin sulfate glycosaminoglycans control proliferation, radial glia cell differentiation and neurogenesis in neural stem/progenitor cells. *Development* 134, 2727–2738. <https://doi.org/10.1242/dev.02871>
- Slaker, M.L., Harkness, J.H., Sorg, B.A., 2016. A standardized and automated method of perineuronal net analysis using *Wisteria floribunda* agglutinin staining intensity. *IBRO Rep.* 1, 54–60. <https://doi.org/10.1016/j.ibror.2016.10.001>
- Smith, D.E., Rapp, P.R., McKay, H.M., Roberts, J.A., Tuszynski, M.H., 2004. Memory Impairment in Aged Primates Is Associated with Focal Death of Cortical Neurons and Atrophy of Subcortical Neurons. *J. Neurosci.* 24, 4373–4381. <https://doi.org/10.1523/JNEUROSCI.4289-03.2004>
- Somerville, R.P.T., Longpre, J.-M., Jungers, K.A., Engle, J.M., Ross, M., Evanko, S., Wight, T.N., Leduc, R., Apte, S.S., 2003. Characterization of ADAMTS-9 and ADAMTS-20 as a Distinct ADAMTS Subfamily Related to *Caenorhabditis elegans* GON-1 \*. *J. Biol. Chem.* 278, 9503–9513. <https://doi.org/10.1074/jbc.M211009200>
- Somiya, M., 2020. Where does the cargo go?: Solutions to provide experimental support for the “extracellular vesicle cargo transfer hypothesis.” *J. Cell Commun. Signal.* 14, 135–146. <https://doi.org/10.1007/s12079-020-00552-9>
- Song, I., Dityatev, A., 2018. Crosstalk between glia, extracellular matrix and neurons. *Brain Res. Bull., Molecular mechanisms of astrocyte-neuron signalling* 136, 101–108. <https://doi.org/10.1016/j.brainresbull.2017.03.003>
- Song, J., Xu, P., Xiang, H., Su, Z., Storer, A.C., Ni, F., 2000. The active-site residue Cys-29 is responsible for the neutral-pH inactivation and the refolding barrier of human cathepsin B. *FEBS Lett.* 475, 157–162. [https://doi.org/10.1016/S0014-5793\(00\)01644-6](https://doi.org/10.1016/S0014-5793(00)01644-6)
- Song, Y.-Q., Karasugi, T., Cheung, K.M.C., Chiba, K., Ho, D.W.H., Miyake, A., Kao, P.Y.P., Sze, K.L., Yee, A., Takahashi, A., Kawaguchi, Y., Mikami, Y., Matsumoto, M., Togawa, D., Kanayama, M., Shi, D., Dai, J., Jiang, Q., Wu, C., Tian, W., Wang, N., Leong, J.C.Y., Luk, K.D.K., Yip, S., Cherny, S.S., Wang, J., Mundlos, S., Kelempisioti, A., Eskola, P.J., Männikkö, M., Mäkelä, P., Karppinen, J., Järvelin, M.-R., O’Reilly, P.F., Kubo, M., Kimura, T., Kubo, T., Toyama, Y., Mizuta, H., Cheah, K.S.E., Tsunoda, T., Sham, P.-C., Ikegawa, S., Chan, D., 2013. Lumbar disc degeneration is linked to a carbohydrate sulfotransferase 3 variant. *J. Clin. Invest.* 123, 4909–4917. <https://doi.org/10.1172/JCI69277>
- Spiegel, S., Foster, D., Kolesnick, R., 1996. Signal transduction through lipid second messengers. *Curr. Opin. Cell Biol.* 8, 159–167. [https://doi.org/10.1016/S0955-0674\(96\)80061-5](https://doi.org/10.1016/S0955-0674(96)80061-5)
- Spilker, C., Nullmeier, S., Grochowska, K.M., Schumacher, A., Butnaru, I., Macharadze, T., Gomes, G.M., Yuanxiang, P., Bayraktar, G., Rodenstein, C., Geiseler, C., Kolodziej, A., Lopez-Rojas, J., Montag, D., Angenstein, F., Bär, J., D’Hanis, W., Roskoden, T., Mikhaylova, M., Budinger, E., Ohl, F.W., Stork, O., Zenclussen, A.C., Karpova, A., Schwegler, H., Kreutz, M.R., 2016. A Jacob/Nsmf Gene Knockout Results in Hippocampal Dysplasia and Impaired BDNF Signaling in Dendritogenesis. *PLoS Genet.* 12, e1005907. <https://doi.org/10.1371/journal.pgen.1005907>
- Squire, L.R., Wixted, J.T., 2011. The Cognitive Neuroscience of Human Memory Since H.M. *Annu. Rev. Neurosci.* 34, 259–288. <https://doi.org/10.1146/annurev-neuro-061010-113720>
- Srivastava, P., Pandey, H., Agarwal, D., Mandal, K., Phadke, S.R., 2017. Spondyloepiphyseal dysplasia Omani type: CHST3 mutation spectrum and phenotypes in three Indian families. *Am. J. Med. Genet. A.* 173, 163–168. <https://doi.org/10.1002/ajmg.a.37996>
- Stanton, H., Rogerson, F.M., East, C.J., Golub, S.B., Lawlor, K.E., Meeker, C.T., Little, C.B., Last, K., Farmer, P.J., Campbell, I.K., Fourie, A.M., Fosang, A.J., 2005. ADAMTS5 is the major

- 
- aggrecanase in mouse cartilage in vivo and in vitro. *Nature* 434, 648–652. <https://doi.org/10.1038/nature03417>
- Steffensen, B., Wallon, U.M., Overall, C.M., 1995. Extracellular Matrix Binding Properties of Recombinant Fibronectin Type II-like Modules of Human 72-kDa Gelatinase/Type IV Collagenase: HIGH AFFINITY BINDING TO NATIVE TYPE I COLLAGEN BUT NOT NATIVE TYPE IV COLLAGEN\*. *J. Biol. Chem.* 270, 11555–11566. <https://doi.org/10.1074/jbc.270.19.11555>
- Sternlicht, M.D., Werb, Z., 2001. HOW MATRIX METALLOPROTEINASES REGULATE CELL BEHAVIOR. *Annu. Rev. Cell Dev. Biol.* 17, 463–516. <https://doi.org/10.1146/annurev.cellbio.17.1.463>
- Strackeljan, L., Baczynska, E., Cangalaya, C., Baidoe-Ansah, D., Wlodarczyk, J., Kaushik, R., Dityatev, A., 2021. Microglia Depletion-Induced Remodeling of Extracellular Matrix and Excitatory Synapses in the Hippocampus of Adult Mice. *Cells* 10, 1862. <https://doi.org/10.3390/cells10081862>
- Strongin, A.Y., Collier, I., Bannikov, G., Marmer, B.L., Grant, G.A., Goldberg, G.I., 1995. Mechanism of cell surface activation of 72-kDa type IV collagenase. Isolation of the activated form of the membrane metalloprotease. *J. Biol. Chem.* 270, 5331–5338. <https://doi.org/10.1074/jbc.270.10.5331>
- Su, S., Grover, J., Roughley, P.J., DiBattista, J.A., Martel-Pelletier, J., Pelletier, J.P., Zafarullah, M., 1999. Expression of the tissue inhibitor of metalloproteinases (TIMP) gene family in normal and osteoarthritic joints. *Rheumatol. Int.* 18, 183–191. <https://doi.org/10.1007/s002960050083>
- Sugahara, K., Mikami, T., Uyama, T., Mizuguchi, S., Nomura, K., Kitagawa, H., 2003. Recent advances in the structural biology of chondroitin sulfate and dermatan sulfate. *Curr. Opin. Struct. Biol.* 13, 612–620. <https://doi.org/10.1016/j.sbi.2003.09.011>
- Sugiyama, S., Di Nardo, A.A., Aizawa, S., Matsuo, I., Volovitch, M., Prochiantz, A., Hensch, T.K., 2008. Experience-dependent transfer of Otx2 homeoprotein into the visual cortex activates postnatal plasticity. *Cell* 134, 508–520. <https://doi.org/10.1016/j.cell.2008.05.054>
- Sun, Z.Y., Bozzelli, P.L., Caccavano, A., Allen, M., Balmuth, J., Vicini, S., Wu, J.-Y., Conant, K., 2018. Disruption of perineuronal nets increases the frequency of sharp wave ripple events. *Hippocampus* 28, 42–52. <https://doi.org/10.1002/hipo.22804>
- Syková, E., Nicholson, C., 2008. Diffusion in Brain Extracellular Space. *Physiol. Rev.* 88, 1277–1340. <https://doi.org/10.1152/physrev.00027.2007>
- Szepesi, Z., Manouchehrian, O., Bachiller, S., Deierborg, T., 2018. Bidirectional Microglia–Neuron Communication in Health and Disease. *Front. Cell. Neurosci.* 12, 323. <https://doi.org/10.3389/fncel.2018.00323>
- Takehara-Nishiuchi, K., 2020. Prefrontal–hippocampal interaction during the encoding of new memories. *Brain Neurosci. Adv.* 4, 2398212820925580. <https://doi.org/10.1177/2398212820925580>
- Takemiya, T., Fumizawa, K., Yamagata, K., Iwakura, Y., Kawakami, M., 2017. Brain Interleukin-1 Facilitates Learning of a Water Maze Spatial Memory Task in Young Mice. *Front. Behav. Neurosci.* 11.
- Takizawa, M., Ohuchi, E., Yamanaka, H., Nakamura, H., Ikeda, E., Ghosh, P., Okada, Y., 2000. Production of tissue inhibitor of metalloproteinases 3 is selectively enhanced by calcium pentosan polysulfate in human rheumatoid synovial fibroblasts. *Arthritis Rheum.* 43, 812–820. [https://doi.org/10.1002/1529-0131\(200004\)43:4<812::AID-ANR11>3.0.CO;2-Y](https://doi.org/10.1002/1529-0131(200004)43:4<812::AID-ANR11>3.0.CO;2-Y)
- Taleb, S., Canello, R., Clément, K., Lacasa, D., 2006. Cathepsin S Promotes Human Preadipocyte Differentiation: Possible Involvement of Fibronectin Degradation. *Endocrinology* 147, 4950–4959. <https://doi.org/10.1210/en.2006-0386>

- 
- Tang, C.-H., Lee, J.-W., Galvez, M.G., Robillard, L., Mole, S.E., Chapman, H.A., 2006. Murine cathepsin F deficiency causes neuronal lipofuscinosis and late-onset neurological disease. *Mol. Cell. Biol.* 26, 2309–2316. <https://doi.org/10.1128/MCB.26.6.2309-2316.2006>
- Tauchi, R., Imagama, S., Natori, T., Ohgomori, T., Muramoto, A., Shinjo, R., Matsuyama, Y., Ishiguro, N., Kadomatsu, K., 2012. The endogenous proteoglycan-degrading enzyme ADAMTS-4 promotes functional recovery after spinal cord injury. *J. Neuroinflammation* 9, 53. <https://doi.org/10.1186/1742-2094-9-53>
- Temido-Ferreira, M., Coelho, J.E., Pousinha, P.A., Lopes, L.V., 2019. Novel Players in the Aging Synapse: Impact on Cognition. *J. Caffeine Adenosine Res.* 9, 104–127. <https://doi.org/10.1089/caff.2019.0013>
- Thibault, O., Landfield, P.W., 1996. Increase in single L-type calcium channels in hippocampal neurons during aging. *Science* 272, 1017–1020. <https://doi.org/10.1126/science.272.5264.1017>
- Thiele, H., Sakano, M., Kitagawa, H., Sugahara, K., Rajab, A., Höhne, W., Ritter, H., Leschik, G., Nürnberg, P., Mundlos, S., 2004. Loss of chondroitin 6-O-sulfotransferase-1 function results in severe human chondrodysplasia with progressive spinal involvement. *Proc. Natl. Acad. Sci. U. S. A.* 101, 10155–10160. <https://doi.org/10.1073/pnas.0400334101>
- Tian, L., Stefanidakis, M., Ning, L., Van Lint, P., Nyman-Huttunen, H., Libert, C., Itoharu, S., Mishina, M., Rauvala, H., Gahmberg, C.G., 2007. Activation of NMDA receptors promotes dendritic spine development through MMP-mediated ICAM-5 cleavage. *J. Cell Biol.* 178, 687–700. <https://doi.org/10.1083/jcb.200612097>
- Todd, L., Palazzo, I., Suarez, L., Liu, X., Volkov, L., Hoang, T.V., Campbell, W.A., Blackshaw, S., Quan, N., Fischer, A.J., 2019. Reactive microglia and IL1 $\beta$ /IL-1R1-signaling mediate neuroprotection in excitotoxin-damaged mouse retina. *J. Neuroinflammation* 16, 118. <https://doi.org/10.1186/s12974-019-1505-5>
- Torres, D.M.C., Cardenas, F.P., 2020. Synaptic plasticity in Alzheimer’s disease and healthy aging. *Rev. Neurosci.* 31, 245–268. <https://doi.org/10.1515/revneuro-2019-0058>
- Tortorella, M., Pratta, M., Liu, R.-Q., Abbaszade, I., Ross, H., Burn, T., Arner, E., 2000. The thrombospondin motif of Aggrecanase-1 (ADAMTS-4) is critical for aggrecan substrate recognition and cleavage. *J. Biol. Chem.* 275, 25791–25797. <https://doi.org/10.1074/jbc.M001065200>
- Tortorella, M.D., Burn, T.C., Pratta, M.A., Abbaszade, I., Hollis, J.M., Liu, R., Rosenfeld, S.A., Copeland, R.A., Decicco, C.P., Wynn, R., Rockwell, A., Yang, F., Duke, J.L., Solomon, K., George, H., Bruckner, R., Nagase, H., Itoh, Y., Ellis, D.M., Ross, H., Wiswall, B.H., Murphy, K., Hillman, M.C., Hollis, G.F., Newton, R.C., Magolda, R.L., Trzaskos, J.M., Arner, E.C., 1999. Purification and Cloning of Aggrecanase-1: A Member of the ADAMTS Family of Proteins. *Science* 284, 1664–1666. <https://doi.org/10.1126/science.284.5420.1664>
- Tortorella, M.D., Liu, R.-Q., Burn, T., Newton, R.C., Arner, E., 2002. Characterization of human aggrecanase 2 (ADAM-TS5): substrate specificity studies and comparison with aggrecanase 1 (ADAM-TS4). *Matrix Biol.* 21, 499–511. [https://doi.org/10.1016/S0945-053X\(02\)00069-0](https://doi.org/10.1016/S0945-053X(02)00069-0)
- Tortorella, M.D., Pratta, M., Liu, R.-Q., Austin, J., Ross, O.H., Abbaszade, I., Burn, T., Arner, E., 2000. Sites of Aggrecan Cleavage by Recombinant Human Aggrecanase-1 (ADAMTS-4)\*. *J. Biol. Chem.* 275, 18566–18573. <https://doi.org/10.1074/jbc.M909383199>
- Tran, A., Silver, J., 2021. Cathepsins in neuronal plasticity. *Neural Regen. Res.* 16, 26. <https://doi.org/10.4103/1673-5374.286948>
- Tran, A.P., Sundar, S., Yu, M., Lang, B.T., Silver, J., 2018a. Modulation of Receptor Protein Tyrosine Phosphatase Sigma Increases Chondroitin Sulfate Proteoglycan Degradation through Cathepsin B Secretion to Enhance Axon Outgrowth. *J. Neurosci.* 38, 5399–5414. <https://doi.org/10.1523/JNEUROSCI.3214-17.2018>

- 
- Tran, A.P., Warren, P.M., Silver, J., 2018b. The Biology of Regeneration Failure and Success After Spinal Cord Injury. *Physiol. Rev.* 98, 881–917. <https://doi.org/10.1152/physrev.00017.2017>
- Traynelis, S.F., Wollmuth, L.P., McBain, C.J., Menniti, F.S., Vance, K.M., Ogden, K.K., Hansen, K.B., Yuan, H., Myers, S.J., Dingledine, R., 2010. Glutamate receptor ion channels: structure, regulation, and function. *Pharmacol. Rev.* 62, 405–496. <https://doi.org/10.1124/pr.109.002451>
- Troeberg, L., Fushimi, K., Scilabra, S.D., Nakamura, H., Dive, V., Thøgersen, I.B., Enghild, J.J., Nagase, H., 2009. The C-terminal domains of ADAMTS-4 and ADAMTS-5 promote association with N-TIMP-3. *Matrix Biol. J. Int. Soc. Matrix Biol.* 28, 463–469. <https://doi.org/10.1016/j.matbio.2009.07.005>
- Tuppo, E.E., Arias, H.R., 2005. The role of inflammation in Alzheimer's disease. *Int. J. Biochem. Cell Biol.* 37, 289–305. <https://doi.org/10.1016/j.biocel.2004.07.009>
- Turk, B., Turk, D., Turk, V., 2000. Lysosomal cysteine proteases: more than scavengers. *Biochim. Biophys. Acta* 1477, 98–111. [https://doi.org/10.1016/s0167-4838\(99\)00263-0](https://doi.org/10.1016/s0167-4838(99)00263-0)
- Turk, V., Stoka, V., Vasiljeva, O., Renko, M., Sun, T., Turk, B., Turk, D., 2012. Cysteine cathepsins: From structure, function and regulation to new frontiers. *Biochim. Biophys. Acta BBA - Proteins Proteomics, Proteolysis 50 years after the discovery of lysosome 1824*, 68–88. <https://doi.org/10.1016/j.bbapap.2011.10.002>
- Ulbrich, P., Khoshneviszadeh, M., Jandke, S., Schreiber, S., Dityatev, A., 2021. Interplay between perivascular and perineuronal extracellular matrix remodelling in neurological and psychiatric diseases. *Eur. J. Neurosci.* 53, 3811–3830. <https://doi.org/10.1111/ejn.14887>
- Unemori, E.N., Hibbs, M.S., Amento, E.P., 1991. Constitutive expression of a 92-kD gelatinase (type V collagenase) by rheumatoid synovial fibroblasts and its induction in normal human fibroblasts by inflammatory cytokines. *J. Clin. Invest.* 88, 1656–1662. <https://doi.org/10.1172/JCI115480>
- Urbán, N., Guillemot, F., 2014. Neurogenesis in the embryonic and adult brain: same regulators, different roles. *Front. Cell. Neurosci.* 8, 396. <https://doi.org/10.3389/fncel.2014.00396>
- Uyama, T., Ishida, M., Izumikawa, T., Trybala, E., Tufaro, F., Bergström, T., Sugahara, K., Kitagawa, H., 2006. Chondroitin 4-O-Sulfotransferase-1 Regulates E Disaccharide Expression of Chondroitin Sulfate Required for Herpes Simplex Virus Infectivity\*. *J. Biol. Chem.* 281, 38668–38674. <https://doi.org/10.1074/jbc.M609320200>
- Uyama, T., Kitagawa, H., Tanaka, J., Tamura, J., Ogawa, T., Sugahara, K., 2003. Molecular Cloning and Expression of a Second Chondroitin N-Acetylgalactosaminyltransferase Involved in the Initiation and Elongation of Chondroitin/Dermatan Sulfate\*. *J. Biol. Chem.* 278, 3072–3078. <https://doi.org/10.1074/jbc.M209446200>
- Vaillant, C., Meissirel, C., Mutin, M., Belin, M.-F., Lund, L.R., Thomasset, N., 2003. MMP-9 deficiency affects axonal outgrowth, migration, and apoptosis in the developing cerebellum. *Mol. Cell. Neurosci.* 24, 395–408. [https://doi.org/10.1016/S1044-7431\(03\)00196-9](https://doi.org/10.1016/S1044-7431(03)00196-9)
- Vainchtein, I.D., Chin, G., Cho, F.S., Kelley, K.W., Miller, J.G., Chien, E.C., Liddelow, S.A., Nguyen, P.T., Nakao-Inoue, H., Dorman, L.C., Akil, O., Joshita, S., Barres, B.A., Paz, J.T., Molofsky, A.B., Molofsky, A.V., 2018. Astrocyte-derived interleukin-33 promotes microglial synapse engulfment and neural circuit development. *Science* 359, 1269–1273. <https://doi.org/10.1126/science.aal3589>
- Vallar, G., 2017. Short-Term Memory☆, in: *Reference Module in Neuroscience and Biobehavioral Psychology*. Elsevier. <https://doi.org/10.1016/B978-0-12-809324-5.03170-9>
- Vanderhaeghen, P., Cheng, H.-J., 2010. Guidance Molecules in Axon Pruning and Cell Death. *Cold Spring Harb. Perspect. Biol.* 2, a001859. <https://doi.org/10.1101/cshperspect.a001859>
- VanGuilder, H.D., Farley, J.A., Yan, H., Van Kirk, C.A., Mitschelen, M., Sonntag, W.E., Freeman, W.M., 2011. Hippocampal dysregulation of synaptic plasticity-associated proteins with age-related cognitive decline. *Neurobiol. Dis.* 43, 201–212. <https://doi.org/10.1016/j.nbd.2011.03.012>

- VanGuilder, H.D., Yan, H., Farley, J.A., Sonntag, W.E., Freeman, W.M., 2010. Aging alters the expression of neurotransmission-regulating proteins in the hippocampal synaptoproteome. *J. Neurochem.* 113, 1577–1588. <https://doi.org/10.1111/j.1471-4159.2010.06719.x>
- Vankemmelbeke, M.N., Holen, I., Wilson, A.G., Ilic, M.Z., Handley, C.J., Kelner, G.S., Clark, M., Liu, C., Maki, R.A., Burnett, D., Buttle, D.J., 2001. Expression and activity of ADAMTS-5 in synovium. *Eur. J. Biochem.* 268, 1259–1268. <https://doi.org/10.1046/j.1432-1327.2001.01990.x>
- Végh, M.J., Heldring, C.M., Kamphuis, W., Hijazi, S., Timmerman, A.J., Li, K.W., van Nierop, P., Mansvelder, H.D., Hol, E.M., Smit, A.B., van Kesteren, R.E., 2014. Reducing hippocampal extracellular matrix reverses early memory deficits in a mouse model of Alzheimer's disease. *Acta Neuropathol. Commun.* 2, 76. <https://doi.org/10.1186/s40478-014-0076-z>
- Vegh, M.J., Rausell, A., Loos, M., Heldring, C.M., Jurkowski, W., van Nierop, P., Paliukhovich, I., Li, K.W., del Sol, A., Smit, A.B., Spijker, S., van Kesteren, R.E., 2014. Hippocampal extracellular matrix levels and stochasticity in synaptic protein expression increase with age and are associated with age-dependent cognitive decline. *Mol Cell Proteomics* 13, 2975–85. <https://doi.org/10.1074/mcp.M113.032086>
- Velasco, J., Li, J., DiPietro, L., Stepp, M.A., Sandy, J.D., Plaas, A., 2011. Adamts5 Deletion Blocks Murine Dermal Repair through CD44-mediated Aggrecan Accumulation and Modulation of Transforming Growth Factor  $\beta$ 1 (TGF $\beta$ 1) Signaling \*. *J. Biol. Chem.* 286, 26016–26027. <https://doi.org/10.1074/jbc.M110.208694>
- Verma, R.P., Hansch, C., 2007. Matrix metalloproteinases (MMPs): Chemical–biological functions and (Q)SARs. *Bioorg. Med. Chem.* 15, 2223–2268. <https://doi.org/10.1016/j.bmc.2007.01.011>
- Verma, S., Dixit, R., Pandey, K.C., 2016. Cysteine Proteases: Modes of Activation and Future Prospects as Pharmacological Targets. *Front. Pharmacol.* 7, 107. <https://doi.org/10.3389/fphar.2016.00107>
- Verslegers, M., Lemmens, K., Van Hove, I., Moons, L., 2013. Matrix metalloproteinase-2 and -9 as promising benefactors in development, plasticity and repair of the nervous system. *Prog. Neurobiol.* 105, 60–78. <https://doi.org/10.1016/j.pneurobio.2013.03.004>
- Vitureira, N., Goda, Y., 2013. The interplay between Hebbian and homeostatic synaptic plasticity. *J. Cell Biol.* 203, 175–186. <https://doi.org/10.1083/jcb.201306030>
- Vogel, C., Marcotte, E.M., 2012. Insights into the regulation of protein abundance from proteomic and transcriptomic analyses. *Nat. Rev. Genet.* 13, 227–232. <https://doi.org/10.1038/nrg3185>
- Vorhees, C.V., Williams, M.T., 2014. Assessing Spatial Learning and Memory in Rodents. *ILAR J.* 55, 310–332. <https://doi.org/10.1093/ilar/ilu013>
- Vu, T.H., Werb, Z., 2000. Matrix metalloproteinases: effectors of development and normal physiology. *Genes Dev.* 14, 2123–2133. <https://doi.org/10.1101/gad.815400>
- Waldmann, V., Jouven, X., Narayanan, K., Piot, O., Chugh, S.S., Albert, C.M., Marijon, E., 2020. Association Between Atrial Fibrillation and Sudden Cardiac Death. *Circ. Res.* 127, 301–309. <https://doi.org/10.1161/CIRCRESAHA.120.316756>
- Wang, H., Katagiri, Y., McCann, T.E., Unsworth, E., Goldsmith, P., Yu, Z.-X., Tan, F., Santiago, L., Mills, E.M., Wang, Y., Symes, A.J., Geller, H.M., 2008. Chondroitin-4-sulfation negatively regulates axonal guidance and growth. *J. Cell Sci.* 121, 3083–3091. <https://doi.org/10.1242/jcs.032649>
- Wang, P., Tortorella, M., England, K., Malfait, A.-M., Thomas, G., Arner, E.C., Pei, D., 2004. Proprotein convertase furin interacts with and cleaves pro-ADAMTS4 (Aggrecanase-1) in the trans-Golgi network. *J. Biol. Chem.* 279, 15434–15440. <https://doi.org/10.1074/jbc.M312797200>
- Wang, X., Bozdagi, O., Nikitczuk, J.S., Zhai, Z.W., Zhou, Q., Huntley, G.W., 2008. Extracellular proteolysis by matrix metalloproteinase-9 drives dendritic spine enlargement and long-term potentiation coordinately. *Proc. Natl. Acad. Sci.* 105, 19520–19525. <https://doi.org/10.1073/pnas.0807248105>

- Wang, X., He, J., Wang, Y., Cui, F.-Z., 2012. Hyaluronic acid-based scaffold for central neural tissue engineering. *Interface Focus* 2, 278–291. <https://doi.org/10.1098/rsfs.2012.0016>
- Wartmann, T., Mayerle, J., Kähne, T., Sahin-Tóth, M., Ruthenbürger, M., Matthias, R., Kruse, A., Reinheckel, T., Peters, C., Weiss, F.U., Sandler, M., Lippert, H., Schulz, H., Aghdassi, A., Dummer, A., Teller, S., Halangk, W., Lerch, M.M., 2010. Cathepsin L Inactivates Human Trypsinogen, Whereas Cathepsin L-Deletion Reduces the Severity of Pancreatitis in Mice. *Gastroenterology* 138, 726–737. <https://doi.org/10.1053/j.gastro.2009.10.048>
- Webb, W.G., 2017. 13 - Pediatric Disorders of Language, in: Webb, W.G. (Ed.), *Neurology for the Speech-Language Pathologist (Sixth Edition)*. Mosby, pp. 272–290. <https://doi.org/10.1016/B978-0-323-10027-4.00013-0>
- Wei, G., Bai, X., Sarkar, A.K., Esko, J.D., 1999. Formation of HNK-1 Determinants and the Glycosaminoglycan Tetrasaccharide Linkage Region by UDP-GlcUA:Galactose  $\beta$ 1,3-Glucuronosyltransferases\*. *J. Biol. Chem.* 274, 7857–7864. <https://doi.org/10.1074/jbc.274.12.7857>
- Weigel, S., Meissner, J., Zharkovsky, A., Arendt, T., Rossner, S., Morawski, M., 2015. Effect of brevican deficiency on neuroplasticity mediating molecules. *SpringerPlus* 4, P55. <https://doi.org/10.1186/2193-1801-4-S1-P55>
- Wen, J., Xiao, J., Rahdar, M., Choudhury, B.P., Cui, J., Taylor, G.S., Esko, J.D., Dixon, J.E., 2014. Xylose phosphorylation functions as a molecular switch to regulate proteoglycan biosynthesis. *Proc. Natl. Acad. Sci.* 111, 15723–15728. <https://doi.org/10.1073/pnas.1417993111>
- Williams, A., Piaton, G., Aigrot, M.-S., Belhadi, A., Théaudin, M., Petermann, F., Thomas, J.-L., Zalc, B., Lubetzki, C., 2007. Semaphorin 3A and 3F: key players in myelin repair in multiple sclerosis? *Brain* 130, 2554–2565. <https://doi.org/10.1093/brain/awm202>
- Williams, M.E., de Wit, J., Ghosh, A., 2010. Molecular Mechanisms of Synaptic Specificity in Developing Neural Circuits. *Neuron* 68, 9–18. <https://doi.org/10.1016/j.neuron.2010.09.007>
- Wingert, J.C., Sorg, B.A., 2021. Impact of Perineuronal Nets on Electrophysiology of Parvalbumin Interneurons, Principal Neurons, and Brain Oscillations: A Review. *Front. Synaptic Neurosci.* 13, 22. <https://doi.org/10.3389/fnsyn.2021.673210>
- Xu, D., Hopf, C., Reddy, R., Cho, R.W., Guo, L., Lanahan, A., Petralia, R.S., Wenthold, R.J., O'Brien, R.J., Worley, P., 2003. Narp and NP1 Form Heterocomplexes that Function in Developmental and Activity-Dependent Synaptic Plasticity. *Neuron* 39, 513–528. [https://doi.org/10.1016/S0896-6273\(03\)00463-X](https://doi.org/10.1016/S0896-6273(03)00463-X)
- Yamaguchi, M., Seki, T., Imayoshi, I., Tamamaki, N., Hayashi, Y., Tatebayashi, Y., Hitoshi, S., 2016. Neural stem cells and neuro/gliogenesis in the central nervous system: understanding the structural and functional plasticity of the developing, mature, and diseased brain. *J. Physiol. Sci.* 66, 197–206. <https://doi.org/10.1007/s12576-015-0421-4>
- Yamazaki, Y., Abe, Y., Fujii, S., Tanaka, K.F., 2021. Oligodendrocytic Na<sup>+</sup>-K<sup>+</sup>-Cl<sup>-</sup> co-transporter 1 activity facilitates axonal conduction and restores plasticity in the adult mouse brain. *Nat. Commun.* 12, 5146. <https://doi.org/10.1038/s41467-021-25488-5>
- Yamazaki, Y., Hozumi, Y., Kaneko, K., Fujii, S., Goto, K., Kato, H., 2010. Oligodendrocytes: Facilitating Axonal Conduction by More Than Myelination. *The Neuroscientist* 16, 11–18. <https://doi.org/10.1177/1073858409334425>
- Yang, S., Gigout, S., Molinaro, A., Naito-Matsui, Y., Hilton, S., Foscarin, S., Nieuwenhuis, B., Tan, C.L., Verhaagen, J., Pizzorusso, T., Saksida, L.M., Bussey, T.M., Kitagawa, H., Kwok, J.C.F., Fawcett, J.W., 2021. Chondroitin 6-sulphate is required for neuroplasticity and memory in ageing. *Mol. Psychiatry* 1–11. <https://doi.org/10.1038/s41380-021-01208-9>

- 
- Yoshihara, Y., Oka, S., Nemoto, Y., Watanabe, Y., Nagata, S., Kagamiyama, H., Mori, K., 1994. An ICAM-related neuronal glycoprotein, telencephalin, with brain segment-specific expression. *Neuron* 12, 541–553. [https://doi.org/10.1016/0896-6273\(94\)90211-9](https://doi.org/10.1016/0896-6273(94)90211-9)
- Young, N.M., Williams, R.E., 1985. Assignment of lectins specific for D-galactose or N-acetyl-D-galactosamine to two groups, based on their circular dichroism. *Can. J. Biochem. Cell Biol. Rev. Can. Biochim. Biol.* 63, 268–271. <https://doi.org/10.1139/o85-039>
- Yu, Q., Stamenkovic, I., 2000. Cell surface-localized matrix metalloproteinase-9 proteolytically activates TGF- $\beta$  and promotes tumor invasion and angiogenesis. *Genes Dev.* 14, 163–176.
- Yuan, J., Lipinski, M., Degtarev, A., 2003. Diversity in the mechanisms of neuronal cell death. *Neuron* 40, 401–413. [https://doi.org/10.1016/s0896-6273\(03\)00601-9](https://doi.org/10.1016/s0896-6273(03)00601-9)
- Yuan, W., Matthews, R.T., Sandy, J.D., Gottschall, P.E., 2002. Association between protease-specific proteolytic cleavage of brevican and synaptic loss in the dentate gyrus of kainate-treated rats. *Neuroscience* 114, 1091–1101. [https://doi.org/10.1016/s0306-4522\(02\)00347-0](https://doi.org/10.1016/s0306-4522(02)00347-0)
- Yuzaki, M., 2018. Two Classes of Secreted Synaptic Organizers in the Central Nervous System. *Annu. Rev. Physiol.* 80, 243–262. <https://doi.org/10.1146/annurev-physiol-021317-121322>
- Zamanian, J.L., Xu, L., Foo, L.C., Nouri, N., Zhou, L., Giffard, R.G., Barres, B.A., 2012. Genomic analysis of reactive astrogliosis. *J. Neurosci. Off. J. Soc. Neurosci.* 32, 6391–6410. <https://doi.org/10.1523/JNEUROSCI.6221-11.2012>
- Zhai, H., Qi, X., Li, Z., Zhang, W., Li, C., Ji, L., Xu, K., Zhong, H., 2018. TIMP-3 suppresses the proliferation and migration of SMCs from the aortic neck of atherosclerotic AAA in rabbits, via decreased MMP-2 and MMP-9 activity, and reduced TNF- $\alpha$  expression. *Mol. Med. Rep.* 18, 2061–2067. <https://doi.org/10.3892/mmr.2018.9224>
- Zhai, J., Kim, H., Han, S.B., Manire, M., Yoo, R., Pang, S., Smith, G.M., Son, Y.-J., 2021. Co-targeting myelin inhibitors and CSPGs markedly enhances regeneration of GDNF-stimulated, but not conditioning-lesioned, sensory axons into the spinal cord. *eLife* 10, e63050. <https://doi.org/10.7554/eLife.63050>
- Zhao, C., Fancy, S.P.J., Franklin, R.J.M., French-Constant, C., 2009. Up-regulation of oligodendrocyte precursor cell  $\alpha$ V integrin and its extracellular ligands during central nervous system remyelination. *J. Neurosci. Res.* 87, 3447–3455. <https://doi.org/10.1002/jnr.22231>
- Zheng, X., Gessel, M.M., Wisniewski, M.L., Viswanathan, K., Wright, D.L., Bahr, B.A., Bowers, M.T., 2012. Z-Phe-Ala-diazomethylketone (PADK) disrupts and remodels early oligomer states of the Alzheimer disease A $\beta$ 42 protein. *J. Biol. Chem.* 287, 6084–6088. <https://doi.org/10.1074/jbc.C111.328575>
- Zhou, Z., Rawnsley, D.R., Goddard, L.M., Pan, W., Cao, X.-J., Jakus, Z., Zheng, H., Yang, J., Arthur, J.S.C., Whitehead, K.J., Li, D., Zhou, B., Garcia, B.A., Zheng, X., Kahn, M.L., 2015. The cerebral cavernous malformation pathway controls cardiac development via regulation of endocardial MEKK3 signaling and KLF expression. *Dev. Cell* 32, 168–180. <https://doi.org/10.1016/j.devcel.2014.12.009>
- Zimmermann, D.R., Dours-Zimmermann, M.T., 2008. Extracellular matrix of the central nervous system: from neglect to challenge. *Histochem. Cell Biol.* 130, 635–653. <https://doi.org/10.1007/s00418-008-0485-9>
- Zonta, B., Desmazieres, A., Rinaldi, A., Tait, S., Sherman, D.L., Nolan, M.F., Brophy, P.J., 2011. A Critical Role for Neurofascin in Regulating Action Potential Initiation through Maintenance of the Axon Initial Segment. *Neuron* 69, 945–956. <https://doi.org/10.1016/j.neuron.2011.02.021>